

On the Synthesis of Switched Output Feedback Controllers for Linear, Time-invariant Systems

by

Keith Robert Santarelli

S.B. Electrical Science and Engineering (1999)
Massachusetts Institute of Technology

M.Eng. Electrical Engineering and Computer Science (2000)
Massachusetts Institute of Technology

Submitted to the Department of Electrical Engineering and Computer
Science

in partial fulfillment of the requirements for the degree of

Doctor of Philosophy in Electrical Engineering and Computer Science

at the

MASSACHUSETTS INSTITUTE OF TECHNOLOGY

February 2007

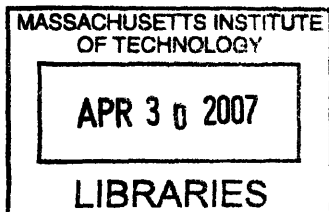
© Massachusetts Institute of Technology 2007. All rights reserved.

Author
Department of Electrical Engineering and Computer Science
January 31, 2007

Certified by
Munther A. Dahleh
Professor of Electrical Engineering
Thesis Supervisor

Accepted by
Terry P. Orlando

Chairman, Department Committee on Graduate Students



ARCHIVES

On the Synthesis of Switched Output Feedback Controllers for Linear, Time-invariant Systems

by

Keith Robert Santarelli

Submitted to the Department of Electrical Engineering and Computer Science
on January 31, 2007, in partial fulfillment of the
requirements for the degree of
Doctor of Philosophy in Electrical Engineering and Computer Science

Abstract

The theory of switching systems has seen many advances in the past decade. Its beginnings were founded primarily due to the physical limitations in devices to implement control such as relays, but today there exists a strong interest in the development of switching systems where switching is introduced as a means of increasing performance. With the newer set of problems that arise from this viewpoint comes the need for many new tools for analysis and design. Analysis tools which include, for instance, the celebrated work on multiple Lyapunov functions are extensive. Tools for the design of switched systems also exist, but, in many cases, the method of designing stabilizing switching laws is often a separate process from the method which is used to determine the set of vector fields between which switching takes place. For instance, one typical method of designing switching controllers for linear, time-invariant (LTI) systems is to first design a set of stabilizing LTI controllers using standard LTI methods, and then design a switching law to increase performance. While such design algorithms can lead to increases in performance, they often impose restrictions that do not allow the designer to take full advantage of the switching architecture being considered. For instance, if one switches between controllers that are individually stabilizing (without any switching), then, effectively, one is forced to switch only between stable systems and, hence, cannot take advantage of the potential benefits of switching between unstable systems in a stable way. It is, therefore, natural to wonder whether design algorithms can be developed which *simultaneously* design both the set of controllers to be switched and a stabilizing switching law.

The work investigated here attempts to take a small step in the above direction. We consider a simple switching architecture that implements switched proportional gain control for second order LTI systems. Examination of this particular structure is motivated by its mathematical simplicity for ease of analysis (and, hence, as a means of gaining insight into the problem-at-large), but, as we will see, the design techniques investigated here can be extended to a larger class of (higher order, potentially non-linear and/or time-varying) systems using standard tools from robust control. The overall problem we investigate is the ability to create algorithms to simultaneously determine a set of switching gains and an associated switching law for a particular plant and performance objective. After determining a set of necessary and sufficient conditions for a given second order plant to be stabilizable via the given switching

architecture, we synthesize an algorithm for constructing controllers for which the corresponding closed-loop system dynamics are finite L_2 gain stable. Also, in an effort to demonstrate that the the given structure can, in fact, be used to increase performance, we consider a step-tracking design problem for a class of plants, where we use overshoot and settling time of the output step response to measure performance. We compare the results obtained using our switching architecture to the performance that can be obtained via two other LTI controller architectures to illustrate some of the performance benefits.

Thesis Supervisor: Munther A. Dahleh
Title: Professor of Electrical Engineering

*In memory of my mother,
Katherine Anne Santarelli,
who left us far too soon.*



Prologue

The instructor said,

*Go home and write
a page tonight.
And let that page come out of you—
Then, it will be true.*

I wonder if it's that simple?

—from Langston Hughes, *Theme for English B*, 1951.

Simplicity. It's a concept that drives all of us everyday. We pack our lives chock-full of different activities, people, and events to play a seemingly endless juggling game: “*What's the easiest route from work to home? I'll squeeze in a workout between lunch and my afternoon appointment? Maybe I can swing by the grocery store on the way to pick up the kids from preschool . . .*” and on and on. Yet during those brief moments of the day in between activities when we get a short moment to catch our breath, we heave a deep mental sigh and think to ourselves “*If only things were simpler.*” At least *I* do, and I have a strong hunch that I'm not alone in this. On the flip-side, however, to actually *achieve* “true” simplicity could require us to cut out entire parts of our lives, and that tends to work against another very important goal: personal fulfillment. So, each day, we play a game between these opposing forces in an effort to find that happy middle ground. Has anybody found it yet? Last I heard, it was somewhere east of Cleveland.

Life as a student at MIT is no exception to this endless game. While many people I know recall their college years in hindsight as a buffer between their childhood and the “real world,” as former MIT president Chuck Vest told my entire freshman class in August of 1995, “Real life begins today. Right here at MIT.”¹ The story of one person's journey through MIT is not limited to the acquisition of knowledge and the honing of practical skills. Rather, it is a journey that traverses several aspects of life. It is a story of building friendships with people from around the world that will last a lifetime, as well as those that don't last beyond orientation. It involves first loves, as well as painful heart breaks. It is a story of broadening horizons, discovering that all issues have shades of grey, becoming an independent thinker, and learning how to speak your mind in a manner that conveys your point while being sensitive to the views of others. It teaches you both how to take care of yourself and how and when to take care of others—and when *not* to take *too* much care of others so that they may learn and benefit from the same powerful lessons that you have learned. It involves life-changing decisions, deep soul-searching and self-discovery about who you really are—your desires, skills, passions, and true goals in life—and learning things about yourself that you never really knew. More importantly, you learn to trust your own

¹Taken from the President's Convocation to the MIT Class of 1999. Available at <http://www-tech.mit.edu/V115/N32/president.32n.html>

intuition and not to limit your judgements and actions based upon the perceptions of others.

In short, life as a student at MIT is *far* from simple.

My journey through MIT has involved all of the aforementioned parts and more. As a whole, the process has transformed me from a shy, awkward boy with narrow focuses (did somebody say integral?) into a confident, outgoing man with far broader horizons (did somebody say KISS 108?). If I had to choose one lesson to sum up my experiences at MIT, it would be this: life—both our life and the lives of all others living in this world—is a fleeting gift that must be cherished and celebrated at all times. In a world that can be very harsh and which can easily distract us with short-term goals, we must always take time to step back and remain cognizant of the fact that, while our time here is limited, our effect on the future of the world is boundless. Hence, we must always make sure that we are utilizing our time and our individual talents in the most useful way possible. While a large part of this time for some of us may be devoted to technical work—sustainable energy, reduction of antibiotic resistance, or even something as trivial as the design of switching controllers for linear systems—we must also remember that we benefit the world by offering a helping hand to individuals in need; not going into lab two nights before your currently defunct bachelor’s project is due to lend an ear to your friend who broke up with her first real boyfriend benefits the world in a very different but equally valuable way. By helping others remain on their feet to realize their full potential, we better the world in ways that are immeasurable. Conversely, we must also learn not always be too proud to reach for a helping hand when it is offered to us since we all need support from time-to-time to get through the complexities of life.

Acknowledgements

To accurately document all of the people and experiences at MIT that have shaped me into the person I am today is a process that could fill volumes. Nevertheless, I will attempt to do my best at highlighting some of the major influences I have had during my time here.

As an undergraduate, life would not have been the same without the support of the many close friends that I developed while living on Conner 4. While the number of close friendships that originated there are numerous, there are a few people whom I’d like to recognize individually. First, many thanks to my former 413A roommates, Nathan St. Michel (whose last name is accurately pronounced stuh-mitchell no matter what he tells you . . .) and the “ghetto-fabulous” Chris Hockert, for putting up with me as a roommate and for always patiently listening to me complain about whatever was on my mind. I’d also like to thank the original “Charlie’s Angels” —Laura Kwinn, Le “Sammi” Truong, and Jade Wang—for always knowing how to make me laugh. Ankur Chandra always knew how to have a good time even in the most dire of situations. Shiva Sandy has always been a strong pillar of support, and I thank him for all the advice he’s dispensed to me over the years. Mike and Steph Harrington were the most amazing floor tutors ever, and, years later as a graduate student, I learned to be an effective GRT through the example they set.

One particular Conner 4 friend who deserves some extra special attention is Veena Thomas. She has become one of my closest friends since I met her as a lowly freshman eight years ago, and she is truly wise beyond her years. Whether having a late-night conversation about the perils of being a graduate student, listening to her offer me insight into the mechanics of the female psyche, or listening to her strategies about how to win a game of Monopoly, I have been very fortunate to benefit from the many pearls of wisdom she has to offer.

In contrast to my undergraduate years, my graduate school years were supported by several different circles of people. First and foremost, I would not be writing this piece today without the aid of my advisor, Prof. Munther Dahleh. Munther introduced me to the wonders of systems theory as an undergraduate when I was fortunate enough to take 6.003 one of the few terms that he lectured the class. As a graduate student, he pushed me to be an independent thinker and demonstrated how to be an effective researcher. I am greatly indebted for all of the sets of skills that I have acquired through him over the years. Other faculty whom I would like to recognize include Prof. Alexandre Megretski for bestowing on me some of his immense technical expertise, Prof. Pablo Parrilo and Prof. Rahul Sarpeshkar for the insights that they both provided during the middle parts of my thesis, and Prof. George Verghese for his immense help during the finishing stages of this work.

I'd further like to thank several of the other students in the Control Systems Group in LIDS: Ola Ayaso, Erin Aylward, Jorge Gonçalves, Isaac Kao, Fadi Karamah, Georgios Kotsalis, Pat Kreidl, Nuno Martins, Mitra Osqui, Mike Rinehart, Mardavij Roozbehani, Sri Sarma, and Holly Waisanen. Special thanks go to Soosan Beheshti and Danielle Tarraf for always providing me with advice.

I also must greatly thank the support of several LIDS Staff members over the years. First, a great big thanks goes out to Ms. Fifi Monserrate for always going out of her way to be tremendously helpful. Not only do I owe her my eternal gratitude, but I'm sure at this point that I owe her *several* bags of candy for all that I stole from her candy dish over the past six years! I'd also additionally like to put out special thanks to Rachel Cohen, Jason Decker, Lynne Dell, Doris Inslee, Brian Jones, Irene Kelliher, Taylore Kelly, Pardis Parsa, Sue Patterson and Petr Swedock for their support over the years.

Outside of the academic realm, life would have been very different were it not for several friends, particularly the *Puffywumps*: Rob Carney, Cathy Hoelscher, Ryan Lang, Kenny Marr, Alisa Marshall, Mat Willmott, Dan Nezich, Rich Ott, Alicia Peralta (to whom I owe an extra special thanks for helping me to edit this document!), Gretchen Poehlman, Rich Redemske, Jeff Simpson, and Margaret Wong. Playing trivia Tuesday nights at the Asgard with all of these fine people, along with all of the other lunches at Subway, trips (Vegas!), and Friday evenings where they would all steal my money while playing a long game of 3-5-7 (yup, Mat, I still haven't let go of that one game . . .), has definitely helped keep me sane through the drudgeries of graduate school. All of these times together are memories that I will forever cherish.

I would be very much amiss if I did not thank all of the students in New House 4 who allowed me to be their GRT for four wonderful years. In letting me become an integral part of their House life, I discovered deep inside of me the ability to be a

leader, something that I never associated with myself up to that point in time. The well-being of each of the many House members whom I was fortunate enough to know meant and still means the world to me. My time spent in New House 4 is the most valuable experience in terms of personal growth that I have ever undergone, and I hope that at least a few of them will still think of me, as I often think of all of them when I look at the *Top 10 Reasons to Become NH4 GRT* poster that they made for me just before I left.

In connection with my years as a GRT, I must also recognize the help and friendship of two of my superiors, Sharon Snaggs and Lauren Wojtkun. Both have extreme drive and passion for helping the student community which has been a source of inspiration for me on more than one occasion. Also, Asha Balakrishnan, Reginald Bryant, Robbin Chapman, Hector Hernandez, Ivory Hills, Krissy Kopp, and Aisha Walcott were great sources of support as fellow GRTs. A special shout goes out to Janice Lansita who, along with partners in crime Amy Englehart and Irina Medvedev, has been an amazing friend from the moment we met in the GRT application process.

The staff and patrons of the Muddy Charles Pub have also been a great outlet for stress during my graduate student years. Some of the great people whom I've had the chance to get to know via my bartending years include: Scott Litzelman, Melissa Mazmanian, John Mills, Troy Simpson, Jess Vey, Sarah Sled, Solar Olugebefola, Monica Rixman, Paige Hopewell, Kevin Duda, Catherine Cresson, Lisa Joslin, Nici Ames, Dan Honiker, Joe Contrada, Bill McKinney, Jan Cornish, Tommy Callahan, Jimmy Carter, Barb Skinner, Paul Campbell, Paul B., Neal...what's your last name Neal?, Kevin Harrison, Mike Cooke, Joost Bonsen, Cory Kidd, and many more. Special thanks go out to Pamela Florek and Susan Stapleton, two of my very good friends (and my two favorite bar patrons!)

Last, but certainly not least, I must thank the wonderful family who has supported me from the moment I first opened my eyes: my father, my older brothers Scott and Bryan, and my older sister Cheryl have always wanted only the best for me. In particular, though, I owe an immense debt of gratitude to my late mother, Katherine, who always supported me through the thick and thin. It has now been over eight years since I last laid eyes on her, yet the image of her smile is as clear in my mind as it is in the picture on the preceding pages. While she may no longer be with us, I have discovered that she is deeply intertwined with almost my every thought and action: my love of laughter, desire to help others, passion for teaching, ability to show compassion, and, most importantly, my ability to love were all learned through her example. There are still days that I miss her just as much as when I first lost her, but, as many people who have lost a parent probably do, I take solace in the fact that I attempt to lead my life in a manner that would make her proud. I love you Mom—always have, always will.

A Word on Truth

Following the advice given at the beginning of this section by Hughes, I have attempted here to be as true—to myself and to the countless invaluable people in my life—as I can. But truth is not something that is always easily put into words, and the

truth of my experience at MIT falls into this category. No words can truly describe the vast wonders that I have witnessed and been a part of over the past decade, and I am content with that. Not all of the pieces that make us into the individuals we are need to be visible to the entire world. It's my belief that the small parts of us that nobody else in the world can really understand preserve our individuality --and individuality is an aspect of ourselves that we should *always* proudly preserve.

I want to emphasize that what follows in these pages is merely *part* of the truth of my experience as a Ph. D. student. Mind you, it is a rather large portion of my experience, and is at the very core of my reasons for obtaining a graduate degree in the first place. But if any of the above ramblings make sense, you, reader, will realize that this work does *not* define who I am; it only defines a part of me.

And that's the truth.

Keith Santarelli
Cambridge, MA
January, 2007

Funding Acknowledgement

Funding for this research has been provided by Air Force Aerospace OSR Grant FA9550-04-1-0052, along with generous contributions from the MIT Department of Electrical Engineering and Computer Science.

Contents

1	Introduction	21
1.1	Switching Systems	21
1.1.1	Example: Temperature Control	22
1.1.2	Example: Switched LTI Controllers	24
1.2	Problem Motivation	26
1.3	Problem Investigation: Controller Synthesis and Performance Comparison	29
1.3.1	Performance Measures	29
1.3.2	Design Algorithm	30
1.4	Related Work	31
1.5	Document Outline	33
2	Preliminary Results: Necessary and Sufficient Conditions for Stabilizability	35
2.1	Introduction	35
2.2	Case Studies	37
2.2.1	Case 1	37
2.2.2	Case 2	41
2.3	Main Result	43
2.4	Design Methodology	45
2.5	Examples	45
2.6	Summary	47
3	Synthesis of Optimal Controllers: Rate of Convergence	49
3.1	Introduction	49
3.2	Rate of Convergence: Definitions	50
3.3	Problem Formulation	52
3.4	Optimal Controller Synthesis for Plants of Relative Degree Two	54
3.5	Summary	68
3.6	Appendix: Proofs of Technical Statements	68
4	L2 Gain Stability of Optimal Controllers and Observer-based Control Laws	71
4.1	Introduction	71
4.2	Preliminaries: Lyapunov Function	73

4.2.1	Auxiliary Switching System	75
4.2.2	Exponential Stability of the Auxiliary Switching System	79
4.2.3	Construction of Piecewise Differentiable Lyapunov Function for Auxiliary System	82
4.3	L2 Gain Stability: Full State Information	88
4.3.1	Storage Functions in Different Coordinates	96
4.4	Observer-based Control	98
4.4.1	Observer Design	99
4.4.2	Finite L2 Gain Stability of Observer-based Controller	100
4.5	Computational Considerations	103
4.6	Summary	107
5	Application: Step Response Performance	109
5.1	Introduction	109
5.2	Switching Architecture Design	111
5.2.1	Step response Performance of Switching Architecture	114
5.2.2	Design Example: Double Integrator	116
5.3	Comparison: First Order LTI Control of a Double Integrator	118
5.3.1	Preliminaries: Controller Constraints	121
5.3.2	First Order Controller Class	127
5.3.3	Computation of Achievable Percentage Overshoot, 1% Settling Time Pairs	131
5.3.4	First Order LTI Control for Other Plants	134
5.4	Comparison: Higher Order LTI Control	136
5.4.1	Time Optimal Control, Part I: Bounds derived from Rise Time	136
5.4.2	Time Optimal Control, Part II: Approximate Bound on Settling Time	143
5.4.3	Designing LTI Controllers with Minimum Settling Time	152
5.5	Summary	160
5.6	Proof of Technical Statements	161
6	Moving Beyond the Phase Plane: Higher Order Design Example	171
6.1	Preliminaries: Small Gain Theorem	171
6.2	Design Example: Robust Design for a Class of Fourth Order LTI Systems	173
6.2.1	Range of τ and L_2 Gain Bound	173
6.2.2	Step Response Performance	178
6.3	Summary	178
7	Conclusion and Future Work	183

List of Figures

1.1.1 Transfer characteristic of a relay with hysteresis.	23
1.1.2 Model of temperature control problem. The relay represents a thermostat, while the linear dynamical system represents the temperature dynamics of the room.	23
1.1.3 Block diagram for control architecture that switches between multiple LTI controllers.	25
1.2.4 Switching architecture under investigation in this document.	27
1.2.5 Structure of supervisor in Fig. 1.2.4.	28
1.3.6 Flow chart which indicates the individual steps in developing the design algorithm for controller synthesis.	32
2.2.1 Illustration of stabilization algorithm for a system which is not static output feedback stabilizable.	40
2.5.2 Root loci for $H_1(s)$, $H_2(s)$, and $H_3(s)$. The root loci for positive k are depicted on the left, while the root loci for negative k are depicted on the right.	46
3.4.1 Graphical depiction of switching law of Eqn. 3.4.11	58
3.4.2 Relative positioning of w_s , w_u , q , and p for Lemma 3.4.3.	59
3.4.3 Illustration of the optimal control law for Example 3.4.	64
3.4.4 Eigenvectors for the matrix $A + v_0BC$ for Example 3.4 (not drawn to scale). 67	
4.2.1 Auxiliary switching system for the different values of ϕ_q . The dashed lines each make an angle of ϕ_0 with w_s and q , and the system dynamics between the pairs of dashed lines surrounding w_s and q , respectively, are chosen to maximize \dot{r}	78
4.3.2 Block diagram depicting where the exogenous signals $g_1(t)$, $g_2(t)$, and $g_3(t)$ enter into the system dynamics for the full state L_2 gain problem. .	89
4.3.3 Graphical depiction of the result of Prop. 4.3.13 when x lies close to w_s . 92	
4.4.4 Block diagram of switching system with observer in place of full-state feedback (the observer is comprised of the blocks $1/(s + k_1)$, k_2 , and k_3). The input w models the net disturbance/noise inputs to the observer. . .	101
4.4.5 Equivalent block diagram of Fig. 4.4.4 with input disturbance w re-configured as an observer output disturbance g_4	103
4.4.6 Block diagram of Fig. 4.4.5 with output of lowpass filter with input w replaced by an <i>arbitrary</i> locally square-integrable signal $g_4(t)$	104

5.2.1 Proposed switching architecture to be used in designing a controller which asymptotically tracks a step input.	111
5.2.2 Supervisor of Fig. 5.2.1 for the plant $P(s)$ given by Eqn. 5.1.1.	114
5.2.3 Example transient response in z coordinates for a plant $P(s)$ of the form Eqn. 5.1.1 controlled by the switching architecture of Fig. 5.2.1.	116
5.2.4 Block diagram of an observer (indicated by the dashed box) for the double integrator which produces an estimate $\hat{x}_2(t)$ of $x_2(t)$	117
5.2.5 Step response of double integrator controlled by the switching architecture of Fig. 5.2.1.	118
5.3.6 Servo control architecture.	119
5.3.7 Example achievability region where the achievable pairs (M, T) are those which satisfy $M \geq 1/T$ (indicated by the shaded region.)	120
5.3.8 Servo architecture with plant input disturbance $w(t)$	122
5.3.9 Partial block diagram for L_2 gain calculation. The exogenous input $w(t)$ is input to the plant $P(s)$ but is not input to the observer.	124
5.3.10 Block diagram of Fig. 5.3.9 under the change of coordinates $z_1 = x_1$, $z_2 = x_2 - x_1$	125
5.3.11 Rearrangement of the block diagram of Fig. 5.3.10.	126
5.3.12 New system which upper bounds the L_2 gain of the system depicted in Fig. 5.3.11 with $-w(t)$ replaced by $w'(t)$	126
5.3.13 Block diagram of a second order system whose joint L_2 gain from the inputs $w(t)$ and $v(t)$ to $y(t)$ upper bounds the L_2 gain from $w(t)$ to $y(t)$ in Fig. 5.3.9.	127
5.3.14 Region described by the boxed-in bounds, with $c_{\min} = 1/(\gamma^2 - \gamma)$, $c_{\max} = \gamma - 1$, $d_{\min} = 1/(\gamma - 1)$, and $d_{\max} = \gamma$	131
5.3.15 Achievable percentage overshoot and 1% settling time pairs that can be achieved via first order LTI control for the given peak control and L_2 gain constraints (shown by 'x' in the picture). The performance of the switching architecture is shown via the circle at the bottom of the figure for comparison.	132
5.3.16 Step responses of double integrator that achieve minimal overshoot and minimal 1% settling time subject to the peak control value and L_2 gain bound constraints given in this section.	133
5.3.17 Realization of transfer function $P(s)$ of Eqn. 5.1.1 where $\Delta = b/\sqrt{a}$	134
5.3.18 Step responses for $P_1(s) = \frac{100}{s(s+1)}$	137
5.3.19 Step responses for $P_2(s) = \frac{100}{s(s-1)}$	138
5.4.20 Plot of $\tilde{h}(\gamma)$ of Eqn. 5.4.24 for $\gamma \in [-1, 1]$	142
5.4.21 Time-optimal control $u^*(t)$ and corresponding optimal output $y(t)$ when $a = 1$ and for $b = -1, 0$ and 1 , respectively.	147
5.4.22 Plot of $h(\gamma)/f(\gamma)$ for $\gamma \in [-1, 1]$	153
5.4.23 Servo configuration	153
5.4.24 Control signal $u(t)$ and step response $y(t)$ which yield minimal 1% settling time (1.85 seconds) for the double integrator $P(s) = 1/s^2$ using a 17th order controller.	159

5.4.25 Control signal $u(t)$ and step response $y(t)$ which yield minimal 1% settling time (1.85 seconds) for the double integrator $P(s) = 1/s^2$ using a reduced order controller (12th order).	159
6.1.1 Block diagram description of systems S and Δ for Small Gain Theorem.	172
6.2.2 Design setup for fourth order plant $P_\tau(s)$	174
6.2.3 Block diagram realization of $P_\tau(s)$	175
6.2.4 Block diagram realization of $P_\tau(s)$ with $\Delta(s)$ given as in Eqn. 6.2.1.	176
6.2.5 Block diagram of system to which we apply the Small Gain Theorem.	176
6.2.6 Block diagram of system for joint L_2 gain calculation.	177
6.2.7 Step response of double integrator.	178

List of Tables

5.1	Summary of results for 5 different plants $P(s)$. The analytical approximation T_0 refers to the approximation for the 1% settling time given by Eqn. 5.4.29.	158
-----	--	-----

Chapter 1

Introduction

In this chapter, we introduce the problem that is to be studied in this document, namely the establishment of a set of analysis and design tools for a particular *switching controller* architecture. We begin by recalling the notion of a *switching system* and provide two common examples of switching systems used in engineering design. Based upon our examination of these two examples (and, in particular, the second example), we pose questions about some of the existing open problems in switching system design to motivate the study of a particular switching architecture. We will then present this architecture, as well as some of the basic questions and areas of investigation that we intend to study in this thesis. Once the architecture has been presented, we will then provide a survey of the existing work in the area of switching systems to compare and contrast the work done here to both well-established results and on-going research efforts. We will conclude this chapter by providing a brief outline of the remainder of the document.

1.1 Switching Systems

We will begin by introducing the notion of a *switching system* which can be modelled in the following manner. We start with the following two main components:

- A set of vector fields $f_p(x, v) : \mathbf{R}^n \times \mathbf{R}^m \rightarrow \mathbf{R}^n$, $p \in \{1, 2, \dots, N\}$.
- A *switching signal* $\sigma(t) : [0, \infty) \rightarrow \{1, 2, \dots, N\}$ where $\sigma(t)$ is piecewise continuous.

A *switching system* with *switching signal* $\sigma(t)$ is the solution to the first order differential equation

$$\dot{x} = f_{\sigma(t)}(x(t), v(t)) \tag{1.1.1}$$

where $x \in \mathbf{R}^n$ represents the continuous state and $v \in \mathbf{R}^m$ represents a vector of exogenous inputs. The notion of switching should immediately become apparent from the above differential equation; because $\sigma(t)$ is piecewise constant, the vector field on the right hand side of Eqn. 1.1.1 changes value every time $\sigma(t)$ changes value and, hence, the vector field “switches” amongst one of a finite number N of vector fields.

Typically, there are several additional mathematical assumptions that are imposed in order to for Eqn. 1.1.1 to make sense. For instance, one often assumes Lipschitz continuity of the vector fields along with assumptions to guarantee that $\sigma(t)$ does not switch infinitely fast [6]. We will assume throughout all parts of this thesis that all switching systems are mathematically well-posed.

While the switching signal $\sigma(t)$ can be viewed as an arbitrary input to the system of Eqn. 1.1.1, in many engineering design problems, $\sigma(t)$ is the output of a *feedback law*

$$\sigma(t^+) = \phi(x(t), v(t), \sigma(t)) \quad (1.1.2)$$

where ϕ is a function of the continuous state x , the exogenous input v , and the current value of σ . A typical design problem involving switching systems is to find some switching scheme (modelled by the function ϕ in Eqn. 1.1.2) such that $x(t)$ which solves Eqn. 1.1.1 satisfies some form of stability (e.g., asymptotic, input-to-state) and also meets a certain performance objective. In order to make the abstract notions discussed here more concrete, we will now investigate two common examples of switching systems found in engineering design.

1.1.1 Example: Temperature Control

Perhaps one of the simplest examples of a switching system—an example with which anyone who lives in the Northeast United States during the winter months will be familiar!—is the problem of controlling the temperature of a room via a thermostat. The operation of a thermostat is well-understood by most everyone; the thermostat is set to a particular “nominal” temperature around which we would like the temperature of the room to vary only slightly. When the temperature of the room drops some fraction below the nominal temperature, the thermostat turns on a furnace to heat the room. When the temperature of the room then rises some fraction *above* the nominal temperature, the thermostat turns the heat off, and the cycle repeats indefinitely.

To model this problem mathematically, we first turn to a mathematical model of the thermostat, which, in its simplest form, can be modelled as a *relay with hysteresis*. The transfer characteristic of a relay with hysteresis is depicted in Fig. 1.1.1 which can be described mathematically by the model below where $u(t) = \text{rel}(y(t))$:

$$u(t) = \text{rel}(y(t)) = \begin{cases} 0 & y(t) > 1, \text{ or } 0 \leq y(t) \leq 1, \ u(t^-) = 0 \\ 1 & y(t) < 0, \text{ or } 0 \leq y(t) \leq 1, \ u(t^-) = 1 \end{cases}.$$

Note that the output $u(t)$ of the relay is only a uniquely defined function of the input when either $y(t) < 0$ or $y(t) > 1$. When $0 \leq y(t) \leq 1$, the output of the relay depends on both $y(t)$ *and* the value of u just prior to the current time, $u(t^-)$; if the previous value of $u(t)$ was 0, then the output of the relay remains 0, while if the previous value was 1, then the output remains at 1. In terms of a temperature control system, this behavior models the fact that if we just turned the heat on, we wish to keep the heat on until the temperature rises above a threshold *different* from the threshold that was used to turn the heat on in the first place.

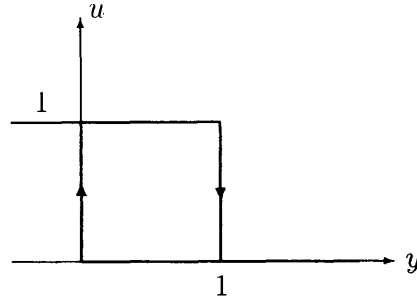


Figure 1.1.1: Transfer characteristic of a relay with hysteresis.

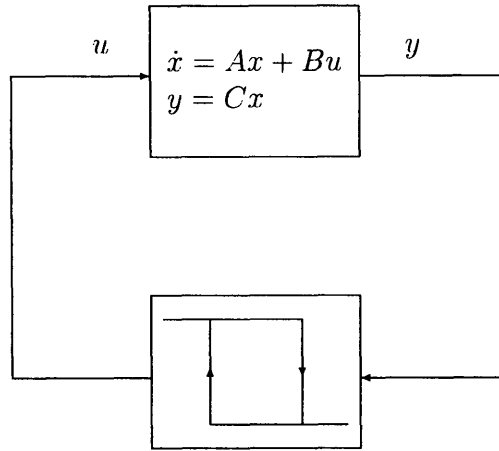


Figure 1.1.2: Model of temperature control problem. The relay represents a thermostat, while the linear dynamical system represents the temperature dynamics of the room.

The simplest possible model for the dynamics of the room whose temperature we are trying to control is given by a linear model

$$\begin{aligned}\dot{x} &= Ax + Bu \\ y &= Cx.\end{aligned}$$

In the above, u represents the control input (whether the heater is turned on or off) and y represents the temperature measured by the thermostat, and the overall temperature control process can be modelled by the closed-loop interconnection of Fig. 1.1.2. More accurate models may take into account the presence of noise disturbances at the input to the sensor by the addition of exogenous input to the relay in Fig. 1.1.2, but we will assume here, for simplicity, that any such noise disturbances are negligible.

In terms of the framework we presented at the beginning of the chapter, the system

of Fig. 1.1.2 switches between two vector fields

$$\begin{aligned} f_1 &= Ax + B \\ f_2 &= Ax \end{aligned}$$

which correspond to the cases $u = 1$ (thermostat on) and $u = 0$ (thermostat off), respectively. Note in this particular example that $u(t)$ is not only an analog input to the temperature dynamics of the room, but $u(t)$ can, also, be viewed as the switching signal $\sigma(t)$ since it is discrete-valued, and the choice of vector field f_1 or f_2 is directly related to the value of $u(t)$. In fact, the relay characteristic $\text{rel}(\cdot)$ can be viewed as the function $\phi(\cdot)$ of Eqn. 1.1.2 since $\text{rel}(y(t)) = \text{rel}(Cx(t))$.

The notion of “stability” that one associates with the regulation of room temperature is not generally the typical notion of asymptotic stability but is rather stability of a *limit cycle*. Roughly speaking, a limit cycle is an periodic solution to a first order ODE $\dot{x} = f(x)$ subject to initial conditions $x(0) = x_0$ lying in a given set (namely, the set of points which lie on the limit cycle). A limit cycle is thought of as *stable* if trajectories with initial conditions which are close to (but do not lie on) the limit cycle eventually converge to the limit cycle. A limit cycle is said to be *globally stable* if trajectories with any initial condition in the state space converge to the limit cycle. To show, then, that a thermostat “works” for the temperature dynamics of a given room, the corresponding mathematical problem is to show existence of a stable limit cycle for the closed-loop interconnection of Fig. 1.1.2. See [14] and the references therein for a more rigorous treatment of limit cycles, as well as some of the existing techniques for establishing stability of limit cycles.

1.1.2 Example: Switched LTI Controllers

In the previous example, switching was introduced into the control problem due to the behavior of the physical devices/machinery being used in the problem (a typical gas or oil furnace does not have multiple temperature settings and can only be turned on or off). By contrast, the example we will investigate here is one in which switching is not a fundamental physical constraint but is a construct which is introduced to increase performance. A block diagram for the form of the system that we consider is shown in Fig. 1.1.3. In this block diagram, we have a continuous-time LTI plant $P(s)$ that we wish to control. We are given a bank of controllers $K_i(s)$, $i = 1, 2, \dots, N$ each of which is individually a stabilizing controller for the plant (i.e., the roots of the equation $1 - P(s)K_i(s) = 0$ all lie in the open left half-plane for $i = 1, 2, \dots, N$). The job of the block denoted “Supervisor” is to choose, at every time t , the output of one of the controller blocks $K_i(s)$ as the input to the plant u . It should be noted that, in general, exogenous inputs are typically present for systems with the basic structure depicted in Fig. 1.1.3 but are omitted for simplicity of the diagram. Now, because each of the individual LTI controllers $K_i(s)$ is individually stabilizing, one should naturally infer that switching is added in this scenario to increase performance in some sense.

Again, to relate this problem to the notion of switching systems that we presented

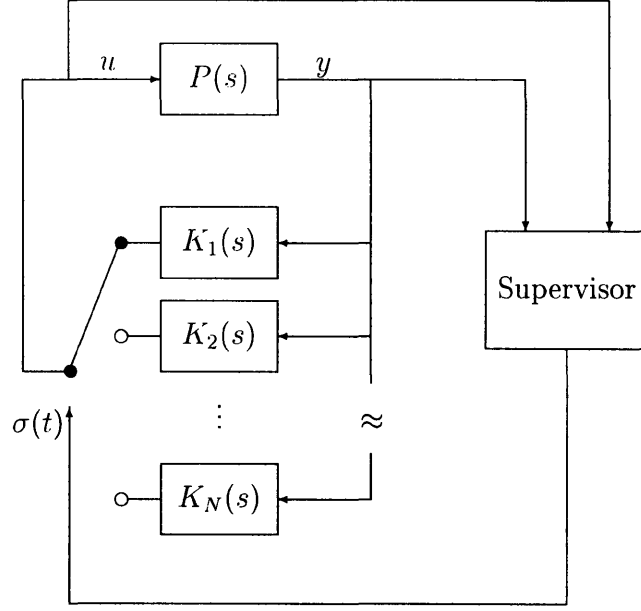


Figure 1.1.3: Block diagram for control architecture that switches between multiple LTI controllers.

at the beginning of this section, we see that the switching signal in this case is given by the output of the supervisor. The vector fields, in this case, are linear vector fields $A_i x$, $i = 1, 2, \dots, N$ where each A_i represents the closed loop dynamics of the interconnection of the plant $P(s)$ with the i -th controller $K_i(s)$.

The structure in Fig. 1.1.3 is very closely related to the work in [18, 38]. In this work, the authors investigate the use of logic-based switching to switch between stabilizing controllers as a way to increase performance¹. The specific technical issue that is addressed is that of finding a controller realization such that the switched system is stable under arbitrary switching (i.e., the switched system is asymptotically stable for *any* switching signal $\sigma(t)$ and, correspondingly, any feedback policy implemented by the supervisor in Fig. 1.1.3). The technique is illustrated on an example involving the dynamics of an aircraft. In the example, two stabilizing LTI controllers are known, one with fast response time and low noise rejection, and one which has slower response time and higher noise rejection. Switching is, hence, introduced to decrease the trade-off between the response time and noise rejection. The example focuses on the design of the controller realization rather than on the specific algorithm that the supervisor implements to decide when to use one controller over the other; however, it is pointed out in the paper that one can use “simple-minded” algorithms to switch between controllers such as estimating the high-frequency noise component and using the “fast” controller only when this estimate is low.

¹While similar, the structure shown in Fig. 1.1.3 is not exactly the structure studied in [18, 38] as the structure in Fig. 1.1.3 also requires that the individual controllers $K_i(s)$ be *stable* in addition to stabilizing. See [18] for a complete discussion.

1.2 Problem Motivation

Both of the examples that we have studied thus far have an element in common in that they both essentially use simple-minded switching algorithms that can be “guessed” a priori. We do not intend to down-play the utility of such algorithms as, often-times, real-world design constraints do lead to simple design algorithms for two key reasons. The first is that the technologies being used have fundamental limitations that restrict the types of algorithms that can actually be implemented. The second is that there may not exist systems-level tools/frameworks for which a given design problem can be posed. The first restriction is not something that can be controlled at a systems level and is something that we cannot change as control engineers (though, thankfully, other branches of engineering such as micro- and nanofabrication research does attempt to push the boundaries to keep increasing performance of physical devices). On the other hand, the second issue—lack of analysis and design tools—is something that we *can* change.

If we examine the design procedure of the second example more closely, we see that it can be broken up into two main steps. In the first step, a set of LTI controllers, each of which individually stabilizes the plant $P(s)$, are constructed using existing tools for the design of LTI controllers for LTI plants. For instance, in the example in [18], the two controllers were determined by solving separate H_2 optimization problems for different cost functions (to reflect different closed-loop system bandwidths). Hence, with respect to the larger issue of designing a switching architecture to increase performance, the continuous-time controllers were essentially *fixed*, and the problem of designing a switching controller reduced to the problem of switching between two fixed, stable closed-loop systems. While such sequential design algorithms can lead to increases in performance, they do not necessarily allow the designer to take full advantage of the switching architecture being considered. For instance, the above set-up does not permit any of the vector fields between which switching takes place to be unstable. While it may not be obvious, as we will see here, switching between unstable subsystems in a stable way can actually lead to performance benefits.

A natural question to ask, then, is the following: can one construct a systematic method of designing both a switching law and a set of controllers *simultaneously*? To do so could not only allow a designer to remove some of the restrictions imposed by a sequential design process, but could also provide additional insight into the capabilities of switching that may have yet to be seen. Moreover, as a very long-term research goal, one could imagine the creation of design engines, much like the design engines for H_2 and H_∞ control for LTI systems, that take as input a plant model and synthesize a set of continuous-time controllers as well as a corresponding switching algorithm that achieve a certain closed-loop performance objective. To answer this last question in any sort of generality is potentially the combined effort of several years of work by multiple researchers. Indeed, algorithms for the design of LTI controllers for LTI plants—which are arguably among the simplest classes of control problems that can be studied—did not develop overnight, and, thus, it would be unreasonable to expect general design algorithms can be synthesized in a single document such as this. Nevertheless, any long journey must begin with a single step, and it is the goal

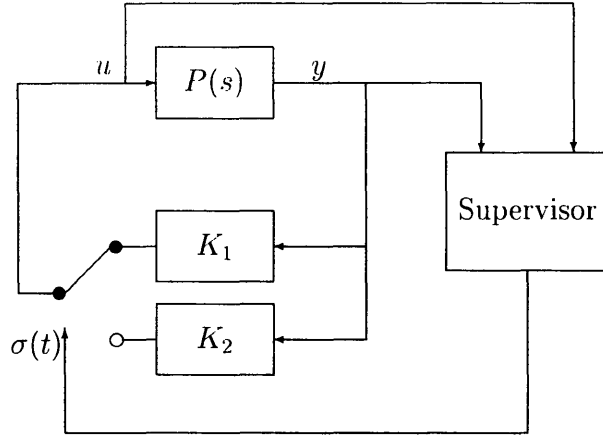


Figure 1.2.4: Switching architecture under investigation in this document.

of this document to provide a step toward the above general direction. So, then, what specific direction will we take here?

The high-level question that this document tries to answer is this: in the context of the system depicted in Fig. 1.1.3, is there some class of LTI plants for which we can establish a design algorithm which takes in a plant $P(s)$ and outputs two objects:

- A set of LTI controllers.
- A supervisor that implements a switching algorithm.

In particular, the switching algorithm should not provide just a certificate(s) of stability for the overall switched system, but it should also be designed with some sort of performance measure in mind (e.g., minimum settling time in a tracking problem for a class of exogenous inputs). The specific structure that we will investigate is a simplified variant of the switching architecture of Fig. 1.1.3 and is shown in Fig. 1.2.4. In this architecture, we primarily consider those LTI plants which are strictly proper, single-input single-output, and second order, i.e. LTI systems of the form

$$\begin{aligned}\dot{x} &= Ax + Bu \\ y &= Cx\end{aligned}$$

where $A \in \mathbf{R}^{2 \times 2}$, $B \in \mathbf{R}^{2 \times 1}$, and $C \in \mathbf{R}^{1 \times 2}$. Furthermore, we consider the case where we switch between two *proportional gain* controllers, i.e., two LTI controllers which implement the control laws $u = K_1 y$ and $u = K_2 y$ with $K_1, K_2 \in \mathbf{R}$. The supervisor is a nonlinear dynamical system which takes as input the plant input u and output y and has structure that is shown in Fig. 1.2.5. The input u and output y of the plant are fed into a first order linear observer to produce an estimate of the plant state, denoted by the outputs \hat{x}_1 and \hat{x}_2 . These state estimates are then input to a memoryless nonlinear switching law which decides at each time t whether to choose gain K_1 or gain K_2 as the feedback gain from the output y to the input u .

Several comments are in order. It is true that one of the major motivations for picking such a simple class of systems to examine is due to the fact that they are

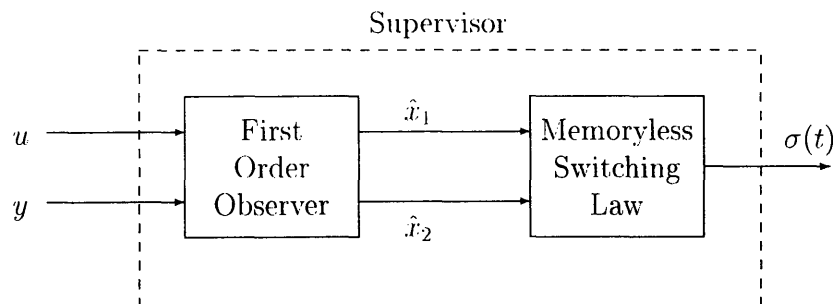


Figure 1.2.5: Structure of supervisor in Fig. 1.2.4.

mathematically simple to analyze. Indeed, many of the initial tools we will use to analyze this class of systems involve phase portrait techniques; tools adapted from sliding mode control, Poincaré maps, etc., will be useful in proving many of the formal statements we will show in this document. One of the major goals of this work is simply to gain some insight into the problem-at-large so as to ascertain future research paths for more complex systems. It should be noted, however, that, while the structure of Fig. 1.2.4 may *appear* extremely simple, the problem is not a trivial one. For instance, even the simplest problem of achieving asymptotic stability by orchestrating a switching algorithm between two proportional gains is not a simple result. Because many second order LTI systems cannot be made stable by a single proportional gain output feedback interconnection, the problem of stabilizing by switching between two proportional gains involves the development of switching algorithms that switch between unstable subsystems in a stable manner. In fact, it turns out that the algorithms we develop here work well *because* they switch between subsystems that are not both stable. The topic of achieving asymptotic stability by means of hybrid output feedback in- and of itself has been a problem which has received a fair amount of attention in the recent literature [3, 26, 31, 32, 68, 69].

While our primary focus will study design algorithms for second order LTI systems, we will, in the end, be able to extend our design algorithms to a larger class of plants which can be well-modelled by a second order LTI plant. The major tool which we will use in performing this extension will be the celebrated *Small Gain Theorem* [52, 67] which will, subsequently, allow us to perform designs for a larger class of systems—including higher order, nonlinear, and time-varying plants—which have a “good” second order LTI model in a sense to be defined.

In addition to mathematical motivations, the switching architecture of Fig. 1.2.4 can also be viewed as attractive due to the relative simplicity of the analog control, namely control via proportional gains. To return briefly to the issue of real-world constraints in the implementation of control laws, the structure of Fig. 1.2.4 is particularly of interest from an applied standpoint when the analog action (i.e., the portion of the structure in Fig. 1.1.3 that relates the control output u to the plant output y) is constrained. As an example from the electronics industry, the design of operational amplifier (“op amp”) circuits typically involves the design of feedback compensators which are passive and first order [15, 22, 59, 62]. Moreover, most of the models used

in op amp design even today are second order LTI models. One may, then, wonder as to whether the switching architecture of Fig. 1.2.4 (which, essentially, can be viewed as a first order nonlinear controller) can be used in place of existing op amp compensator designs to improve performance in some sense. In fact, this particular question actually motivated one of the last pieces of work we investigate in this document, namely a comparison of our switching architecture with different forms of LTI control. Clearly, there are implementation-level issues that arise when one considers such practical problems, but we will not dwell on those here; the work in this document is viewed strictly from a systems-level perspective. We will return to this issue of designing switching controllers for op amp circuits in the conclusion as one of the potential paths for future work.

As a last aside before we begin to discuss the intended areas of investigation, we would like to point out two “generalities” of the setup in Fig. 1.2.4. First, we note that the assumption that the plant be strictly proper is not essential. Indeed, if we consider a plant with output $y' = Cx + Du$ where $D \neq 0$, then applying a standard feedforward cancellation $y = y' - Du$ will transform any problem involving a proper (but not strictly proper) plant into a problem involving a strictly proper plant. Second, while it may seem restrictive to switch only between two proportional gains rather than to allow the number of switching gains to be potentially larger, we will actually show as one of our first results that, when a second order plant can be stabilized by switching between multiple gains, it can be stabilized by switching between only *two* gains in a prescribed manner.²

1.3 Problem Investigation: Controller Synthesis and Performance Comparison

For a given second order plant, our goal is to be able to design a controller of the form indicated in Fig. 1.1.3 and 1.2.5 that achieves “good” performance. We will first discuss the measures of performance we will consider in this work and will then proceed to describe the manner in which we approach the problem of controller design.

1.3.1 Performance Measures

We will consider multiple performance objectives throughout this work. In the beginning of our studies, we will consider a setup in which no additional exogenous inputs are present³, and we will consider an asymptotic stabilizability problem where we measure performance in terms of rate of convergence of the state trajectories to the origin. In setting up an optimal control problem to maximize this rate of convergence

²The actual result we prove is slightly more general than this since we actually consider the case of switching between a *continuum* of gains rather than just a discrete set.

³While Fig. 1.2.4 does not indicate the presence of exogenous inputs, we will consider the more general case where inputs (both command inputs and disturbance/noise inputs) are present. We defer a discussion of the manner in which these inputs enter the system dynamics until Chapter 4.

we will, in essence, develop one of the key components that leads to a general design algorithm for synthesizing switching controllers of the form being studied here.

One of the main goals of this work is to investigate whether the switching architecture we consider here has the potential to outperform existing controller architectures that we already know how to design. On a high level, this is equivalent to investigating whether the introduction of switching into systems-level design can, in fact, increase performance. To this end, a large part of the work toward the end of this document is dedicated to a particular study in which we design a switching controller like the one depicted in Fig. 1.2.4 and 1.2.5 to track a step input. Here, we will measure performance in terms of settling time and overshoot, and we will compare the performance of the switching controller to that of two other LTI controller architectures to illustrate some of the benefits of using this particular switching architecture.

1.3.2 Design Algorithm

In developing an algorithm for synthesizing switching controllers in our framework, we will break down the design process into two separate parts:

- Solving a “full-state” problem in which we find proportional gains $K_1, K_2 \in \mathbf{R}$, and a memoryless switching law $v(x_1, x_2) : \mathbf{R}^2 \rightarrow \{1, 2\}$ which takes as input the state of the plant $P(s)$ (denoted by $x = [x_1, x_2]'$) and outputs a stabilizing switching signal $\sigma(t)$.
- Design of an appropriate observer that takes the plant input u and output y as inputs and produces an estimate $\hat{x} = [\hat{x}_1 \ \hat{x}_2]'$ of the plant state x .

The two steps described above are similar to the steps taken in the standard pole placement problem from linear systems theory [46]; we first consider a simpler problem where the controller architecture (or, in this case, *part* of the controller architecture) has full access to the state of the plant. We then consider the harder problem where the controller does *not* have full state information, and we design an appropriate observer to obtain a good estimate of the true plant state, where “good” in this context refers to an estimate which converges exponentially to the true state when no disturbance inputs are present. The output of the observer is fed into the memoryless switching law designed for full state access (as shown in Fig. 1.2.5), and the control design is complete.

In order for any control algorithm to be useful, it must yield a closed-loop interconnection that is stable—but stable in what sense? The major theoretical contribution that we provide in this work is that the controllers that we design via the process above yield closed loop systems that are *finite L_2 gain stable*. Roughly speaking, this result states that if exogenous signals of finite power are input the closed loop system described by Fig. 1.2.4 and 1.2.5, the power of any corresponding outputs (viewed as linear combinations of the system state and exogenous inputs) is also finite. Moreover, the process of determining an upper bound on the L_2 gain is a tractable problem which can be computed numerically in MATLAB by searching for a piecewise quadratic storage function. This particular computational component will

be relevant when we perform a comparison between the switching controller here to LTI controller architectures as the L_2 gain will be used as a means of measuring noise sensitivity for the different architectures. It will also be useful when we consider a design example for a system which is *not* a second order LTI system as computation of an appropriate L_2 gain will provide us with guaranteed performance bounds.

The process of developing observer-based controllers which are finite L_2 gain stabilizing is an incremental one. The process we used to develop such algorithms is shown in the flow chart of Fig. 1.3.6. We first start by considering one of the most basic question we can ask about the switching architecture, namely the development of necessary and sufficient conditions on the second order plant $P(s)$ which will guarantee existence of a switching controller which asymptotically stabilizes the closed loop interconnection. We assume for this problem, and for the first few problems that we will consider, that the memoryless switching law $v(\cdot)$ indicated above has access to the *true* state of the plant x rather than an observer estimate. In this part, we will also develop an explicit switching law that can be used to achieve asymptotic stability for plants which satisfy the necessary and sufficient conditions we develop.

We will, next, proceed to consider the development of switching laws which optimize the rate of convergence of the state trajectories to the origin. The controllers that we develop here will serve as the basis for the controllers we will use in later design examples when we consider performance comparisons, and a method of explicitly designing optimal “full-state” controllers will be outlined.

We will then proceed to the problem of finite L_2 gain stability. We will first show that the controllers developed to maximize the rate of convergence to the origin are, also, finite L_2 gain stabilizing, again when the switching law has full access to (a possibly noise-corrupted version of) the true state. Once we have proved this, we will then show how to design an appropriate observer such that L_2 gain stability is preserved when the optimal switching laws receive estimates of the state rather than the true state. We will also discuss how to formulate the problem of determining the upper bounds on the L_2 gain for a particular closed-loop interconnection as a semi-definite program.

Once all of the design tools have been synthesized, we will then be able to consider the design of a switching controller for the step tracking problem mentioned in the previous section. We will show explicitly through examples how to design a controller which asymptotically tracks a step input and will compare its performance to two different forms of LTI control, one in which the LTI control is low order, and one in which the order of the LTI controller is unconstrained. Also, by making use of our L_2 gain tools, we will be able to investigate design of switching controllers which stabilize systems other than second order LTI systems, and a specific design example will be considered in the last chapter of this work.

1.4 Related Work

The history of switching systems finds many of its original roots in the study of relay control. The work by Tsypkin in the 1950s [65] is one of the classical texts on this

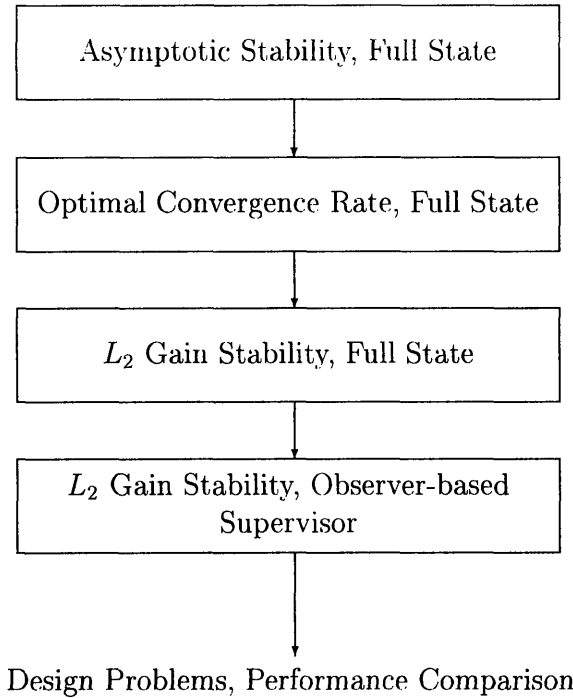


Figure 1.3.6: Flow chart which indicates the individual steps in developing the design algorithm for controller synthesis.

subject. The first chapter is devoted to a myriad of engineering examples involving the use of relays, and the remainder of the book develops a number of techniques for assessing the stability and limit cycle behavior of systems involving relays. This was later followed by the work of Flügge-Lotz [11] who developed additional frequency and phase plane techniques, and who showed that certain classes of optimal control problems lead to discontinuous (e.g., “bang-bang”) control laws. The work of Åström et. al. on PID Controllers [64] utilizes relays as a method of creating steady-state oscillations to estimate system parameters in adaptive control problems, and several books have been published on the related area of sliding mode control (e.g., [49]).

In the 1980s, a large amount of work was performed for developing *periodic output feedback* controllers to stabilize linear systems. The discrete-time case was considered by several sources such as [2, 16, 24] where it was discovered that, under certain mild conditions, LTI systems could be stabilized by using periodic output feedback that switches between n gains where n is the order of the system. Kabamba investigated the continuous-time case [23] using continuous-time waveforms rather than a discrete set of gains, though it can be shown that, for mild assumptions on the sampling interval, a continuous-time system can also be stabilized via periodic output feedback by switching between n gains and employing a sampled-data controller. The work has some positive results for robustness with respect to *linear* perturbations. For example, Kabamba in [23] develops a robustness condition for stable LTI perturbations that do not change the number of unstable modes in the original model. In [47], Khargonekar et. al. examine a robust design problem for a compact class of discrete-time LTI

plants using periodic compensation. To the knowledge of the author, however, no results have been developed using induced system norms (L_2 gain or otherwise) to provide robustness analysis tools for these systems that can be used to treat nonlinear uncertainty. Some recent work by Yanesi et. al. in [70] investigates the problem of designing periodic feedback controllers to minimize a quadratic cost functional of the state and input.

In the 1990s, much work was performed to study *piecewise linear systems* (see, for instance, [57]). Branicky developed *multiple Lyapunov functions* [6, 7] which can be applied to certain classes of piecewise linear systems, and Johansson et. al. developed associated computational tools in [21]. Additional computational tools were developed by Kulkarni et. al. for time-delay hybrid systems in [50]. Gonçalves et. al. developed a method of examining the stability of equilibrium points and limit cycles using the notion of *quadratic surface Lyapunov functions* for a wide array of piecewise linear systems including relay feedback systems, on/off systems, and saturation systems [12, 13, 14, 35, 36]. The majority of the work performed in both of these areas is primarily for the case when no exogenous inputs are present, though Gonçalves does have results for an optimal design problem to minimize the L_2 gain in which the presence of the exogenous input does not affect the switching signal [14]. In addition, some work by Hespanha [20] and Zhai et. al. [33, 34] consider the problem of establishing finite L_2 gain for systems that switch between Hurwitz/Schur stable matrices. Some recent work by Zhao et. al. [71] investigates the design of state-dependent switching laws which establish finite L_2 gain interconnections even when the switching matrices are not strictly stable, and an example is provided that switches between marginally stable matrices to achieve L_2 gain stability.

Several other general results on switching systems exist in the literature today. Liberzon [28] summarizes many of the current results on stability and design of switching systems. A more concise version of the basic problems that exist in stability and design of switched systems can be found in [27]. [45] considers the problem of input-to-state stability of switched systems via supervisory control using a notion of bounded state rather than L_2 gain. [8] considers stability of stochastic switched systems using multiple Lyapunov functions. [29] examines Lie algebraic conditions for stability when switching between two globally asymptotically stable vector fields.

The work of Hespanha in [19] provides a framework for studying logic based switching control. [17] considers an extension of LaSalle's Invariance Principle to switched linear systems. [39] considers switching algorithms for uncertain systems with hysteresis involved in the switching law, and [37] considers logic-based switching for nonholonomic systems. In [10], the authors consider a hybrid control strategy that switches between a time-optimal controller and PID controller to achieve stability and increase performance.

1.5 Document Outline

The remainder of the document follows the structure of the flow chart depicted in Fig. 1.3.6. Chapter two examines necessary and sufficient conditions for asymptotic

stabilizability of a second order LTI plant assuming that the supervisor has full access to the state. Chapter 3 considers the problem of designing controllers to maximize the rate of convergence. The fourth chapter examines the problem of finite L_2 gain, first for a full state problem. It then discusses how to design an appropriate first order observer, proves finite L_2 gain stability with an observer in place, and then briefly discusses a method of computing upper bounds on the L_2 gain. Chapter 5 considers the problem of designing switching controllers to asymptotically track a step input for a certain class of LTI plants and performs the aforementioned comparisons to two different forms of LTI control. Chapter 6 explores a design example for a fourth order LTI system using Small Gain techniques. We will conclude in Chapter 7 with some directions for future work. Many of the results presented here already exist in the literature (either in final or preliminary form) [40, 41, 42, 43].

The reader is assumed to be familiar with certain basic concepts in mathematics, signals and systems, and control design. A thorough view of signals and systems theory can be found in either [63] or [56]. A review of basic classical control techniques can be found in [44], and a review of modern robust control can be found in [67]. A review of analysis can be found in either [60] or [30], and [1] and [9] are excellent references for a review of a review of measure theory, Fourier theory, and Hilbert spaces.

Chapter 2

Preliminary Results: Necessary and Sufficient Conditions for Stabilizability

In this chapter, we derive necessary and sufficient conditions on a second order LTI plant that guarantee stabilizability via the switching architecture presented in the last chapter when the supervisor has full access to the state of the plant. Specifically, we consider the problem of stabilizing a second order SISO LTI system of the form $\dot{x} = Ax + Bu, y = Cx$ with feedback of the form $u(x) = v(x)Cx$, where $v(x)$ is real-valued and has domain which is all of \mathbf{R}^2 . We will show that, when stabilization is possible, $v(x)$ can be chosen to take on no more than two values throughout the entire state space (i.e., $v(x) \in \{v_1, v_2\}$ for all x and for some v_1, v_2), and an algorithm for finding a specific choice of $v(x)$ will be presented. It will also be shown that the classical root locus of the corresponding transfer function $C(sI - A)^{-1}B$ has a strong connection to this stabilization problem, and its utility will be demonstrated through multiple examples.

2.1 Introduction

Stabilization of continuous time systems via hybrid feedback (in which a controller which possesses both continuous and discrete dynamics is employed) is a problem that has received much attention in the recent literature. Artstein first raised this question via examples [3]. Litsyn et. al. show in [32] that the linear system

$$\dot{x} = Ax + Bu, \quad y = Cx \tag{2.1.1}$$

with (A, B) reachable and (C, A) observable can be stabilized via a hybrid feedback controller which uses a countable number of discrete states (and no continuous states) and which only depends upon the output y as opposed to the entire continuous state x . A natural question arises as to whether a hybrid feedback controller can be designed which uses a *finite* number of states instead. For the most part, the answer to this

question is still open, though a partial answer has been given by Hu et. al. in [31] based upon the so-called conic switching laws of [69] and [68]. In [31], it is shown that, for a certain class of single-input, single-output (SISO) second order systems which are reachable and observable, there exists a feedback control law of the form $u(x) = v(x)Cx$ where

$$v(x) = \begin{cases} v_1, & \text{if } x_1x_2 \geq 0 \\ v_2, & \text{if } x_1x_2 < 0 \end{cases} \quad (2.1.2)$$

with $x = [x_1 \ x_2]'$ such that the resulting closed-loop system

$$\dot{x} = Ax + v(x)BCx \quad (2.1.3)$$

is globally exponentially stable. A control law of the form Eqn. 2.1.2 is desirable as it can be implemented as a switch between two static gains which multiplies the output $y = Cx$. Note that, in general, the above strategy does not always work as the result of [32] sometimes requires a more complicated hybrid feedback structure to achieve stability, even when the system described by Eqn. 2.1.1 is reachable and observable.

Example 2.1.1 Consider Eqn. 2.1.1 with

$$A = \begin{bmatrix} 2 & -1 \\ -1 & 2 \end{bmatrix}, B = \begin{bmatrix} 0 \\ 1 \end{bmatrix}, C = [0 \ 1].$$

The system is reachable and observable, but Eqn. 2.1.3 is not stable for *any* real-valued choice of $v(x) \equiv v(x_1, x_2)$ whose domain is all of \mathbf{R}^2 , not just $v(x_1, x_2)$ of the form Eqn. 2.1.2.¹ To see this, first note that the region $x_1 < 0, x_2 > 0$ is invariant under the flow of Eqn. 2.1.3 for any choice of $v(x_1, x_2)$. Indeed, when $x_1 = 0, \dot{x}_1 = -x_2 < 0$, and when $x_2 = 0, \dot{x}_2 = -x_1 > 0$ for all choices of $v(x)$. Moreover, when $x_1(0) < 0$ and $x_2(0) > 0, \dot{x}_1 = 2x_1 - x_2 < 0$, which means that $x_1(t)$ is strictly decreasing, and, hence, does not decay to zero regardless of the choice of $v(x_1, x_2)$. \square

The goal of this chapter is to answer the following questions: under what conditions on $A \in \mathbf{R}^{2 \times 2}, B \in \mathbf{R}^{2 \times 1}$ and $C \in \mathbf{R}^{1 \times 2}$ can the closed-loop system Eqn. 2.1.3 be made asymptotically stable for some choice of $v(x_1, x_2)$? And, moreover, when stability is achievable, how may one design $v(x_1, x_2)$ explicitly? As it turns out, the answer to the first question has a strong connection to the classical control notion of root locus. Essentially, if one considers control laws of the form $v(x_1, x_2) = k$ for some constant k where k varies continuously over \mathbf{R} , then the system Eqn. 2.1.3 is stabilizable in only one of two situations:

- There exists a value of k such that the matrix $A + kBC$ is Hurwitz and, hence, Eqn. 2.1.3 is exponentially stabilizable via static output feedback.
- There is no value of k for which $A + kBC$ is Hurwitz, but there does exist a value of k for which the eigenvalues of $A + kBC$ are complex. In this case,

¹We will implicitly make this assumption on the domain of $v(x)$ throughout the paper. Note that this eliminates choices of $v(x)$ which blow up for some value(s) of x , such as $v(x)$ which attempt to divide by the output $y = Cx$.

$v(x_1, x_2)$ can be chosen to take on only two values v_1 and v_2 throughout the entire state-space, i.e., $v(x_1, x_2) \in \{v_1, v_2\}$, where v_1 and v_2 are appropriately selected real constants, and global exponential stability can be achieved.

A third situation can exist in which there exists no value of k for which $A + kBC$ is Hurwitz and the eigenvalues of $A + kBC$ are real for all k . It is precisely these situations for which no choice of $v(x_1, x_2)$ will yield asymptotic stability.

The structure of this chapter is as follows. First, we examine two particular case studies in which the form of the B and C vectors have special structure and analyze the conditions on the matrix A which will guarantee stability. Also, we will derive explicit forms for $v(x_1, x_2)$ which can be used to achieve stability when it is possible to do so. Next, we will show that, through appropriate coordinate transformations, all nontrivial² problems can be transformed into either one of these two case studies and then will use this to establish the main result. Finally, we explore a general method of designing such controllers (when they exist) and provide several examples to illustrate the methodology.

2.2 Case Studies

In this section, we explore two specific case studies in which the A , B and C matrices of Eqn. 2.1.1 have particular structures. Using appropriate coordinate transformations, we will then relate the results of this section to derive the main result for general A , B , and C .

2.2.1 Case 1

We first assume a system of the following structure:

$$A = \begin{bmatrix} a & b \\ c & 0 \end{bmatrix}, B = \begin{bmatrix} 0 \\ 1 \end{bmatrix}, C = [0 \quad 1], \quad (2.2.4)$$

where $a, c \in \mathbf{R}$, and $b \geq 0$. Here, Eqn. 2.1.3 takes the form

$$\begin{bmatrix} \dot{x}_1 \\ \dot{x}_2 \end{bmatrix} = \begin{bmatrix} a & b \\ c & v(x_1, x_2) \end{bmatrix} \begin{bmatrix} x_1 \\ x_2 \end{bmatrix} \quad (2.2.5)$$

We summarize the possibilities for stabilizability as a function of the parameters a , b , and c in the proposition below:

Proposition 2.2.1 *For the system Eqn. 2.2.5:*

1. *If $bc = 0$, then Eqn. 2.2.5 is exponentially stabilizable via static output feedback if $a < 0$ and is not stabilizable for any choice of $v(x_1, x_2)$ otherwise.*

²By “nontrivial”, we refer to problems in which neither B nor C is identically 0.

2. If $b > 0$ and $c > 0$, when $v(x_1, x_2) = k$ for some constant k , then the eigenvalues of Eqn. 2.2.5 are real for all k , and Eqn. 2.2.5 is either exponentially stabilizable via static output feedback or is not stabilizable by any choice of $v(x_1, x_2)$.
3. If $b > 0$ and $c < 0$, when $v(x_1, x_2) = k$ for some constant k , then the eigenvalues of Eqn. 2.2.5 are not real for all k , and Eqn. 2.2.5 is exponentially stabilizable either by static output feedback or by feedback of the form

$$v(x_1, x_2) = \begin{cases} k_1, & \text{if } w_1'x = 0 \\ k_2, & \text{if } w_1'x \neq 0 \end{cases}$$

for some appropriate choice of w_1 , k_1 and k_2 .

We prove each part separately below.

Proof of Part 1

Note that if $b = 0$, the system described by Eqn. 2.2.4 has an uncontrollable mode. In this case, stabilizability is possible if and only if $a < 0$ and can be achieved via $v(x_1, x_2) = k$, where $k < 0$. In a similar vein, if $c = 0$, Eqn. 2.2.4 has an unobservable mode. Noting that any initial condition with $x_2(0) = 0$ satisfies $x_2(t) = 0$ for all t , it is again clear that stabilizability is possible if and only if $a < 0$ and can be achieved by setting $v(x_1, x_2)$ to a negative real constant.

Proof of Part 2

If we set $v(x_1, x_2) = k$ for some constant k , the characteristic polynomial of Eqn. 2.2.5 is given by

$$s^2 - (a + k)s + ak - bc. \quad (2.2.6)$$

First note that both roots of Eqn. 2.2.6 are real for any value of k since the discriminant $(a + k)^2 - 4ak + 4bc = (a - k)^2 + 4bc > 0$ for all k . Now, both eigenvalues of Eqn. 2.2.5 can be placed in the open left half plane if and only if there exists a value of k such that $a + k < 0$ and $ak - bc > 0$. When $a < 0$, there always exists a value of k which satisfies both of these constraints and, hence, Eqn. 2.2.5 is stabilizable via static output feedback.

When $a \geq 0$, there is no value k which can satisfy both inequalities simultaneously when $b > 0$ and $c > 0$. Hence, Eqn. 2.2.5 cannot be stabilized via static output feedback. To show that Eqn. 2.2.5 cannot be stabilized for *any* choice of $v(x_1, x_2)$, first recognize that, when $b > 0$, and $c > 0$, the conic region $x_1 > 0$, $x_2 > 0$ is invariant under the flow of Eqn. 2.2.5 for any choice of $v(x_1, x_2)$. To show this, assume that the statement is not true, and that there exists a trajectory with $x_1(0) > 0$, $x_2(0) > 0$ that leaves the open first quadrant by crossing the axis $x_1 = 0$. At the point of time that the trajectory crosses the x_1 axis, the corresponding value of \dot{x}_1 is given by $bx_2 > 0$ which means that $x_1(t)$ must be *increasing* when it crosses the x_1 axis, an obvious contradiction. Similarly, if there exists some choice of $v(x_1, x_2)$ such that

a trajectory escapes the open first quadrant by crossing the x_2 axis, at the time of crossing, $\dot{x}_2 = cx_1 > 0$.

If $a \geq 0$, $b > 0$, $c > 0$, then Eqn. 2.2.5 is not stabilizable for any choice of $v(x_1, x_2)$ for essentially the same reason as was presented in Example Eqn. 2.1. By virtue of the above, if $x_1(0) > 0, x_2(0) > 0$, then $\dot{x}_1 = ax_1 + bx_2 > 0$, which means that $x_1(t)$ is always increasing for any choice of $v(x_1, x_2)$.

Proof of Part 3

When $c < 0$, the roots of Eqn. 2.2.6 can be made to lie in the open left half plane when $a < 0$. When $a \geq 0$, the roots can also be made to lie in the open left half plane if and only if $a^2 < -bc$. Hence, Eqn. 2.2.5 is not static output feedback stabilizable if $a^2 \geq -bc$, yet, as we now show, there exists a choice of $v(x_1, x_2)$ which yields global exponential stability. Closer examination of the characteristic polynomial Eqn. 2.2.6 with $b > 0$, $c < 0$, and $a^2 \geq -bc$ yields the following two statements:

- The roots of Eqn. 2.2.6 are complex with nonnegative real part whenever $a - 2\sqrt{-bc} < k < a + 2\sqrt{-bc}$.
- There exists a negative real root of Eqn. 2.2.6 whenever $k < -a$.

Since the roots of Eqn. 2.2.6 can be calculated explicitly as

$$s = \frac{a+k}{2} \pm \frac{\sqrt{(a-k)^2 + 4bc}}{2}, \quad (2.2.7)$$

it is clear that the roots are complex whenever the first bulleted item holds. Moreover, the real part of the roots is nonnegative since, due to the fact that $a^2 \geq -bc$,

$$\frac{a+k}{2} > a - \sqrt{-bc} \geq 0.$$

Now, when $k < -a$, the discriminant satisfies

$$(a-k)^2 + 4bc > 4a^2 + 4bc \geq 0,$$

hence, the roots are real. Moreover, because the sum of the roots $(a+k)/2 < 0$, one root must be negative.

Informally speaking, to find a choice of $v(x_1, x_2)$ which asymptotically stabilizes Eqn. 2.2.5, we use the following basic design strategy. The above analysis shows that there exists a value of k_1 which yields a real eigenvalue $\lambda_1 < 0$ and corresponding real eigenvector q_1 . If we set $v(x_1, x_2) = k_1$ along q_1 , then any initial condition which lies along q_1 will decay exponentially with rate λ_1 . For all other values of x_1 and x_2 which do not lie along q_1 , we find a value k_2 for which the eigenvalues are complex. If we set $v(x_1, x_2) = k_2$ everywhere else in the state-space, then any initial condition which does not lie along q_1 will rotate until it eventually “hits” q_1 and will decay exponentially thereafter. This idea is illustrated graphically in Fig. 2.2.1. Here, the

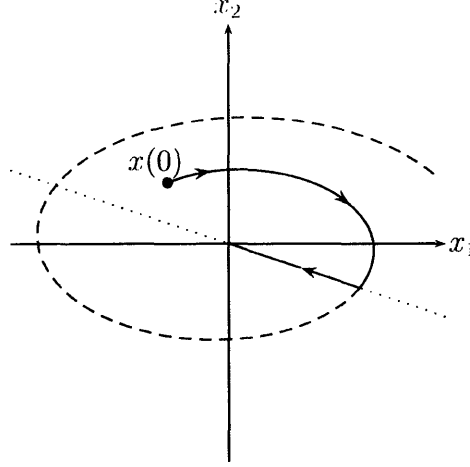


Figure 2.2.1: Illustration of stabilization algorithm for a system which is not static output feedback stabilizable.

dotted line represents the stable eigenvector q_1 when $v(x_1, x_2) = k_1$, the dashed line represents a sample phase portrait with initial condition $x(0)$ when $v(x_1, x_2) = k_2$ throughout the entire state-space, and the solid curve represents the trajectory with initial condition $x(0)$ when $v(x_1, x_2) = k_1$ along q_1 and $v(x_1, x_2) = k_2$ everywhere else in the state-space.

Before we prove this result formally, we need the following lemma:

Lemma 2.2.1 *Consider the linear system $\dot{z} = Az$ where $A \in \mathbf{R}^{2 \times 2}$ has two complex conjugate eigenvalues. Then for any $w \in \mathbf{R}^2$ and any $z(0)$, there exists $t_0 \in \mathbf{R}$ such that $w'z(t_0) = 0$.*

Proof If $w'z(0) = 0$, then the statement immediately follows. Otherwise, without loss of generality, assume that $w'z(0) > 0$. Because the eigenvalues of A are complex, the entries of the corresponding state transition matrix $\exp(At)$ are linear combinations of the terms $\exp(\sigma_0 t) \cos(\omega_0 t)$ and $\exp(\sigma_0 t) \sin(\omega_0 t)$ where $\sigma_0, \omega_0 > 0$. Hence,

$$w'z\left(\frac{\pi}{\omega_0}\right) = -\exp\left(\frac{\sigma_0 \pi}{\omega_0}\right) w'z(0) < 0.$$

By continuity of $z(t)$, it then follows that there exists some time $t_0 < \pi/\omega_0$ such that $w'z(t_0) = 0$. \square

We now formally prove that the above informal description yields an exponentially stable system.

Proposition 2.2.2 *For the system Eqn. 2.2.5 with $b > 0$, $c < 0$, and $a^2 \geq -bc$, suppose that k_1 is chosen such that Eqn. 2.2.5 with $v(x_1, x_2) = k_1$ has a stable eigenvector q_1 with corresponding eigenvalue $\lambda_1 < 0$, and k_2 is chosen such that Eqn. 2.2.5 has two complex eigenvalues. Let w_1 satisfy $w_1'q_1 = 0$ and consider*

$$v(x_1, x_2) = \begin{cases} k_1, & \text{if } w_1'x = 0 \\ k_2, & \text{if } w_1'x \neq 0 \end{cases}.$$

Then Eqn. 2.2.5 is globally exponentially stable for the above choice of $v(x_1, x_2)$ with decay rate λ_1 .

Proof If $x(0) = \alpha q_1$ for some $\alpha \in \mathbf{R}$, then $x(t) = \exp(\lambda_1 t)x(0)$ and the statement holds. Otherwise, $w'_1 x(0) \neq 0$, and, by virtue of Lemma 2.2.1, there exists some value of t_0 such that $w'_1 x(t_0) = 0$. Now, $x(t) = \exp(\lambda_1(t - t_0))x(t_0)$ for all $t > t_0$. \square

2.2.2 Case 2

Now we assume a system of the following structure:

$$A = \begin{bmatrix} a & b \\ 0 & c \end{bmatrix}, B = \begin{bmatrix} 0 \\ 1 \end{bmatrix}, C = [1 \quad 0], \quad (2.2.8)$$

where $a, c \in \mathbf{R}$, and $b \geq 0$. Here, Eqn. 2.1.3 takes the form

$$\begin{bmatrix} \dot{x}_1 \\ \dot{x}_2 \end{bmatrix} = \begin{bmatrix} a & b \\ v(x_1, x_2) & c \end{bmatrix} \begin{bmatrix} x_1 \\ x_2 \end{bmatrix} \quad (2.2.9)$$

We summarize the possibilities for stabilizability as a function of the parameters a, b , and c in the proposition below:

Proposition 2.2.3 *For the system Eqn. 2.2.9:*

1. *If $b = 0$, then Eqn. 2.2.9 is exponentially stabilizable via static output feedback if $a < 0$ and $c < 0$ and is not stabilizable for any choice of $v(x_1, x_2)$ otherwise.*
2. *If $b > 0$, when $v(x_1, x_2) = k$ for some constant k , the eigenvalues of Eqn. 2.2.9 are not real for all k , and Eqn. 2.2.9 is exponentially stabilizable either by static output feedback or by feedback of the form*

$$v(x_1, x_2) = \begin{cases} k_1, & \text{if } w'_1 x = 0 \\ k_2, & \text{if } w'_1 x \neq 0 \end{cases}$$

for some appropriate choice of w_1, k_1 and k_2 .

We prove each part separately below.

Proof of Part 1

If $b = 0$, the system described by Eqn. 2.2.8 is both uncontrollable and unobservable. In this case, Eqn. 2.2.9 is stabilizable if and only if $a < 0$ and $c < 0$. That Eqn. 2.2.9 is unstable if $a \geq 0$ is clear; if $c \geq 0$, then any solution with initial condition $x_1(0) = 0$ satisfies $\dot{x}_2 = cx_2$ and, hence, Eqn. 2.2.9 is unstable for any choice of $v(x_1, x_2)$.

Proof of Part 2

If we set $v(x_1, x_2) = k$ for some constant k , the characteristic polynomial of Eqn. 2.2.9 is

$$s^2 - (a + c)s + ac - bk. \quad (2.2.10)$$

It is clear that if $a + c < 0$, then there always exists a choice of k such that $ac - bk > 0$, and hence Eqn. 2.2.9 can be stabilized via static output feedback. If $a + c \geq 0$, then Eqn. 2.2.9 can be stabilized via a choice of $v(x_1, x_2)$ which takes on two values throughout the entire state space in a manner similar to that of Case 1. A more detailed observation of the roots of Eqn. 2.2.10 when $a + c \geq 0$ reveal the following two facts:

- The roots of Eqn. 2.2.10 are complex with nonnegative real part whenever $k < -(a - c)^2/4b$.
- There exists a negative real root of Eqn. 2.2.10 whenever $k > ac/b$.

Because the roots of Eqn. 2.2.10 can be calculated explicitly as

$$s = \frac{a + c}{2} \pm \frac{\sqrt{(a - c)^2 + 4bk}}{2}, \quad (2.2.11)$$

it is clear that the roots are complex whenever the first bulleted item holds.

Now, if k is chosen such that a negative real root exists, then the inequality $a + c < \sqrt{(a - c)^2 + 4bk}$ must be satisfied. A simple calculation shows that this is equivalent to the second bulleted item.

Using this result, we can derive a stabilization algorithm which is completely analogous to the algorithm of the previous case:

Proposition 2.2.4 *For the system Eqn. 2.2.9 with $b > 0$ and $a + c \geq 0$, suppose that k_1 is chosen such that Eqn. 2.2.9 has a stable eigenvector q_1 with corresponding eigenvalue $\lambda_1 < 0$, and k_2 is chosen such that Eqn. 2.2.9 has two complex eigenvalues. Let w_1 satisfy $w_1'q_1 = 0$, and consider*

$$v(x_1, x_2) = \begin{cases} k_1, & \text{if } w_1'x = 0 \\ k_2, & \text{if } w_1'x \neq 0 \end{cases}.$$

Then Eqn. 2.2.5 is globally exponentially stable for the above choice of $v(x_1, x_2)$ with decay rate λ_1 .

Proof Same as the proof of Proposition 2.2.2. □

Remark While it is easy to get lost in the details of the above two case studies due to the number of subcases used in carrying out analysis, an important feature to note about both cases is that the existence of complex eigenvalues in the root locus of the corresponding linear systems (i.e., $v(x_1, x_2) = k$ for all x_1, x_2) is a sufficient condition for stabilizability when static output feedback cannot stabilize the system (indeed, in

Case 1, this is also a *necessary* condition as well). As we will see in the next section, existence of complex eigenvalues in the root locus is *always* a necessary and sufficient condition whenever Eqn. 2.1.3 is not static output feedback stabilizable.

2.3 Main Result

While the case studies of the prior section may seem constrained due to the very special structure of the A, B , and C matrices, an appropriate change of coordinates reveals that any second order system of the form Eqn. 2.1.1 and can be transformed into either Case 1 or Case 2.

Lemma 2.3.2 *Consider matrices $A \in \mathbf{R}^{2 \times 2}$, $B \in \mathbf{R}^{2 \times 1}$, and $C \in \mathbf{R}^{1 \times 2}$ where neither B nor C is identically 0. For any invertible matrix $T \in \mathbf{R}^{2 \times 2}$, define the triplet $(\tilde{A}, \tilde{B}, \tilde{C})$ as $(T^{-1}AT, T^{-1}B, CT)$, and let*

$$\tilde{A} \equiv \begin{bmatrix} a & b \\ c & d \end{bmatrix}.$$

Then the following statements hold:

1. *If $CB \neq 0$, then $\exists T$ such that*

$$\tilde{B} = \begin{bmatrix} 0 \\ 1 \end{bmatrix}, \tilde{C} = [0 \quad \alpha]$$

with $\alpha \neq 0$ and $b \geq 0$.

2. *If $CB = 0$, then $\exists T$ such that*

$$\tilde{B} = \begin{bmatrix} 0 \\ 1 \end{bmatrix}, \tilde{C} = [\alpha \quad 0]$$

with $\alpha \neq 0$ and $b \geq 0$.

Proof Let $B = [\beta_1 \quad \beta_2]'$, $C = [\gamma_1 \quad \gamma_2]$. To prove the first result, direct computation shows that the matrix

$$T = \begin{bmatrix} \gamma_2 & \beta_1 \\ -\gamma_1 & \beta_2 \end{bmatrix}$$

is invertible since $\det(T) = \gamma_1\beta_1 + \gamma_2\beta_2 = CB \neq 0$. Moreover, $\tilde{B} = [0 \quad 1]'$, $\tilde{C} = [0 \quad \alpha]$ where $\alpha = CB \neq 0$. If $b \geq 0$, then the statement follows. Otherwise, the transformation

$$T_2 = T \begin{bmatrix} -1 & 0 \\ 0 & 1 \end{bmatrix} = \begin{bmatrix} -\gamma_2 & \beta_1 \\ \gamma_1 & \beta_2 \end{bmatrix}$$

will satisfy all of the desired properties.

To prove the second part of the statement, consider the matrix

$$T = \begin{bmatrix} \beta_2 & \beta_1 \\ -\beta_1 & \beta_2 \end{bmatrix}.$$

Then $\det(T) = \beta_1^2 + \beta_2^2 \neq 0$, and, hence, T is invertible. Note that any nonzero C which satisfies $CB = 0$ may be written as $C = [\delta\beta_2 \quad -\delta\beta_1]$, where $\delta \neq 0$. Hence, $\tilde{B} = [0 \quad 1]'$, $\tilde{C} = [\alpha \quad 0]$, where $\alpha = \delta(\beta_1^2 + \beta_2^2) \neq 0$. If $b \geq 0$, then the statement holds. Otherwise, the transformation

$$T_2 = T \begin{bmatrix} -1 & 0 \\ 0 & 1 \end{bmatrix} = \begin{bmatrix} -\beta_2 & \beta_1 \\ \beta_1 & \beta_2 \end{bmatrix}$$

will satisfy all of the desired properties. \square

We are now ready to present the main result of the paper.

Theorem 2.3.1 *Consider the system Eqn. 2.1.1 with $A \in \mathbf{R}^{2 \times 2}$, $B \in \mathbf{R}^{2 \times 1}$, and $C \in \mathbf{R}^{1 \times 2}$ where neither C nor B is identically 0. Define the root locus of this system to be the locus of eigenvalues of Eqn. 2.1.3 when $v(x_1, x_2) = k$ as k varies continuously over \mathbf{R} . Then exactly one of the following statements is true:*

1. *The system is static output feedback stabilizable.*
2. *The system is not static output feedback stabilizable, but it has root locus which takes on complex values for some values of $k \in \mathbf{R}$ and is stabilizable by a control law $v(x_1, x_2)$ which takes on one of two values throughout the entire state space.*
3. *The system has a root locus which is real for all values of $k \in \mathbf{R}$ and is not stabilizable by control of the form Eqn. 2.1.3 for any choice of $v(x_1, x_2)$.*

Proof Using Lemma 2.3.2, whenever C and B are not identically 0, there exists a coordinate transformation where Eqn. 2.1.3 is either of the form

$$\begin{bmatrix} \dot{x}_1 \\ \dot{x}_2 \end{bmatrix} = \begin{bmatrix} a & b \\ c & d + \alpha v(x_1, x_2) \end{bmatrix} \begin{bmatrix} x_1 \\ x_2 \end{bmatrix}$$

or the form

$$\begin{bmatrix} \dot{x}_1 \\ \dot{x}_2 \end{bmatrix} = \begin{bmatrix} a & b \\ c + \alpha v(x_1, x_2) & d \end{bmatrix} \begin{bmatrix} x_1 \\ x_2 \end{bmatrix},$$

with $\alpha \neq 0$ and $b \geq 0$. Since $\alpha \neq 0$, the substitutions $\tilde{u}(x_1, x_2) = d + \alpha v(x_1, x_2)$ and $\tilde{u}(x_1, x_2) = c + \alpha v(x_1, x_2)$ are invertible. Hence, any system of the form Eqn. 2.1.1 for which neither C nor B is identically 0 can be transformed into the form of either Case 1 or Case 2 of the previous section. Since the statements of the theorem were shown to be true for both of these case studies, it then follows that the result must hold in the more general setting. \square

2.4 Design Methodology

Note that in order to obtain a stabilizing controller (when it exists), one need not carry out the transformations described in Lemma 2.3.2. Rather, one may analyze the root locus of the matrix $A + kBC$ directly and (when necessary) find a stable eigenvector to derive an appropriate control law $v(x_1, x_2)$. Moreover, when (A, B) is reachable and (C, A) is observable, we may employ classical root locus techniques to the corresponding transfer function $C(sI - A)^{-1}B$ to quickly ascertain the geometric behavior of the root locus. When either (A, B) is not reachable and/or (C, A) is not observable, we may still use classical root locus techniques on the transfer function $C(sI - A)^{-1}B$, but we must take care to include the unreachable and/or unobservable modes in our analysis.

The following basic algorithm will yield a stabilizing controller when one exists:

1. Compute the transfer function $C(sI - A)^{-1}B$ and examine the corresponding root locus of Eqn. 2.1.1 (i.e. the roots of $1 - kC(sI - A)^{-1}B$ as k varies over \mathbf{R} , along with any fixed unreachable and/or unobservable modes of the original state-space model).
2. If examination of the root locus shows that $\exists k_0$ for which both of the eigenvalues of $A + k_0BC$ lie in the open left half-plane, find such a value of k_0 and choose $v(x_1, x_2) = k_0$ for all x .
3. If examination of the root locus indicates that there exists a value k_1 for which one of the eigenvalues $A + k_1BC$ lies in the open left half-plane and a value k_2 for which the imaginary part of the eigenvalues is nonzero, find corresponding values of k_1 and k_2 , along with the (real) eigenvector w_1 of $A + k_1BC$ corresponding to the stable eigenvalue. Choose $v(x_1, x_2)$ such that

$$v(x_1, x_2) = \begin{cases} k_1, & \text{if } w_1'x = 0 \\ k_2, & \text{if } w_1'x \neq 0 \end{cases}$$

where w_1 satisfies $w_1'q_1 = 0$.

4. If neither 2) nor 3) holds, declare the system unstabilizable by any choice of $v(x_1, x_2)$.

2.5 Examples

Example 2.5.2 We consider three reachable, observable systems of the form

$$\dot{x} = A_i x + B_i u, \quad y = C_i x, \quad i \in \{1, 2, 3\}$$

$$A_1 = \begin{bmatrix} -6 & -6 \\ -6 & 7 \end{bmatrix} \quad A_2 = \begin{bmatrix} 0 & 1 \\ 6 & 1 \end{bmatrix} \quad A_3 = \begin{bmatrix} 0 & 1 \\ -12 & 7 \end{bmatrix}$$

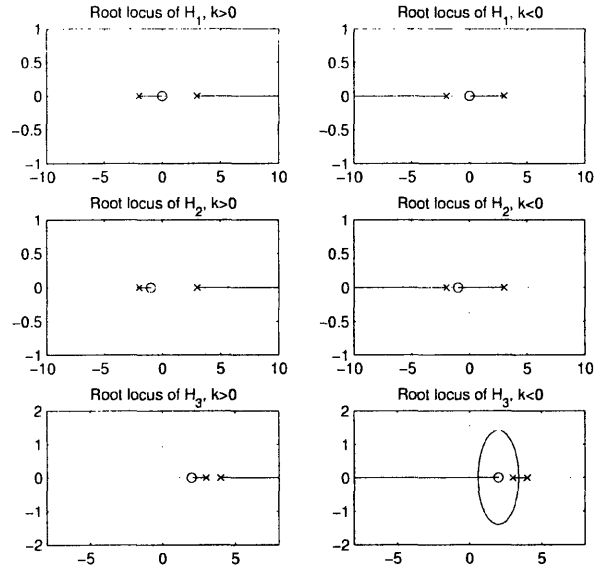


Figure 2.5.2: Root loci for $H_1(s)$, $H_2(s)$, and $H_3(s)$. The root loci for positive k are depicted on the left, while the root loci for negative k are depicted on the right.

$$B_1 = \begin{bmatrix} -1 \\ 1 \end{bmatrix} \quad B_2 = \begin{bmatrix} 0 \\ 1 \end{bmatrix} \quad B_3 = \begin{bmatrix} 0 \\ 1 \end{bmatrix}$$

$$C_1 = \begin{bmatrix} 0 & 1 \end{bmatrix} \quad C_2 = \begin{bmatrix} 1 & 1 \end{bmatrix} \quad C_3 = \begin{bmatrix} -2 & 1 \end{bmatrix}.$$

The transfer functions $H_i(s)$ corresponding to each of these state space descriptions are given by

$$H_1(s) = \frac{s}{s^2 - s - 6}$$

$$H_2(s) = \frac{s + 1}{s^2 - s - 6}$$

$$H_3(s) = \frac{s - 2}{s^2 - 7s + 12}$$

The root locus for each of the above transfer functions is depicted in Fig. 2.5.2. From the first root locus diagram for $H_1(s)$, it is clear that the root locus is real for all k , but the zero at $s = 0$ prevents one eigenvalue from entering the left half plane. Hence, there is no switching control law of the form Eqn. 2.1.2 which can asymptotically stabilize this system.

While the root locus for $H_2(s)$ is also real for all k , the presence of the zero at $s = -1$ allows both eigenvalues to lie in the open left half plane for sufficiently negative values of k . Indeed, when $k = -7$, the eigenvalues are approximately -5.83 and -0.17 . Hence, the second system can be made stable via static output feedback.

The third system $H_3(s)$ has a root locus that takes on complex values for some negative values of k , but both eigenvalues never lie in the left half plane simultaneously. Nevertheless, *one* of the eigenvalues can be made negative for sufficiently

negative values of k . Indeed, when $k = -20/3$, -1 is an eigenvalue of $A_3 + kB_3C_3$ with corresponding eigenvector $q_1 = \begin{bmatrix} 1 & -1 \end{bmatrix}'$. When $k = -1$, the eigenvalues of $A_3 + kB_3C_3$ are complex ($3 \pm i$). Noting that $w_1 = \begin{bmatrix} 1 & 1 \end{bmatrix}'$ satisfies $w_1'q_1 = 0$, a stabilizing switching controller is given by $u(x_1, x_2) = v(x_1, x_2)C_3x$, where $v(x_1, x_2)$ is given by

$$v(x_1, x_2) = \begin{cases} -\frac{20}{3}, & \text{if } x_1 + x_2 = 0 \\ -1, & \text{if } x_1 + x_2 \neq 0 \end{cases}.$$

□

The purpose of the root locus diagrams in the previous example is to illustrate how one can almost immediately tell whether stability can be achieved by a single gain, two gains, or by no control of the form $u(x_1, x_2) = v(x_1, x_2)Cx$. Using the standard root locus techniques on the transfer function $C(sI - A)^{-1}B$, it is fairly quick and easy to determine the basic geometric features of the locus and, hence, determine in which of the three stabilization categories a given system lies.

Example 2.5.3 We now consider two unreachable systems of the form

$$\dot{x} = A_i x + Bu, \quad y = Cx,$$

where $B = \begin{bmatrix} 1 & 0 \end{bmatrix}$, $C = \begin{bmatrix} 1 & 1 \end{bmatrix}$ and

$$A_1 = \begin{bmatrix} -1 & 1 \\ 0 & 1 \end{bmatrix}, \quad A_2 = \begin{bmatrix} -1 & 1 \\ 0 & -1 \end{bmatrix}.$$

In both cases, the transfer function $C(sI - A_i)^{-1}B = 1/(s + 1)$, from which it is clear that the root locus lies along the negative real line for an appropriately chosen value of the gain k . However, since the root locus of the entire system is given by the root locus of the transfer function united with the fixed, unreachable modes, only the second system is stabilizable in this case since the unreachable mode lies in the open left half plane. The first system has a root locus which is real for all k , but an unstable eigenvalue at $s = 1$ always exists. Hence, no feedback of the form $u(x_1, x_2) = v(x_1, x_2)Cx$ can stabilize the first system for any $v(x_1, x_2)$. □

2.6 Summary

In this chapter, we derived necessary and sufficient conditions on the stabilizability of a given second order LTI plant via the given switching architecture where the supervisor has full state information. The reader may be alarmed at this point that the switching control laws derived here suggest using a gain on a measure zero set. Indeed, such control laws are not practically implementable as they are not robust with respect to time delays. Rest assured, however, that in the chapters that follow, we will derive control laws for which we will be able to prove certain robustness properties (the specific issue of robustness with respect to time delays will be discussed in Chapter 4).

We will also take this opportunity to point out that, in higher dimensions, similar sets of *sufficient* conditions exist that guarantee stabilizability by switching between two gains. For instance, in an n -dimensional system, if there exists a value of k_1 such that $A + k_1 BC$ has a pair of dominant complex-conjugate eigenvalues, and there exists a value k_2 such that $A + k_2 BC$ has only one unstable mode, then a generalization of the switching law presented here will yield global exponential stability. Existence of general necessary and sufficient conditions in higher dimensions is still an open problem.

Chapter 3

Synthesis of Optimal Controllers: Rate of Convergence

In this chapter, we will develop algorithms for designing asymptotically stabilizing controllers using the proposed switching architecture which optimize the *rate of convergence* of the state trajectories to the origin. We will first provide a formal definition of convergence rate and will then explore an algorithm which optimizes the rate of convergence when the set of switching gains is symmetric and bounded, i.e., $v(x) \in [-v_0, v_0]$ where $v_0 > 0$. The specific algorithm we will investigate will design optimal switching laws for the specific case where the second order LTI plants $P(s)$ has relative degree two.

3.1 Introduction

The previous chapter provides for us necessary and sufficient conditions for a given LTI plant $P(s)$ to be asymptotically stabilizable using the proposed switching architecture and provides a switching algorithm (represented by the switching law $v(x)$) and a set of gains for achieving stability when possible. In this chapter, we extend the results of the previous chapter by attaching a performance measure to the stabilization problem and solving an optimal control problem that yields a switching controller which maximizes the performance measure. The benefits of solving such a problem are three-fold. First, and most obviously, one is typically interested in providing more than just stability in any realistic control problem; finding a controller which behaves “well” in some sense is typically important for any real application. Second, in solving this optimal control problem, we will arrive at an actual algorithm that can be used to pick a controller, rather than just a set of necessary and sufficient conditions for stability. Finally, as a byproduct of solving the optimal control problem we will present here, we will arrive at a switching algorithm which yields a control law that achieves not only asymptotic stability, but also achieves a form of input-output stability in the form of *finite L_2 gain stability*. This last point, however, is the subject of discussion for Chapter 4.

The structure of this chapter is as follows. First, we will introduce the performance

measure that we wish to associate with our controller design, namely the notion of *rate of convergence*. We will present a formal definition of the rate of convergence and will then use this definition to formulate an optimal control problem when the set of gains that are implementable via the switching architecture is a *bounded, symmetric set*, i.e., $v(x) \in [-v_0, v_0]$ for some $v_0 > 0$ and for all $x \in \mathbf{R}^2$. In order to find an optimal control law (and, correspondingly, the optimal rate of convergence) for a second order plant $P(s)$ that can be stabilized via the switching algorithm of the previous chapter, one needs to consider separately two sub-cases, the first in which $P(s)$ has relative degree two, and the second in which $P(s)$ has relative degree one. Our focus in this chapter is to develop switching algorithms only for the first of these two cases; the case where the plant has relative degree one has very similar design algorithms, but we focus only on the case of relative degree two as this case directly relates to a specific application area that we will examine in a later chapter.

3.2 Rate of Convergence: Definitions

In this section, we introduce the metric of *rate of convergence* over which our ensuing designs will be optimized. We begin with some definitions:

Definition 3.2.1 *The autonomous system described by $\dot{x} = f(x)$ ¹ is said to be globally exponentially stable if there exist constants $M, \beta > 0$ such that, for all solutions $x(t)$,*

$$\|x(t)\|_2 \leq M e^{-\beta t} \|x(0)\|_2 \quad \forall t \geq 0. \quad (3.2.1)$$

Note that we will often-times omit the word “globally” when referring to exponential stability in what follows.

Definition 3.2.2 *A function $f(x)$ is said to be homogeneous if for every $c \in \mathbf{R}$, $f(cx) = cf(x)$.*

Definition 3.2.3 *For a globally exponentially stable autonomous system of the form $\dot{x} = f(x)$, $x(0) = x_0$ where $f(x)$ is homogeneous and piecewise continuous, we define the rate of convergence R as*

$$R = \min_{\|x_0\|=1} \liminf_{T \rightarrow \infty} -\frac{1}{2T} \ln (\|x(T)\|^2).$$

Def. 3.2.3 finds the *largest* real number β such that all solutions of the differential equation satisfy $\|x(t)\| \leq M e^{-\beta t} \|x(0)\|$ for some $M > 0$. Note that, because of the

¹We assume throughout this chapter that all vector fields are defined such that a unique solution exists for every initial condition $x(0)$.

assumed exponential stability of the system. $R > 0$, since for any initial condition $x(0)$,

$$R \geq \liminf_{T \rightarrow \infty} -\frac{1}{2T} \ln (M^2 e^{-2\beta T} \|x(0)\|^2) = \beta.$$

While for general nonlinear systems, this definition may not be well-defined (the limit infimum may approach $+\infty$ or the minimization over the unit circle may not capture the behavior of all solutions), the assumptions of homogeneity and piecewise continuity ensure that the definition of R is a sensible one, a fact we now show.

First, note that if a solution $x_1(t)$ has initial condition $x_1(0) = x_0$, the corresponding solution $x_2(t)$ to the initial condition $x_2(0) = cx_0$ is given by $x_2(t) = cx_1(t)$. Indeed,

$$\dot{x}_2(t) = c\dot{x}_1(t) = cf(x_1(t)) = f(cx_1(t)) = f(x_2(t)).$$

Moreover, since $\ln cx = \ln c + \ln x$,

$$\liminf_{T \rightarrow \infty} -\frac{1}{2T} \ln (c^2 \|x(T)\|^2) = \liminf_{T \rightarrow \infty} -\frac{1}{2T} \ln (\|x(T)\|^2),$$

we see that minimization with respect to $\|x_0\| = 1$ is equivalent to computing the infimum over all $\|x_0\| \neq 0$ so that the definition captures the behavior of *all* solutions $x(t)$.

Next, to see that the \liminf operation is well-defined, we note the following:

$$\frac{d}{dt} \|x(t)\|^2 = 2x'f(x) = 2\|x\|^2 \theta f(\theta),$$

where $\theta = x/\|x\|$ for $x \neq 0$. Since θ lies on the unit sphere, which is a compact set, and since $f(x)$ is assumed piecewise continuous, it follows that $\theta f(\theta)$ has a minimum value α on the unit sphere. Hence,

$$\frac{d}{dt} \|x(t)\|^2 \geq 2\alpha \|x\|^2$$

which implies that

$$\|x(t)\|^2 \geq e^{2\alpha t} \|x(0)\|^2.$$

But this in turn implies that

$$\begin{aligned} -\frac{1}{2T} \ln (\|x(T)\|^2) &\leq -\frac{1}{2T} \ln (e^{2\alpha T} \|x(0)\|^2) \\ &= -\alpha - \frac{\ln \|x(0)\|}{T}. \end{aligned}$$

Because the right hand side in the above inequality is bounded above for large T , it is clear that the limit inferior exists and satisfies

$$\liminf_{T \rightarrow \infty} -\frac{1}{2T} \ln (\|x(T)\|^2) \leq -\alpha.$$

It is useful to point out that, in many cases, including the cases that we will examine in this chapter, the rate of convergence is both independent of the initial condition $x(0)$ and the limit inferior can be replaced by a strict limit, i.e.,

$$R = \lim_{T \rightarrow \infty} -\frac{1}{2T} \ln (||x(T)||^2)$$

A useful property about the rate of convergence that we will utilize in our optimization study is the following:

Corollary 1 *Define the P -rate of convergence R_P as*

$$\min_{||x_0||=1} \liminf_{T \rightarrow \infty} -\frac{1}{2T} \ln (x(T)'Px(T))$$

where $P = P' > 0$. Then $R_P = R_I = R$.

Proof From the inequality

$$\lambda_{\min}(P)||x||^2 \leq x'Px \leq \lambda_{\max}(P)||x||^2,$$

we find that

$$\begin{aligned} -\frac{\ln(\lambda_{\max}(P))}{2T} + r(T) &\leq -\frac{1}{2T} \ln(x(T)'Px(T)) \\ &\leq -\frac{\ln(\lambda_{\min}(P))}{2T} + r(T) \end{aligned}$$

where

$$r(T) = -\frac{1}{2T} \ln (||x(T)||^2).$$

Since

$$\min_{||x(0)||=1} \liminf_{T \rightarrow \infty} r(T) = R,$$

it follows by the squeeze theorem that

$$\min_{||x(0)||=1} \liminf_{T \rightarrow \infty} -\frac{1}{2T} \ln(x(T)'Px(T)) = R.$$

□

3.3 Problem Formulation

Now that we have formally defined our optimization metric, we can formulate the problem under investigation. Consider a second order single-input, single-output LTI system of relative degree two of the form

$$\dot{x} = Ax + Bu, \quad y = Cx, \tag{3.3.2}$$

and further consider a feedback control law of the form $u(x) = v(x)Cx$ where $u(x)$ is homogeneous so that the overall interconnected system is an autonomous system which takes the form

$$\dot{x} = Ax + v(x)BCx, \quad x(0) = x_0: \text{ given.} \quad (3.3.3)$$

Here, the scalar function $v(x)$ satisfies the condition $v(x) \in [v_{\min}, v_{\max}] \forall x \in \mathbf{R}^2$ where v_{\min} and v_{\max} satisfy the following properties:

- There exists v_1 with $v_1 \in [v_{\min}, v_{\max}]$ such that the eigenvalues of $A + v_1BC$ form a complex conjugate pair.
- There exists v_2 with $v_2 \in [v_{\min}, v_{\max}]$ such that at least one of the eigenvalues of $A + v_2BC$ lies strictly in the open left half plane.

It is easily verified that any choice of $v(x)$ that satisfies the bulleted criteria above will admit a stabilizing controller as described in the previous chapter. In addition to the above, the assumed homogeneity of $u(x)$ implies that $v(x)$ satisfies the following property:

Proposition 3.3.5 *If $u(x)$ is homogeneous and $u(x)$ and $v(x)$ are related by the transformation $u(x) = v(x)Cx$, then $v(x) = v(\alpha x)$ for all x with $Cx \neq 0$ and for all $\alpha \neq 0$.*

Proof For any $\alpha \neq 0$

$$\begin{aligned} u(\alpha x) &= \alpha v(\alpha x)Cx \\ \alpha u(x) &= \alpha v(x)Cx \end{aligned}$$

Since $u(\alpha x) = \alpha u(x)$, equating the two expressions and dividing by αCx yields the result. \square

For simplicity, we will examine choices of $v(x)$ for which $v(\alpha x) = v(x)$ for *all* x as this will not affect our choice of an optimal controller.

It is clear that, for each choice of $v(x)$, the autonomous system Eqn. 3.3.3 has an associated rate of convergence R . For a given plant Eqn. 3.3.2 and given values of v_{\min} and v_{\max} , the task at hand, then, is to find a choice of $v(x) \in [v_{\min}, v_{\max}]$ such that the corresponding rate R is maximum. Note that the optimal R is implicitly a function of v_{\min} and v_{\max} , and, hence, we use the notation

$$R^*(v_{\min}, v_{\max}) = \max_{v(x) \in [v_{\min}, v_{\max}]} R(v(x))$$

to denote this optimal value.

For general v_{\min} and v_{\max} , it is often difficult to compute the optimal rate of convergence for a given stabilizable plant $P(s)$ exactly. If, however, the range of $v(x)$ is *symmetric*, i.e., $v(x) \in [-v_0, v_0]$ where $v_0 > 0$ is sufficiently large, then the optimal rate of convergence is exactly computable, and corresponding optimal controllers can

be readily designed. The remainder of this chapter focuses on determining optimal controllers and corresponding rates for this particular case.

In the sections that follow, we will find a choice of $v^*(x) \in [-v_0, v_0]$ which achieves the maximal rate (which we now denote as $R^*(v_0)$) in the above optimization problem and will also explicitly characterize the optimal value $R^*(v_0)$ in terms of v_0 and the parameters of the plant transfer function $C(sI - A)^{-1}B$. We will prove optimality of the resulting controllers by first finding an optimal controller for a particular state-space realization of a plant with transfer function $P(s)$. We will then show that the problem of finding an optimal controller in an arbitrary state-space description can be obtained by performing a design in this particular state-space realization and then performing an appropriate change of coordinates. We will end this chapter by forming a design algorithm for an arbitrary state-space description that does not require changing coordinates.

3.4 Optimal Controller Synthesis for Plants of Relative Degree Two

In this section, we consider the design of a controller which maximizes the rate of convergence for a second order plant of the form

$$P(s) = \frac{c}{s^2 + as + b} \quad (3.4.4)$$

where a , b , and $c \in \mathbf{R}$. In particular, we will focus our attention on the case where $c = 1$. We note if $c \neq 1$, then the problem of finding an optimal controller for $v(x)$ which lie in the bounded region $[-v_0, v_0]$ is equivalent to solving an optimal control problem with the plant numerator coefficient equal to one and where $v(x)$ lies in the bounded region $[-|c|v_0, |c|v_0]$ ², and, hence, we make this assumption without loss of generality. We will first consider the problem of control design for the case where the plant has state-space description given by

$$\begin{bmatrix} \dot{x}_1 \\ \dot{x}_2 \end{bmatrix} = \begin{bmatrix} -\frac{a}{2} & \gamma \\ \frac{-b + \frac{a^2}{4}}{\gamma} & -\frac{a}{2} \end{bmatrix} \begin{bmatrix} x_1 \\ x_2 \end{bmatrix} + \begin{bmatrix} 0 \\ \frac{1}{\gamma} \end{bmatrix} u \quad (3.4.5)$$

$$y = x_1 \quad (3.4.6)$$

where $\gamma > 0$ is a free parameter that we will choose. Under the feedback law $u = vx_1$, the characteristic polynomial of the closed-loop system is given by

$$s^2 + as + b - v = 0$$

which has roots

$$s = \frac{-a \pm \sqrt{a^2 - 4b + 4v}}{2}.$$

²We ignore the trivial case when $c = 0$.

A straightforward calculation shows that, in order for the system to be stabilizable via the switching algorithm of the previous chapter, v_0 must satisfy the following condition:

$$v_0 > \begin{cases} \left| \frac{a^2}{4} - b \right|, & a > 0 \\ \max \left\{ \frac{a^2}{4} - b, b \right\}, & a \leq 0 \end{cases}. \quad (3.4.7)$$

We will actually enforce a somewhat stronger condition on the value of v_0 , namely that

$$v_0 > \max\{|a^2/4 - b|, b\} \quad (3.4.8)$$

for all $a \in \mathbf{R}$. While this stronger condition is not necessary for the work we are investigating in this chapter, it will make a difference when we begin to investigate input-output stability.

Upper Bound on Optimal Rate of Convergence

Our first goal is to prove the following statement:

Theorem 3.4.2 *Consider the system of Eqn. 3.4.5 and 3.4.6 under the feedback law $u(x) = v(x)y$ with $v(x) \in [-v_0, v_0]$ for all $x \in \mathbf{R}^2$ where v_0 satisfies the conditions of Eqn. 3.4.8, and suppose that v_0 satisfies the additional constraint that*

$$v_0 \geq 2b - \frac{a^2}{2}. \quad (3.4.9)$$

Then the optimal rate of convergence $R^(v_0)$ satisfies the inequality*

$$R^*(v_0) \leq -\lambda_{\min}(A + v_0 BC)$$

where A , B , and C are the corresponding matrices of the state-space description in Eqn. 3.4.5 and 3.4.6, and $\lambda_{\min}(\cdot)$ denotes the minimum eigenvalue of a square matrix.

In the sequel we will see that the above upper bound can be achieved with equality by an appropriate controller selection.

Proof Let \tilde{A} be given by

$$\tilde{A}(v(x)) = A + v(x)BC = \begin{bmatrix} -\frac{a}{2} & \gamma \\ \frac{-b + \frac{a^2}{4} + v(x)}{\gamma} & -\frac{a}{2} \end{bmatrix}.$$

Along the trajectories of the system we have

$$\begin{aligned} \frac{d}{dt} \|x(t)\|^2 &= x(t)' \left(\tilde{A}(v(x(t))) + \tilde{A}'(v(x(t))) \right) x(t) \\ &\geq \min_{|v| \leq v_0} \lambda_{\min} \left(\tilde{A}(v) + \tilde{A}'(v) \right) \|x(t)\|^2 \end{aligned}$$

Now, a simple calculation shows that

$$\lambda_{\min} \left(\tilde{A}(v) + \tilde{A}'(v) \right) = -a - \left| \gamma + \frac{v - b + \frac{a^2}{4}}{\gamma} \right|.$$

by factoring out $1/\gamma$, we see that minimization of the above eigenvalue over all v that satisfy $|v| \leq v_0$ is equivalent to computing

$$\max_{|v| \leq v_0} \left| \gamma^2 + v - b + \frac{a^2}{4} \right|.$$

Note that the lower bound we derived on the derivative of the squared Euclidean norm of $x(t)$ must hold for *any* $\gamma > 0$. Hence, we can fix γ to be a convenient value³ of γ and compute the corresponding maximum in the above expression. If we choose $\gamma = \sqrt{\frac{a^2}{4} - b + v_0}$, then we find

$$\begin{aligned} \left| \gamma^2 + v - b + \frac{a^2}{4} \right| &= \left| v + v_0 - 2b + \frac{a^2}{4} \right| \\ &= |v + \alpha| \end{aligned}$$

where $\alpha \geq 0$ and where we have used the inequality Eqn. 3.4.9 in deriving the last equality. Because $\alpha \geq 0$, the maximum value of the last expression over the set $|v| \leq v_0$ occurs when $v = v_0$, and we find that

$$\begin{aligned} \min_{|v| \leq v_0} \lambda_{\min} \left(\tilde{A}(v) + \tilde{A}'(v) \right) &= -a - \sqrt{a^2 - 4b + 4v_0} \\ &= 2\lambda_{\min}(A + v_0 BC) \\ &\triangleq 2\tilde{\lambda}. \end{aligned}$$

Solving the resulting differential inequality, we find

$$||x(t)||^2 \geq e^{2\tilde{\lambda}t} ||x(0)||^2.$$

Now

$$\begin{aligned} R^*(v_0) &= \min_{||x(0)||=1} \liminf_{T \rightarrow \infty} -\frac{1}{2T} \ln (||x(T)||^2) \\ &\leq \min_{||x(0)||=1} \liminf_{T \rightarrow \infty} -\frac{1}{2T} \ln \left(e^{2\tilde{\lambda}T} ||x(0)||^2 \right) \\ &= \min_{||x(0)||=1} \liminf_{T \rightarrow \infty} -\frac{1}{2T} \ln (||x(0)||^2) - \tilde{\lambda} \\ &= -\tilde{\lambda}. \end{aligned}$$

³As we will see shortly, the value of γ that we choose here yields the *least* upper bound on $R^*(v_0)$.

□

Achieving the Upper Bound: Optimal Controller Structure

We will now derive a generic control law $v(x)$ for which the corresponding rate of convergence achieves the upper bound of Thm. 3.4.2. We will first find a controller $v(x)$ for the state-space description of Eqn. 3.4.5 and 3.4.6, and will then show how to derive optimal controllers for arbitrary state-space descriptions through an appropriate coordinate transformation.

As it turns out, a controller which achieves the upper bound on the rate of convergence we derived in the previous section is a so-called “bang-bang” controller, i.e., a controller which switches between the two extreme values, v_0 and $-v_0$. To begin, we will first find the eigenspace of the matrix $A + v_0 BC$ where A , B , and C are the state-space matrices of the state-space description in Eqn. 3.4.5 and 3.4.6 when $\gamma = \sqrt{\frac{a^2}{4} - b + v_0}$:

$$A + v_0 BC = \begin{bmatrix} -\frac{a}{2} & \gamma \\ \gamma & -\frac{a}{2} \end{bmatrix},$$

the eigenvalues of which are given by

$$\lambda(A + v_0 BC) = -\frac{a}{2} \pm \gamma.$$

If we denote the minimum and maximum eigenvalues as λ_s and λ_u , respectively, then the corresponding eigenvectors w_s and w_u are given by

$$w_s = \begin{bmatrix} -1 \\ 1 \end{bmatrix}, \quad w_u = \begin{bmatrix} 1 \\ 1 \end{bmatrix}. \quad (3.4.10)$$

The basic algorithm that we will use to achieve stability (and the upper bound on the rate of convergence) is essentially the same as the one we used in the last chapter: we choose a value of gain that yields complex eigenvalues to induce rotation and switch the value of the gain to v_0 when the state trajectory lands on the stable manifold. The exact algorithm we use is described in the following Theorem:

Theorem 3.4.3 *Let w_s and w_u be given as in Eqn. 3.4.10, and let \tilde{w}_s and \tilde{w}_u be defined such that $\tilde{w}_s' w_s = 0$ and $\tilde{w}_u' w_u = 0$ where \tilde{w}_s and \tilde{w}_u are both oriented in a clockwise orientation. Suppose that $q = \begin{bmatrix} q_1 & q_2 \end{bmatrix}'$ satisfies the conditions $q_2 > 0$ and*

$$(\tilde{w}_s' q)(\tilde{w}_u' q) < 0,$$

and let \tilde{q} be defined in such a way that $\tilde{q}' q = 0$ where \tilde{q} is oriented clockwise. Then the control law

$$v(x) = \begin{cases} v_0 & x'(\tilde{w}_s \tilde{q}')x \leq 0 \\ -v_0 & x'(\tilde{w}_s \tilde{q}')x > 0 \end{cases} \quad (3.4.11)$$

asymptotically stabilizes the plant of Eqn. 3.4.5 and 3.4.6 when $\gamma = \sqrt{a^2/4 - b + v_0}$

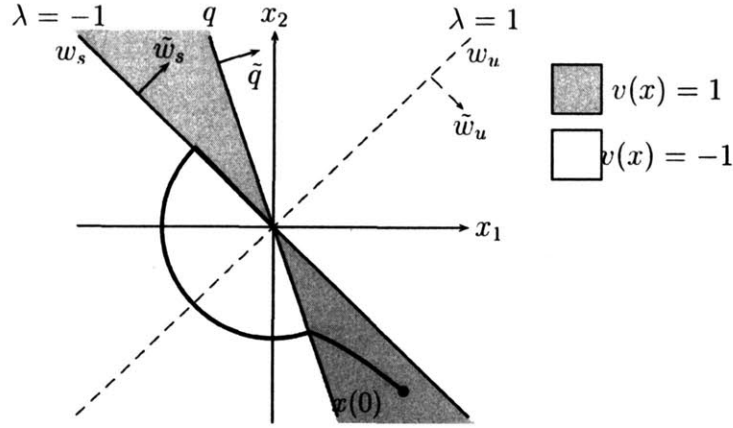


Figure 3.4.1: Graphical depiction of switching law of Eqn. 3.4.11

with rate

$$R = -\lambda_{\min}(A + v_0 BC).$$

An immediate corollary to Thm. 3.4.3 is the following.

Corollary 2 *The optimal rate of convergence for the plant of Eqn. 3.4.5 and Eqn. 3.4.6 when $v(x)$ is constrained to lie in the range $[-v_0, v_0]$ is*

$$R^*(v_0) = -\lambda_{\min}(A + v_0 BC).$$

The control law of Eqn. 3.4.11 is depicted graphically in Fig. 3.4.1. Essentially, if we pick any vector q that lies to the right of one of the eigenvectors and to the left of the other, then this induces a partition on the state-space where we use the gain $v(x) = v_0$ in the region bound by the w_s and q , and where we use $v(x) = -v_0$ in the region bound by w_u and q . A sample phase portrait for an initial condition $x(0)$ which lies in the region of the state-space where $v(x) = v_0$ is depicted in the figure, as well.

In order to prove Thm. 3.4.3, we will need the result of the following Lemma.

Lemma 3.4.3 *Consider a diagonalizable matrix $A \in \mathbf{R}^{2 \times 2}$ which has eigenvalues λ_s and λ_u , $\lambda_u > \lambda_s$, and corresponding eigenvectors w_s and w_u , respectively. Define \tilde{w}_s and \tilde{w}_u in such a way that $\tilde{w}_s' w_s = 0$ and $\tilde{w}_u' w_u = 0$, and consider vectors q and p that satisfy the following conditions:*

$$\begin{aligned} \tilde{w}_s' q &> 0 \\ \tilde{w}_u' q &< 0 \\ \tilde{w}_s' p &> 0 \\ \tilde{q}' p &< 0 \end{aligned}$$

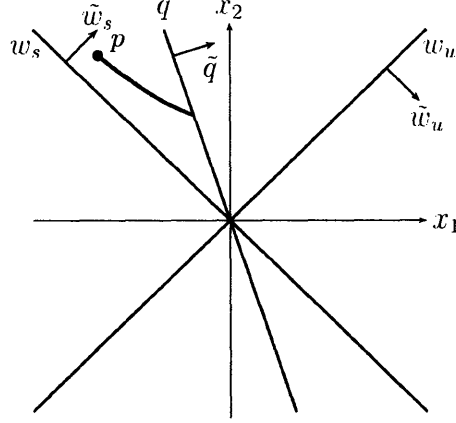


Figure 3.4.2: Relative positioning of w_s , w_u , q , and p for Lemma 3.4.3.

where \tilde{q} satisfies $\tilde{q}'q = 0$. Assume that \tilde{w}_s , \tilde{w}_u , and \tilde{q} are all oriented in the same direction (either clockwise or counterclockwise) and that $\tilde{w}_s'w_u \geq 0$. Then there exists $t > 0$ such that the state trajectory $x(t)$ of the system

$$\dot{x} = Ax, \quad x(0) = p$$

satisfies the condition $x(t) = \alpha q$ for some $\alpha \in \mathbf{R}$.

A geometric interpretation of Lemma 3.4.3 is given in Fig. 3.4.2. The conditions in the lemma reflect the relative positioning of q and p with respect to the two eigenvectors w_s and w_u . The conditions on p and q ensure that there is no eigenvector between p and q , and that p is closer in angle to w_s than q . Since $\lambda_u > \lambda_s$, one should expect the phase portraits to approach w_u as $t \rightarrow \infty$. The overall statement, then, reflects the following intuitive notion: since p lies closer to the eigenvector with smaller eigenvalue λ_s than the vector q , the state trajectory $x(t)$ must cross the line defined by the vector q at some finite, positive time. We leave the proof of this statement to an appendix at the end of the chapter.

Proof [Proof of Thm. 3.4.3] We will first show the following: the closed loop system $\dot{x} = (A + v(x)BC)x$ satisfies the condition that, for every initial condition $x(0)$, there exists $t_0 > 0$ such that $x(t_0) = \alpha w_s$ for some $\alpha \in \mathbf{R}$, i.e., that every initial condition is driven onto the stable manifold in finite time. We first consider the case when $x(0)$ lies in the region

$$x(0)'(\tilde{w}_s\tilde{q}')x(0) > 0.$$

In this region, we have the $v(x(0)) = -v_0$. The eigenvalues of the matrix $A - v_0BC$ in this region are of the form $-a/2 \pm j\omega_0$ where $\omega_0 = \sqrt{v_0 + b - a^2/4}$. Now, it is clear from Lemma 2.2.1 of the previous chapter that there exists some time $t_0 < \pi/\omega_0$ for which $x(t_0)'(\tilde{w}_s\tilde{q}')x(t_0) = 0$ and for which $v(x(t)) = -v_0$ for all $t < t_0$. This, in turn, implies that one of the following conditions holds

$$\tilde{w}_s'x(t_0) = 0 \quad \text{or} \quad \tilde{q}'x(t_0) = 0.$$

We will show that the former condition must hold by showing that the latter condition is impossible. Suppose that at time t_0 , $\tilde{q}'x(t_0) = 0$. We may equivalently write this condition as

$$x(t_0) = \beta \begin{bmatrix} q_1 \\ q_2 \end{bmatrix}, \quad (3.4.12)$$

where $\beta \in \mathbf{R}$, and let \tilde{q} be the clockwise oriented vector $\tilde{q} = \begin{bmatrix} q_2 & -q_1 \end{bmatrix}'$. Now,

$$\frac{d}{dt} (x(t)'(\tilde{w}_s \tilde{q}')x(t)) = x(t)'(A - v_0 BC)'(\tilde{w}_s \tilde{q}')x(t) + x(t)'(\tilde{w}_s \tilde{q}')(A - v_0 BC)x(t). \quad (3.4.13)$$

If Eqn. 3.4.13 is satisfied, the above derivative reduces to

$$\frac{d}{dt} (x(t)'(\tilde{w}_s \tilde{q}')x(t)) = \beta^2 (q_1 + q_2) \left(\frac{\omega_0^2}{\gamma} q_1^2 + \gamma q_2^2 \right).$$

Recalling the conditions $(\tilde{w}_s' q)(\tilde{w}_u' q) < 0$ and $q_2 > 0$, we find that $q_1 + q_2 > 0$ which means that the above derivative is positive. But if $\tilde{q}'x(t_0) = 0$ and the above derivative is positive, then it follows that

$$x(t_0^-)'(\tilde{w}_s \tilde{q}')x(t_0^-) < 0$$

which implies that $v(x(t_0^-)) = v_0$, i.e., that a switch from $-v_0$ to v_0 has already occurred, which is an obvious contradiction. Hence, we conclude that there exists $t_0 < \pi/\omega_0$ such that $\tilde{w}_s'x(t_0) = 0$ or, equivalently, $x(t_0) = \alpha w_s$ for some $\alpha \in \mathbf{R}$.

Now consider the case where the initial condition $x(0)$ satisfies

$$x(0)'(\tilde{w}_s \tilde{q}')x(0) \leq 0.$$

We will break the above condition down into three separate cases

1. $x(0) = \alpha w_s$, $\alpha \in \mathbf{R}$.
2. $x(0) = \beta q$, $\beta \in \mathbf{R}$.
3. $x(0)'(\tilde{w}_s \tilde{q}')x(0) < 0$.

The first case immediately yields the result that we desire. For the second case, the analysis above shows that if $x(0) = \beta q$ for some $\beta \in \mathbf{R}$, then

$$x(0^+)'\tilde{w}_s \tilde{q}'x(0^+) > 0$$

where the inequality is strict. Employing the time-invariance of the interconnected system, the problem now reduces to showing that there exists $t_0 > 0$ such that the state trajectory $\hat{x}(t)$ with initial state $\hat{x}(0) = x(0^+)$ satisfies $\hat{x}(t) = \alpha w_s$ for some $\alpha \in \mathbf{R}$, which we already showed above.

To consider the final case, we will use the result of Lemma 3.4.3. By our assumptions, we have that \tilde{w}_s , \tilde{w}_u , and \tilde{q} are all oriented in the same direction (clockwise),

and we also have that $\tilde{w}'_s q > 0$, $\tilde{w}'_u q < 0$. Now, if we let $p = x(0)$, one of the following sets of conditions must hold

$$\tilde{w}'_s p > 0 \quad \text{and} \quad \tilde{q}' p < 0$$

or

$$\tilde{w}'_s p > 0 \quad \text{and} \quad \tilde{q}' p < 0.$$

Because the interconnected system is homogeneous, we may assume without loss of generality that the first set of conditions holds. Indeed, if p does not satisfy the first set of conditions, $-p$ does satisfy the first set of conditions. Furthermore, the trajectory $z(t) = -x(t)$ that satisfies the differential equation

$$\dot{z} = (A + v(z)BC)z, \quad z(0) = -p$$

crosses the stable manifold for some $t_0 > 0$ if and only if $x(t)$ crosses the stable manifold in the same time t_0 .

Under these assumptions, Lemma 3.4.3 guarantees that there exists some time $t_1 > 0$ for which $x(t) = \beta q$ for some $\beta \in \mathbf{R}$. But if we now consider the new initial condition $z(0) = x(t_1)$, we know from the second case that there exists t_2 such that $z(t_2) = x(t_1 + t_2) = \alpha w_s$, $\alpha \in \mathbf{R}$. Hence, we may take $t_0 = t_1 + t_2$.

Now, if we let $\tilde{\lambda} = \lambda_{\min}(A + v_0 BC) < 0$, we see that, for every initial condition $x(0)$, there exists $t_0 \geq 0$ and $\alpha \in \mathbf{R}$ such that

$$x(t) = \alpha e^{\tilde{\lambda}(t-t_0)} w_s$$

from which asymptotic stability immediately follows. To establish the result on the corresponding rate R , we note that

$$\liminf_{T \rightarrow \infty} -\frac{1}{2T} \ln (\|x(T)\|^2) = \lim_{T \rightarrow \infty} -\frac{1}{2T} \ln \left(e^{2\tilde{\lambda}(T-t_0)} \|w_s\|^2 \right) = -\tilde{\lambda}.$$

Since this results holds true for all $x(0) \in \mathbf{R}^2$, we conclude that

$$R = -\lambda_{\min}(A + v_0 BC).$$

□

A few comments are in order. First, it is clear that controllers that achieve the optimal rate are not unique; the parameter q is a free design parameter (subject to the constraints imposed in Thm. 3.4.3). While we will not attempt to discuss this in a formal manner, it is typically that case that one generally chooses q to be sufficiently far (in an angular sense) from both of the eigenvectors w_s and w_u . Choosing q to be very close to w_u leads to “practical” instability since, for initial conditions that lie in the shaded area of Fig. 3.4.1, the Euclidean norm of the state vector may grow very large before the gain is switched from v_0 to $-v_0$. Choosing q too close to w_s , on the other hand, leads to a robustness issue whose roots will become apparent in the next

chapter. One particular ad hoc method of choosing q when the state-space description of the plant takes the form of Eqn. 3.4.5 and 3.4.6 is to select q as the angle bisector of the eigenvectors w_s and w_u . We will see in later chapters that this particular choice of q often performs well in certain design problems (see [42, 43] to understand where this particular ad-hoc choice originated). Note, however, that the relative performance achieved by choosing q in such a manner is *highly* a function of the state-space description of the plant; just because choosing q to be the angle bisector of w_s and w_u yields good performance in this state-space description does *not* mean that choosing q to be the angle bisector will achieve good performance for an *arbitrary* state-space description. In the next section, we will discuss a method of designing controllers where we transform the state-space description into the form studied here and then transform back into the original coordinate system. By doing this, if we map the angle bisector in the coordinate system shown here into an equivalent vector q in the original state-space coordinates (which may not be close to the angle bisector of the vectors w_s and w_u at all).

The reader may also note that the choice of $v(x) = -v_0$ in the unshaded region of Fig. 3.4.1 is not critical for achieving the maximum rate of convergence, as picking $v(x)$ to be any value of $v < 0$ for which the discriminant $a^2/4 - b + v < 0$ will yield the same rate. In this case, however, choosing the $v(x)$ to lie along the lower boundary of the range is a natural choice, as this value maximizes the frequency of rotation. As we will see in later chapters, choosing $v(x) = -v_0$ in the unshaded region of Fig. 3.4.1 can lead to system responses with desirable transient behavior.

Optimal Controllers for Arbitrary State-space descriptions

To obtain an optimal design for all other state-space realizations of a given second order transfer function of relative degree two, essentially, one need only apply a simple change of coordinates:

Proposition 3.4.6 *Consider an exponentially stable system of the form $\dot{x} = Ax + v(x)BCx$ with rate R where $v(x)$ takes the form*

$$v(x) = \begin{cases} v_1 & x'F_1F_2'x \leq 0 \\ v_2 & x'F_1F_2'x > 0 \end{cases}$$

where F_1, F_2 are column vectors of appropriate dimension. Then the system $\dot{z} = \tilde{A}z + \tilde{v}(z)\tilde{B}\tilde{C}z$ with $\tilde{v}(z)$ given by

$$\tilde{v}(z) = \begin{cases} v_1 & z'\tilde{F}_1\tilde{F}_2'z \leq 0 \\ v_2 & z'\tilde{F}_1\tilde{F}_2'z > 0 \end{cases}$$

with

$$\tilde{A} = T^{-1}AT, \tilde{B} = T^{-1}B, \tilde{C} = CT, \tilde{F}_i = T'F_i, i = 1, 2$$

where T is an invertible matrix is also exponentially stable with rate R .

Proof Performing the change of coordinates $x = Tz$ shows that the above system defined by z has P -rate of convergence equal to R with $P = T'T$. But Cor. 1 implies

that the rate of convergence of the new system defined by z is equal to R , as well. \square

Prop. 3.4.6 allows us to design optimal controllers for systems of relative degree two with arbitrary state-space descriptions in the following way: we first find a state-space description of the corresponding transfer function $P(s) = C(sI - A)^{-1}B$ in the form of Eqn. 3.4.5 and 3.4.6 with $\gamma = \sqrt{a^2/4 - b + v_0}$. We then design a controller which optimizes the rate of convergence in this set of coordinates, and then find an appropriate change of coordinates that transforms the state-space description in which we performed the design into the state-space description that we started with. An optimal controller is then obtained by using the relationships listed in Prop. 3.4.6. We illustrate this process through an example.

Example 3.4.4 Consider the unstable LTI plant

$$\begin{aligned} \begin{bmatrix} \dot{z}_1 \\ \dot{z}_2 \end{bmatrix} &= \begin{bmatrix} 0 & 1 \\ -12 & 7 \end{bmatrix} \begin{bmatrix} z_1 \\ z_2 \end{bmatrix} + \begin{bmatrix} 0 \\ 1 \end{bmatrix} u \\ y &= z_1. \end{aligned}$$

with transfer function

$$P(s) = \frac{1}{s^2 - 7s + 12}.$$

We wish to find a switching controller of the form $u(x) = v(x)y$ which asymptotically stabilizes this plant with maximum rate of convergence when $v(x)$ satisfies the bound $|v(x)| \leq 99.75$ for all $x \in \mathbf{R}^2$. If we take $a = -7$, $b = 12$, and $v_0 = 99.75$, we first note that the conditions $v_0 > \max\{a^2/4 - b, b\}$ and $v_0 > 2b - a^2/4$ are satisfied and, therefore, conclude that the results of Thm. 3.4.2 and 3.4.3 are valid. Hence, we may use these results to go about the business of finding an optimal controller.

With $\gamma = \sqrt{a^2/4 - b + v_0}$, the state-space description of Eqn. 3.4.5 and 3.4.6 is given by

$$\begin{aligned} \begin{bmatrix} \dot{x}_1 \\ \dot{x}_2 \end{bmatrix} &= \begin{bmatrix} 3.5 & 10 \\ 0.025 & 3.5 \end{bmatrix} \begin{bmatrix} x_1 \\ x_2 \end{bmatrix} + \begin{bmatrix} 0 \\ 0.1 \end{bmatrix} u \\ y &= x_1. \end{aligned}$$

Recalling that the stable and unstable eigenvectors of the matrix $A + v_0 BC$ are given by $w_s = \begin{bmatrix} -1 & 1 \end{bmatrix}'$ and $w_u = \begin{bmatrix} 1 & 1 \end{bmatrix}'$, respectively, and choosing q to be the angle bisector of these two vectors ($q = \begin{bmatrix} 0 & 1 \end{bmatrix}'$), we find that the following control law achieves the maximum rate of convergence:

$$v(x) = \begin{cases} 99.75 & x_1(x_1 + x_2) \leq 0 \\ -99.75 & x_1(x_1 + x_2) > 0 \end{cases}.$$

The optimal rate of convergence in this case is given by $R^*(99.75) = -\lambda_{\min}(A + v_0 BC) = 6.5$.

By diagonalizing the “ A ” matrix for both state-space descriptions, a simple calculation shows that the two descriptions can be related via the coordinate transfor-

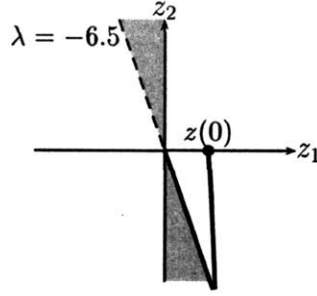


Figure 3.4.3: Illustration of the optimal control law for Example 3.4.

mation $x = Tz$ where

$$T = \begin{bmatrix} 1 & 0 \\ -.35 & .1 \end{bmatrix}.$$

Using this transformation to compute \tilde{F}_i , $i = 1, 2$ of Prop. 3.4.6, we establish the following optimal control law in terms of the original state-space description:

$$v^*(x) = \begin{cases} 99.75 & x_1(6.5x_1 + x_2) \leq 0 \\ -99.75 & x_1(6.5x_1 + x_2) > 0 \end{cases} \quad (3.4.14)$$

which is depicted graphically along with a sample trajectory in Fig. 3.4.3. Notice that one of the boundaries of the cone in which $v(x) = 99.75$ is the stable eigenvector of the matrix

$$\begin{bmatrix} 0 & 1 \\ 87.75 & 7 \end{bmatrix}$$

and that the state trajectory follows this eigenvector for large time. Notice also that the corresponding stable eigenvalue of the above matrix is -6.5 which, as we computed earlier, is our optimal rate $R^*(99.75)$.

Designing Controllers Without an Explicit Coordinate Change

While the above process does allow us to find an optimal controller for arbitrary state-space descriptions, it is not necessarily the most desirable method as it requires finding an explicit change of coordinates to relate the state-space description for which we wish to design a control law to a “canonical” state-space description. We will now describe a method which does not require an explicit change of coordinates, i.e., a method of designing switching controllers directly in the coordinate frame of interest.

The control laws we have been constructing take the form shown in Prop. 3.4.6 with $F_1 = \tilde{w}_s$ and $F_2 = \tilde{q}$. From the proof of Lemma 3.4.3, we see that an invertible change of coordinates will yield the following results, the proofs of which are immediate and left to the reader:

- If $F_1 = \tilde{w}_s$ is a vector which is normal to the stable eigenvector of $A + v_0 BC$, then the transformed vector \tilde{F}_1 is a vector which is normal to the stable eigenvector

of $T^{-1}(A + v_0 BC)T$.

- If \tilde{w}_s , \tilde{w}_u and q satisfy the relationships $\tilde{w}_s' q > 0$ and $\tilde{w}_u' q < 0$, then the transformed vectors $\hat{\tilde{w}}_s' \hat{q} > 0$ and $\hat{\tilde{w}}_u' \hat{q} < 0$ where $\hat{\tilde{w}}_s = T' \tilde{w}_s$, $\hat{\tilde{w}}_u = T' \tilde{w}_u$, and $\hat{q} = T^{-1} q$.

In layman's terms, the above conditions tell us that, for *any* state-space description, one can choose an optimal controller by choosing one switching boundary to be the stable eigenvector and choosing the other boundary to be a vector q that lies “between” the stable eigenvector and the unstable eigenvector. Here, however, lies some ambiguity: for any eigenvectors w_s and w_u with corresponding normal vectors \tilde{w}_s and \tilde{w}_u , the state-space can be partitioned into two regions: the region of $x \in \mathbf{R}^2$ which satisfies $x' \tilde{w}_s \tilde{w}_u' x \geq 0$ and the region which satisfies $x' \tilde{w}_s \tilde{w}_u' x < 0$. If one were to blindly apply the results of Thm. 3.4.3, one would pick q in the second region since, in that region, $q' \tilde{w}_s \tilde{w}_u' q < 0$. However, note that we equally could have chosen $v_s = -w_s$ as a stable eigenvector with corresponding normal vector $\tilde{v}_s = -\tilde{w}_s$, in which case the *first* region would appear to the region for which we want to place q . How do we resolve this issue?

If we re-examine the particular state-space description of Thm. 3.4.3, one important feature that led us to choose q in the region that we did was the following: along the switching boundary, the vector field for both $A + v_0 BC$ and $A - v_0 BC$ points in the same direction. Formally, this is equivalent to saying that $\tilde{q}'(A + v_0 BC)q$ and $\tilde{q}'(A - v_0 BC)q$ are of the same sign. Again taking $q = \begin{bmatrix} q_1 & q_2 \end{bmatrix}'$ and $\tilde{q} = \begin{bmatrix} q_2 & -q_1 \end{bmatrix}'$, we find that

$$\tilde{q}'(A + v_0 BC)q = \gamma(q_2^2 - q_1^2) \quad (3.4.15)$$

$$\tilde{q}'(A - v_0 BC)q = \gamma q_2^2 + \frac{v_0 - b + \frac{a^2}{4}}{\gamma} q_1^2. \quad (3.4.16)$$

By the assumptions on v_0 , we have that $v_0 - b + a^2/4$ is positive, and, hence, Eqn. 3.4.16 is positive for any $q \in \mathbf{R}^2$. Geometrically, this indicates that the phase portraits of the system $\dot{x} = (A - v_0 BC)x$ are rotating in a clockwise manner. Note that Eqn. 3.4.15 is only positive in the region $q_1^2 > q_2^2$. This is the region where we chose q to be in Thm. 3.4.3. Note that if we had chosen q to lie in the other region, then Eqn. 3.4.15 would be negative, i.e., the vector fields on either side of q would be “pointing at” each other and, hence, the resulting switching system would be ill-posed. In real-world implementations, the situation in which the vector fields point at each other induces a phenomenon known as *chatter* (see, e.g., [11, 65]) which is, generally, an undesirable phenomenon.

From the above, we see that we pick q to lie in the region for which the state trajectories for both $\dot{x} = (A + v_0 BC)x$ and $\dot{x} = (A - v_0 BC)x$ will move in the same direction across the switching boundary which, in practice, can be done via a graphical examination of the phase portraits of $\dot{x} = (A + v_0 BC)x$ and $\dot{x} = (A - v_0 BC)x$. We illustrate this by re-visiting our first example.

Example 3.4.5 Consider the unstable LTI plant

$$\begin{bmatrix} \dot{x}_1 \\ \dot{x}_2 \end{bmatrix} = \begin{bmatrix} 0 & 1 \\ -12 & 7 \end{bmatrix} \begin{bmatrix} x_1 \\ x_2 \end{bmatrix} + \begin{bmatrix} 0 \\ 1 \end{bmatrix} u$$

$$y = x_1.$$

and the associated task of finding a switching controller $v(x)$ which achieves maximal convergence rate for $|v(x)| \leq 99.75$. We begin by computing the eigenvectors of the matrix $A + v_0 BC$:

$$w_s = \begin{bmatrix} -1 \\ 6.5 \end{bmatrix}, \quad w_u = \begin{bmatrix} 1 \\ 13.5 \end{bmatrix}$$

which are depicted graphically in Fig. 3.4.4. In order to determine the region where we should place q (either the region bound by the eigenvectors which contains the x_2 axis, or the region bound by the eigenvectors that contains the x_1 axis), we first determine the orientation of rotation for the phase portraits of $A - v_0 BC$. Note that $\dot{x} = (A - v_0 BC)x$ satisfies the property that, when $x_1 = 0$, $\dot{x}_1 = x_2$. From this, we immediately conclude that the phase portraits of $\dot{x} = (A - v_0 BC)x$ are rotating in a clockwise manner. By examining the relative placement of the eigenvectors in Fig. 3.4.4, we see that the phase portraits of $\dot{x} = (A + v_0 BC)x$ are rotating in a clockwise manner in the region which contains the positive x_2 axis. Hence, we may choose any q in this region to define our control law. Picking $q = \begin{bmatrix} 0 & 1 \end{bmatrix}'$ yields the control law we found in the first example:

$$v(x) = \begin{cases} 99.75 & x_1(6.5x_1 + x_2) \leq 0 \\ -99.75 & x_1(6.5x_1 + x_2) > 0 \end{cases}.$$

As an alternative, if we use the ad-hoc procedure of choosing q to be the angle bisector of the stable and unstable eigenvectors, we arrive at the control law

$$v(x) = \begin{cases} 99.75 & (x_1 + .0394x_2)(6.5x_1 + x_2) \leq 0 \\ -99.75 & (x_1 + .0394x_2)(6.5x_1 + x_2) > 0 \end{cases}.$$

Note, for this example, that the angle between the corresponding q vectors in each of the above control laws is only 2.26° .

Overall Design Algorithm without a Coordinate Change

To summarize, we may design optimal rate controllers for a second order system of relative degree two of the form

$$P(s) = \frac{1}{s^2 + as + b}$$

by performing the following steps:

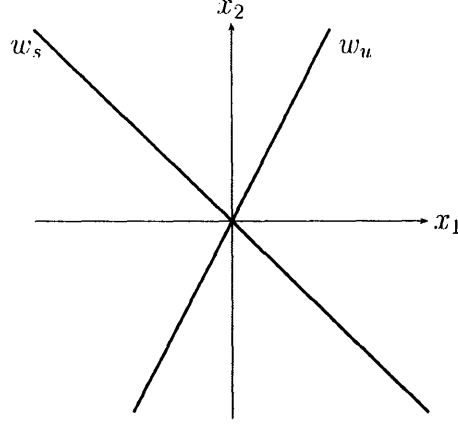


Figure 3.4.4: Eigenvectors for the matrix $A + v_0 BC$ for Example 3.4 (not drawn to scale).

1. For a given gain bound v_0 , check to make sure that the conditions

$$v_0 > \begin{cases} \left| \frac{a^2}{4} - b \right|, & a > 0 \\ \max \left\{ \frac{a^2}{4} - b, b \right\}, & a \leq 0 \end{cases}.$$

and

$$v_0 > 2b - \frac{a^2}{4}$$

are satisfied. If so, proceed to step 2.

2. Compute the eigenvectors of $A + v_0 BC$ and the direction of the phase portraits of $\dot{x} = (A - v_0 BC)x$ (clockwise or counterclockwise).
3. Determine the appropriate region of the state-space to place the vector q . Choose q to be the angle bisector of the eigenvectors w_s and w_u in this region, or choose any other vector q in this region.
4. An optimal controller is given by

$$v(x) = \begin{cases} v_0 & x' \tilde{w}_s \tilde{q}' x \leq 0 \\ -v_0 & x' \tilde{w}_s \tilde{q}' x > 0 \end{cases}$$

where \tilde{w}_s and \tilde{q} are normal vectors to w_s and q , respectively, that are oriented in the same direction.

The above algorithm will always yield a stabilizing controller with maximum rate $R^*(v_0) = -\lambda_{\min}(A + v_0 BC)$. It should be noted that while we have focused on systems of relative degree two here, a similar algorithm exists for systems of relative degree one.

3.5 Summary

In this chapter, we devised a method of constructing controllers which optimize the rate of convergence of the state trajectory to the origin. Note that, in addition to providing the plant $P(s)$, one must also provide a (sufficiently large) value of the gain bound v_0 in order to determine an optimal controller. Such a requirement is not restrictive in practice since any real implementation will, naturally, impose limits on the maximum gains that can be implemented.

Note that the algorithm described above is not “automatic” in the sense that it does not provide one specific controller but, rather, provides a set of simply-parameterized controllers. From the perspective of asymptotic stability, any one of these controllers is as good as the next, but for general design problems that involve more than just asymptotic stability, the ability to choose amongst a set of controllers offers the designer increased flexibility. This is not an issue that we will discuss in this document as the specific manner in which we choose a controller is, generally, very much tied to a specific application/performance objective, but we merely wish to point out that this non-uniqueness aspect should be viewed as a benefit.

Also, in regards to the ad-hoc procedure of choosing the angle bisector for the original state-space description Eqn. 3.4.5 and 3.4.6, this specific choice was not simply motivated by the (rather obvious) idea of maximizing the minimum angle between q and the eigenvectors w_s and w_u , but is actually mathematically motivated by the fact that this particular solution is actually the limiting solution of a similar *finite time-horizon* problem. For details on the specifics of this problem, the interested reader is referred to some of our previous work that can be found in [42, 43].

3.6 Appendix: Proofs of Technical Statements

Proof of Lemma. 3.4.3

We will prove the statement under the assumption that \tilde{w}_s , \tilde{w}_u , and \tilde{q} are all oriented clockwise; the proof for the case where they are all oriented counterclockwise is similar and is left to the reader. We will begin by showing that the problem is invariant to an invertible change of coordinates. If we let $z = Tx$, then we can prove the equivalent statement that there exists $t > 0$ such that the trajectory $z(t)$ of the system

$$\dot{z} = T^{-1}ATz, \quad z(0) = \hat{p}$$

satisfies the relationship $z(t) = \alpha \hat{q}$ for some $\alpha \in \mathbf{R}$ where $\hat{p} = Tp$ and $\hat{q} = Tq$. We note that, under a coordinate change, the eigenvectors w_s and w_u map to new eigenvectors in z coordinates given by $\hat{w}_s = Tw_s$ and $\hat{w}_u = Tw_u$. We also note that the vectors \tilde{w}_s , \tilde{w}_u , and \tilde{q} are mapped to new vectors $\hat{\tilde{w}}_s = (T^{-1})'\tilde{w}_s$, $\hat{\tilde{w}}_u = (T^{-1})'\tilde{w}_u$, and $\hat{\tilde{q}} = (T^{-1})'\tilde{q}$, by noting, for instance, that

$$\tilde{w}_s' w_s = 0 \implies \hat{\tilde{w}}_s' T^{-1} \hat{w}_s = 0.$$

If we then note that $\hat{w}'_s \hat{q} = \tilde{w}'_s T^{-1} T q = \tilde{w}_s q$ and notice that all other similar inner products satisfy the same preservation of inner products, then we find that the following conditions are satisfied:

$$\hat{w}'_s \hat{q} > 0 \quad (3.6.17)$$

$$\hat{w}'_u \hat{q} < 0 \quad (3.6.18)$$

$$\hat{w}'_s \hat{p} > 0 \quad (3.6.19)$$

$$\hat{q}' \hat{p} < 0 \quad (3.6.20)$$

$$\hat{w}'_s \hat{w}_u \geq 0. \quad (3.6.21)$$

The only thing that remains to be proved is that the clockwise orientation of the vectors \hat{w}_s , \hat{w}_u , and \hat{q} can be preserved under the coordinate transformation. First, note for any vector $w = [w_1 \ w_2]'$ that a clockwise-oriented normal vector is given by $\tilde{w} = \beta [w_2 \ -w_1]'$ where $\beta > 0$. Now

$$Tw = \begin{bmatrix} t_1 & t_2 \\ t_3 & t_4 \end{bmatrix} \begin{bmatrix} w_1 \\ w_2 \end{bmatrix} = \begin{bmatrix} t_1 w_1 + t_2 w_2 \\ t_3 w_1 + t_4 w_2 \end{bmatrix}$$

and

$$(T^{-1})' \tilde{w} = \frac{1}{\det(T)} \begin{bmatrix} t_4 & -t_3 \\ -t_2 & t_1 \end{bmatrix} \begin{bmatrix} w_2 \\ -w_1 \end{bmatrix} = \frac{1}{\det(T)} \begin{bmatrix} t_3 w_1 + t_4 w_2 \\ -t_1 w_1 - t_2 w_2 \end{bmatrix}.$$

If $\det(T) > 0$, it is clear from the above that all three of \hat{w}_s , \hat{w}_u , and \hat{q} are oriented in the clockwise direction. If $\det(T) < 0$, we may, instead, take $\hat{w}_s = -(T^{-1})' \tilde{w}_s$, $\hat{w}_u = -(T^{-1})' \tilde{w}_u$, and $\hat{q} = -(T^{-1})' \tilde{q}$, and the inequalities Eqn. 3.6.17, 3.6.18, and 3.6.19 will still be satisfied.

Without loss of generality, then, we take

$$w_s = \begin{bmatrix} 0 \\ 1 \end{bmatrix}, \quad w_u = \begin{bmatrix} 1 \\ 0 \end{bmatrix}$$

and, correspondingly,

$$\tilde{w}_s = \begin{bmatrix} 1 \\ 0 \end{bmatrix}, \quad \tilde{w}_u = \begin{bmatrix} 0 \\ -1 \end{bmatrix}.$$

Now, if we let $p = [p_1 \ p_2]'$, and $q = [q_1 \ q_2]'$ the inequalities of Eqn. 3.6.17, 3.6.18, and 3.6.19⁴ reduce to $q_1 > 0$, $q_2 > 0$, and $p_1 > 0$, respectively.

Now, in the given coordinates, the solution to $\dot{x} = Ax$, $x(0) = p$ can be written explicitly as

$$x(t) = p_2 \begin{bmatrix} 1 \\ 0 \end{bmatrix} e^{\lambda_s t} + p_1 \begin{bmatrix} 0 \\ 1 \end{bmatrix} e^{\lambda_u t}.$$

We wish to show that there exists $t > 0$ such that $x(t) = \alpha q$ for some $\alpha \in \mathbf{R}$.

⁴Here we replace all “hatted” variables by their “unhatted” form to simplify notation.

This, however, is equivalent to showing that $\tilde{q}'x(t) = 0$ for some $t > 0$. If we take $\tilde{q} = \begin{bmatrix} q_2 & -q_1 \end{bmatrix}$, we find that the constraint $\tilde{q}'x(t) = 0$ has an explicit solution in terms of t given by

$$t = \frac{1}{\lambda_u - \lambda_s} \ln \left(\frac{q_1 p_2}{q_2 p_1} \right).$$

Since $\lambda_u > \lambda_s$, we only need show that the quotient $q_1 p_2 / q_2 p_1$ is greater than 1. Note that the condition of Eqn. 3.6.20 reduces to

$$q_2 p_1 - q_1 p_2 < 0.$$

Since $p_2 > 0$, this is equivalent to

$$q_1 p_2 > q_2 p_1.$$

Now, because $q_2 p_1 > 0$, division by $q_2 p_1$ shows that the quotient in the logarithm is greater than 1, and existence of $t > 0$ is established.

Chapter 4

L2 Gain Stability of Optimal Controllers and Observer-based Control Laws

In this chapter, we prove that the switching laws of the previous chapter that maximize the rate of convergence also satisfy a form of input-output stability known as *finite L_2 gain stability*. After a brief review of the definition of L_2 gain, we begin by establishing that the optimal switching systems of the previous chapter admit a Lyapunov function of a certain structure that we will, eventually, be able to prove acts as a storage function when exogenous inputs are present. Once we have proved this result, we will then discuss the problem of designing observers when only the output of the plant is known rather than the full state. We will show that we can always find a first order observer to estimate the missing state information which, when appropriately combined with the original full-state switching laws we have been studying, retains L_2 gain stability of the overall interconnected system. We will end with some computational considerations for computing upper bounds on the L_2 gain in standard software packages such as MATLAB.

4.1 Introduction

The previous chapters have focused on developing algorithms for designing controllers which are asymptotically stabilizing. If the ultimate goal of our work, however, is to design switching systems for real-world applications, we require another form of stability, namely input-output stability. In typical applications, exogenous inputs to a system are the result of one of the following:

External Command Inputs In most forms of system design, the objective of the design is to process an exogenous input in particular manner so as to produce an output within a certain class. For example, the objective of lowpass filter design is to process the input signal in such a way as to remove its high frequency components. An example more common to control theorists—and one that we will explore in great detail in the next chapter—is that of reference tracking.

Namely, for a given class of input signals $w(t)$, a system is designed so that the output $y(t)$ tracks the input $w(t)$ asymptotically, in the sense that $\lim_{t \rightarrow \infty} |y(t) - w(t)| = 0$.

Disturbances and Noise Even when the objective is simply asymptotic stability and no external inputs are purposely injected into the system dynamics, external inputs in the form of plant disturbances or sensor noise are often present. Indeed, it is because of the presence of these (and other) forms of uncertainty that feedback controllers are a useful construct in the real world. Without uncertainty, some of the simplest illustrations of the use of feedback control would not exist (e.g., we would all be able to balance a pencil on the tip of our finger effortlessly!)

For either of these cases, notions of input-output stability are important as they provide some certificate that the designed system will behave within certain “reasonable” limits. In this chapter, we will prove that the systems we developed in the last chapter satisfy a form of input-output stability known as *L_2 gain stability*. We begin with a definition, borrowed from [52]:

Definition The L_2 gain of a continuous-time system S with input w and output y is the smallest (infimal) value of $\gamma \geq 0$ such that

$$\inf_{T \geq 0} \int_0^T (\gamma^2 \|w(t)\|^2 - \|y(t)\|^2) dt > -\infty$$

for all input/output pairs $y = S(w)$ where input w is square integrable over arbitrary finite intervals.¹

Informally speaking, L_2 gain provides a sort of “power bound.” That is, if a signal $w(t)$ with unit power is input to a system S with L_2 gain γ , the corresponding output $y(t)$ will have power less than or equal to γ . A system is called *L_2 gain stable* if it has finite L_2 gain $\gamma \geq 0$.

The definition of L_2 gain above can often be difficult to use when trying to prove that a particular system S has finite L_2 gain. An often-times more convenient method of proving that a system has finite L_2 gain is to prove existence of a (*generalized*) *storage function* [51, 58]. Informally speaking, a storage function $V(x(t))$ with quadratic supply rate $\sigma(w, x)$ is a positive definite function $V(x)$ which satisfies the relationship

$$\int_0^t \sigma(w(t), x(t)) dt \geq V(x(t)) - V(x(0)) \quad (4.1.1)$$

where x is the system state, and w is an exogenous input. If we consider the quadratic supply rate

$$\sigma(x, w) = \gamma^2 \|w\|^2 - \|y\|^2$$

where $y = h(x, w)$ is a system output, it is clear that existence of a generalized storage function is a sufficient condition for finite L_2 gain stability. What is less obvious (see

¹We will assume this throughout the remainder of the document.

[58, 51] for a proof) is that existence of a storage function is also a *necessary* condition for finite L_2 gain stability. By differentiating Eqn. 4.1.1 with respect to time, we, therefore, find that an equivalent condition for finite L_2 gain stability with L_2 gain γ is existence of a storage function $V(x)$ such that

$$\gamma^2 \|w\|^2 - \|y\|^2 - \frac{d}{dt}V(x(t)) \geq 0$$

along system trajectories. One of the main goals for this chapter is to prove existence of a storage function $V(\cdot)$ such that the above inequality holds along the trajectories of the switching systems we designed in the last chapter. We will do this in two steps: first, we will find a Lyapunov function for the case when the exogenous input vector $w = 0$ that satisfies certain useful properties. We will then use this Lyapunov function as a base for finding a storage function when $w \neq 0$, and will prove finite L_2 gain stability by an appropriate scaling of the Lyapunov function.

Once we have proved that the switching system of the previous chapter is finite L_2 gain stable, we will then investigate the problem of *observer based feedback*. Specifically, we will show that, if the supervisor only has access to the input and output of the plant rather than the full state, an appropriate first order observer can be designed to estimate the missing state information in such a way that the overall interconnected system still preserves finite L_2 gain stability (and, hence, preserves asymptotic stability when no exogenous inputs are present). We will conclude this chapter by briefly discussing methods of actually *computing* numerical upper bounds on the L_2 gain for the switching systems we discuss here by searching for piecewise-quadratic storage functions using MATLAB.

4.2 Preliminaries: Lyapunov Function

We begin by restating the state-space description of the plant of the previous chapter along with the corresponding optimal switching law. The plant dynamics are described via

$$\begin{bmatrix} \dot{x}_1 \\ \dot{x}_2 \end{bmatrix} = \begin{bmatrix} -\frac{a}{2} & \gamma \\ \frac{-b+\frac{a^2}{4}}{\gamma} & -\frac{a}{2} \end{bmatrix} \begin{bmatrix} x_1 \\ x_2 \end{bmatrix} + \begin{bmatrix} 0 \\ \frac{1}{\gamma} \end{bmatrix} u \quad (4.2.2)$$

$$y = x_1 \quad (4.2.3)$$

where $\gamma = \sqrt{a^2/4 - b + v_0}$, and where v_0 satisfies the condition

$$v_0 > \max \left\{ \left| \frac{a^2}{4} - b \right|, 2b - \frac{a^2}{2}, b \right\}. \quad (4.2.4)$$

The control law that we designed to maximize the rate of convergence took the form $u(x) = v(x)y$ with $v(x)$ given by

$$v(x) = \begin{cases} v_0 & x'(\tilde{w}_s \tilde{q}')x \leq 0 \\ -v_0 & x'(\tilde{w}_s \tilde{q}')x > 0 \end{cases} \quad (4.2.5)$$

where $\tilde{q} = [q_2 \quad -q_1]'$ satisfies $q_2 > 0$ along with the condition

$$(\tilde{w}_s' q)(\tilde{w}_u' q) < 0 \quad (4.2.6)$$

where $q = [q_1 \quad q_2]'$. Here, \tilde{w}_s and \tilde{w}_u are the clockwise-oriented normal vectors to the stable and unstable eigenvectors w_s and w_u of the matrix $A + v_0 BC$ where A , B , and C , are the state-space matrices that correspond to the state-space description of Eqn. 4.2.2 and 4.2.3:

$$w_s = \begin{bmatrix} -1 \\ 1 \end{bmatrix}, \quad w_u = \begin{bmatrix} 1 \\ 1 \end{bmatrix}$$

and

$$\tilde{w}_s = \begin{bmatrix} 1 \\ 1 \end{bmatrix}, \quad \tilde{w}_u = \begin{bmatrix} 1 \\ -1 \end{bmatrix}.$$

For convenience, we will abbreviate the closed-loop dynamics of the system $\dot{x} = (A + v(x)BC)x$ in the following way:

$$\dot{x} = \begin{cases} A_1 x & x'(\tilde{w}_s \tilde{q}')x \leq 0 \\ A_2 x & x'(\tilde{w}_s \tilde{q}')x > 0 \end{cases} \quad (4.2.7)$$

where the matrices A_1 and A_2 are given by

$$A_1 = \begin{bmatrix} -\frac{a}{2} & \gamma \\ \gamma & -\frac{a}{2} \end{bmatrix}, \quad A_2 = \begin{bmatrix} -\frac{a}{2} & \gamma \\ \gamma - \frac{2v_0}{\gamma} & -\frac{a}{2} \end{bmatrix} \quad (4.2.8)$$

In the last chapter, we proved that the closed-loop system described by Eqn. 4.2.7 is exponentially stable and, hence, admits a Lyapunov function $V(x)$ which is monotonically decreasing along the system trajectories. Assuming, for the moment, that a smooth Lyapunov function exists, then it will satisfy the conditions

$$-\nabla V(x)A_1 x > 0 \quad x'(\tilde{w}_s \tilde{q}')x \leq 0 \quad (4.2.9)$$

$$-\nabla V(x)A_2 x > 0 \quad x'(\tilde{w}_s \tilde{q}')x > 0. \quad (4.2.10)$$

While the above conditions are sufficient for proving asymptotic stability, the above conditions by themselves are not sufficient for finding a storage function when exogenous inputs are added to the system. To illustrate one of the key issues that arises by trying to use a Lyapunov function that only satisfies the conditions Eqn. 4.2.9 and 4.2.10 as a model for a storage function, consider the case when the switching law

$v(x)$ evolves according to

$$v(x) = \begin{cases} v_0 & (x+g)'(\tilde{w}_s\tilde{q}')(x+g) \leq 0 \\ -v_0 & (x+g)'(\tilde{w}_s\tilde{q}')(x+g) > 0 \end{cases}$$

where $g = g(t)$ is an exogenous input which can be thought of as noise component that corrupts the switching law. It is clear that, for any value of x in the state-space, a value of g can always be chosen so as to “fool” the supervisor, e.g., g is such that $(x+g)'(\tilde{w}_s\tilde{q}')(x+g) \leq 0$ but $x'(\tilde{w}_s\tilde{q}')x > 0$. Without corruption, the dynamics would evolve according to $\dot{x} = A_2x$, but, instead, they evolve according to $\dot{x} = A_1x$, and it is quite possible that $-\nabla V(x)A_1x < 0$. When g is small compared to x (so that x lies close in angle to either q or w_s), this is particularly problematic since, informally speaking, positivity of the expression

$$\gamma^2 \|g\|^2 - \|y\|^2 - \frac{d}{dt}V(x(t))$$

essentially reduces to positivity of $-\nabla V(x)A_1x$ for small g .

We attempt to fix the above problem in the following way: in addition to requiring that $-\nabla V(x)A_1x > 0$ whenever $x'(\tilde{w}_s\tilde{q}')x \leq 0$ and, $-\nabla V(x)A_2x > 0$ whenever $x'(\tilde{w}_s\tilde{q}')x < 0$, we wish to find a Lyapunov function for which $-\nabla V(x)A_ix > 0$ for both $i = 1, 2$ whenever x is close to either q or w_s in an angular sense. While it is not obvious, if we prove existence of a Lyapunov function which satisfies these additional requirements, in the end, we will be able to use it as a storage function to prove that the systems under study have finite L_2 gain.

The main goal of this section is to prove that there exists a piecewise differentiable Lyapunov function for the system of Eqn. 4.2.7 which satisfies the above additional properties. In our effort to prove this, we will actually find a Lyapunov function for a *different* (but related) system and will then prove, in the end, that the Lyapunov function we found for the different system also acts as a Lyapunov function for the first system with the additional requirements we desire to impose.

4.2.1 Auxiliary Switching System

Before we begin our discussion of the new switching system we wish to study, we will re-describe Eqn. 4.2.7 in polar coordinates as it provides a more convenient description for analyzing and proving the results we intend to investigate in this section. The radial component r and the angular component θ can be described via the following dynamics:

$$\begin{bmatrix} \dot{r} \\ \dot{\theta} \end{bmatrix} = \begin{cases} f_1(r, \theta) & \phi_q \leq \theta \leq \frac{3\pi}{4} \text{ or} \\ f_2(r, \theta) & \phi_q + \pi \leq \theta \leq \frac{7\pi}{4} \\ & \text{otherwise} \end{cases} \quad (4.2.11)$$

where $\phi_q \in (\pi/4, 3\pi/4)$ is the angle that the vector q makes with respect to the positive x_1 axis, and the functions $f_1(r, \theta)$ and $f_2(r, \theta)$ are given by

$$f_1(r, \theta) = \begin{bmatrix} -\frac{a}{2}r + \gamma r \sin 2\theta \\ \gamma \cos 2\theta \end{bmatrix}, \quad f_2(r, \theta) = \begin{bmatrix} -\frac{a}{2}r + \left(\gamma - \frac{v_0}{\gamma}\right) r \sin 2\theta \\ \left(\gamma - \frac{v_0}{\gamma}\right) \cos 2\theta - \frac{v_0}{\gamma} \end{bmatrix}. \quad (4.2.12)$$

For a given value of θ , consider now the problem of determining the vector field f_1 or f_2 which maximizes \dot{r} . Since $\gamma > \gamma - v_0/\gamma$, we see that f_1 maximizes \dot{r} for θ lying in the first and third quadrants, while f_2 maximizes \dot{r} for θ lying in the second and fourth quadrants. The new switching system that we will study has dynamics which can be described as follows: the values of θ for which we choose to use f_1 and f_2 in Eqn. 4.2.11 will be almost exactly the same in our new system, with the following exception: around the switchings boundaries w_s (corresponding to θ values of $3\pi/4$ and $7\pi/4$) and q (corresponding to θ values of ϕ_q and $\phi_q + \pi$), we will construct a small cone for which the system dynamics will evolve according to whichever vector field maximizes \dot{r} . Depending upon the value of ϕ_q , this gives rise to three possible situations which are depicted graphically in Fig. 4.2.1. When $\phi_q > \pi/2$, we consider a system which evolves according to the dynamics

$$\begin{bmatrix} \dot{r} \\ \dot{\theta} \end{bmatrix} = \begin{cases} f_1(r, \theta) & \phi_q + \phi_0 \leq \theta \leq \frac{3\pi}{4} - \phi_0 \text{ or} \\ & \phi_q + \phi_0 + \pi \leq \theta \leq \frac{7\pi}{4} - \phi_0 \\ f_2(r, \theta) & \text{otherwise} \end{cases} \quad (4.2.13)$$

where $\phi_0 > 0$ is a small angle. We arrived at this description in the following way: we first investigate the cone described by $3\pi/4 - \phi_0 \leq \theta \leq 3\pi/4 + \phi_0$ (depicted in part (a) of Fig. 4.2.1 as the sector formed by the two dotted lines that surround w_s) and consider the task of choosing the vector field that maximizes \dot{r} in this region. From the analysis in the previous paragraph, we see that f_2 maximizes \dot{r} everywhere in a small cone, so we choose this vector field in the small cone. Similarly, we construct a small cone about q ($\phi_q - \phi_0 \leq \theta \leq \phi_q + \phi_0$) and, again, choose the vector field which maximizes \dot{r} in this region. For $\phi > \pi/2$, we find that, again, f_2 maximizes \dot{r} everywhere in this cone. When ϕ_q is less than $\pi/2$, it turns out that f_1 maximizes \dot{r} everywhere in the cone (depicted in part (b) of the figure), and the corresponding switching system dynamics are described via

$$\begin{bmatrix} \dot{r} \\ \dot{\theta} \end{bmatrix} = \begin{cases} f_1(r, \theta) & \phi_q - \phi_0 \leq \theta \leq \frac{3\pi}{4} - \phi_0 \text{ or} \\ & \phi_q - \phi_0 + \pi \leq \theta \leq \frac{7\pi}{4} - \phi_0 \\ f_2(r, \theta) & \text{otherwise} \end{cases}. \quad (4.2.14)$$

When $\phi_q = \pi/2$, it turns out that f_2 maximizes \dot{r} in the region $\pi/2 \leq \theta \leq \pi/2 + \phi_0$, and that f_1 maximizes \dot{r} in the region $\pi/2 - \phi_0 \leq \theta < \pi/2$, and the corresponding

dynamics are described by

$$\begin{bmatrix} \dot{r} \\ \dot{\theta} \end{bmatrix} = \begin{cases} f_1(r, \theta) & \frac{\pi}{2} + \phi_0 \leq \theta \leq \frac{3\pi}{4} - \phi_0 \quad \text{or} \\ & \frac{3\pi}{2} + \phi_0 + \pi \leq \theta \leq \frac{7\pi}{4} - \phi_0 \quad \text{or} \\ & \frac{\pi}{2} - \phi_0 \leq \theta < \frac{\pi}{2} \quad \text{or} \\ & \frac{3\pi}{2} - \phi_0 \leq \theta < \frac{3\pi}{2} \\ f_2(r, \theta) & \text{otherwise} \end{cases}. \quad (4.2.15)$$

As we will show shortly, in any of the above three cases, for ϕ_0 sufficiently small, the resulting switching systems are exponentially stable. Before we prove this formally, we would like to point out a useful consequence of this statement which, while tangential to our current overall goal of finding a storage function for our original switching system, is a very useful result in its own right.

Stability under Time Delays

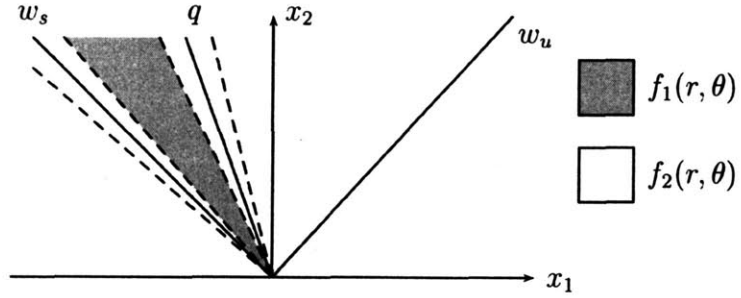
Suppose that the switching law for our original system has a time delay; that is, suppose our switching law is actually $x(t - \tau)' \tilde{w}_s \tilde{q}' x(t - \tau)$ for some $\tau > 0$. For the system of Eqn. 4.2.7, we can rewrite the quadratic form as $x(t)' e^{A_2 \tau} \tilde{w}_s \tilde{q}' e^{A_1 \tau} x(t)$. Hence, under a time delay, our switching law $v(x)$ becomes

$$v(x) = \begin{cases} v_0 & x' F_1 F_2' x \leq 0 \\ -v_0 & x' F_1 F_2' x > 0 \end{cases}$$

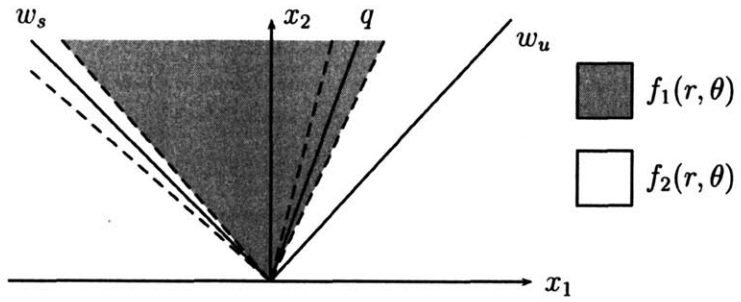
where $F_1 = e^{A_2 \tau} \tilde{w}_s$ and $F_2 = e^{A_1 \tau} \tilde{q}$. Now, because $e^{At} \rightarrow I$ as $t \rightarrow 0$, it is clear that, for τ sufficiently small, the angular difference between F_1 and \tilde{w}_s and the angular difference between F_2 and \tilde{q} tends to 0 as $\tau \rightarrow 0$.

Suppose now that our result regarding the stability of the auxiliary switched system holds, namely that, for ϕ_0 sufficiently small, the auxiliary switched system is exponentially stable. Suppose that τ is small enough to guarantee that the angles between F_1 and \tilde{w}_s and between F_2 and \tilde{q} are both less than θ_0 . Because we designed the auxiliary switching system to maximize \dot{r} in the small cones about \tilde{w}_s and \tilde{q} , it follows that $\dot{r}_{td}(t) \leq \dot{r}_{aux}(t)$ for all $t > 0$, where $\dot{r}_{td}(t)$ represents the radial dynamics of the time delayed system, and where $\dot{r}_{aux}(t)$ represents the radial dynamics of the auxiliary switching system we have designed. For identical initial conditions $r_{td}(0) = r_{aux}(0) = r_0$, it then follows that $r_{td}(t) \leq r_{aux}(t)$ for all $t > 0$. But if the auxiliary switching system is exponentially stable, then it follows that $r_{td}(t) \rightarrow 0$ exponentially as $t \rightarrow \infty$. Hence, if the auxiliary switching system is stable, we can conclude that our original system remains exponentially stable even in the presence of time delays, provided that the time delays are not too large. From a practical standpoint this is an *extremely* important statement, as any practical implementation of the switching systems we present here will inherently possess some time delay.

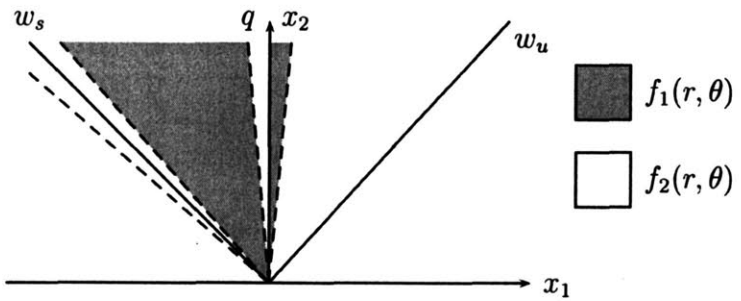
Note that the time delay τ need not be fixed for the above argument to work. Indeed, the above can be extended to hold for a variable time delay $\tau(t) \in [0, \tau_0]$ provided that τ_0 is sufficiently small.



(a) $\phi_q > \pi/2$



(b) $\phi_q < \pi/2$



(c) $\phi_q = \pi/2$

Figure 4.2.1: Auxiliary switching system for the different values of ϕ_q . The dashed lines each make an angle of ϕ_0 with w_s and q , and the system dynamics between the pairs of dashed lines surrounding w_s and q , respectively, are chosen to maximize \dot{r} .

Lyapunov Function Construction

It is clear that if the auxiliary switching system is stable, it admits a Lyapunov function that proves stability. It is also clear that if the auxiliary switched system is stable, then the original system is stable as well (take τ to be 0 for the time-delayed system above). What is not necessarily clear—and which we will spend a fair bit of time proving at the end of this section—is that if we find a Lyapunov function of a particular form for the auxiliary system, this Lyapunov function is also a Lyapunov function for our original system which satisfies the additional criterion that the Lyapunov function is decreasing for *both* vector fields in a small cone around w_s and in a small cone around q .

The remainder of this section is devoted to two technical issues. First, we will prove that the auxiliary switching system that we have defined is exponentially stable for sufficiently small values of ϕ_0 . From this, we will be able to construct a piecewise-differentiable Lyapunov function we will then prove serves as a Lyapunov function for the original system with the extra desired constraints.

4.2.2 Exponential Stability of the Auxiliary Switching System

We will prove stability of the auxiliary switching system of the previous section via *Poincaré maps* [25]. Formally, we will only prove this result for the case where $\phi_q > \pi/2$. The cases where $\phi_q < \pi/2$ and $\phi_q = \pi/2$ follow nearly identical arguments and are left as an exercise for the reader. Examining the top portion of Fig. 4.2.1, we see there is a cone in which the dynamics evolve according to $f_1(r, \theta)$, one of whose boundaries lies very close to the stable eigenvector w_s . Informally speaking, the closer the left-most boundary of that cone lies to the stable eigenvector, the more initial shrinkage the phase portraits will exhibit in the Euclidean norm. It is precisely this fact that we will use to prove exponential stability for sufficiently small ϕ_0 . Specifically, we will prove that the initial shrinkage in the Euclidean norm due to the vector field $f_1(r, \theta)$ can be made arbitrarily small as ϕ_0 tends to 0. Moreover, we will show that any growth in the Euclidean norm due to the vector field $f_2(r, \theta)$ is bounded, and that any phase portrait which starts with an angle of $\theta = 3\pi/4 - \phi_0$ must periodically cross this ray, each time with a Euclidean norm that is smaller than the previous time. From this, we will be able to argue global exponential stability. We will formally prove exponential stability of the auxiliary system through a sequence of propositions.

Proposition 4.2.7 *Consider the system whose dynamics evolve according to Eqn. 4.2.13 with $\phi_q > \pi/2$ and such that $3\pi/4 - \phi_0 > \phi_q + \phi_0$. Consider a trajectory of the system with angular initial condition $\theta(0) = 3\pi/4 - \phi_0$. Then there exists $t_1 > 0$ such that $\theta(t_1) = \phi_q + \phi_0$. Moreover, for every $\epsilon > 0$, there exists δ' such that if $|\phi_0| < \delta'$, $r(t_1) < \epsilon r(0)$.*

Proof We will actually prove this statement in rectangular coordinates. First, note than any initial angular condition $\theta(0) = 3\pi/4 - \phi_0$ with $\phi_0 > 0$ can be thought of

as a scalar multiple of the (rectangular coordinate) initial condition $w_s + \delta w_u$, where $\delta > 0$. As $\delta \rightarrow 0$, the above vector approaches the stable eigenvector w_s , so it is clear that the angle between the above vector and w_s approaches 0 as $\delta \rightarrow 0$. Hence, making ϕ_0 sufficiently small in polar coordinates is equivalent to making δ sufficiently small in rectangular coordinates.

Now, if we let $\lambda_s = \lambda_{\min}(A + v_0 BC)$ and $\lambda_u = \lambda_{\max}(A + v_0 BC)$ (here we note that $A + v_0 BC$ is the matrix which corresponds to the vector field $f_1(r, \theta)$), the condition we wish to show, in terms of rectangular coordinates, can be expressed as existence of $t_1 > 0$ such that

$$w_s e^{\lambda_s t_1} + \delta w_u e^{\lambda_u t_1} = \alpha q_0$$

for some $\alpha \in \mathbf{R}$ where q_0 is a vector with angle $\phi_q + \phi_0$. If we assume that \tilde{q}_0 is oriented clockwise where $\tilde{q}_0' q_0 = 0$, then we find that this condition is equivalent to

$$\tilde{q}_0' w_s e^{\lambda_s t_1} + \delta \tilde{q}_0' w_u e^{\lambda_u t_1} = 0.$$

Now, because \tilde{q}_0 is oriented clockwise, and because $\pi/2 < \phi_q + \phi_0 < 3\pi/4$, we find that \tilde{q}_0 takes the form $\tilde{q}_0 = \begin{bmatrix} q_2 & q_1 \end{bmatrix}'$ with $q_2 > q_1 > 0$. Hence, $\alpha_1 = -\tilde{q}_0' w_s > 0$ and $\alpha_2 = \tilde{q}_0' w_u > 0$, and we find that the above equation has solution

$$t_1 = \frac{1}{\lambda_u - \lambda_s} \ln \left(\frac{\alpha_1}{\delta \alpha_2} \right).$$

Now, note that $r(0) = \|w_s + \delta w_u\| = \sqrt{1 + \delta^2}$. Plugging the expression for t_1 into the expression $w_s \exp(\lambda_s t_1) + \delta w_u \exp(\lambda_u t_1)$ yields

$$r(t_1) = \delta^{-\frac{\lambda_s}{\lambda_u - \lambda_s}} \left(\left(\frac{\alpha_1}{\alpha_2} \right)^{\frac{\lambda_s}{\lambda_u - \lambda_s}} + \left(\frac{\alpha_1}{\alpha_2} \right)^{\frac{\lambda_u}{\lambda_u - \lambda_s}} \right).$$

By assumption, $\lambda_s < 0$, and hence the right-hand side of the above expression tends toward 0 as $\delta \rightarrow 0$, whereas $r(0) \geq 1$ for all $\delta > 0$, and, therefore, the statement holds. □

Proposition 4.2.8 *Consider the system whose dynamics evolve according to Eqn. 4.2.13 with $\phi_q > \pi/2$ and such that $3\pi/4 - \phi_0 > \phi_q + \phi_0$. Consider a trajectory of this system with initial angular condition given by $\theta(0) = \phi_q + \phi_0$. There exists $t_2 > 0$ for which $\theta(t_2) = -\pi/4 - \phi_0$ and such that the following conditions are satisfied:*

1. *For every $\phi_0 < 3\pi/8 + 0.5\phi_q$, there exists $T > 0$ such that $t_2 = t_2(\phi_0) < T$.*
2. *$\theta((k+1)t_1 + kt_2) = 3\pi/4 - \phi_0 - k\pi$ for every $k \in \mathbf{Z}^+$ where t_1 is defined as in Prop. 4.2.7.*

Informally, Prop. 4.2.8 tells us that any trajectory that starts on the ray $\phi_q + \phi_0$ must cross eventually cross the ray $-\pi/4 - \phi_0$ in bounded time. Combining this with

the result of Prop. 4.2.7, we arrive at the second numbered item. namely that any trajectory which starts on the line determined by the ray $\theta = 3\pi/4 - \phi_0$ must cross this line periodically.

Proof If $\theta(0) = \phi_q + \phi_0$, then the system evolves according to $f_2(r, \theta)$ until the state trajectory crosses the ray $\theta = -\pi/4 - \phi_0$. To see this, first note that

$$\dot{\theta} = \left(\gamma - \frac{v_0}{\gamma} \right) \cos 2\theta - \frac{v_0}{\gamma} \leq \max \left\{ \gamma - \frac{2v_0}{\gamma}, -\gamma \right\} \triangleq \beta.$$

By our assumption that $v_0 > 2b - a^2/2$, both terms in the above maximization are strictly negative, so $\beta < 0$. Hence, we find that t_2 such that $\theta(t_2) = -\pi/4 - \phi_0$ exists and satisfies

$$t_2 < \frac{\phi_q + \frac{\pi}{4} + 2\phi_0}{\beta}.$$

Moreover, since $\phi_0 < 3\pi/8 + 0.5\phi_q$, we can further upper bound this by

$$t_2 < \frac{2\phi_q + \pi}{\beta} \triangleq T. \quad (4.2.16)$$

Now, from the result of Prop. 4.2.7, if $\theta(-t_1) = 3\pi/4 - \phi_0$, then $\theta(0) = \phi_q + \phi_0$ as desired, and $\theta(t_2) = -\pi/4 - \phi_0$. Now, since this switching system is both homogeneous and time invariant, it follows that, starting at time t_2 , θ will decrease another π radians to $-5\pi/4 - \phi_0$ in another $t_1 + t_2$ seconds. Continuing on in an inductive manner, we, indeed find that $\theta((k+1)t_1 + kt_2) = -\pi/4 - \phi_0 - k\pi$. \square

Proposition 4.2.9 *Consider the system whose dynamics evolve according to Eqn. 4.2.13 with $\phi_q > \pi/2$ and such that $3\pi/4 - \phi_0 > \phi_q + \phi_0$. Consider a trajectory of this system with initial angular condition given by $\theta(0) = 3\pi/4 - \phi_0$. Then, for every $\alpha \in (0, 1)$, there exists sufficiently small $\phi_0 > 0$ such that $r(k(t_1 + t_2)) < \alpha^k r(0)$ for all $k \in \mathbf{Z}^+$ where t_1 and t_2 are defined as in Prop. 4.2.7 and 4.2.8.*

Proof By Prop. 4.2.7, we know that we can choose ϕ_0 sufficiently small so that $r(t_1) < \epsilon r(0)$ for every $\epsilon > 0$. Now, because $t_2 < T$ of Eqn. 4.2.16 for all values of ϕ_0 sufficiently small, we find that $r(t_1 + t_2) < \exp(MT)r(t_1)$ where M is given by

$$M = \max_{\theta \in [0, 2\pi]} \left(-\frac{a}{2} + \gamma \sin 2\theta \right).$$

It hence follows that $r(t_1 + t_2) < \epsilon M r(0)$. Letting $\epsilon = \alpha/M$, we have that $r(t_1 + t_2) < \alpha r(0)$. If we again invoke the fact that the system is both homogeneous and time invariant, we obtain the more general result that $r(k(t_1 + t_2)) < \alpha^k r(0)$ for all $k \in \mathbf{Z}^+$. \square

Proposition 4.2.10 *The system whose dynamics evolve according to Eqn. 4.2.13 with $\phi_q > \pi/2$ is globally exponentially stable for sufficiently small ϕ_0 .*

Proof First, note that any initial angle $\theta(0)$ must lie along a trajectory which passes through the line determined by the ray $\theta = 3\pi/4 - \phi_0$. If this were not the case, then our result that $\theta(t)$ traverses from $3\pi/4 - \phi_0$ to $-\pi/4 - \phi_0$ in $t_1 + t_2$ units of time would not be true for the following reason: suppose that there exists some angle θ_0 such that if $\theta(0) = \theta_0$, $\theta(t) \neq 3\pi/4 - \phi_0 - k\pi$ for any $k \in \mathbf{Z}$. Now consider a trajectory for which $\theta'(0) = 3\pi/4 - \phi_0$. By continuity of $\theta'(t)$, it follows that there exists some time $t_3 > 0$ for which $\theta'(t_3) = \theta_0$. But by time invariance, it then follows $\theta'(t) \neq 3\pi/4 - \phi_0 - 2k\pi$ for any $k \in \mathbf{Z}$ and for any $t > t_3$, which clearly contradicts the result of Prop. 4.2.8.

Now, for any initial angle $\theta(0)$, it follows that there exists $t_4 \geq 0$ such that $\theta(t_4) = 3\pi/4 - \phi_0$ or $\theta(t_4) = -\pi/4 - \phi_0$. Moreover, we have that $\theta(t_4 + k(t_1 + t_2)) = 3\pi/4 - \phi_0 - k\pi$ or $\theta(t_4 + k(t_1 + t_2)) = -\pi/4 - \phi_0 - k\pi$ for all $k \in \mathbf{Z}^+$. Hence, for ϕ_0 sufficiently small, we conclude from Prop. 4.2.9 that we can find $\alpha \in (0, 1)$ such that

$$r(t_4 + k(t_1 + t_2)) < \alpha^k r(t_4) \rightarrow 0$$

as $k \rightarrow \infty$. Hence, a certain set of *samples* of $r(t)$ are guaranteed to tend to 0 as $t \rightarrow \infty$. To extend this result to general t , we note the following: for any value of t such that $t_4 + k(t_1 + t_2) \leq t \leq t_4 + (k+1)(t_1 + t_2)$,

$$r(t) \leq e^{M(t_1+t_2)} r(t_4 + k(t_1 + t_2))$$

where M is defined as in Prop. 4.2.9. Since the right-hand side of the above inequality tends to 0 exponentially as $k \rightarrow \infty$, we conclude that $r(t) \rightarrow 0$ exponentially as $t \rightarrow \infty$. \square

4.2.3 Construction of Piecewise Differentiable Lyapunov Function for Auxiliary System

Now that we have proved that the auxiliary system is exponentially stable, we will prove that it has a Lyapunov function which is strictly decreasing along system trajectories and which is piecewise differentiable. We will prove these statements in rectangular coordinates as, ultimately, we would like to express our storage function in rectangular coordinates. As before, we will prove these statements only for the case when $\phi_q > \pi/2$ and leave the other two cases to the reader. The first formal statement that we will show is the following:

Proposition 4.2.11 *Consider the system*

$$\dot{x} = f(x) = \begin{cases} (A + v_0 BC)x & x' F_1 F_2' x \leq 0 \\ (A - v_0 BC)x & x' F_1 F_2' x > 0 \end{cases} \quad (4.2.17)$$

where A , B , and C are the state-space matrices corresponding to 4.2.2 and 4.2.3, and where F_1 is the clockwise-oriented normal vector to the ray $\theta = 3\pi/4 - \phi_0$ and F_2 is the clockwise-oriented normal vector to the ray $\theta = \phi_q + \phi_0$. Then for ϕ_0 sufficiently

small, the function

$$V(x_0) = \int_0^\infty \|x(\tau)\|^2 d\tau$$

where $x(t)$ is the solution to Eqn. 4.2.17 with initial condition $x(0) = x_0$ is a Lyapunov function which is strictly decreasing along the trajectories of Eqn. 4.2.17.

Proof First, note that as a result of Prop. 4.2.10, if ϕ_0 is sufficiently small, then Eqn. 4.2.17 is exponentially stable and hence admits constants $M, \beta > 0$ such that

$$\|x(t)\| \leq M e^{-\beta t} \|x(0)\|$$

along all trajectories of the system. Hence, $V(x_0)$ is well defined as the the integral converges for each $x(0) \in \mathbf{R}^2$.

It is clear that $V(x_0)$ is positive definite. Indeed, $V(x_0) = 0$ if and only if $\|x(t)\| = 0$ for all $t > 0$, but this can only happen for the system of Eqn. 4.2.17 if $x_0 = 0$. Also, $V(x_0) \rightarrow \infty$ as $x_0 \rightarrow \infty$. Indeed, due to the homogeneity of Eqn. 4.2.17, $V(\lambda x_0) = \lambda^2 V(x_0)$ which tends toward infinity as $\lambda \rightarrow \infty$ for any nonzero x_0 . Hence, $V(x_0)$ is a viable candidate Lyapunov function for proving global exponential stability.

In order to show that the candidate Lyapunov function is strictly decreasing along the system trajectories, we need to show that for any system trajectory $x(t)$ and for any times $t_2 > t_1$, then $V(x(t_1)) > V(x(t_2))$. Consider any trajectory of Eqn. 4.2.17 and denote $x(t_1) = x_1$ and $x(t_2) = x_2$ for any times $t_2 > t_1$. By definition,

$$V(x(t_1)) = V(x_1) = \int_0^\infty \|\tilde{x}(\tau)\|^2 d\tau$$

for a state trajectory $\tilde{x}(t)$ with initial condition $\tilde{x}(0) = x_1$. Now, for any $x_1 \neq 0$,

$$\begin{aligned} V(x_1) &= \int_0^\infty \|\tilde{x}(\tau)\|^2 d\tau \\ &= \int_0^{t_2-t_1} \|\tilde{x}(\tau)\|^2 d\tau + \int_{t_2-t_1}^\infty \|\tilde{x}(\tau)\|^2 d\tau \\ &> \int_{t_2-t_1}^\infty \|\tilde{x}(\tau)\|^2 d\tau \\ &= \int_0^\infty \|\hat{x}(\tau)\|^2 d\tau \\ &= V(\hat{x}(0)). \end{aligned}$$

where $\hat{x}(t) = \tilde{x}(t + (t_2 - t_1))$. Note that $\hat{x}(0) = \tilde{x}(t_2 - t_1)$. Also note, due to the time invariant nature of Eqn. 4.2.17 that $x(t + t_1) = \tilde{x}(t)$ for all $t > 0$. Hence, $\hat{x}(0) = x(t_2) = x_2$, and we conclude that

$$V(x(t_1)) = V(x_1) > V(x_2) = V(x(t_2))$$

as desired. □

We would now like to show that the Lyapunov function $V(x)$ of Prop. 4.2.11 is piecewise differentiable. More specifically, we wish to show the following:

Proposition 4.2.12 *Consider the Lyapunov function $V(x_0)$ of Prop. 4.2.11. Within each cone $x'F_1F_2'x \leq 0$ and $x'F_1F_2'x > 0$ where F_1 and F_2 are given as in Prop. 4.2.11, the partial derivatives $\partial V/\partial x_1$ and $\partial V/\partial x_2$ exist and are continuous.*

The proof of this statement will rely on the following result from Functional Analysis, taken directly from [25]:

Theorem 4.2.4 (Implicit Function Theorem) *Assume that $f : \mathbf{R}^n \rightarrow \mathbf{R}^m \rightarrow \mathbf{R}^n$ is continuously differentiable at each point (x, y) of an open set $S \subset \mathbf{R}^n \times \mathbf{R}^m$. Let (x_0, y_0) be a point in S for which $f(x_0, y_0) = 0$ and for which the Jacobian matrix $[\partial f/\partial x](x_0, y_0)$ is nonsingular. Then there exist neighborhoods $U \subset \mathbf{R}^n$ of x_0 and $V \subset \mathbf{R}^m$ of y_0 such that for each $y \in V$ the equation $f(x, y) = 0$ has a unique solution $x \in U$. Moreover, this solution can be written in the form $x = g(y)$ where g is continuously differentiable at $y = y_0$.*

Proof [Proof of Prop. 4.2.12] We will prove the statement for a point $x_0 = [x_1 \ x_2]'$ which lies in the set $x_0'F_1F_2'x_0 > 0$; the proof for $x_0'F_1F_2'x_0 \leq 0$ is similar. For each initial condition $x(0) = x_0$ such that $x_0'F_1F_2'x_0 > 0$, there exists a time $T(x_0)$ for which $x(t) = \alpha G_1$ where G_1 corresponds to the ray $\theta = 3\pi/4 - \phi_0$ and $\alpha \in \mathbf{R}$, and where we assume G_1 is normalized to have Euclidean length 1. Note that we can write $V(x_0)$ as

$$\begin{aligned} V(x_0) &= \int_0^\infty \|e^{A_2\tau} x_0\|^2 d\tau \\ &= \int_0^{T(x_0)} \|e^{A_2\tau} x_0\|^2 d\tau + \int_{T(x_0)}^\infty \|x(t)\|^2 d\tau \end{aligned}$$

where A_2 is given as in Eqn. 4.2.8. Performing a time-invariance argument similar to the one used in the Proof of Prop. 4.2.11, the second integral can be expressed as

$$\int_{T(x_0)}^\infty \|x(t)\|^2 d\tau = V(\|e^{A_2T(x_0)} x_0\|^2 G_1) = \|e^{A_2T(x_0)} x_0\|^2 V(G_1)$$

where the last equality follows from the fact that V is homogeneous of degree 2. Hence,

$$V(x_0) = \int_0^{T(x_0)} \|e^{A_2\tau} x_0\|^2 d\tau + \|e^{A_2T(x_0)} x_0\|^2 V(G_1).$$

Assuming for the moment that the partial derivatives of V exist, they can be expressed as

$$\begin{aligned} \frac{\partial V}{\partial x_i} &= \int_0^{T(x_0)} \frac{\partial}{\partial x_i} (x_0' e^{A_2\tau} e^{A_2\tau} x_0) d\tau + \|e^{A_2T(x_0)} x_0\|^2 \frac{\partial T}{\partial x_i} \\ &\quad + V(G_1) \frac{\partial}{\partial x_i} (x_0' e^{A_2T(x_0)} e^{A_2T(x_0)} x_0) \end{aligned}$$

for $i = 1, 2$. Because the partial derivatives of the quadratic forms in the above expression are continuously differentiable everywhere, we see that the partial derivatives of V will be continuously differentiable within the cone $x'F_1F_2'x > 0$ if the partial derivatives of $T(x_0)$ are continuously differentiable within the cone. We will now proceed to show that this is, indeed, the case.

First, note that $T(x_0)$ can be characterized implicitly by the constraint

$$F_2'e^{A_2T(x_0)}x_0 = 0.$$

Note that the left-hand side of the above can be viewed as a function $f(T, x_0) : \mathbf{R} \times \mathbf{R}^2 \rightarrow \mathbf{R}$. It is clear that f is continuously differentiable on the open set $\mathbf{R}^+ \times S$ where $S = \{x_0 : x_0'F_1F_2'x_0 > 0\}$, and that $T(x_0)$ is implicitly defined by the relation $f(T, x_0) = 0$. We now wish to show that the Jacobian matrix

$$\frac{\partial f}{\partial T} = F_2'A_2e^{A_2T}x_0 \neq 0$$

for any $T \in \mathbf{R}^+, x_0 \in S$ such that $f(T, x_0) = 0$. Suppose that the Jacobian is 0. This then implies that the equation

$$\begin{bmatrix} F_1'e^{A_2T} \\ F_1'A_2e^{A_2T} \end{bmatrix} x_0 = 0$$

has a solution for some nonzero x_0 . Because e^{A_2T} is invertible for all T , this implies that the matrix

$$\begin{bmatrix} F_1 \\ F_1A_2 \end{bmatrix}$$

is singular. Since F_1 is nonzero, the above matrix will be singular if and only if $F_1A_2 = \lambda F_1$ for some $\lambda \in \mathbf{R}$, i.e., if F_1 is a left eigenvector of A_2 . By construction, A_2 is a real matrix with complex eigenvalues, and, hence, its eigenvectors have nonzero imaginary part, whereas F_1 is purely real-valued. Therefore, F_1 cannot be a left eigenvector of A_2 and we conclude that if $f(T, x_0) = 0$, then $[\partial f / \partial T](T, x_0)$ must be nonzero. By the Implicit Function Theorem, Thm. 4.2.4, we conclude that, for each $x_0 \in S$, there exists an open neighborhood for which $T(x_0)$ is continuously differentiable. Since this result holds for *every* $x_0 \in S$, we conclude that $T(x_0)$ is continuously differentiable over the entire cone. Combining this with our previous results show that $\partial V / \partial x_i$ for $i = 1, 2$ exist and are continuous over the entire cone. \square

Robust Lyapunov Function for Original System

Our final result—the original goal of this section—is to show the following:

Theorem 4.2.5 *Consider the function $V(\cdot)$ of Prop. 4.2.11 where ϕ_0 is sufficiently small to guarantee that $V(x_0)$ is a Lyapunov function for the system of Eqn. 4.2.11. Then $V(\cdot)$ is a Lyapunov function for the original system of Eqn. 4.2.2 and Eqn.*

4.2.3 and satisfies the conditions

$$\begin{aligned} -\nabla V(x)A_1x &> 0, \quad x'\tilde{w}_s'\tilde{q}x \leq 0 \\ -\nabla V(x)A_2x &> 0, \quad x'\tilde{w}_s'\tilde{q}x > 0. \end{aligned}$$

Moreover, there exists a small cone about the vectors w_s and q for which the Lyapunov function is decreasing along both vector fields, i.e.

$$-\nabla V(x)A_i x > 0, \quad x'H_{1i}H'_{2i}x \leq 0$$

for $i = 1, 2$, where A_i are given as in Eqn. 4.2.8, H_{11} and H_{21} are clockwise-oriented normal vectors to the rays $\theta = 3\pi/4 - \phi_1$ and $\theta = 3\pi/4 + \phi_1$, and where H_{21} and H_{22} are clockwise-oriented normal vectors to the rays $\theta = \phi_q - \phi_1$ and $\theta = \phi_q + \phi_1$ where $\phi_1 > 0$ is sufficiently small.

Proof For one final time, we will return to polar coordinates to prove this statement. Note that, in polar coordinates, V can be expressed as

$$V(r, \theta) = r^2 f(\theta)$$

since V is homogeneous of degree 2. Moreover, the partial derivatives $\partial V/\partial r$ and $\partial V/\partial \theta$ are continuous within $x'F_1F'_2x \leq 0$ and $x'F_1F'_2x > 0$ where F_1, F_2 are defined as in Prop. 4.2.11. To see this, note that, since, $x_1 = r \cos \theta$ and $x_2 = r \sin \theta$,

$$\begin{aligned} \frac{\partial V}{\partial r} &= \frac{\partial V}{\partial x_1} \cos \theta + \frac{\partial V}{\partial x_2} \sin \theta \\ \frac{\partial V}{\partial \theta} &= -\frac{\partial V}{\partial x_1} r \sin \theta + \frac{\partial V}{\partial x_2} r \cos \theta \end{aligned}$$

from which continuous differentiability in the indicated regions is clear. ²

For $\phi_q > \pi/2$, by construction, the vector field of the auxiliary system and the original system are the same in the regions $x'H_{11}H'_{22}x \leq 0$ and $x'H_{12}H'_{21}x > 0$ (for a graphical depiction of this, in Fig. 4.2.1, $x'H_{11}H'_{22}x \leq 0$ corresponds to the shaded region, and $x'H_{12}H'_{21}x > 0$ corresponds to the non-shaded region excluding the small regions containing w_s and q that are bound by the dashed lines). Hence, we have that $-\nabla V(x)A_1x > 0$ in the region $x'H_{11}H'_{22}x \leq 0$ and $-\nabla V(x)A_2x > 0$ in the region $x'H_{12}H'_{21}x > 0$, as desired. We also have that $-\nabla V(x)A_2x > 0$ in the regions $x'H_{11}H'_{12}x \leq 0$ and $x'H_{21}H'_{22}x \leq 0$ by virtue of the fact that V is a Lyapunov function for the auxiliary system. The only thing that remains to be shown, then, is that $-\nabla V(x)A_1x > 0$ in the regions $x'H_{11}H'_{12}x \leq 0$ and $x'H_{21}H'_{22}x \leq 0$. In polar coordinates, this amounts to showing that

$$\frac{\partial V}{\partial r} f_{11}(r, \theta) + \frac{\partial V}{\partial \theta} f_{12}(r, \theta) > 0$$

²Strictly speaking, the partial derivatives are continuous in the *open* region $x'F_1F'_2x < 0$ rather than the closed region $x'F_1F'_2x \leq 0$, but this subtlety will not make a difference in our analysis.

for $\theta \in [3\pi/4 - \phi_1, 3\pi/4 + \phi_1]$ and $\theta \in [\phi_q - \phi_1, \phi_q + \phi_1]$ for sufficiently small $\phi_1 > 0$, where $f_{11}(r, \theta)$ and $f_{12}(r, \theta)$ are the first and second components, respectively, of the vector field $f_1(r, \theta)$ of Eqn. 4.2.12. Direct computation shows that the above expression can be written as

$$-2r^2 f(\theta) \left(-\frac{a}{2} + \gamma \sin 2\theta \right) - r^2 f'(\theta) \gamma \cos 2\theta > 0 \quad (4.2.18)$$

where $f'(\theta) = df/d\theta$. We consider the cases $\theta \in [3\pi/4 - \phi_1, 3\pi/4 + \phi_1]$ and $\theta \in [\phi_q - \phi_1, \phi_q + \phi_1]$ separately, considering the former case first. Note that since $\theta = 3\pi/4$ corresponds to the stable eigenvector w_s of the matrix A_1 , $(-a/2 + \gamma) < 0$. Moreover, since $f(\theta) > 0$ for all θ by construction, we have that $-2r^2 f(\theta)(-a/2 + \gamma) < 0$. Now, by continuity of $f(\theta)$, there exists $\phi_2 > 0$ and a positive real number M such that

$$-2r^2 f(\theta) \left(-\frac{a}{2} + \gamma \sin 2\theta \right) \geq Mr^2 > 0$$

for all $\theta \in [3\pi/4 - \phi_2, 3\pi/4 + \phi_2]$. Consider, now, values of ϕ_2 such that $\phi_0 > \phi_2 > 0$. By construction, $f'(\theta)$ exists and is continuous in the region $\theta \in [3\pi/4 - \phi_0, 3\pi/4 + \phi_0]$ and, hence, is continuous in the region $\theta \in [3\pi/4 - \phi_2, 3\pi/4 + \phi_2]$. Now because $\cos 2\theta \rightarrow 0$ as $\theta \rightarrow 3\pi/4$, it follows that for ϕ_2 sufficiently small,

$$r^2 f'(\theta) \gamma \cos 2\theta > -\frac{M}{2} r^2$$

for all $\theta \in [3\pi/4 - \phi_2, 3\pi/4 + \phi_2]$. Thus, it follows that

$$-2r^2 f(\theta) \left(-\frac{a}{2} + \gamma \sin 2\theta \right) - r^2 f'(\theta) \gamma \cos 2\theta > \frac{M}{2} r^2 > 0$$

for all $\theta \in [3\pi/4 - \phi_2, 3\pi/4 + \phi_2]$.

To prove positivity of Eqn. 4.2.18 in the region $\theta \in [\phi_q - \phi_1, \phi_q + \phi_1]$ for $\phi_1 > 0$ sufficiently small, note that by virtue of the fact that $-\nabla V(x)A_2x > 0$ in the region $\theta \in [\phi_q - \phi_0, \phi_q + \phi_0]$, we have the inequality

$$-2r^2 f(\theta) \left(-\frac{a}{2} + \left(\gamma - \frac{v_0}{\gamma} \right) \sin 2\theta \right) - r^2 f'(\theta) \left(\left(\gamma - \frac{v_0}{\gamma} \right) \cos 2\theta - \frac{v_0}{\gamma} \right) > 0 \quad (4.2.19)$$

in this region. Eqn. 4.2.19 implicitly defines a lower bound bound on $f'(\theta)$ in the region $\theta \in [\phi_q - \phi_0, \phi_q + \phi_0]$. Noting that for $\phi_q > \pi/2$ and $\phi_0 > 0$ sufficiently small, $-\cos 2\theta > 0$ for all $\theta \in [\phi_q - \phi_0, \phi_q + \phi_0]$, if we solve for $f'(\theta)$ in Eqn. 4.2.19 and plug the resulting lower bound into Eqn. 4.2.18, we arrive at the following lower bound for Eqn. 4.2.18 in the region $\theta \in [\phi_q - \phi_0, \phi_q + \phi_0]$:

$$-2r^2 f(\theta) \left(-\frac{a}{2} + \gamma \sin 2\theta \right) - r^2 f'(\theta) \gamma \cos 2\theta > v_0 r^2 f(\theta) \left(-2 \sin 2\theta + \frac{a}{\gamma} \cos 2\theta + \frac{a}{\gamma} \right).$$

We will now verify that the quantity

$$g(\theta) = -2 \sin 2\theta + \frac{a}{\gamma} \cos 2\theta + \frac{a}{\gamma} \quad (4.2.20)$$

is positive for all $\theta \in (\pi/2, 3\pi/4)$ (and, hence, for $\theta \in [\phi_q - \phi_0, \phi_q + \phi_0]$ for all $a \in \mathbf{R}$ where, as always, $\gamma = \sqrt{a^2/4 - b + v_0}$ with $v_0 \geq b$). First, note that for $a \geq 0$

$$-2 \sin 2\theta + \frac{a}{\gamma} \cos 2\theta + \frac{a}{\gamma} \geq -2 \sin 2\theta > 0$$

for $\theta \in (\pi/2, 3\pi/4)$. Now, for $a < 0$, notice that Eqn. 4.2.20 has a local maximum inside the range $(\pi/2, 3\pi/4)$. Indeed, differentiating once shows that $g(\theta)$ has a critical point θ^* when $\tan 2\theta^* = -2\gamma/a$. Since $a < 0$, this implies that both $\sin 2\theta^*$ and $\cos 2\theta^*$ are both negative (since $-2\gamma/a > 0$ and $2\theta^*$ lies in the third quadrant), from which we deduce

$$\sin 2\theta^* = \frac{-2\gamma}{\sqrt{4\gamma^2 + a^2}}, \quad \cos 2\theta^* = \frac{a}{\sqrt{4\gamma^2 + a^2}}.$$

If we now compute $g''(\theta^*)$, we find that it is equal to

$$g''(\theta^*) = -\frac{4}{\gamma} \sqrt{4\gamma^2 + a^2} < 0$$

which implies that $g(\theta)$ takes on local maximum at θ^* . Hence, for $\theta \in [\pi/2, 3\pi/4]$, $g(\theta)$ takes on its minimal value at either $\theta = \pi/2$ or $\theta = 3\pi/4$. If both of these quantities are nonnegative, this will imply that $g(\theta) > 0$ in the open interval $\theta \in (\pi/2, 3\pi/4)$. Moreover, since $g(\pi/2) = 0$, positivity will follow if $g(3\pi/4) \geq 0$. Now

$$g\left(\frac{\pi}{4}\right) = 2 + \frac{a}{\gamma}.$$

Using our assumption that $v_0 \geq b$, we find that $|a/\gamma| \leq 2$ and, hence $g(3\pi/4) \geq 0$. Finally, if we take

$$\phi_1 = \min\{\phi_0, \phi_2\} = \phi_2,$$

we see that our Lyapunov function is decreasing along both vector fields A_1x and A_2x in a small cone about w_s and q , as desired. Note that the proof for the cases when $\phi_q < \pi/2$ and $\phi_q = \pi/2$ are similar and are left to the reader. \square

4.3 L2 Gain Stability: Full State Information

We are now ready to consider the problem of proving that the systems under investigation are finite L_2 gain stable. Specifically, we wish to investigate the following setup: consider signals $g_i(t)$ for $i = 1, 2$, and 3 and consider the following system

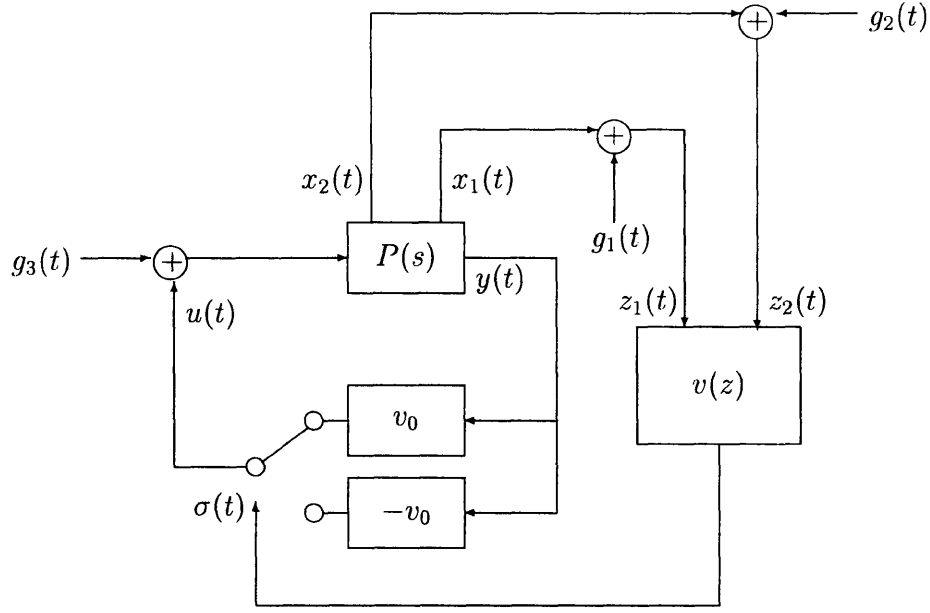


Figure 4.3.2: Block diagram depicting where the exogenous signals $g_1(t)$, $g_2(t)$, and $g_3(t)$ enter into the system dynamics for the full state L_2 gain problem.

dynamics:

$$\begin{bmatrix} \dot{x}_1 \\ \dot{x}_2 \end{bmatrix} = \begin{bmatrix} -\frac{a}{2} & \gamma \\ \frac{-b+\frac{a^2}{4}}{\gamma} & -\frac{a}{2} \end{bmatrix} \begin{bmatrix} x_1 \\ x_2 \end{bmatrix} + \begin{bmatrix} 0 \\ \frac{1}{\gamma} \end{bmatrix} (u + g_3(t)) \quad (4.3.21)$$

$$y = x_1 \quad (4.3.22)$$

where, as before, $\gamma = \sqrt{a^2/4 - b + v_0}$. We now consider a control law of the form $u(z) = v(z)y$ where $z = x + \hat{g}$ with $\hat{g} = [g_1(t) \ g_2(t)]'$, and where $v(z)$ is given by

$$v(z) = \begin{cases} v_0 & z'(\tilde{w}_s \tilde{q}')z \leq 0 \\ -v_0 & z'(\tilde{w}_s \tilde{q}')z > 0 \end{cases} \quad (4.3.23)$$

If we define $g \triangleq [g_1(t) \ g_2(t) \ g_3(t)]'$, the formal statement that we wish to prove in this section is the following: under the assumptions on v_0 given by Eqn. 4.2.4, for any matrices $E \in \mathbf{R}^{m \times 2}$ and $F \in \mathbf{R}^{m \times 3}$ where $m \in \mathbf{Z}^+$, there exists $\gamma > 0$ such that

$$\inf_{T>0} \int_0^T (\gamma^2 \|g\|^2 - \|Ex + Fg\|^2) dt > -\infty.$$

In other words, we wish to prove that the L_2 gain from the vector g to any linear combination of the state and output is finite.

Fig. 4.3.2 depicts graphically where the signals $g_1(t)$, $g_2(t)$, and $g_3(t)$ enter the system dynamics. We see that $g_1(t)$ and $g_2(t)$ “corrupt” the information that is

passed to the switching law $v(z)$ (which, in the absence of either $g_1(t)$ or $g_2(t)$ is equal to the optimal switching law $v(x)$ of the previous section and the previous chapter), while $g_3(t)$ corrupts the control input $u(t)$. A few words on the generality of this model are in order. There are three additional spots in the block diagram where exogenous inputs could be added: one at the input to the gain v_0 , another at the input to the gain $-v_0$, and another at the output of the supervisor $v(z)$. The first two inputs are effectively modelled by the input $g_3(t)$, as we show now. First note that the control signal $u(t)$ can be expressed as

$$u(t) = v_0 y(t) f(t) - v_0 y(t) (1 - f(t)) + v_0 g_4(t) f(t) - v_0 g_5(t) (1 - f(t))$$

where $f(t) \in \{0, 1\}$ for all t , $g_4(t)$ is an exogenous input added to the block with gain v_0 , and $g_5(t)$ is an exogenous input added to the block with gain $-v_0$. We see that $f(t)$ represents the times for which the switching signal $\sigma(t)$ selects v_0 as the feedback gain, whereas $1 - f(t)$ represents the times for which $\sigma(t)$ selects $-v_0$ as the gain. Note that $f(t)$ is *not* a fixed waveform, but, instead depends upon all exogenous inputs and the initial state of the system. Nevertheless, we can model the signal $u(t)$ via

$$u(t) = v_0 y(t) f(t) - v_0 y(t) (1 - f(t)) + g'_3(t)$$

where

$$g'_3(t) = v_0 g_4(t) f(t) - v_0 g_5(t) (1 - f(t)),$$

i.e., we can model the disturbances $g_4(t)$ and $g_5(t)$ present at the *input* to the switching gains as an equivalent disturbance at the *output* of the switching gains. Now, $g'_3(t)$ plays the role of $g_3(t)$ depicted in Fig. 4.3.2. The key question that remains is whether the L_2 gain from $g_4(t)$ and $g_5(t)$ to any linear function of the state and input will be finite. Suppose for the moment that the result of this section holds and that L_2 gain due to the equivalent input $g'_3(t)$ to any linear function of the state and input is finite. Then the L_2 gain from the inputs $g_4(t)$ and $g_5(t)$ to any linear combination of the state and input must be finite as well as a result of the *submultiplicative property* of L_2 gains (see Prop. 5.3.16 of Chapter 5). Indeed, the L_2 gain from $g_4(t)$ and $g_5(t)$ to any linear combination of the state and input $Ex + Fg$ is upper bounded by the product of two L_2 gains: the product of the L_2 gain from $g'_3(t)$ to $Ex + Fg$ and the L_2 gain from $g_4(t)$ and $g_5(t)$ to $g'_3(t)$. Hence, if the L_2 gain from $g_4(t)$ and $g_5(t)$ to $g'_3(t)$ is finite, the problem of finite L_2 gain from $g_4(t)$ and $g_5(t)$ to any linear combination of the state and input will reduce to the finite L_2 gain of the set-up shown in Fig. 4.3.2. As we show now, the L_2 gain from $g_4(t)$ and $g_5(t)$ to $g'_3(t)$ is upper bounded by v_0 . Indeed

$$\begin{aligned} \int_0^T (v_0^2(g_4^2(t) + g_5^2(t)) - v_0^2(f(t)g_4(t) - (1 - f(t))g_5(t))^2) dt &= \\ \int_0^T (v_0^2(g_4^2(t) + g_5^2(t)) - v_0^2(f^2(t)g_4^2(t) + (1 - f(t))^2g_5^2(t))) dt & \end{aligned}$$

by virtue of the fact that $f(t)(1 - f(t)) = 0$ for all t . But, now, since $|f(t)| \leq 1$ for

all t and $|1 - f(t)| \leq 1$ for all t ,

$$\int_0^T (v_0^2(g_4^2(t) + g_5^2(t)) - v_0^2(f^2(t)g_4^2(t) + (1 - f(t))^2g_5^2(t))) dt \geq 0.$$

Since the above holds for any $g_4(t)$ and $g_5(t)$ (and, correspondingly, any associated $f(t)$), we conclude that the L_2 gain from $g_4(t)$ and $g_5(t)$ to $g'_3(t)$ is upper bounded by v_0 .

As for the remaining potential input to the output of the supervisor $v(z)$, we see that this is not a sensible place to add an arbitrary signal since the output of $v(z)$ is discrete-valued. Moreover, if the physical interpretation of an exogenous input to the output of the supervisor $v(z)$ is analog noise, then any reasonable electronic implementation of the control law $v(z)$ can be made to have no noise sensitivity under the additional provision that the noise values are bounded sufficiently small. We will not discuss this concept formally here (the interested reader is referred to a discussion of the topics of noise margins in digital circuits in any basic text on digital logic, e.g. [66]), but we provide this information to show that lack of an exogenous input at the output of $v(z)$ is not an oversight.

In order to prove that the system under investigation has finite L_2 gain, we will prove that there exists a storage function for the quadratic supply rate $\gamma^2||g||^2 - ||Ex + Fg||^2$ whenever γ is sufficiently large. Our storage function we will be based on the Lyapunov function of the previous section (in fact, it will be a scalar multiple of it). Our proof will rely on considering two separate cases, one in which $||g|| \leq \epsilon||x||$ and one in which $||g|| \geq \epsilon||x||$ where $\epsilon > 0$ is a sufficiently small real number. The proof for the former case will rely on the result of the following Proposition:

Proposition 4.3.13 *Consider vectors $x, g \in \mathbf{R}^2$ such that*

$$\text{sgn}(x'\tilde{w}_s\tilde{q}'x) \neq \text{sgn}((x + g)'\tilde{w}_s\tilde{q}'(x + g))$$

where $\text{sgn}(\cdot)$ is the standard signum function. Then for every $\delta > 0$, there exists $\epsilon > 0$ such that if $||g|| \leq \epsilon||x||$, then one of the following must hold:

$$x'G_1G_2'x \leq 0 \quad \text{or} \quad x'H_1H_2'x \leq 0$$

where G_1 and G_2 are clockwise-oriented normal vectors to the rays $\theta = 3\pi/4 - \delta$ and $\theta = 3\pi/4 + \delta$ and H_1 and H_2 are clockwise-oriented normal vectors to the rays $\theta = \phi_q - \delta$ and $\theta = \phi_q + \delta$ where ϕ_q represents the angle of the vector q with respect to the positive x_1 axis.

In layman's terms, Prop. 4.3.13 says that if g is small compared to x , and x and $x + g$ lie in different cones, then x must be close in angle to one of the boundaries, either w_s or q . This idea is illustrated graphically in the case that x is close to w_s in Fig. 4.3.3. In the picture, x has a Euclidean angle that is larger than $3\pi/4$, but g is just large enough so as to make the vector $x + g$ have a Euclidean angle less than $3\pi/4$. From the picture, it is clear that the farther that x lies in angle from the stable eigenvector w_s , the larger g has to be in order to change the sign.

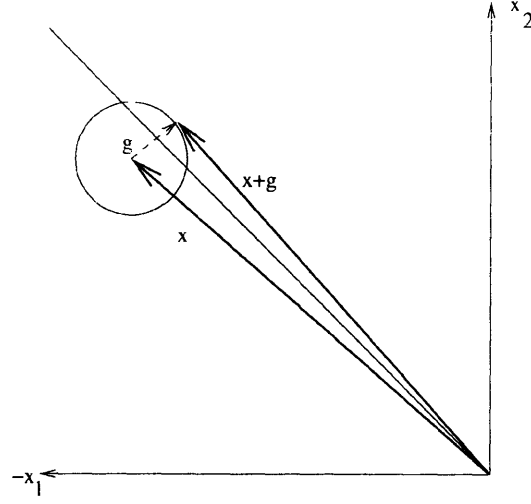


Figure 4.3.3: Graphical depiction of the result of Prop. 4.3.13 when x lies close to w_s .

Proof [Proof of Prop. 4.3.13] We will first prove the following intermediate statement: for every $\delta_2 > 0$, there exists $\epsilon > 0$ such that, if $\|g\| \leq \epsilon\|x\|$, the Euclidean angle ψ between the vectors x and $x + g$ can be made smaller than δ , i.e., $|\psi| \leq \delta$. To prove this, recall that $|\sin \psi|$ can be expressed as the magnitude of the cross product of x and $x + g$ divided by the product of the norms of x and $x + g$. The cross product of x and $x + g$ is given by the value of the determinant

$$\left| \begin{bmatrix} \hat{i} & \hat{j} & \hat{k} \\ x_1 & x_2 & 0 \\ x_1 + g_1 & x_2 + g_2 & 0 \end{bmatrix} \right|$$

where $x = \begin{bmatrix} x_1 & x_2 \end{bmatrix}'$ and $g = \begin{bmatrix} g_1 & g_2 \end{bmatrix}'$ from which it follows that

$$|\sin \psi| = \frac{|x_1 g_2 - x_2 g_1|}{\|x\| \|x + g\|}.$$

Now, if $\epsilon < 0.5$, $\|x + g\| > 0.5\|x\|$, and we find that

$$|\sin \psi| \leq 2 \frac{|x_1 g_2 - x_2 g_1|}{\|x\|^2}.$$

If we parameterize g_1 and g_2 as $g_1 = \epsilon\|x\| \cos \phi$ and $g_2 = \epsilon\|x\| \sin \phi$, we can perform a simple one variable maximization over ϕ in the range of $\phi \in [0, 2\pi]$ to find that the right hand side of the above inequality is upper bounded by 2ϵ . Hence, if $\delta = \arcsin(2\epsilon)$, we can guarantee that $|\psi| \leq \delta$ for every $\delta > 0$ when $\epsilon > 0$ is sufficiently small.

Now, let ϕ_1 represent the Euclidean angle of the vector x in the range $\phi_1 \in [-\pi/4, 7\pi/4]$, and let ϕ_2 represent the Euclidean angle of the vector $x + g$ under the

same restriction. There are eight possibilities for the relative locations of ϕ_1 and ϕ_2 which will yield different signs. If $\phi_2 > \phi_1$, four of the possibilities are

1. $-\pi/4 \leq \phi_1 < \phi_q, \phi_q \leq \phi_2 < 3\pi/4$.
2. $\phi_q \leq \phi_1 < 3\pi/4, 3\pi/4 \leq \phi_2 < \phi_q + \pi$.
3. $3\pi/4 \leq \phi_1 < \phi_q + \pi, \phi_q + \pi \leq \phi_2 < 7\pi/4$.
4. $\phi_q + \pi \leq \phi_1 < 7\pi/4, -\pi/4 \leq \phi_2 < \phi_q$.

Another four conditions arise when we interchange ϕ_1 and ϕ_2 above (i.e., when $\phi_2 < \phi_1$). We will prove that the result is true for one of these cases as the remaining cases follow from appropriate adjustments and/or symmetry arguments. To this end, we will pick case 1 above. The relevant information that we will use here is that $\phi_1 < \phi_q$ and that $\phi_2 \geq \phi_q$. Now, if ϵ is sufficiently small, we can guarantee that $\phi_2 - \phi_1 \leq \delta$. But this implies that $\phi_1 \geq \phi_2 - \delta \geq \phi_q - \delta$. Hence,

$$\phi_q - \delta \leq \phi_1 \leq \phi_q$$

and we find that x satisfies $x'H_1H_2'x \leq 0$. The remaining cases follow in a similar fashion. \square

We are now ready to prove one of the main theorems of this chapter.

Theorem 4.3.6 (Finite L2 Gain Theorem) *Consider the Lyapunov function $V(\cdot)$ of Prop. 4.2.11. There exist positive constants α and γ such that the function $\alpha V(x)$ is a storage function for the quadratic supply rate $\gamma^2 \|g\|^2 - \|Ex + Fg\|^2$ along the system trajectories described by Eqn. 4.3.21, 4.3.22, and 4.3.23.*

Proof We wish to show that for all $x \in \mathbf{R}^2$ and all $g \in \mathbf{R}^3$ (not both identically 0) that there exist constants α and γ both positive such that

$$\gamma^2 \|g\|^2 - \|Ex + Fg\|^2 - \alpha \frac{d}{dt} V(x(t)) > 0$$

which can, equivalently, be expressed as

$$\gamma^2 \|g\|^2 - \|Ex\|^2 - \|Fg\|^2 - 2x'E'Fg - \alpha \nabla V(x)(A_i x + Bg_3) > 0 \quad (4.3.24)$$

for $i = 1, 2$ where A_i are given as in Eqn. 4.2.8 and where

$$i = \begin{cases} 1 & (x + \hat{g})' \tilde{w}_s \tilde{q}(x + \hat{g}) \leq 0 \\ 2 & (x + \hat{g})' \tilde{w}_s \tilde{q}(x + \hat{g}) > 0 \end{cases}.$$

As mentioned before, we will break the proof up into two cases: one in which $\|g\| \leq \epsilon \|x\|$ and one in which $\|g\| \geq \epsilon \|x\|$ where $\epsilon > 0$ will be chosen sufficiently small.

Case 1: Small g

Consider the first case where g is small compared to x . We wish to show first that

$$-\nabla V(x)A_i x > 0$$

along the system trajectories under the constraint that $\|g\| \leq \epsilon\|x\|$ for $\epsilon > 0$ sufficiently small. When $x'\tilde{w}_s\tilde{q}'x$ and $(x + \hat{g})'\tilde{w}_s\tilde{q}'(x + \hat{g})$ have the same sign, the above statement is trivially true since $V(x)$ is a Lyapunov function for the autonomous system with no exogenous inputs. When $x'\tilde{w}_s\tilde{q}'x$ and $(x + \hat{g})'\tilde{w}_s\tilde{q}'(x + \hat{g})$ are of *different* signs, however, this conclusion does not hold, in general, since the “wrong” vector field is being chosen. As we will show, now, however, under the assumption that g is sufficiently small compared to x , the statement *is* true, and the proof is actually rather simple. First, note that by picking ϵ sufficiently small, Prop. 4.3.13 tells us that, whenever $x'\tilde{w}_s\tilde{q}'x$ and $(x + \hat{g})'\tilde{w}_s\tilde{q}'(x + \hat{g})$ have different signs, x must lie in a small cone about either w_s or q . But now by Thm. 4.2.5, there exists a small cone about w_s and a small cone about q for which

$$-\nabla V(x)A_i x$$

is decreasing for both $i = 1$ and $i = 2$.

Now, consider the difference

$$-\alpha\nabla V(x)A_i x - \|Ex\|^2.$$

If we let $\eta = x/\|x\|$ for $x \neq 0$, we can express the above as

$$(-\alpha\nabla V(\eta)A_i\eta - \|E\eta\|^2)\|x\|^2 > (-\alpha\nabla V(\eta)A_i\eta - \|E\|^2)\|x\|^2.$$

Now, since η is a compact set, we have

$$\min_{\eta, i=1,2} -\nabla V(x)A_i x = \beta > 0$$

and, hence,

$$(-\alpha\nabla V(\eta)A_i\eta - \|E\|^2)\|x\|^2 > (\alpha\beta - \|E\|^2)\|x\|^2 > \beta\|x\|^2$$

when $\alpha > 1 + \|E\|^2/\beta$. Hence, the left-hand side of Eqn. 4.3.24 can be lower bounded by

$$g'(\gamma^2 I - F'F)g - 2x'E'Fg - \alpha\nabla V(x)Bg_3 + \beta\|x\|^2.$$

For notational convenience, if we define $\tilde{\gamma}^2 = \gamma^2 - \lambda_{\max}(F'F)$ for $\gamma^2 > \lambda_{\max}(F'F)$, we can further lower bound the above by

$$\tilde{\gamma}^2\|g\|^2 - 2x'E'Fg - \alpha\nabla V(x)Bg_3 + \beta\|x\|^2.$$

The above expression takes the form

$$f(g, x) = \tilde{\gamma}^2 \|g\|^2 - 2p(x)'g + \beta \|x\|^2$$

where $p(x)$ is continuous and homogeneous of degree one. For each fixed $x \in \mathbf{R}^2$, the above is a quadratic form in g which has minimal value

$$-\frac{p^2(x)}{\tilde{\gamma}^2} + \beta \|x\|^2.$$

If we again let $\eta = x/\|x\|$, the above can reparameterized as

$$\left(\beta - \frac{p^2(\eta)}{\tilde{\gamma}^2} \right) \|x\|^2.$$

Since η is a compact set and $p(x)$ is continuous, it follows that $\omega = \max_{\eta} p^2(\eta)$ exists and

$$\left(\beta - \frac{p^2(\eta)}{\tilde{\gamma}^2} \right) \|x\|^2 > \left(\beta - \frac{\omega}{\tilde{\gamma}^2} \right) \|x\|^2 > \frac{\beta}{2} \|x\|^2$$

when $\tilde{\gamma}^2 > 2\omega/\beta$. Hence, we have shown that, under the constraint $\|g\| \leq \epsilon \|x\|$, Eqn. 4.3.24 is positive definite for α and γ sufficiently large.

Case 2: Large g

We now wish to show that if $\|g\| \geq \epsilon \|x\|$, γ can still be chosen sufficiently large to ensure that Eqn. 4.3.24 is positive for all $x \in \mathbf{R}^2$, $g \in \mathbf{R}^3$ which are not both identically 0. If we define $\tilde{\gamma}^2$ as in the previous section and if we define $h(x) = \min_{i=1,2} -\alpha \nabla V(x) A_i x$, then the left-hand side of Eqn. 4.3.24 is lower bounded by

$$\tilde{\gamma}^2 \|g\|^2 - 2x' E' F g - \alpha \nabla V(x) B g_3 - \|Ex\|^2 - h(x).$$

Note that the above can be written in the form

$$\tilde{\gamma}^2 \|g\|^2 - 2p(x)'g - q(x)$$

where $p(x)$ is continuous and homogeneous of degree one and $q(x)$ is continuous and homogeneous of degree 2. Again using the parameterization $\eta = x/\|x\|$, if we consider all g which satisfy $\|g\| = t\|x\|$ for some $t > 0$, we can rewrite the above in the form

$$(\tilde{\gamma}^2 t^2 - 2p(\eta)' \tilde{g} t - q(\eta)) \|x\|^2$$

where $\tilde{g} = g/\|g\|$. What we wish to show now that the expression in parentheses above is increasing for $t \geq \epsilon$ for all unit-length η and \tilde{g} if $\tilde{\gamma}^2$ is sufficiently large. Indeed, differentiating the expression in parentheses with respect to t shows that the

derivative is increasing whenever

$$t > \frac{p(\eta)' \tilde{g}}{\tilde{\gamma}^2}.$$

Again, since η and \tilde{g} lie in compact sets and p is continuous,

$$\omega = \max_{\eta, \tilde{g}} p(\eta)' \tilde{g}$$

exists, and the indicated function of t is increasing whenever

$$t > \frac{\omega}{\tilde{\gamma}^2}.$$

Taking $\tilde{\gamma}^2 > \omega/\epsilon$ guarantees that the expression in parentheses is increasing for $t \geq \epsilon$. Thus, for all g which satisfy $\|g\| \geq \epsilon\|x\|$,

$$(\tilde{\gamma}^2 t^2 - 2p(\eta)' \tilde{g} t - q(\eta)) \|x\|^2 > (\tilde{\gamma}^2 \epsilon^2 - 2p(\eta)' \tilde{g} \epsilon - q(\eta)) \|x\|^2.$$

Defining

$$\nu = \min_{\eta, \tilde{g}} (-2p(\eta)' \tilde{g} \epsilon - q(\eta)),$$

we have

$$(\tilde{\gamma}^2 \epsilon^2 - 2p(\eta)' \tilde{g} \epsilon - q(\eta)) \|x\|^2 > (\tilde{\gamma}^2 \epsilon^2 - \nu) \|x\|^2 > 0$$

for $\tilde{\gamma}^2 > \nu/\epsilon^2$.

We have now shown that $\tilde{\gamma}$ (and, equivalently γ), can be chosen sufficiently large to ensure that Eqn. 4.3.24 is positive for *all* g and x that are not both identically 0. Hence $\alpha V(x)$ is a storage function for α sufficiently large, and the given system has finite L_2 gain. \square

4.3.1 Storage Functions in Different Coordinates

Thm. 4.3.6 proves finite L_2 gain for a particular coordinate description of the plant $P(s)$. However, as we will show now, one can find storage functions to prove finite L_2 gain for *any* minimal state-space description of the second order plant $P(s)$ of relative degree one:

Proposition 4.3.14 *Consider a linear system*

$$\begin{aligned} \dot{x} &= Ax + Bu + Bg_3 \\ y &= Ex + Fg \end{aligned}$$

under the control law $u(x) = v(x)y$ with

$$v(x) = \begin{cases} v_0 & (x + \hat{g})' F_1 F_2' (x + \hat{g}) \leq 0 \\ -v_0 & (x + \hat{g})' F_1 F_2' (x + \hat{g}) > 0 \end{cases}$$

where $\hat{g} = [g_1(t) \ g_2(t)]'$, and where $F_j \in \mathbf{R}^{2 \times 1}$ for $j = 1, 2$. Suppose for some value $\gamma > 0$, the quadratic supply rate $\gamma^2 \|g\|^2 - \|Ex + Fg\|^2$ has associated nonnegative storage function $V(x)$ where $g \triangleq [g_1(t) \ g_2(t) \ g_3(t)]'$. Then for any invertible $T \in \mathbf{R}^{2 \times 2}$, the system

$$\begin{aligned}\dot{z} &= T^{-1}ATz + T^{-1}Bu + T^{-1}Bg_3 \\ y &= ETz + Fg\end{aligned}$$

under the control law $u(z) = v(z)y$ with

$$u(z) = \begin{cases} v_0 & (z + \tilde{g})' \tilde{F}_1 \tilde{F}_2'(z + \tilde{g}) \leq 0 \\ -v_0 & (z + \tilde{g})' \tilde{F}_1 \tilde{F}_2'(z + \tilde{g}) > 0 \end{cases}$$

where $\tilde{g} = T^{-1}\hat{g}$ and $\tilde{F}_j = T'F_j$ for $j = 1, 2$ has quadratic supply rate $\gamma^2 \|g'\|^2 - \|ETz + Fg\|^2$ where g' is given by

$$g' = \begin{bmatrix} T^{-1} & 0 \\ 0 & 1 \end{bmatrix} \begin{bmatrix} \hat{g} \\ g_3 \end{bmatrix} \quad (4.3.25)$$

has associated nonnegative storage function $V(Tz)$.

Proof Immediate upon making the substitution $x = Tz$. □

From Prop. 4.3.14, we conclude that if the closed-loop interconnection for one state-space description of our plant has finite L_2 gain, then any other state-space description will have finite L_2 gain as well upon appropriately transforming the coordinates of the control law; however, the actual *value* of the L_2 gain between the two coordinate descriptions for a given input vector g may differ. Note that, in z -coordinates, the input vector in Prop. 4.3.14 is *different* than the input vector in the original coordinates; the input vector g' in transformed coordinates is related to the original input vector g via Eqn. 4.3.25. The fact that the two input vectors are different does not invalidate our conclusion the L_2 gain is finite for the *same* input vector when the state-space description of the plant (and, correspondingly, the controller $v(\cdot)$) changes, as we will now show. If we write

$$g = \begin{bmatrix} T & 0 \\ 0 & 1 \end{bmatrix} g', \quad (4.3.26)$$

we see that the L_2 gain of the system with input g in z -coordinates can be viewed as the L_2 gain of the series interconnection of two systems, the first of which is the memoryless linear transformation described above in Eqn. 4.3.26 and the second of which is the system with input g' described in the second part of Prop. 4.3.14. If we denote the L_2 gain of the system in z -coordinates with input g as γ_g , then, by the submultiplicative property of L_2 gains (Prop. 5.3.16 of the next chapter), we find that

$$\gamma_g \leq M\gamma$$

where

$$M = \sigma_{\max} \left(\begin{bmatrix} T & 0 \\ 0 & 1 \end{bmatrix} \right)$$

where $\sigma_{\max}(\cdot)$ denotes the largest singular value of a matrix.

4.4 Observer-based Control

Up until this point, we have assumed that the switching law v has access to the full state of the plant in making its decision (i.e., $v = v(x_1, x_2)$ where x_1 and x_2 are the states of the plant $P(s)$). In practice, it is not the case that the supervisor will have this luxury, and it will have to rely on some estimate $\begin{bmatrix} \hat{x}_1 & \hat{x}_2 \end{bmatrix}'$ of the true state $\begin{bmatrix} x_1 & x_2 \end{bmatrix}$ to make its decisions. If the estimate is “good enough,” one should expect that the overall interconnected system using the switching law that is a function of the estimated state should be sufficiently well-behaved.

The problem that we study in this section is akin to the pole placement problem in linear systems theory [46]. In the pole placement problem, we consider the task of placing the poles of a finite order LTI system at arbitrary locations by building a feedback compensator that is a function of the plant output. Under conditions of reachability and observability, the solution to this problem has a separation structure: we first design a state feedback controller, assuming that the true state of the plant x is known. Then, we design an estimator (observer) to produce an estimate \hat{x} which we then use in place of the true state. The certificate of being “sufficiently well-behaved” for this particular problem is a statement that an appropriately designed linear observer leads to an interconnected system with poles that can be placed at arbitrary locations.

As we will see now, we actually have a similar separation structure for the class of controllers that we are dealing with here. We have already studied how to design switching controllers of the given structure when the full state is known to the observer. We will show now that, by designing a simple observer, we can design switching controllers which do *not* rely on access to the full state of the plant and which yield closed-loop interconnections that are finite L_2 gain stable. We will begin by showing that one can design a reduced-order (first order observer) to estimate the “missing” state information that is not present in the output. Once we have done this, we will show that using the output of this observer in place of the true missing state information will still yield an overall interconnected system which is finite L_2 gain stable. We will show this by computing an upper bound on the L_2 gain of the system with the observer in place that will transform our problem into a problem in which the switching law has full access to the state, the problem we studied in the previous section. Since finite L_2 gain stability has already been established for the full-state problem, finite L_2 gain stability with an observer in place will then follow.

4.4.1 Observer Design

The design of the observer we will use is, essentially, a straightforward application of the existing theory on reduced order observers for LTI systems (see Exercise 29.2 in [46]). Consider an observable second order LTI system of the form

$$\begin{aligned} \begin{bmatrix} \dot{w}_1 \\ \dot{w}_2 \end{bmatrix} &= \begin{bmatrix} a_{11} & a_{12} \\ a_{21} & a_{22} \end{bmatrix} \begin{bmatrix} w_1 \\ w_2 \end{bmatrix} + \begin{bmatrix} b_1 \\ b_2 \end{bmatrix} u \\ y &= w_1 \end{aligned}$$

Note that the class of plants we have been studying, namely second order plants of relative degree two, always have a state-space description that can be written in the above format. Since the output is, itself, the first state of the plant, we only need to estimate the second state of the plant \hat{w}_2 in order to obtain an estimate of the full state vector (where, in this case, one of the estimates is the true value of the state itself!). Now, if $a_{22} < 0$, the state estimator

$$\dot{\hat{w}}_2 = a_{22}\hat{w}_2 + a_{21}y + b_2u$$

is a good one in the sense that the error dynamics of $e = w_2 - \hat{w}_2$ are given by

$$\dot{e} = a_{22}e$$

and are hence, stable, i.e., $\hat{w}_2(t) \rightarrow w_2(t)$ exponentially as $t \rightarrow \infty$. If $a_{22} \geq 0$, however, the error dynamics may *grow* exponentially, an obviously undesirable phenomenon. The “trick” to estimate a new variable which we will call \hat{x}_2 that attempts to estimate $w_2 + lw_1$, where l is some to-be-determined gain. If one makes the change of coordinates

$$\begin{bmatrix} x_1 \\ x_2 \end{bmatrix} = \begin{bmatrix} 1 & 0 \\ l & 1 \end{bmatrix} \begin{bmatrix} w_1 \\ w_2 \end{bmatrix}, \quad (4.4.27)$$

the dynamics are now expressed as

$$\begin{bmatrix} \dot{x}_1 \\ \dot{x}_2 \end{bmatrix} = \begin{bmatrix} a_{11} - la_{12} & a_{12} \\ a_{21} + l(a_{11} - a_{22}) - l^2a_{12} & a_{22} + la_{12} \end{bmatrix} \begin{bmatrix} x_1 \\ x_2 \end{bmatrix} \quad (4.4.28)$$

$$+ \begin{bmatrix} b_1 \\ lb_1 + b_2 \end{bmatrix} u \quad (4.4.29)$$

$$y = x_1. \quad (4.4.30)$$

Note that the error dynamics of the observer

$$\dot{\hat{x}}_2 = -k_1\hat{x}_2 + k_2y + k_3u \quad (4.4.31)$$

where

$$k_1 = -a_{22} - la_{12} \quad (4.4.32)$$

$$k_2 = a_{21} + l(a_{11} - a_{22}) - l^2 a_{12} \quad (4.4.33)$$

$$k_3 = b_2 + lb_1 \quad (4.4.34)$$

are given by

$$\dot{e} = -k_2 e$$

where $e = x_2 - \hat{x}_2$. If $a_{12} \neq 0$, then it is clear that k_1 can be made positive for some choice of l , and $\hat{x}_2(t) \rightarrow x_2(t)$ exponentially as $t \rightarrow \infty$. Indeed, a_{12} *must* be nonzero by the assumed observability of the plant. This can be seen by constructing the associated observability matrix

$$\begin{bmatrix} C \\ CA \end{bmatrix}$$

and noting that this matrix is rank one if $a_{12} = 0$.

Equation 4.4.31 is the form of the observer we will use. Note that, without loss of generality, for the more specific problem of designing an observer for the switching system under consideration, we can automatically *assume* that our plant is in the form given by Eqn. 4.4.29 and 4.4.30 for some value of l which makes $k_1 > 0$; if this is not the case, we make a change of coordinates for some appropriate value of l to change the plant into the form of Eqn. 4.4.29 and 4.4.30, and we *also* change coordinates on the switching law as described in the previous chapter; that is, if the switching law $v(w)$ yields an asymptotically (and finite L_2 gain) stable interconnection $\dot{w} = A + v(w)BCw$ where A , B and C are the corresponding state-space matrices for the plant in w -coordinates, the result of Proposition 3.4.6 in Chapter 3 tells us that the control law $\tilde{v}(x) = v(T^{-1}x)$ yields an asymptotically (and finite L_2 gain) stable interconnection $\dot{x} = \tilde{A}x + \tilde{v}(x)\tilde{B}\tilde{C}x$, where \tilde{A} , \tilde{B} and \tilde{C} are given by

$$\tilde{A} = TAT^{-1}, \quad \tilde{B} = TB, \quad \tilde{C} = CT^{-1}$$

where T is given by the matrix in Eqn. 4.4.27. Hence, we can always assume that our switching law has been designed for a coordinate system where the second state yields an observer of the form Eqn. 4.4.31 with stable error dynamics.

4.4.2 Finite L2 Gain Stability of Observer-based Controller

A block diagram of the closed-loop system with the observer of Eqn. 4.4.31 in place is shown in Fig. 4.4.4. Recall from the previous section that, by assumption, we assume a state-space description where $y(t) = x_1(t)$. Hence, we can directly feed $y(t)$ into the first input of the switching law $v(z_1, z_2)$ (where we still assume that $z_1(t)$ is potentially “corrupted” by an additive disturbance $g_1(t)$). We employ the estimator Eqn. 4.4.31 of the previous section to produce an estimate $\hat{x}_2(t)$ of the true second state $x_2(t)$ where we select $k_1 > 0$ in the block with transfer function $1/(s + k_1)$.

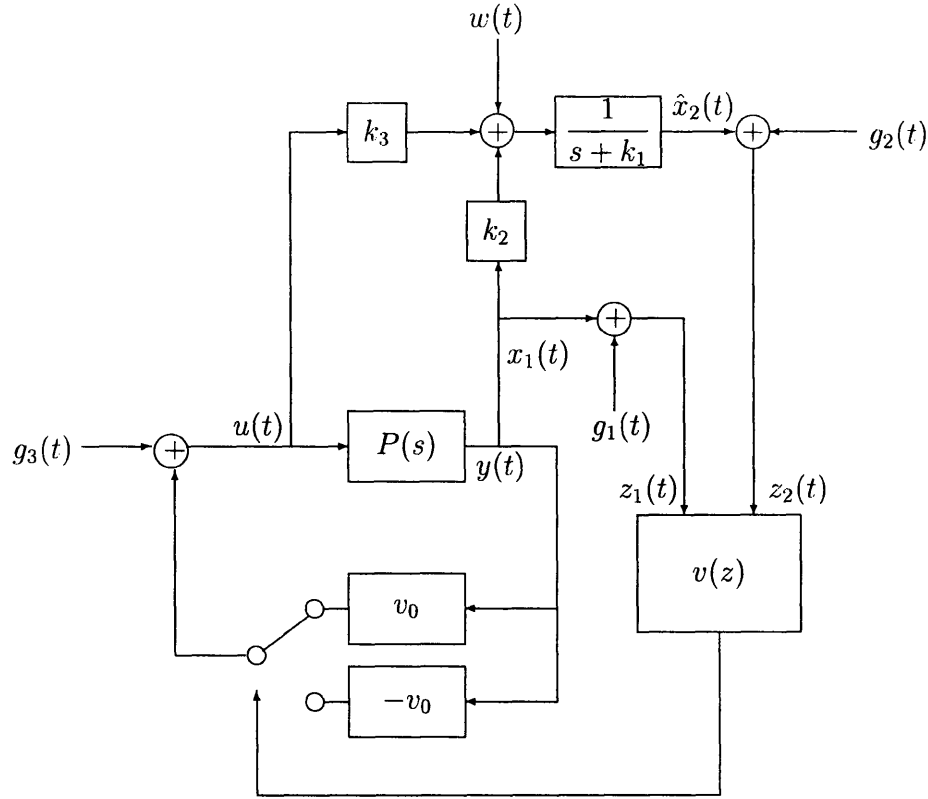


Figure 4.4.4: Block diagram of switching system with observer in place of full-state feedback (the observer is comprised of the blocks $1/(s + k_1)$, k_2 , and k_3). The input w models the net disturbance/noise inputs to the observer.

As in the full-state problem of Fig. 4.3.2, we allow the addition of the three exogenous inputs $g_1(t)$, $g_2(t)$, and $g_3(t)$ as before, but we now also allow an additional exogenous input $w(t)$ to the input of the observer dynamics. The observer is designed such that, under the assumption that the input $u(t)$ is the same for both the plant and the observer, the estimate $\hat{x}_2(t)$ converges exponentially to $x_2(t)$ as $t \rightarrow \infty$. In reality, however, it is unrealistic to expect that the input to the plant and observer are both *exactly* the same for all time, and the exogenous input $w(t)$ accounts for this fact.

The task at hand now is to show the following:

Theorem 4.4.7 (Observer-based Finite L_2 Gain Theorem) *Consider the system depicted in Fig. 4.4.4 where, under the assumption $w(t) = 0$ identically, the observer output $\hat{x}_2(t) \rightarrow x_2(t)$ exponentially as $t \rightarrow \infty$ where $x_2(t)$ is the second state of the second order plant $P(s)$. Assume that the system of Fig. 4.3.2 is finite L_2 gain stable for the same plant $P(s)$, switching law $v(z)$, and switching gains v_0 and $-v_0$. Then the system of Fig. 4.4.4 is also finite L_2 gain stable.*

Proof We begin by re-drawing the block diagram of Fig. 4.4.4 into the form shown in Fig. 4.4.5. Consider the task of assessing whether the system with exogenous inputs

$g_i(t)$, $i = 1, 2, 3$ and 4 has finite L_2 gain where $g_4(t)$ is labeled as in Fig. 4.4.6 and where we are assuming that the input $g_4(t)$ is an *arbitrary* input rather than being the output of the lowpass filter $1/(s + k_1)$ with input $w(t)$, as shown in Fig. 4.4.5. If the L_2 gain of the system in Fig. 4.4.6 with g_4 as an arbitrary input is finite, then it follows that the L_2 gain of the system with $w(t)$ as input is finite, as well, since, by the submultiplicative property of L_2 gains, we have

$$\gamma_w \leq M\gamma_{g_4}$$

where

$$M = \left\| \begin{bmatrix} 1 & & & \\ & 1 & & \\ & & 1 & \\ & & & \frac{1}{s+k_1} \end{bmatrix} \right\|_\infty = \max\{1, 1/k_1\}$$

and where γ_w and γ_{g_4} represent the L_2 gains of Fig. 4.4.4 with input $w(t)$ and Fig. 4.4.6 with (exogenous) input $g_4(t)$, respectively. Hence, if we can show that the system of Fig. 4.4.6 is finite L_2 gain stable, L_2 gain stability of the original system of Fig. 4.4.4 will immediately follow.

We note, now, that in redrawing the block diagram of Fig. 4.4.4, into the form shown in Fig. 4.4.6, the input to the observer structure is exactly the same as the input to the plant. Because of this, it follows that $\hat{x}_2(t)$ is related to $x_2(t)$ via the relationship

$$x_2(t) = \hat{x}_2(t) + (x_2(0) - \hat{x}_2(0))e^{-k_1 t}.$$

Formally, the systems of Fig. 4.4.4 and 4.4.5 are third order systems and, hence, the applicability of the storage function we found for the full-state problem does not appear to immediately apply. However, we note that via the definition of L_2 gain given at the beginning of the chapter, the L_2 gain is *independent* of initial conditions since existence of a nonnegative storage function $V(\cdot)$ implies that

$$\inf_{T \geq 0} \int_0^T (\gamma^2 \|w(t)\|^2 - \|y(t)\|^2) dt \geq \inf_{T \geq 0} V(x(T)) - V(x(0)) \geq -V(x(0))$$

for any dynamics system with input w and output y . Hence, the system of Fig. 4.4.6 is finite gain L_2 stable if and only if it is finite gain L_2 stable when the initial conditions $x_2(0)$ and $\hat{x}_2(0)$ are exactly equal, in which case we have that

$$x_2(t) = \hat{x}_2(t)$$

for all $t \geq 0$. But if we now define a new exogenous input to the input of the second argument of the switching law z_2 given by

$$g'_2(t) = g_2(t) + g_4(t),$$

we find that this is *exactly* the same setup as in the full-state problem of Fig. 4.3.2. Hence, if the system of Fig. 4.3.2 is finite L_2 gain stable, the system of Fig. 4.4.4 is

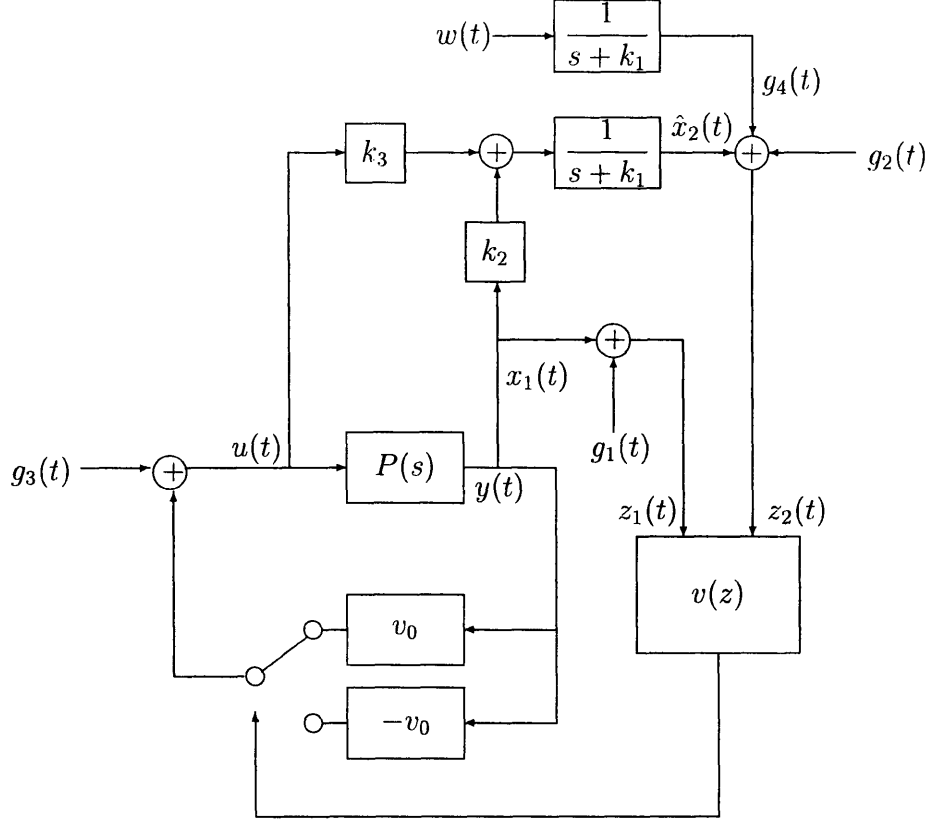


Figure 4.4.5: Equivalent block diagram of Fig. 4.4.4 with input disturbance w re-configured as an observer output disturbance g_1 .

finite L_2 gain stable as well. □

Note that the previous proof can easily be augmented to show that the the system of Fig. 4.4.4 is *asymptotically* stable when all exogenous inputs are 0. Indeed, when all inputs are 0, we again have that

$$x_2(t) = \hat{x}_2(t) + (x_2(0) - \hat{x}_2(0))e^{-k_1 t}.$$

Noting that this simply corresponds to a different initial condition for the “full-state” problem (with no observer), asymptotic stability is immediately apparent.

4.5 Computational Considerations

Up to this point, our focus has been on proving that the L_2 gain of a particular system is finite without regard to what the actual *value* of the L_2 gain may be. We begin with the comment that, while the storage function of Eqn. 4.1.1 is useful for proving existence of a finite L_2 gain, it is often-times somewhat difficult to express in an analytical form that is useful for computation. In this section, we briefly discuss a methodology

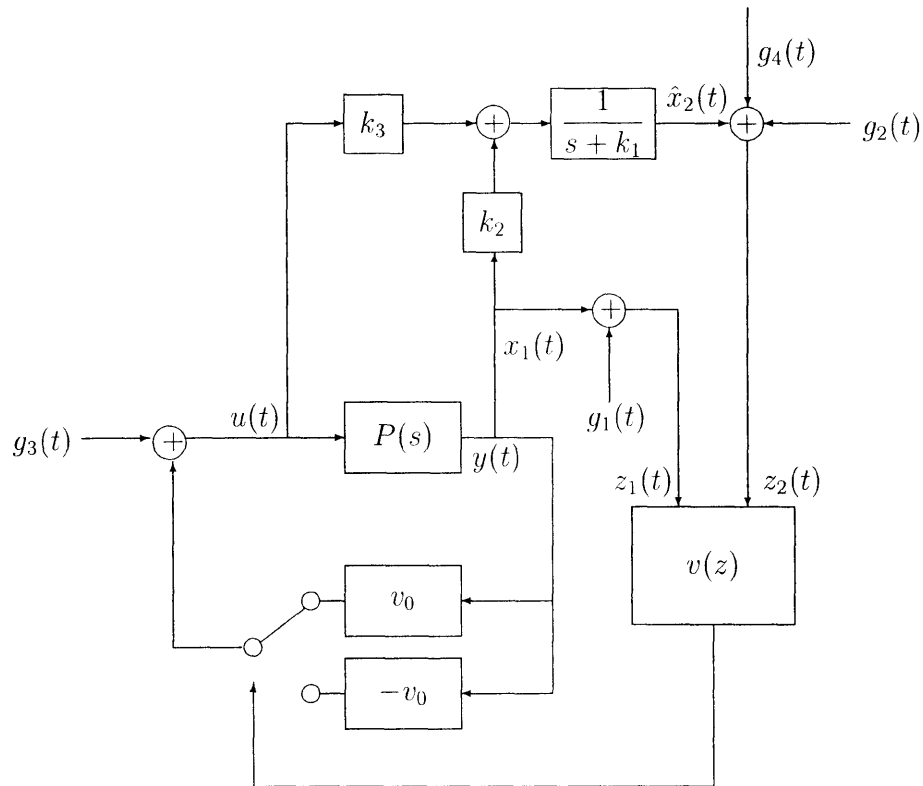


Figure 4.4.6: Block diagram of Fig. 4.4.5 with output of lowpass filter with input w replaced by an *arbitrary* locally square-integrable signal $g_4(t)$.

for computing upper bounds on the L_2 gain for the switching systems under consideration by computing *piecewise-quadratic storage functions*. More specifically, consider a partition of \mathbf{R}^2 into N cones of the form $x'M_i x \leq 0$ $i = 1, 2, \dots, N$ where M_i are symmetric matrices for $i = 1, 2, \dots, N$ whose interiors $X_i = \{x : x'M_i x < 0\}$ are mutually disjoint, i.e. $X_i \cap X_j = \emptyset$ for all $i \neq j$ and such that the closures of each set span all of \mathbf{R}^2 , i.e. $\cup_{i=1}^N \bar{X}_i = \mathbf{R}^2$, where $\bar{X}_i = \{x : x'M_i x \leq 0\}$. We consider storage function candidates $V(x)$ of the form

$$V(x) = x'P_i x \quad \forall x : x'M_i x \leq 0$$

where the matrices P_i are symmetric matrices which are positive on the cones for which they are defined, i.e.,

$$x'P_i x > 0 \quad \forall x : x'M_i x \leq 0$$

whenever $x \neq 0$ and such that $V(x)$ is continuous along cone boundaries, i.e., if $E_{ij} \in \bar{X}_i \cap \bar{X}_j$, then

$$E'_{ij}P_i E_{ij} = E'_{ij}P_j E_{ij}.$$

The overall task at hand is to find a storage function $V(\cdot)$ and $\gamma > 0$ such that the inequality

$$\gamma^2 \|g\|^2 - \|Ex + Fg\|^2 - \frac{d}{dt}V(x(t)) > 0$$

is satisfied along system trajectories. If $V(\cdot)$ and γ can be found which satisfy the above condition, the γ is an *upper bound* on the L_2 gain from g to $Ex + Fg$. Note, in general, it is quite difficult to determine the *exact* value of the L_2 gain for a given system (special exceptions to this rule including LTI systems and certain memoryless nonlinearities), and an upper bound on the L_2 gain is typically all that can be found.

Now, if we focus our attention for the moment on a switching law which has full access to the state ³, the dynamics of the systems we have been studying take the form

$$\dot{x} = \begin{cases} A_1 x + Bg_3 & (x + \hat{g})'F_1 F_2'(x + \hat{g}) \leq 0 \\ A_2 x + Bg_3 & (x + \hat{g})'F_1 F_2'(x + \hat{g}) > 0 \end{cases}$$

where, again, $\hat{g} = [g_1 \ g_2]'$, $A_i \in \mathbf{R}^{2 \times 2}$, $F_i \in \mathbf{R}^{2 \times 1}$ for $i = 1, 2$, and $B \in \mathbf{R}^{2 \times 1}$. We, therefore, wish to find a storage function $V(x)$ such that

$$\begin{aligned} \gamma^2 \|g\|^2 - \|Ex + Fg\|^2 - \nabla V(x)(A_1 x + Bg_3) &> 0, \quad (x + \hat{g})'F_1 F_2'(x + \hat{g}) \leq 0 \\ \gamma^2 \|g\|^2 - \|Ex + Fg\|^2 - \nabla V(x)(A_2 x + Bg_3) &> 0, \quad (x + \hat{g})'F_1 F_2'(x + \hat{g}) > 0. \end{aligned}$$

³We will show in the next chapter how to compute the L_2 gain for a system with an observer in place.

Now, if we restrict $V(x)$ to be piecewise-quadratic, the above can be written as

$$\gamma^2 \|g\|^2 - \|Ex + Fg\|^2 - 2x'P_i(A_1x + Bg_3) > 0, (x + \hat{g})'F_1F_2'(x + \hat{g}) \leq 0 \quad (4.5.35)$$

$$\text{and } x'M_ix \leq 0 \quad (4.5.36)$$

$$\gamma^2 \|g\|^2 - \|Ex + Fg\|^2 - 2x'P_i(A_2x + Bg_3) > 0, (x + \hat{g})'F_1F_2'(x + \hat{g}) > 0 \quad (4.5.37)$$

$$\text{and } x'M_ix \leq 0. \quad (4.5.38)$$

The above constraints can all be written in the form

$$z'Qz > 0 \quad \text{subject to } z'Rz \geq 0, \quad z'Sz \geq 0 \quad (4.5.39)$$

where $z = \begin{bmatrix} x & g \end{bmatrix}'$ and Q , R , and S are matrices of appropriate dimension. By virtue of the \mathcal{S} -procedure [48], a constraint of the above form will hold if there exist constants $\tau_1 \geq 0$ and $\tau_2 \geq 0$ such that

$$Q - \tau_1 R - \tau_2 S \geq 0 \quad (4.5.40)$$

where the notation “ ≥ 0 ” refers to a matrix on the left-hand side that is positive semidefinite. Now, for a given partition (or, equivalently, set of symmetric matrices M_i), the constraints of Eqn. 4.5.36 and 4.5.38 are linear in both γ^2 and the entries of the P_i matrices. Hence, the corresponding matrix Q is linear with respect to these variables as well, and the problem of computing an upper bound on the L_2 gain can be expressed as a *semidefinite program*. We will not delve into the many details of semi-definite programming here (the interested reader is referred to [48]), but we will simply point out that there exist several numerical packages for solving semidefinite programming problems in software such as MATLAB. Moreover, the problem of trying to minimize the upper bound on the L_2 gain using piecewise quadratic Lyapunov functions within a given partition can be solved automatically by setting up a problem of the form

$$\min \gamma : \quad Q_j - \tau_{j1}R - \tau_{j2}S \geq 0,$$

where $j = 1, 2, \dots, M$ for some appropriately chosen M . While the above semidefinite program is not guaranteed to be feasible for any particular partition, the author has yet to find an example where the semi-definite program has failed to converge for some not-too-large number of partitions (all examples that have been studied have converged with fewer than 12 partitions). We will conclude this section with an example.

Example 4.5.6 Consider the following system:

$$\begin{aligned} \begin{bmatrix} \dot{x}_1 \\ \dot{x}_2 \end{bmatrix} &= \begin{bmatrix} 0 & 1 \\ 0 & 0 \end{bmatrix} \begin{bmatrix} x_1 \\ x_2 \end{bmatrix} + \begin{bmatrix} 0 \\ 1 \end{bmatrix} u \\ y &= x_1 \end{aligned}$$

where $u(t) = r(t) + v(x(t))y(t)$, where $r(t)$ is an exogenous input and the switching

law $v(x)$ is given by

$$v(x) = \begin{cases} 1 & x_1(x_1 + x_2) \leq 0 \\ -1 & x_1(x_1 + x_2) > 0 \end{cases}.$$

Without the presence of the exogenous input r , the switching law $v(x)$ implements a controller which maximizes the rate of convergence under the constraint $|v(x)| \leq 1$. The task at hand, now, is to determine an upper bound on the L_2 gain from the input r to the output y , i.e., we wish to find $\gamma > 0$ as small as possible such that there exists a nonnegative storage function $V(x)$ such that

$$\gamma^2 r^2 - x_1^2 - \frac{d}{dt}V(x(t)) > 0$$

along the system trajectories. If we break up the state space into 11 partitions and implement the semidefinite programming problem described above in MATLAB, we find that 6.82 is an upper bound on the L_2 gain from r to y for this system. The question naturally arises as to the degree of conservatism of this estimate; could the L_2 gain be a much smaller quantity, say, for instance 0.01? While we will not go through the full analysis here, it can be shown (and will be shown in the next chapter), that when $r(t) = 1$ for all $t \geq 0$, the output $y(t) \rightarrow 1$ exponentially as $t \rightarrow \infty$. Moreover, if $x_1(0) = 1$ and $x_2(0) = 0$, $y(t) = 1$ for all $t \geq 0$. Now, if the true L_2 gain γ satisfies the constraint that

$$\inf_{T \geq 0} \int_0^T (\gamma^2 r^2(t) - y^2(t)) dt > -\infty$$

for *all* input output pairs $(r(t), y(t))$, then it follows for the specific input-output pair $r(t) = 1$, $y(t) = 1$ that

$$\inf_{T \geq 0} \int_0^T (\gamma^2 - 1) dt > -\infty$$

from which we conclude that $\gamma \geq 1$. Hence, the true L_2 gain satisfies the inequality constraint

$$1 \leq \gamma \leq 6.28$$

from which we deduce that the upper bound is less than one order of magnitude higher than the true L_2 gain.

4.6 Summary

In this chapter, we have shown that the optimal switching laws of the previous chapter, which were designed only for asymptotic stability, admit a form of input-output stability. From this, we were able to derive an observer-based switching controller which does not rely on the full state to implement switching, and we separately investigated the problem of computing the L_2 gain for a given plant and switching controller. With these new tools in hand, we now are able to investigate the use of the switching controllers that we have been studying for some simple design problems, the topic of the next chapter.

Chapter 5

Application: Step Response Performance

In this chapter, we explore an application where we design a switching controller of the form studied to this point to asymptotically track a step input for a class of LTI plants. We then evaluate the performance (which, in this chapter, will be measured via the percentage overshoot and 1% settling time of the zero-state step response) of two different forms of LTI control, one in which the controller is constrained to be first order (to match the order of the switching controller dynamics), and one in which the order is unconstrained. As we shall see, for a particular class of plants, the performance of the switching architecture can greatly outperform the performance of the first order LTI controller under mild constraints on the set of permissible first order controllers. We shall also see that the performance of the switching architecture does not greatly under-perform when compared to the performance achievable via arbitrarily high-order LTI control. Moreover, a methodical way of designing an LTI controller to achieve close-to-optimal performance will be shown which, in the context of specific design examples, will yield very high order LTI controllers.

5.1 Introduction

In this chapter, we consider a class of plants of the form

$$P(s) = \frac{a}{s(s - b)} \quad (5.1.1)$$

where $a > 0$ and $b \in \mathbf{R}$ and consider the task of designing a switching controller within the architecture we have been studying to this point to asymptotically track a step input, paying particular attention to the class of plants for which $a \gg b^2$ (we shall quantify this relationship more formally in later sections). We shall assess the quality of the step response in terms of the percentage overshoot and 1% settling time

when the input is a step, i.e. for an exogenous input $r(t)$ of the form

$$r(t) = \begin{cases} 0 & t < 0 \\ r & t \geq 0 \end{cases}$$

with $r > 0$. Under the assumption that the step response $s(t)$ asymptotically tracks the input $r(t)$, then for a step input of amplitude $r > 0$, we define the percentage overshoot of the zero-state unit step response $s(t)$ as the smallest value of $M > 0$ such that

$$s(t) \leq r(M + 1) \quad \forall t > 0$$

and define the 1% settling time as the smallest value of $T > 0$ such that

$$|s(t) - r| \leq 0.01r \quad \forall t \geq T.$$

Our objective in this chapter is the following: we wish to compare the performance that can be achieved via the switching architecture (in terms of the above performance measures) to the performance we can achieve via two different linear controller designs.¹ Specifically, we wish to compare the performance of the switching architecture to two other scenarios:

- Design via an LTI controller that is first order.
- Design via a finite order LTI controller of unconstrained order.

The motivation for making the first comparison lies in the fact that the switching controller we will design has first order dynamics. By comparing its response to that of a first order LTI controller, we obtain some qualitative information as to how the introduction of switching can improve performance. The objective of the second comparison is to assess how “close” the first order switching architecture can get to the fundamental limits of LTI control. As we shall see, while the fundamental performance of LTI control outperforms the simple switching architecture, for a certain subclass of the set of plants described by Eqn. 5.1.1, the ratio of the settling time that can be achieved via arbitrarily high order LTI control to that which can be achieved via the switching architecture is bounded. Moreover, we will demonstrate through examples that a methodical procedure for designing an LTI controller which achieves close-to-optimal performance does, indeed, yield a *very* high order LTI controller.

We shall first evaluate the performance of the switching architecture for a particular example, namely for the case where the plant is a double integrator, and compare the performance achieved here to that which can be achieved via first order LTI control and will then present a weak generalization of this result for a class of plants which are sufficiently “close” to a double integrator. Finally, we will compare the settling time of the switching architecture to that which can be achieved via arbitrarily high-order LTI control by establishing the aforementioned bound on the ratio of these settling times.

¹We delay an explanation of the *exact* way in which we will utilize the above performance measures to make a comparison until we formally present the problem in subsequent sections.

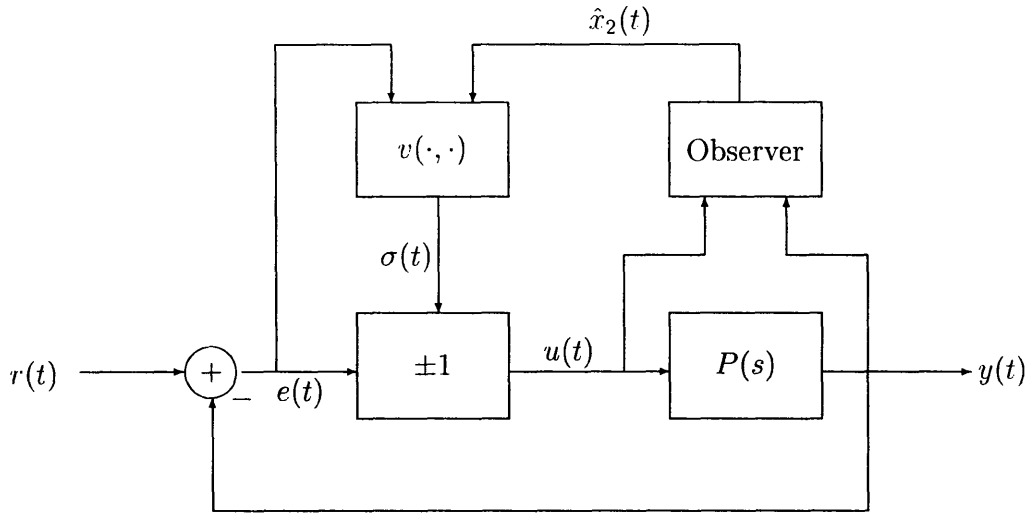


Figure 5.2.1: Proposed switching architecture to be used in designing a controller which asymptotically tracks a step input.

5.2 Switching Architecture Design

A block diagram of the switching architecture to be designed in this section is depicted in Fig. 5.2.1. Several comments are in order.

First Order Observer

First, we will design a partial observer with output $\hat{x}_2(t)$ —which is an estimate of the second state of the plant $x_2(t)$ for a particular state space description—that is a first order LTI system. Indeed, if we assume a state space description of the plant for which the output y is equal to the first state x_1 , i.e., $P(s)$ can be described via

$$\begin{bmatrix} \dot{x}_1 \\ \dot{x}_2 \end{bmatrix} = \begin{bmatrix} 0 & \sqrt{a} \\ 0 & b \end{bmatrix} \begin{bmatrix} x_1 \\ x_2 \end{bmatrix} + \begin{bmatrix} 0 \\ \sqrt{a} \end{bmatrix} u \quad (5.2.2)$$

$$y = x_1, \quad (5.2.3)$$

then we only need to obtain some estimate of x_2 in order to have a complete estimate of the state of the system. As we discussed in Chapter 4, if instead of estimating $x_2(t)$ we estimate $z(t) = x_2(t) - lx_1(t)$ where l is a free parameter, we find that the evolution of $z(t)$ is given by

$$\dot{z}(t) = (b - l\sqrt{a})z + l(b - l\sqrt{a})y + \sqrt{a}u.$$

By building an observer $\hat{z}(t)$ which mimics the above dynamics, i.e.,

$$\dot{\hat{z}}(t) = (b - l\sqrt{a})\hat{z} + l(b - l\sqrt{a})y + \sqrt{a}u,$$

we find that the dynamics of the error $d(t) = z(t) - \hat{z}(t)$ satisfy

$$\dot{d}(t) = (b - l\sqrt{a})d$$

and, hence, by choosing $l > b/\sqrt{a}$, the estimate $\hat{z}(t)$ will converge to $z(t)$ exponentially. It, hence, follows, that we can obtain an estimate $\hat{x}_2(t) = \hat{z}(t) + lx_1(t) = \hat{z}(t) + ly(t)$ which converges exponentially to $x_2(t)$ at the same rate $(b - l\sqrt{a})$.

Switching Gains

As in previous chapters, we will devote our attention to the case where the switching gains are symmetric, i.e., the gain at any given time is either $+K$ or $-K$ for some $K > 0$. The motivation for this is one of practical interest since it is sometimes the case that symmetric gains have certain implementation benefits over asymmetric gains. It should be noted that the design that we present in this section can be extended to the case of asymmetric gains, and that by restricting our examination to symmetric gains, we essentially provide lower bounds on the achievable performance of the switching structure shown in Fig. 5.2.1.

The motivation for choosing gains of $+1$ and -1 as indicated in the block diagram Fig. 5.2.1 is due to a constraint that we will impose on the design of the linear controller structures in subsequent sections. In order to make sure that the linear controllers that we design provide “reasonable” control inputs, we will impose the constraint that the control signal $u(t)$ be bounded for all time. Specifically, we will impose the constraint that $|u(t)| \leq 1$ for all $t \geq 0$. The choice of the bound of 1 imposes a constraint that the peak control value should not exceed the peak value of the exogenous input $r(t)$.²

Given the constraint that $|u(t)| \leq 1$ for all $t \geq 0$, it is necessary in any symmetric gain implementation for the gain K to satisfy $0 < K \leq 1$. Indeed, under the assumption of zero initial state, $|u(0)| = K|r(0)| = K$ from which it immediately follows that K must be less than or equal to 1. We choose to study the specific case where $K = 1$ since this value of K maximizes the rate of convergence to the origin when the input $r(t) = 0$. Indeed, via the results of Chapter 3, straightforward calculation shows that the rate of convergence for the plant $P(s)$ of Eqn. 5.1.1 is with switching gains $+K$ and $-K$ is given by

$$R = \frac{-b + \sqrt{b^2 + 4aK}}{2}.$$

It is clear from the above expression that the rate of convergence is maximized when we choose $K = 1$. It may be unclear as to why we wish to choose the value of K which maximizes the rate of convergence above, but, as we shall see in the next section, the zero-state step response of the switching architecture is closely related to the transient behavior of an equivalent system with zero input.

²Note, again, that we impose this constraint for a *unit* step input. For a step input of amplitude B , the corresponding control bound would be $|u(t)| \leq B$ for all $t \geq 0$ due to the homogeneity of the system dynamics.

Supervisor Design

To begin, note from the block diagram Fig. 5.2.1 that one of the inputs to the supervisor is the tracking error $e(t) \triangleq r(t) - y(t)$ rather than simply $y(t)$ as in previous chapters. On an intuitive level, this should not come as a surprise since our objective is drive the output $y(t)$ toward the command input $r(t)$, and, hence, we want the tracking error $e(t)$ to be small in some sense. On a more formal mathematical level, we make the following observation. Consider a constant input $r(t) = r$ for all $t > 0$. Then at any given time $t > 0$, the dynamics of the plant $P(s)$ of Eqn. 5.1.1 evolve according to

$$\begin{bmatrix} \dot{x}_1 \\ \dot{x}_2 \end{bmatrix} = \begin{bmatrix} 0 & \sqrt{a} \\ 0 & b \end{bmatrix} \begin{bmatrix} x_1 \\ x_2 \end{bmatrix} \pm \begin{bmatrix} 0 \\ \sqrt{a} \end{bmatrix} (r - x_1) \quad (5.2.4)$$

where the “ \pm ” is determined as either $+$ or $-$ via the output of the memoryless switching law $v(\cdot)$.

If we define the new variables $z_1(t) = x_1(t) - r$ and $z_2(t) = x_2(t)$, then it follows that the state-space description Eqn. 5.2.4 can be rewritten as follows:

$$\begin{bmatrix} \dot{z}_1 \\ \dot{z}_2 \end{bmatrix} = \begin{bmatrix} 0 & \sqrt{a} \\ \mp\sqrt{a} & b \end{bmatrix} \begin{bmatrix} z_1 \\ z_2 \end{bmatrix}. \quad (5.2.5)$$

From the above, we see that the zero-state response of the plant $P(s)$ to a constant input can be modelled as the zero-input response of the plant shown in Eqn. 5.2.5 with corresponding initial conditions $z_1(0) = x_1(0) - r$ and $z_2(0) = x_2(0)$ and output $y(t) = z_1(t) + r$. Hence, we may view the problem of designing a supervisor to track a step input as a problem in which we design an asymptotically stabilizing controller in the new variables z_1 and z_2 . Since $e(t) = -z_1(t)$, we can define an equivalent memoryless switching law in terms of the variables $e(t)$ and $\hat{z}_2(t) \triangleq \hat{x}_2(t)$.

We are now ready to design an asymptotically stabilizing memoryless switching law. When the switching signal $\sigma(t) = -1$, the eigenvectors of the matrix in Eqn. 5.2.5 are real and are given by

$$w_s = \begin{bmatrix} 2\sqrt{a} \\ b - \sqrt{b^2 + 4a} \end{bmatrix}, \quad w_u = \begin{bmatrix} 2\sqrt{a} \\ b + \sqrt{b^2 + 4a} \end{bmatrix},$$

where, as usual, w_s represents the stable eigenvector and w_u represents the unstable eigenvector. When $a \gg b^2$, we find that

$$w_s \approx \begin{bmatrix} 2 \\ -2 \end{bmatrix}, \quad w_u \approx \begin{bmatrix} 2 \\ 2 \end{bmatrix}.$$

Note that the vector $\begin{bmatrix} 0 & 1 \end{bmatrix}$ bisects the angle between the above two vectors, so, following the procedure of Chapter 3, we choose the following supervisor:

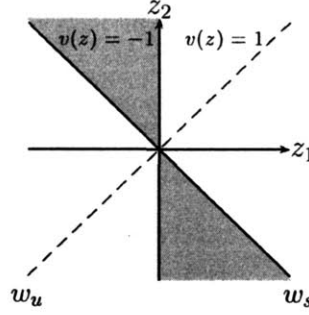


Figure 5.2.2: Supervisor of Fig. 5.2.1 for the plant $P(s)$ given by Eqn. 5.1.1.

$$v(z_1, \hat{z}_2) = \begin{cases} -1 & z_1((b - \sqrt{b^2 + 4a})z_1 - 2\sqrt{a}z_2) \leq 0 \\ 1 & z_1((b - \sqrt{b^2 + 4a})z_1 - 2\sqrt{a}z_2) > 0 \end{cases} \quad (5.2.6)$$

which, in terms of the original coordinates of the plant, can be written as

$$v(x_1 - r, \hat{x}_2) = \begin{cases} -1 & (x_1 - r)((b - \sqrt{b^2 + 4a})(x_1 - r) - 2\sqrt{a}x_2) \leq 0 \\ 1 & (x_1 - r)((b - \sqrt{b^2 + 4a})(x_1 - r) - 2\sqrt{a}x_2) > 0 \end{cases} \quad (5.2.7)$$

The supervisor is depicted graphically in terms of z coordinates in Fig. 5.2.2.

5.2.1 Step response Performance of Switching Architecture

We are now ready to describe some of the qualitative attributes of the step response of the switching architecture Fig. 5.2.1 for plants $P(s)$ of the form Eqn. 5.1.1, namely the 1% settling time and peak overshoot of the unit step response. We will specifically examine the case in which the parameters of the plant $P(s)$ satisfy the constraint that $a > b^2$. To begin, we first note that, under the assumption of zero initial state, the output of the observer $\hat{z}_2(t)$ is perfect, i.e. $\hat{z}_2(t) = z_2(t)$ for all $t \geq 0$. Hence, in computing the step response, we may ignore the observer entirely and treat the problem as if the switching law has full state access.

We will first compute an expression for the 1% settling time T_s of the step response. Note that this can be represented in terms of the variable z_1 as the smallest time $T_s > 0$ such that

$$|z_1(t)| \leq 0.01 \quad \forall t \geq T_s.$$

For a unit step input, the initial condition in z coordinates is $z(0) = \begin{bmatrix} -1 & 0 \end{bmatrix}$. Since this state lies outside of the shaded region in Fig. 5.2.2, $v(z)$ is initially 1, and a simple calculation shows that the state evolution is initially given via

$$z(t) = e^{\frac{b}{2}t} \begin{bmatrix} -\cos \beta t + \frac{b}{\sqrt{4a-b^2}} \sin \beta t \\ \frac{2\sqrt{a}}{4a-b^2} \sin \beta t \end{bmatrix} \quad (5.2.8)$$

where $\beta = \frac{1}{2}\sqrt{4a-b^2}$. The state $z(t)$ evolves in the above manner until a certain time which we will denote T_1 at which point $z(t)$ crosses the stable eigenvector w_s

which can be expressed as

$$z(T_1) = \gamma w_s$$

for some $\gamma \in \mathbf{R}$. Simple calculations show that this time T_1 is given by

$$T_1 = \frac{2}{\sqrt{4a - b^2}} \operatorname{arccot} \left(\frac{2b + \sqrt{b^2 + 4a}}{\sqrt{4a - b^2}} \right). \quad (5.2.9)$$

For times $t \geq T_1$, the state then evolves according to

$$z(t) = e^{\delta t} z(T_1) \quad (5.2.10)$$

where $\delta = \frac{1}{2}(b - \sqrt{b^2 + 4a})$ is the stable eigenvalue of the matrix in Eqn. 5.2.5 when $v(z) = -1$. We find that, for $t > T_1$,

$$z_1(t) = -\frac{1}{\sqrt{2}} e^{\frac{b}{2}T_1} e^{\delta(t-T_1)}. \quad (5.2.11)$$

Under the constraint $a > b^2$, it can be shown that the quantity $\exp(bT_1/2)/\sqrt{2} > 0.01$. Indeed,

$$\begin{aligned} \left| \frac{bT_1}{2} \right| &= \left| \frac{b}{\sqrt{4a - b^2}} \operatorname{arccot} \left(\frac{2b + \sqrt{b^2 + 4a}}{\sqrt{4a - b^2}} \right) \right| \\ &< \left| \frac{1}{\sqrt{3}} \operatorname{arccot} \left(\frac{2b + \sqrt{b^2 + 4a}}{\sqrt{4a - b^2}} \right) \right| \\ &< \frac{\pi}{2\sqrt{3}} \end{aligned}$$

from which it follows that

$$\frac{\exp(\frac{bT_1}{2})}{\sqrt{2}} > \frac{\exp(-\frac{\pi}{2\sqrt{3}})}{\sqrt{2}} > 0.01.$$

It, hence, follows that the 1% settling time T_s is the value of t in Eqn. 5.2.11 for which $z_1(t) = -.01$, which can be written explicitly as

$$T_s = \frac{1}{\delta} \ln \left(\frac{\sqrt{2}}{100} \right) + \left(1 - \frac{b}{2\delta} \right) T_1. \quad (5.2.12)$$

A sample phase portrait in z coordinates is depicted in Fig. 5.2.3. The portion of the phase portrait which lies along the depicted circular arc represents the initial T_1 seconds of evolution where the state is described by Eqn. 5.2.8, while the portion which lies along the stable manifold is the portion which is described by Eqn. 5.2.10. The phase portrait indicates that $z_1(t) < 0$ for all $t \geq 0$ which, in turn, implies that $y(t) = z_1(t) + r < r$ for all $t \geq 0$, which, in turn, implies that the step response

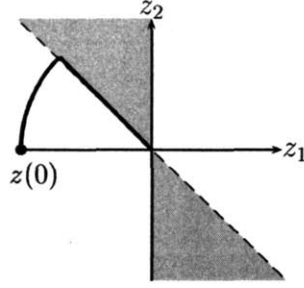


Figure 5.2.3: Example transient response in z coordinates for a plant $P(s)$ of the form Eqn. 5.1.1 controlled by the switching architecture of Fig. 5.2.1.

has no overshoot. Indeed, with the constraint $a > b^2$ in place³, this statement is true. Examining the expression for $z_2(t)$ in Eqn. 5.2.8, we see that $z_2(t) \geq 0$ for $0 \leq t \leq \pi/\beta$. Because $\dot{z}_1 = \sqrt{a}z_2$, it follows that $z_1(t)$ is increasing for $0 \leq t \leq \pi/\beta$. Now, since $z_1(T_1) = -\exp(bT_1/2)\sqrt{2} < 0$, it follows that $z_1(t) < 0$ for $0 \leq t \leq T_1$. Moreover, since $z_1(t)$ is given by Eqn. 5.2.11 for $t \geq T_1$, it follows that $z_1(t) < 0$ for all $t \geq 0$, and, hence, $y(t)$ exhibits no overshoot.

5.2.2 Design Example: Double Integrator

In order to solidify the design procedures and associated results on the settling time and overshoot presented in this section so far, we will now explore a specific example in which the plant is a double integrator $P(s) = 1/s^2$. The objective, as before, is to design a controller of the form shown in the block diagram of Fig. 5.2.1 to asymptotically track a step input. In keeping with the assumption that the output of our plant is equal to the first state of the plant, i.e. $y = x_1$, we use the following state space description:

$$\begin{bmatrix} \dot{x}_1 \\ \dot{x}_2 \end{bmatrix} = \begin{bmatrix} 0 & 1 \\ 0 & 0 \end{bmatrix} \begin{bmatrix} x_1 \\ x_2 \end{bmatrix} + \begin{bmatrix} 0 \\ 1 \end{bmatrix} u \quad (5.2.13)$$

In order to specify a design, we need to supply two objects:

- A first order observer which provides an estimate $\hat{x}_2(t)$ of the state $x_2(t)$.
- A supervisor $v(z_1, z_2)$ that implements the switching law.

Observer Design

The procedure outlined in the previous section for designing an observer consisted of two steps. First, we find an observer $\hat{z}(t)$ for the quantity $z(t) = x_2(t) - lx_1(t)$ where

³The careful reader will note that we only require $a > (b/2)^2$ for the same conclusion to be valid. Since, however, we required $a > b^2$ in deriving statements about the 1% settling time, we impose the same constraint here to focus on a class of systems for which we can make statements about *both* the settling time and overshoot.

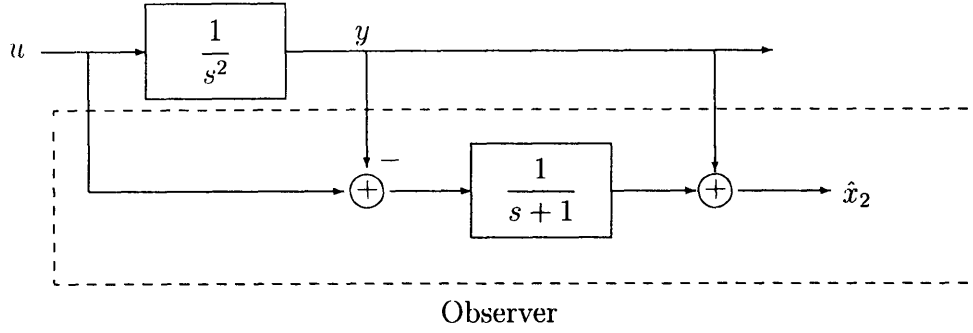


Figure 5.2.4: Block diagram of an observer (indicated by the dashed box) for the double integrator which produces an estimate $\hat{x}_2(t)$ of $x_2(t)$.

l is chosen to yield stable error dynamics. We then form an estimate $\hat{x}_2(t)$ for $x_2(t)$ via $\hat{x}_2(t) = \hat{z}(t) + lx_1(t)$. For the double integrator, the dynamics of $z(t)$ are given by

$$\dot{z} = -lz - l^2y + u$$

from which it immediately follows that any $l > 0$ will achieve stable error dynamics. For simplicity, we choose $l = 1$. Our observer is, therefore, given by

$$\begin{aligned}\dot{\hat{z}} &= -\hat{z} - y + u \\ \hat{x}_2 &= \hat{z} + y\end{aligned}$$

which is shown in block diagram form in Fig. 5.2.4.

Supervisor Design

Following the recipe of the previous section, for a constant input r , if we define the variables $z_1 = x_1 - r$, $z_2 = x_2$, their evolution at any time t can be described via

$$\begin{bmatrix} \dot{z}_1 \\ \dot{z}_2 \end{bmatrix} = \begin{bmatrix} 0 & 1 \\ \pm 1 & 0 \end{bmatrix} \begin{bmatrix} z_1 \\ z_2 \end{bmatrix}$$

where, again, either “+” or “−” are selected via the memoryless switching law. When the lower left-hand element of the matrix above is +1, the stable eigenvector w_s and unstable eigenvector w_u are given by

$$w_s = \begin{bmatrix} 1 \\ -1 \end{bmatrix}, \quad w_u = \begin{bmatrix} 1 \\ 1 \end{bmatrix}.$$

Hence, we choose as our supervisor

$$v(z_1, z_2) = \begin{cases} -1 & z_1(z_1 + z_2) \leq 0 \\ 1 & z_1(z_1 + z_2) > 0 \end{cases}.$$

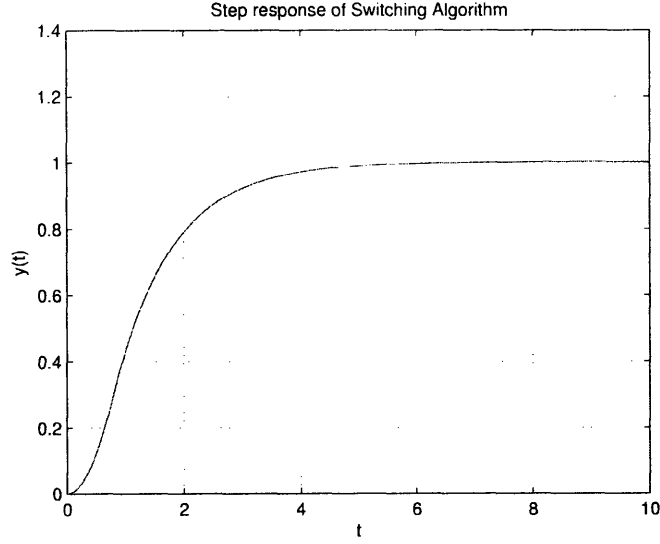


Figure 5.2.5: Step response of double integrator controlled by the switching architecture of Fig. 5.2.1.

The above supervisor is one which assumes access to the full state of the plant. As is indicated in Fig. 5.2.1, the actual inputs to the supervisor are $e(t) = -z_1(t)$ and $\hat{x}_2(t)$. In terms of these variables, the supervisor can be expressed as

$$v(e, \hat{x}_2) = \begin{cases} 1 & e(-e + \hat{x}_2) \leq 0 \\ -1 & e(-e + \hat{x}_2) > 0 \end{cases}.$$

Results

The step response using the above observer and supervisor is depicted in Fig. 5.2.5. As was proved in the prior section, the step response exhibits no overshoot. The 1% settling time for the double integrator (corresponding to the values $a = 1, b = 0$) is $T_s = \pi/4 + \ln(100/\sqrt{2}) \approx 5.04$.

5.3 Comparison: First Order LTI Control of a Double Integrator

The main objective of this chapter is not just to characterize the behavior of the step response for the switching architecture in Fig. 5.2.1, but it is, rather, to obtain an understanding of how the switching architecture performs compared to other more traditional forms of control. In this section, we wish to compare the performance of the step response that is achieved via our switching architecture to the performance of the set of step responses which are achievable via first order LTI control. The specific architecture we will consider is the so-called *servo* configuration shown in Fig. 5.3.6

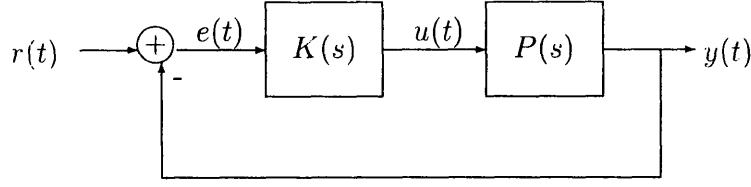


Figure 5.3.6: Servo control architecture.

where, for the present time, we restrict $K(s)$ to be a first order LTI system:

$$K(s) = k \frac{s + c}{s + d} \quad (5.3.14)$$

with $k, c, d \in \mathbf{R}$.

As a first goal, we will undergo the process of designing a first order controller $K(s)$ for the specific case where the plant is, again, a double integrator $P(s) = 1/s^2$. This will allow us to quantitatively compare the performance of the switching architecture to the achievable performance of a first order LTI controller for a specific case study and, as we will see, provide some insight into the performance capabilities of the switching architecture. In a later section, we will then extend the results shown here to a class of plants $P(s)$ which, again, are of the form

$$P(s) = \frac{a}{s(s - b)}$$

for which we will be able to make a somewhat more general performance statement.

The performance measures which we will use to evaluate the quality of a step response are the 1% settling time of the step response, as well as the percentage overshoot of the unit step response. Unlike the step response of the switching architecture, which exhibits no overshoot for a double integrator, the step response of any stabilizing first order LTI controller *must* exhibit overshoot, a fact which we now show. If we denote by $H_{re}(s)$ the transfer function from the input $r(t)$ to the tracking error $e(t)$ in the block diagram of Fig. 5.3.6, a simple application of Black's Formula yields

$$H_{re}(s) = \frac{s^2(s + d)}{s^3 + ds^2 + ks + kc}.$$

When $r(t)$ is a unit step input, $E(s)$, the Laplace transform of $e(t)$, is given by

$$E(s) = \frac{s(s + d)}{s^3 + ds^2 + ks + kc}.$$

Since $E(0) = 0$, it follows that

$$\int_0^\infty e(t) dt = 0.$$

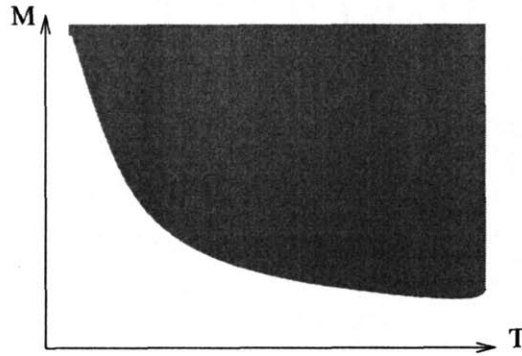


Figure 5.3.7: Example achievability region where the achievable pairs (M, T) are those which satisfy $M \geq 1/T$ (indicated by the shaded region.)

Noting also that $e(0) = \lim_{s \rightarrow \infty} sE(s) = 1$, we conclude from the above integral constraint that there exists some value of t for which $e(t) < 0$. Since $e(t) = r(t) - y(t)$, this equivalently implies that there exists some value of t for which $y(t) > r(t)$ which implies that the step response of any stabilizing first order controller will always exhibit overshoot.

The way that we will compare the performance that can be achieved via first order LTI control to the performance obtained via the switching architecture will be to determine the *achievability region* of percentage overshoot and 1% settling time. More specifically, if we denote by M and T the peak overshoot and 1% settling time, respectively, of a particular stabilizing first order LTI controller $K(s)$, then we wish to determine the set of ordered pairs (M, T) which result as we allow $K(s)$ to range over an entire class of first order LTI controllers. The reason that we wish to compute such an achievability region rather than trying to compute the controller which produces the minimal overshoot and/or the minimal 1% settling time is to gather information about potential tradeoffs between percentage overshoot and settling time for a particular class of controllers. As a hypothetical example, suppose that for a particular class of first order controllers, we find that the set of achievable pairs (M, T) satisfy the relationship

$$M \geq \frac{1}{T}$$

which is depicted graphically in Fig. 5.3.7. If we consider the problems of minimizing the percentage overshoot and minimizing the 1% settling time separately, it is clear that both of these quantities can be made arbitrarily small; however, since the product of M and T is always greater than or equal to 1, any design which makes one quantity small automatically implies that the other quantity will be large. Hence, very small settling times will require large percentage overshoot and vice-versa.

5.3.1 Preliminaries: Controller Constraints

Note in the above description that we wish to determine the achievability region for a *class* of first order controllers. Why do we simply not determine the achievability region as $K(s)$ ranges over *all* first order controllers? If we do not impose some limitations on the set of controllers, we will potentially allow ourselves to use controllers that may exhibit “unreasonable” behavior even if they provide good performance in terms of percentage overshoot and 1% settling time. We illustrate this point through an example.

Example 5.3.7 For the double integrator $P(s) = 1/s^2$, consider the first order controller

$$K(s) = \frac{\alpha^2 s}{s + 2\alpha}.$$

The associated closed-loop transfer function from $r(t)$ to $y(t)$ for this controller is given by

$$H_{ry}(s) = \frac{\alpha^2}{(s + \alpha)^2}.$$

Because the impulse response $h_{ry}(t) = \alpha^2 t \exp(-\alpha t) > 0$ for all t , it is clear that the corresponding step response

$$s(t) = \int_0^t h_{ry}(\tau) d\tau$$

is monotonically increasing and, hence, does not exhibit any overshoot. Moreover, as $\alpha \rightarrow \infty$, it is clear that the 1% settling time of the step response tends to 0. To see this, consider the case when $\alpha = 1$, and let T_0 denote the corresponding 1% settling time, i.e., $s(T_0) = .99$ when $\alpha = 1$. A simple change of variable in the above integral shows that $s(t)$ can be equivalently characterized as

$$s(t) = \int_0^{\alpha t} u e^{-u} du.$$

Hence,

$$s\left(\frac{T_0}{\alpha}\right) = \int_0^{T_0} u e^{-u} du$$

is constant for all α . Thus, T_0/α is the 1% settling time for arbitrary $\alpha > 0$ which tends to 0 as $\alpha \rightarrow \infty$.

The reader should be alarmed that the step response does not exhibit any overshoot, and with good reason! This statement is seemingly in contradiction with the statement we proved earlier that any stabilizing first order controller cannot exhibit any overshoot. As we show now, the caveat is that the controller that we are exploring here is *not* a stabilizing controller. Consider the case where a disturbance is present at the input to the plant as shown in Fig. 5.3.8. The transfer function $H_{wy}(s)$ from $w(t)$ to $y(t)$ is given by

$$H_{wy}(s) = \frac{s + 2\alpha}{s(s + \alpha)^2}$$

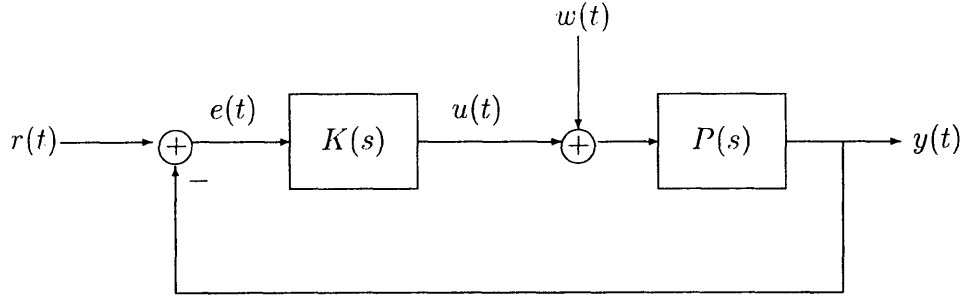


Figure 5.3.8: Servo architecture with plant input disturbance $w(t)$.

and is, hence, unstable. The instability in the above transfer function is a result of an unstable pole-zero cancellation at $s = 0$ between the controller $K(s)$ and the plant $P(s)$. One could conceivably consider a slightly different controller of the form

$$K(s) = \alpha^2 \frac{s + \epsilon}{s + 2\alpha}$$

where ϵ is a small number since one would expect the step response with this controller in place to be close to the original step response for ϵ sufficiently small. In this case, $H_{wy}(s)$ becomes

$$H_{wy}(s) = \frac{s + 2\alpha}{s^3 + 2\alpha s^2 + \alpha^2 s + \alpha^2 \epsilon}$$

which, by the Routh-Hurwitz criterion [63], will be stable for $\alpha > 0$, $\epsilon > 0$, $\alpha > \epsilon/2$. Note, however, in this case that, for ϵ very small, the H-infinity norm of $H_{wy}(s)$ will be very large. Indeed,

$$\|H_{wy}\|_{\infty} \geq |H(0)| = \frac{2}{\alpha\epsilon}$$

from which we conclude that $\|H_{wy}\|_{\infty} \rightarrow \infty$ as $\epsilon \rightarrow 0$. Because this H-infinity norm represents the L_2 gain from $w(t)$ to $y(t)$, we see that low-frequency disturbance inputs will have a large impact on the output $y(t)$ when ϵ is small which, typically, is undesirable.

In addition to the above problem, an additional problem exists in that, for large values of α , the peak control value is very high. Indeed, for a unit step input, $U(s)$, the Laplace transform of the control output $u(t)$ is given by

$$U(s) = \frac{\alpha^2 s}{(s + \alpha)^2}.$$

From this, we deduce that $u(0) = \lim_{s \rightarrow \infty} sU(s) = \alpha^2$. Thus, the smaller we want the 1% settling time, the larger the peak control value.

The preceding example suggests two key constraints to impose on the closed-loop servo configuration of Fig. 5.3.8:

- A bound on the peak control response, i.e., for some $B > 0$, constraining

$$|u(t)| \leq B \text{ for all } t > 0.$$

- A bound on the closed-loop L_2 gain from w to y , i.e., for some $C > 0$, considering only those first order controllers $K(s)$ for which the corresponding closed-loop transfer function from w to y satisfies $\|H_{wy}\|_\infty \leq C$.

In forming a comparison between the performance we can achieve via first order LTI control and the performance of the switching architecture we have constructed, we must take care to ensure the same set of constraints for both architectures. Because we are considering only a single design within the framework of the switching architecture, the values of these constraints are determined de facto.

Switching Architecture: Peak Control Bound

As was mentioned in the process of designing the switching architecture, the choice of switching between gains of $+1$ and -1 was related to the fact that, in the end, we desired to constrain the peak control value to be one, i.e., we wanted to impose the constraint that $|u(t)| \leq 1$ for all $t > 0$, a fact we now show.

First, note that $|u(t)| = |r(t) - y(t)| = |e(t)|$, so it suffices to show that $|e(t)|$ never exceeds one when $r(t)$ is a unit step input. Now, we have already shown that the output $y(t)$ is monotonically increasing for all $t > 0$ and satisfies the constraints

$$y(0) = 0, \quad \lim_{t \rightarrow \infty} y(t) = 1.$$

It then follows that $e(t)$ is monotonically decreasing for $t > 0$ and satisfies the conditions

$$e(0) = 1, \quad \lim_{t \rightarrow \infty} e(t) = 0.$$

Hence $0 \leq e(t) \leq 1$ for all $t > 0$, and it follows that $|u(t)| \leq 1$ for all $t \geq 0$.

Switching Architecture: L_2 gain from $w(t)$ to $y(t)$

As we mentioned in Chapter 4, while it is generally impossible to determine the exact L_2 gain from a given input to a given output in a nonlinear system such as ours, we can find an upper bound on the L_2 gain from $w(t)$ to $y(t)$ for the switching architecture.

A partial block diagram which depicts the L_2 gain calculation we wish to perform is depicted in Fig. 5.3.9. Because the plant $P(s)$ is second order and the observer is first order, the overall plant dynamics are third order. This does not fit within the framework of the computational techniques that were developed in Chapter 4 (which could handle only second order dynamics), but, as we will see now, we can develop an upper bound on the L_2 gain from $w(t)$ to $y(t)$ which involves computing the L_2 gain for a second order system.

To begin, we will make the change of coordinates $z_1 = x_1$, $z_2 = x_2 - x_1$, for which

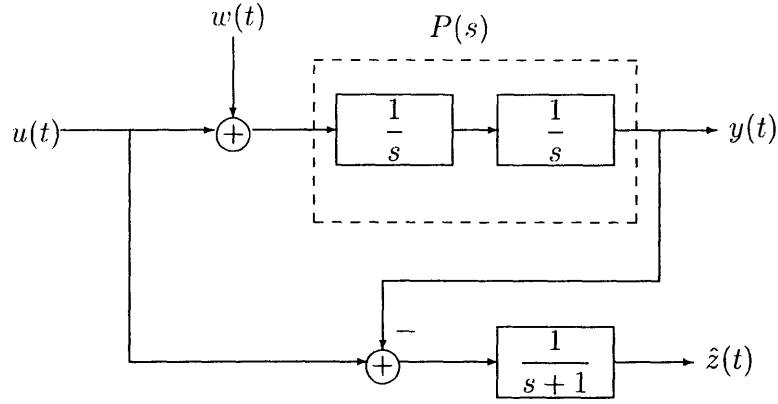


Figure 5.3.9: Partial block diagram for L_2 gain calculation. The exogenous input $w(t)$ is input to the plant $P(s)$ but is not input to the observer.

we obtain the state-space description

$$\begin{bmatrix} \dot{z}_1 \\ \dot{z}_2 \end{bmatrix} = \begin{bmatrix} 1 & 1 \\ -1 & -1 \end{bmatrix} \begin{bmatrix} z_1 \\ z_2 \end{bmatrix} + \begin{bmatrix} 0 \\ 1 \end{bmatrix} u \quad (5.3.15)$$

$$y = z_1 \quad (5.3.16)$$

which is depicted graphically in Fig. 5.3.10. Notice that there are two blocks which both have transfer function $1/(s+1)$. If the input $w(t)$ were not present (i.e., $w(t) = 0$ for all t), then the outputs of the two blocks would be related by

$$z_2(t) = \hat{z}(t) + (z_2(0) - \hat{z}(0))e^{-t}$$

for all $t \geq 0$ where the decaying exponential term is due to the difference in initial conditions between $z_2(t)$ and $\hat{z}(t)$. Because this decaying signal would not affect the L_2 gain calculation, we would be able to perform the calculation by eliminating the observer block entirely and performing the calculation as if we had access to the full state $\begin{bmatrix} z_1 & z_2 \end{bmatrix}'$.

While it is true that we cannot make the above conclusion when $w(t)$ is present, it turns out that we can compute another L_2 gain in which *both* the plant and observer have access to the input $w(t)$ and which provides an upper bound on the L_2 gain from $w(t)$ to $y(t)$ in the original setup of Fig. 5.3.9. To begin, first note that we may redraw the block diagram of Fig. 5.3.10 to appear as what is depicted in Fig. 5.3.11. Now, suppose that we replace the input $-w(t)$ by an arbitrary signal $w'(t)$. We will invoke the following results whose proofs are given in the last section of this chapter:

Proposition 5.3.15 *Consider a two-input, single-output system $y = \Delta(w, w')$ such that the joint L_2 gain from $\begin{bmatrix} w(t) & w'(t) \end{bmatrix}$ to $y(t)$ is finite. Suppose that γ is an upper bound on the L_2 gain from $\begin{bmatrix} w(t) & w'(t) \end{bmatrix}$ to $y(t)$. Then $\sqrt{2}\gamma$ is an upper bound on the L_2 gain from $w(t)$ to $y(t)$ when $w(t)$ and $w'(t)$ are related by the constraint $|w(t)| = |w'(t)|$ for all t .*

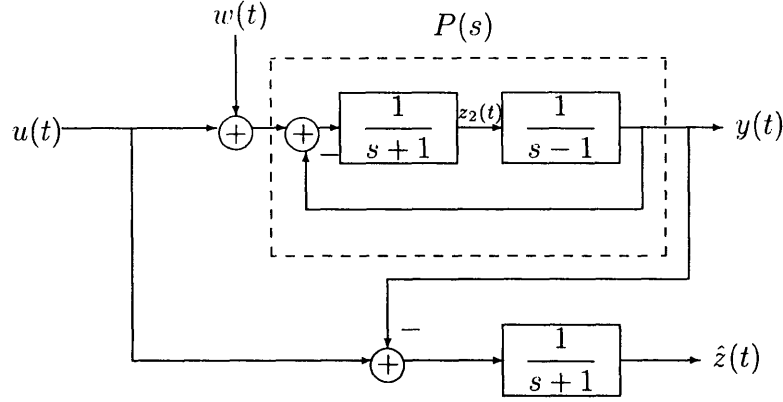


Figure 5.3.10: Block diagram of Fig. 5.3.9 under the change of coordinates $z_1 = x_1$, $z_2 = x_2 - x_1$.

Proposition 5.3.16 *Consider systems Δ_1 and Δ_2 , both with finite L_2 gain. Suppose that γ_1 is an upper bound on the L_2 gain of Δ_1 , and that γ_2 is an upper bound on the L_2 gain of Δ_2 . Then $\gamma_1\gamma_2$ is an upper bound on the L_2 gain of the composition $\Delta_1 \circ \Delta_2$, i.e. $\gamma_1\gamma_2$ is an upper bound on the L_2 gain of the system $y = \Delta_1(\Delta_2(w))$.*

We will utilize the result of Prop. 5.3.15 in the following way: if we replace the input $-w(t)$ by an arbitrary input $w'(t)$ and compute an upper bound γ on the L_2 gain from $\begin{bmatrix} w(t) & w'(t) \end{bmatrix}$ to $y(t)$, then we will know that $\sqrt{2}\gamma$ is an upper bound on the L_2 gain from $w(t)$ to $y(t)$ in the original problem. While the utility of this statement may not be immediately apparent, we proceed forward.

Note that the system of Fig. 5.3.11 can be modelled as the composition of two systems $y = \Delta_1(\Delta_2(w, w'))$, where

$$\Delta_2(w, w') = \begin{bmatrix} 1 & 0 \\ 0 & \frac{1}{s+1} \end{bmatrix} \begin{bmatrix} w \\ w' \end{bmatrix}$$

and where $\Delta_1 \triangleq \Delta_1(w, v)$ characterizes the remaining dynamics of the system. Since the L_2 gain of Δ_2 is equal to 1, Prop. 5.3.16 tells us that the L_2 gain of $y = \Delta_1(\Delta_2(w, w'))$ is upper bounded by the L_2 gain of $y = \Delta_1(w, v)$. Fig. 5.3.12 depicts this new L_2 gain calculation. We now notice in this diagram that $w(t)$ drives *both* the input to the plant and the observer, from which we conclude that

$$z_2(t) = \hat{z}(t) + (z_2(0) - \hat{z}(0))e^{-t}$$

for all $t > 0$. Hence, we can safely remove the observer from the L_2 gain calculation and assume that we have access to the plant state $z_2(t)$. Fig. 5.3.13 depicts this calculation. Notice that this is a second order system and the techniques of Chapter 4 directly apply.

To summarize, finding an upper bound on the L_2 gain from $w(t)$ to $y(t)$ in Fig. 5.3.9 can be accomplished in two steps:

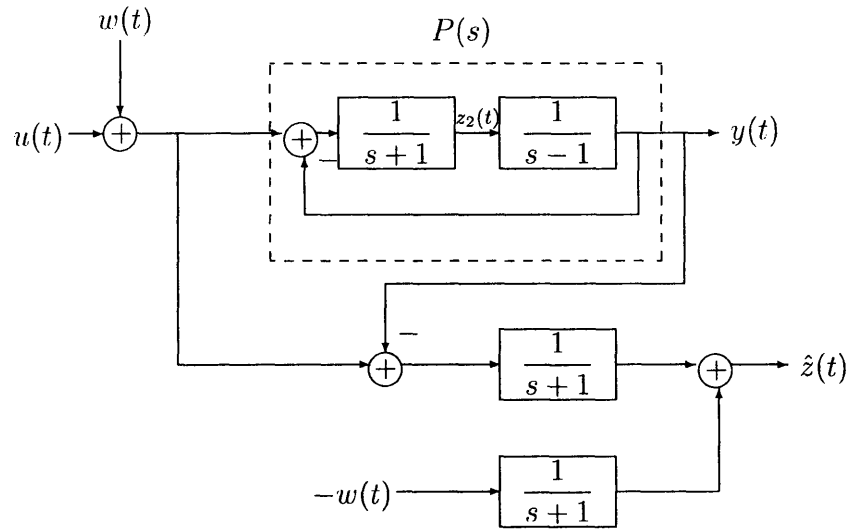


Figure 5.3.11: Rearrangement of the block diagram of Fig. 5.3.10.

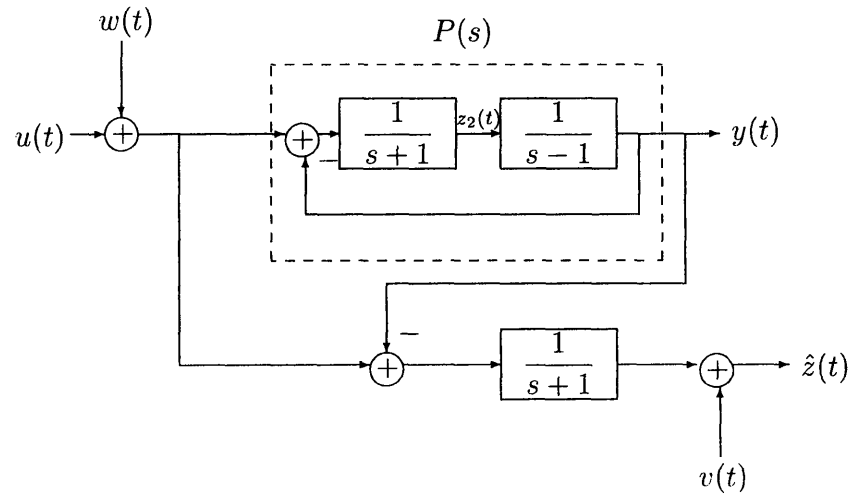


Figure 5.3.12: New system which upper bounds the L_2 gain of the system depicted in Fig. 5.3.11 with $-w(t)$ replaced by $w'(t)$.

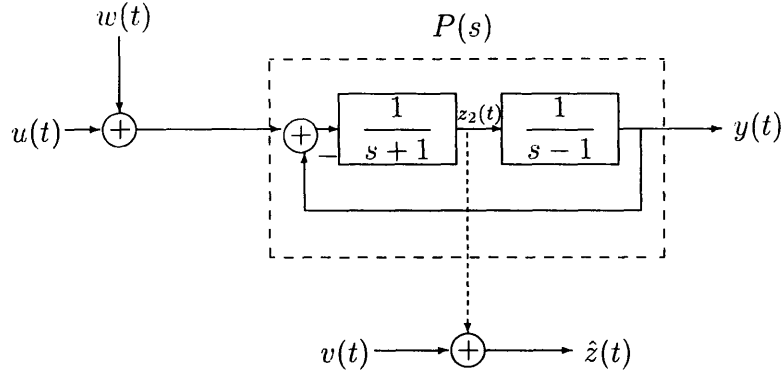


Figure 5.3.13: Block diagram of a second order system whose joint L_2 gain from the inputs $w(t)$ and $v(t)$ to $y(t)$ upper bounds the L_2 gain from $w(t)$ to $y(t)$ in Fig. 5.3.9.

- Computing the joint L_2 gain from $\begin{bmatrix} w(t) & v(t) \end{bmatrix}$ to $y(t)$ in Fig. 5.3.13.
- Multiplying this joint L_2 gain by $\sqrt{2}$.

The dynamics of the joint L_2 gain calculation for the double integrator can be described via the equations

$$\begin{aligned}\dot{z}_1 &= z_1 + z_2 \\ \dot{z}_2 &= -z_1 - z_2 + f(z_1, z_2, v)y + w \\ y &= z_1\end{aligned}$$

where $f(z_1, z_2, v)$ is given by

$$f(z_1, z_2, v) = \begin{cases} 1 & z_1(2z_1 + z_2 + v) \leq 0 \\ -1 & z_1(2z_1 + z_2 + v) > 0 \end{cases}.$$

Computing the above joint L_2 gain from $\begin{bmatrix} w(t) & v(t) \end{bmatrix}'$ to $y(t)$ in MATLAB yields an upper bound of 5.92. Multiplying this by $\sqrt{2}$ yields an upper bound of 8.38 for the L_2 gain from $w(t)$ to $y(t)$ in Fig. 5.3.9.

5.3.2 First Order Controller Class

Now that we have computed the constraints that we wish to impose on the closed-loop system of Fig. 5.3.8, we are in the position of being able to compute the constraints on the associated first order controller $K(s)$ of the form

$$K(s) = k \frac{s + c}{s + d}.$$

We will first determine constraints on the value of k that are induced by the peak control bound, and will then determine constraints on the values of c and d imposed

by the constraint on the L_2 gain from w to y .

Peak Control Bound

When $P(s) = 1/s^2$ and $K(s)$ is as shown above, the closed loop transfer function from $r(t)$ to $u(t)$ in the servo configuration of Fig. 5.3.8 is given by

$$H_{ru}(s) = \frac{ks^2(s+c)}{s^3 + ds^2 + ks + kc}. \quad (5.3.17)$$

When the input $r(t)$ is a unit step with Laplace transform $R(s) = 1/s$, the initial value theorem tells us that $u(0) = \lim_{s \rightarrow \infty} sU(s) = k$. Hence, if we wish to constrain the peak value of the control to be less than 1 for all $t \geq 0$, it follows that $|k| \leq 1$. Moreover, by examining the denominator of Eqn. 5.3.17, the Routh criterion constrains k to be positive. Hence, we only consider values of k for which $0 < k \leq 1$.

As it turns out, the value of k which yields the “best” performance is the value $k = 1$. Intuitively, as $k \rightarrow 0$, the block diagram of Fig. 5.3.8 approaches an “open-loop” configuration and, hence, we would expect poor performance (in terms of overshoot and/or settling time) for small values of k . The formal statement we can make is the following:

Proposition 5.3.17 *Consider the system of Fig. 5.3.8 where $P(s) = 1/s^2$ and where $K(s)$ is a first order controller of the form Eqn. 5.3.14:*

$$K(s) = k \frac{s+c}{s+d}$$

with k strictly less than one, and denote by M and T the percentage overshoot and 1% settling time of the unit step response $y(t)$. Suppose that $K(s)$ satisfies the constraint

$$\left\| \frac{P(s)}{1 + P(s)K(s)} \right\|_{\infty} < \gamma$$

for some $\gamma > 0$. Then the following statements are true

1. *The peak control value to a unit step input is equal to k .*
2. *The controller*

$$\tilde{K}(s) = \frac{s + \frac{c}{\sqrt{k}}}{s + \frac{d}{\sqrt{k}}}$$

satisfies the constraint

$$\left\| \frac{P(s)}{1 + P(s)\tilde{K}(s)} \right\|_{\infty} < \gamma.$$

Moreover, the peak control effort $u(t)$ in response to a unit step input with the controller $\tilde{K}(s)$ in place of $K(s)$ is equal to 1, and the overshoot and 1% settling time of the corresponding step response $y(t)$ are given by M and $T\sqrt{k}$, respectively.

The proof of Prop. 5.3.17 is rather technical and is left to the appendix at the end of the chapter. In layman's terms, the result of the proposition is the following: if we can find a controller with peak gain strictly less than 1 for which the closed-loop L_2 gain from $w(t)$ to $y(t)$ (characterized by the H_∞ norm constraint) is less than a certain value γ , then we can always find another controller for which the peak gain is exactly equal to 1 and for which the L_2 gain constraint is still satisfied. Moreover, this new controller has a percentage overshoot that is exactly the same as the original controller but with a 1% settling time that is reduced by a factor of \sqrt{k} . Hence, it is sufficient to search over the set of controllers $K(s)$ of the form Eqn. 5.3.14 with $k = 1$.

L_2 Gain Bound

Based upon the results of the previous section, it is sufficient to limit the set of controllers over which we search to those which take the form

$$K(s) = \frac{s + c}{s + d}. \quad (5.3.18)$$

Hence, the set of controllers which we want to examine are those for which the closed loop L_2 gain from $w(t)$ to $y(t)$ in Fig. 5.3.8 is bounded above by $\gamma = 8.38$. This requirement can be expressed as searching over the set of $(c, d) \in \mathbf{R}^2$ for which

$$\|H(s)\|_\infty = \left\| \frac{s + d}{s^3 + ds^2 + s + c} \right\|_\infty \leq \gamma. \quad (5.3.19)$$

As we will show now, the set of pairs $(c, d) \in \mathbf{R}^2$ which satisfy the condition of Eqn. 5.3.19 for any $\gamma > 0$ lies in a bounded set. While it is difficult to analytically compute the exact set of pairs (c, d) which satisfy the above condition, we will find an outer approximation of this region which will allow us to be able to estimate the achievability region that we want to calculate.

To begin, define

$$W = \{(c, d) \in \mathbf{R}^2 : c > 0, d > 0, d > c\}.$$

The set W is the set of $(c, d) \in \mathbf{R}^2$ for which all of the roots of the polynomial $s^3 + ds^2 + s + c$ lie in the open left half plane and, hence, represents the domain for which the H_∞ norm of Eqn. 5.3.19 is well-defined. Define

$$f(c, d) = \left\| \frac{s + d}{s^3 + ds^2 + s + c} \right\|_\infty$$

for $(c, d) \in W$, and let V_γ be defined by the condition

$$V_\gamma = \{(c, d) \in W : f(c, d) \leq \gamma\} \quad (5.3.20)$$

for some $\gamma > 0$. It is precisely the set V_γ that we wish to show is bounded.

To show that V_γ is bounded, we compute $|H(j\omega)|$ of Eqn. 5.3.19 at a few select frequencies. First, note that $|H(0)| = d/c$. If the infinity norm of $H(s)$ is to be less than some value γ then $|H(j\omega)|$ must be less than γ for every frequency ω , which implies that $|H(0)| \leq \gamma$ or that

$$\boxed{d \leq \gamma c.}$$

If we now compute $|H(j\omega)|$ at $\omega = 1$, we have

$$|H(j)| = \left| \frac{j + d}{c - d} \right| \geq \frac{1}{1 - \frac{c}{d}}.$$

Recognizing that the rightmost inequality must be less than or equal to γ yields the condition

$$\boxed{d \geq \frac{\gamma}{\gamma-1}c.}$$

Continuing in a similar vein,

$$\begin{aligned} \left| H \left(j \sqrt{\frac{c}{d}} \right) \right| &= \left| \frac{j \sqrt{\frac{c}{d}} + d}{j \sqrt{\frac{c}{d}} (1 - \frac{c}{d})} \right| \\ &\geq \frac{d}{\sqrt{\frac{c}{d}} (1 - \frac{c}{d})} \\ &\geq \frac{d}{\left(\frac{\gamma-1}{\gamma} \right)^{\frac{3}{2}}} \end{aligned}$$

which yields the bound

$$\boxed{d \leq \gamma \left(\frac{\gamma-1}{\gamma} \right)^{\frac{3}{2}} \leq \gamma.}$$

Now, revisiting $|H(j)|$, we have

$$\begin{aligned} |H(j)| = \left| \frac{j + d}{c - d} \right| &\geq \frac{1}{d - c} \\ &= \frac{1}{d \left(1 - \frac{c}{d} \right)} \\ &\geq \frac{1}{d \left(1 - \frac{1}{\gamma} \right)} \end{aligned}$$

from which we conclude

$$\boxed{d \geq \frac{1}{\gamma-1}.$$

Finally, manipulating the above inequalities appropriately, we obtain the bounds

$$\boxed{\frac{1}{\gamma(\gamma-1)} \leq c \leq \gamma - 1.}$$

A graphical depiction of the region described by the boxed-in inequalities above is shown in Fig. 5.3.14. Note that in order for the above bounds on c and d to make

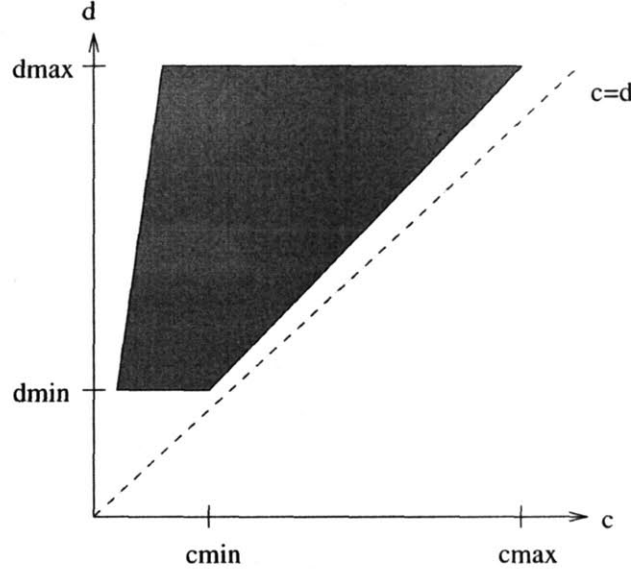


Figure 5.3.14: Region described by the boxed-in bounds, with $c_{\min} = 1/(\gamma^2 - \gamma)$, $c_{\max} = \gamma - 1$, $d_{\min} = 1/(\gamma - 1)$, and $d_{\max} = \gamma$.

sense, we require that

$$\begin{aligned}\gamma &\geq \frac{1}{\gamma - 1} \\ \gamma - 1 &\geq \frac{1}{\gamma(\gamma - 1)}.\end{aligned}$$

A simple numerical evaluation confirms that if $\gamma > 1.76$ then the above inequalities are satisfied. Mathematically, this implies that V_γ is empty for $\gamma \leq 1.76$, i.e., 1.76 is a lower bound on the infinity norm of $H(s)$ in Eqn. 5.3.19 for *any* values $(c, d) \in W$.

Note that, in general the region V_γ of Eqn. 5.3.20 is *not* the region that is defined by the boxed-in inequalities above. Rather, V_γ is a subset of this region.

5.3.3 Computation of Achievable Percentage Overshoot, 1% Settling Time Pairs

We have now limited the process of computing the set of achievable pairs (M, T) of percentage overshoot and 1% settling time pairs to a search over a bounded region of \mathbf{R}^2 . Because overshoot and settling time are not analytically parameterizable, we attempt to compute an approximation of the achievable set of pairs (M, T) by finely gridding the bounded region described in the previous section. For each grid point (c_i, d_j) in the polygon described by Fig. 5.3.14, we first determine whether whether $(c_i, d_j) \in V_\gamma$, i.e., whether the corresponding closed loop transfer function $H(s)$ of Eqn. 5.3.19 satisfies the imposed norm bound condition. Once we have found the set of points in the grid which lie in V_γ , we simulate the corresponding unit step response

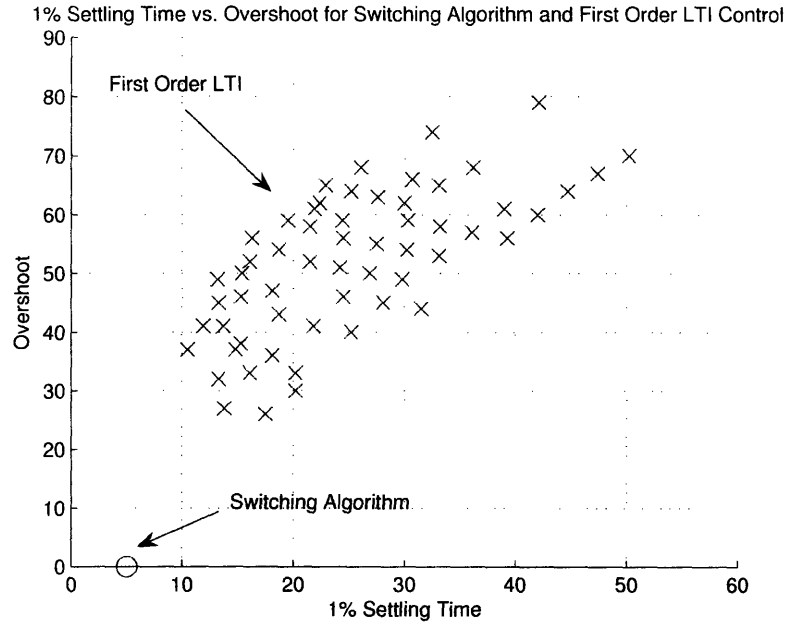
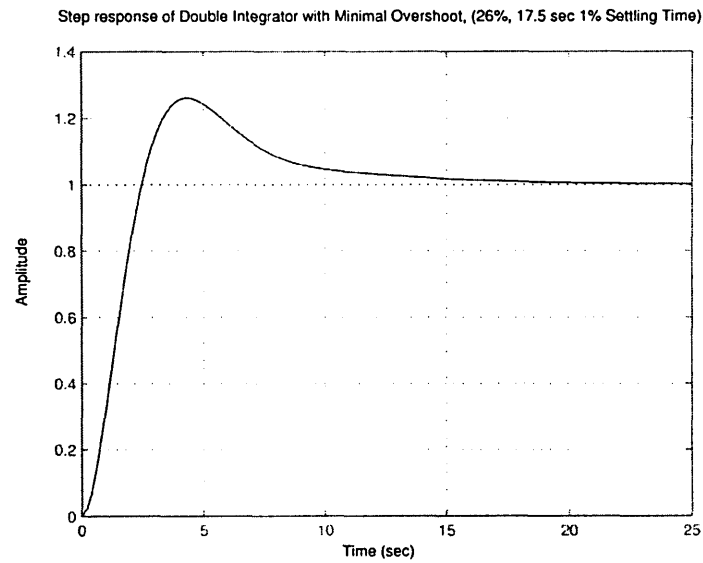


Figure 5.3.15: Achievable percentage overshoot and 1% settling time time pairs that can be achieved via first order LTI control for the given peak control and L_2 gain constraints (shown by 'x' in the picture). The performance of the switching architecture is shown via the circle at the bottom of the figure for comparison.

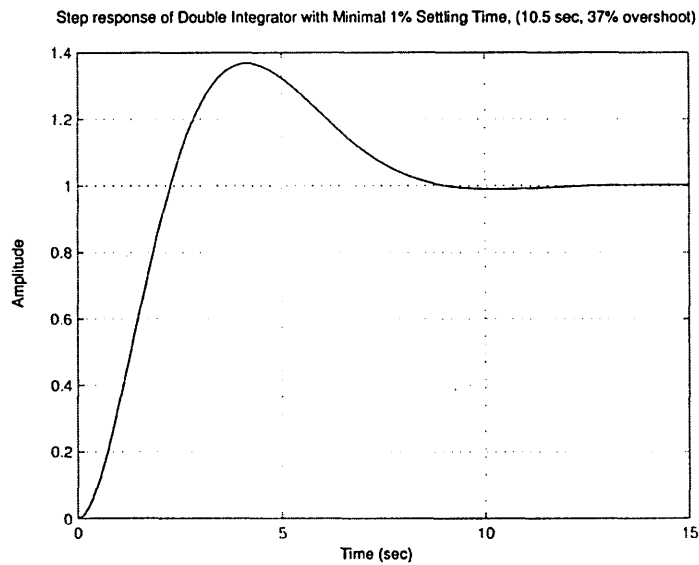
in MATLAB and measure the percentage overshoot and 1% settling time for each grid point in V_γ .

The results of this gridding process are shown in Fig. 5.3.15. The overshoot and 1% settling time pairs that are achievable via first order LTI control under the given peak control and L_2 gain constraints are depicted by the 'x' symbols, while the performance of the switching architecture that we designed in the first section is shown via the circle at the bottom of the figure for comparison. Note that the LTI control does exhibit a tradeoff between percentage overshoot and 1% settling time; the minimal percentage overshoot of 26% has a settling time of 17.5 seconds, while the minimal 1% settling time of 10.5 seconds has a corresponding peak overshoot of 37%. A plot of the step response with minimal percentage overshoot and a plot of the step response with minimal 1% settling time are shown in Fig. 5.3.16.

While it is impossible to obtain the exact minimal values of percentage overshoot and 1% settling time via a gridding procedure, Fig. 5.3.15 is clearly indicative of a finite gap between the minimal 1% settling time and minimal percentage overshoot that can be achieved via first order LTI control vs. what can be achieved via the switching algorithm designed in the first section.



(a) Minimal overshoot.



(b) Minimal 1% settling time.

Figure 5.3.16: Step responses of double integrator that achieve minimal overshoot and minimal 1% settling time subject to the peak control value and L_2 gain bound constraints given in this section.

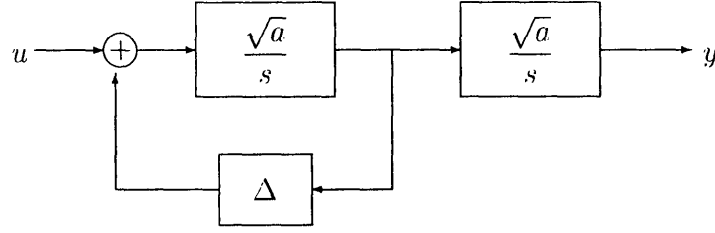


Figure 5.3.17: Realization of transfer function $P(s)$ of Eqn. 5.1.1 where $\Delta = b/\sqrt{a}$.

5.3.4 First Order LTI Control for Other Plants

We can perform similar comparisons between the performance of the switching architecture and the performance that is achievable via first order LTI control for plants other than the double integrator, as well. Here, we will consider two additional plants:

$$P_1(s) = \frac{100}{s(s+1)}, \quad P_2(s) = \frac{100}{s(s-1)}$$

Informally, the above plants are “close” to a double integrator in the sense that the corresponding values of a and b for each plant satisfy the constraint that $a \gg b^2$ (in both cases $a/b^2 = 100$). In a slightly more formal setting, we can view the transfer function $P(s)$ of Eqn. 5.1.1 as a *perturbation* of a double integrator in the following manner: the transfer function $P(s)$ can be realized via the block diagram of Fig. 5.3.17 where $\Delta = b/\sqrt{a}$. The case when $a \gg b^2$ can, therefore, be viewed as a case where Δ is small in Fig. 5.3.17, hence motivating the informal notion of closeness we have been describing to this point.

Returning now to our performance comparison, we design switching controllers for the plants $P_1(s)$ and $P_2(s)$ using the algorithm presented in the first section of this chapter, and then we evaluate the performance of a first order LTI controller subject to the same peak gain condition $|u(t)| \leq 1$ for all $t \geq 0$ and a similar L_2 gain bound condition (where, obviously, the L_2 gain bounds are the bounds which we numerically compute for the switching architectures that control $P_1(s)$ and $P_2(s)$, respectively). The results for $P_1(s)$ and $P_2(s)$ are shown in Fig. 5.3.18 and Fig. 5.3.19, respectively. Part (a) of each figure shows the step response that is obtained via the switching algorithm presented in the first section of this chapter, while parts (b) and (c) of each figure show the step response with a first order LTI controller $K(s)$ placed in a servo configuration of Fig. 5.3.6 that achieves minimal overshoot and minimal 1% settling time, respectively.

It is difficult to make general statements about a class of systems for which the use of the switching architecture presented in this chapter has clear benefits over using a first order LTI controller. Part of this is simply due to the fact that quantities such as percentage overshoot and 1% settling time are not quantities which are, in general, easily analytically parameterizable. Nevertheless, while we cannot currently provide a broad general class, we can offer the following weak generalization.

Proposition 5.3.18 Consider a plant $P(s)$ and controller $K(s)$ of the form

$$P(s) = \frac{a}{s(s-b)} \quad K(s) = k \frac{s+c}{s+d}$$

with $a > 0$, $k > 0$, $b, c, d \in \mathbf{R}$, and define

$$H_1(s) = \frac{K(s)}{1 + P(s)K(s)} \quad H_2(s) = \frac{P(s)K(s)}{1 + P(s)K(s)}.$$

Suppose that the following two properties hold:

1. The step response $u(t)$ of the system $H_1(s)$ satisfies the condition $|u(t)| \leq 1$ for all $t \geq 0$.
2. $\|H_2(s)\|_\infty$ is finite and satisfies $\|H_2(s)\|_\infty \leq \gamma$ for some $\gamma > 0$.
3. The unit step response $s(t)$ of $H_2(s)$ has percentage overshoot M and 1% settling time T .

Then the transfer functions $\tilde{H}_1(s)$ and $\tilde{H}_2(s)$ given by

$$\tilde{H}_1(s) = \frac{\tilde{K}(s)}{1 + \tilde{P}(s)\tilde{K}(s)} \quad \tilde{H}_2(s) = \frac{\tilde{P}(s)\tilde{K}(s)}{1 + \tilde{P}(s)\tilde{K}(s)}$$

with

$$\tilde{P}(s) = \frac{a\alpha^2}{s(s-b\alpha)} \quad \tilde{K}(s) = k \frac{s+c\alpha}{s+d\alpha}$$

for some $\alpha > 0$ satisfy the following conditions.

1. The step response $\tilde{u}(t)$ of the system $\tilde{H}_1(s)$ satisfies the condition $|\tilde{u}(t)| \leq 1$ for all $t \geq 0$.
2. $\|\tilde{H}_2(s)\|_\infty$ is finite and satisfies $\|\tilde{H}_2(s)\|_\infty \leq \gamma$.
3. The unit step response $\tilde{s}(t)$ of $\tilde{H}_2(s)$ has percentage overshoot M and 1% settling time T/α .

Proof The proof of this statement is very similar to the second part of the proof of Prop. 5.3.17 and is left to the reader. \square

Prop. 5.3.18 tells us that, in optimizing for performance in terms of percentage overshoot and/or 1% settling time for a single plant, we effectively compute the optimal percentage overshoot and/or 1% settling time for an entire *class* of plants. For example, consider the plant

$$P_3(s) = \frac{1}{s(s-.1)}$$

which is related to the plant $P_2(s)$ above via $P_3(s) = P_2(10s)$. Using the result of Prop. 5.3.18 for $\alpha = 0.1$, we conclude that, since the minimum achievable overshoot using first order control for $P_2(s)$ was measured to be 38%, the minimum achievable overshoot using first order control for $P_3(s)$ is also 38%. Moreover, since the minimum achievable 1% settling time was measured to be 1.35 sec for $P_2(s)$, we conclude that the minimum achievable 1% settling time for $P_3(s)$ is 13.5 sec. In general, if we know that the minimal percentage overshoot and 1% settling time for a plant $P(s)$ are given by M and T , respectively, then the minimal percentage overshoot and settling time of $P(s/\alpha)$ are given by M and T/α , respectively.

5.4 Comparison: Higher Order LTI Control

In this section, we would like to compare the performance of the switching architecture of the first section to fundamental performance limits of LTI control. Specifically, we would like to compare the 1% settling time of the switching controller for a given plant $P(s)$ of Eqn. 5.1.1 to the 1% settling time that can be achieved via a rational LTI controller $K(s)$ connected in the servo configuration of Fig. 5.3.6 where $K(s)$ is of unconstrained order.

We will derive bounds on the ratio of the 1% settling time achievable via the switching architecture vs. that which is achievable via LTI control by first examining two *time-optimal* control problems. That is, we will initially remove the restriction that the control input $u(t)$ must be the output of an LTI feedback interconnection and derive a lower bound on the 1% settling time that can be achieved by searching over all control inputs $u(t)$ with $|u(t)| \leq 1$ for all $t \geq 0$. We will first derive a weak (conservative) lower bound on the 1% settling time achievable via bounded control to establish a formal bound on the ratio of the two settling times (switching algorithm vs. bounded control input), and then will derive an approximate lower bound which, in many cases, yields a more accurate ratio.

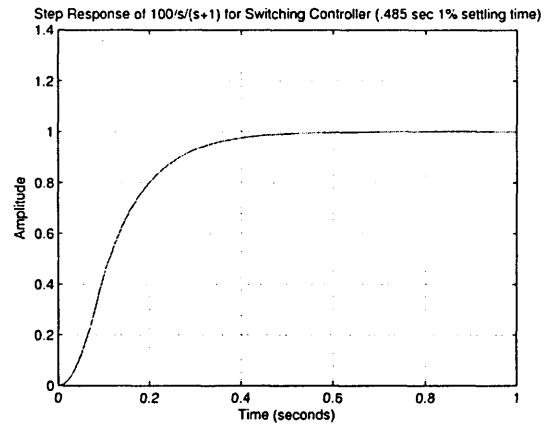
Once we have derived the above bounds, we will examine a method of designing LTI controllers that minimize 1% settling time with less than 1% overshoot (we will see that this extra constraint on overshoot does not affect our ability to get close-to-optimal 1% settling times). As we will see, this problem can be formulated as an infinite dimensional linear programming problem that can be solved numerically using standard software packages. We will examine the method for several plants $P(s)$ to investigate the order of a controller $K(s)$ which achieves close-to-optimal performance that can be obtained via this method as a function of the plant parameters a and b .

5.4.1 Time Optimal Control, Part I: Bounds derived from Rise Time

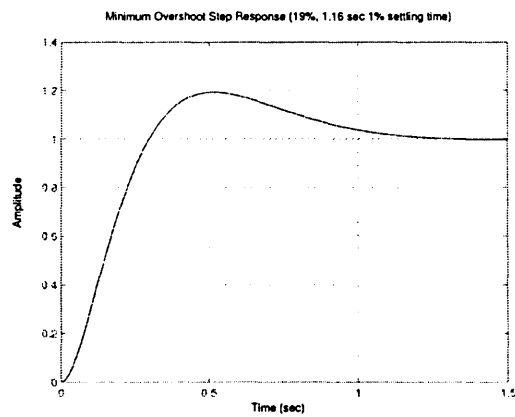
We begin with two definitions that we will encounter frequently in this section:

Definition 5.4.4 The ϵ -settling time T of a real-valued signal $y(t)$ is the smallest value of $T > 0$ such that

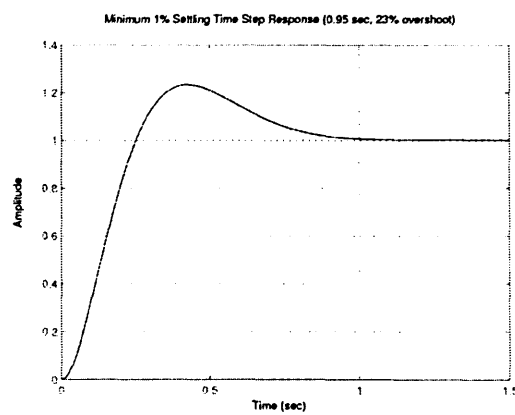
$$|y(t) - 1| \leq \epsilon \quad \forall t \geq T.$$



(a) Switching algorithm step response (0.485 sec 1% settling time).

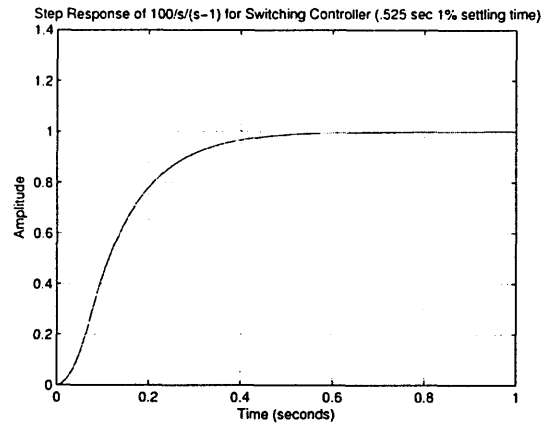


(b) Minimum overshoot with first order LTI control (19% overshoot, 1.16 sec 1% settling time).

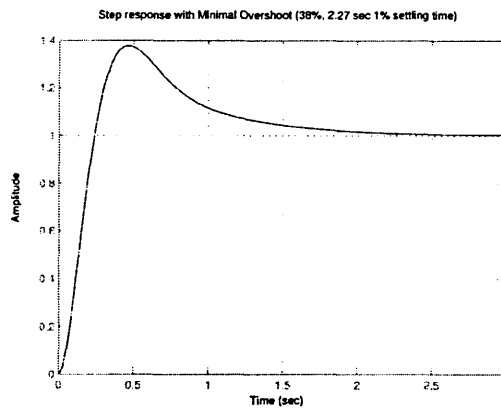


(c) Minimum 1% settling time with first order LTI control (0.95 sec 1% settling time, 23% overshoot).

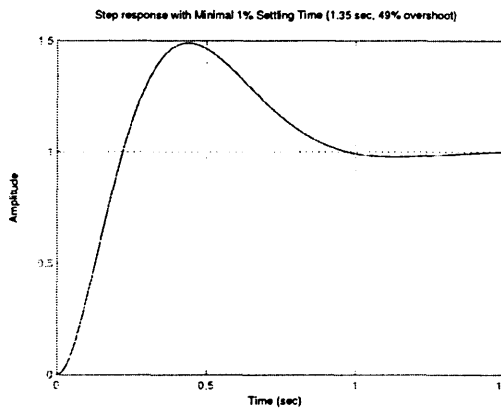
Figure 5.3.18: Step responses for $P_1(s) = \frac{100}{s(s+1)}$.



(a) Switching algorithm step response (0.525 sec 1% settling time) .



(b) Minimum overshoot with first order LTI control (38% overshoot, 2.27 sec 1% settling time).



(c) Minimum 1% settling time with first order LTI control (1.35 sec 1% settling time, 49% overshoot).

Figure 5.3.19: Step responses for $P_2(s) = \frac{100}{s(s-1)}$.

If no value of T exists that satisfies the above constraint, then $T = \infty$.

Definition 5.4.5 The ϵ -rise time T_r of a real-valued signal $y(t)$ is the smallest value of $T_r > 0$ such that

$$y(T_r) = 1 - \epsilon$$

If no value of T_r exists that satisfies the above constraint, then $T_r = \infty$.

The 1% settling time of a signal $y(t)$ is, according to Def. 5.4.4, an ϵ -settling time with $\epsilon = 0.01$. It is clear from the above definitions that any real-valued signal $y(t)$ that has finite ϵ -settling time T_s also has finite ϵ -rise time T_r (for the same value of ϵ), and that $T_r \leq T_s$. Hence, the ϵ -rise time is always a lower bound for the ϵ -settling time.

The goal of this section is to find an upper bound on the ratio of the 1% settling time of the switching architecture to the smallest possible 1% settling time that can be achieved via any bounded control input $|u(t)| \leq 1$. In order to establish this bound, we will find a lower bound on the 1% rise time achievable via bounded control and an upper bound on the 1% settling time of the switching architecture. An upper bound on the ratio will then be the upper bound of the 1% settling time of the switching architecture divided by the lower bound on the 1% rise time for bounded control inputs.

All of the bounds we develop here will be for the case where $a \geq b^2$; the case where $a \gg b^2$ (which correspond to cases where the switching architecture has performance benefits over a first order LTI controller, as demonstrated in the last section) is therefore a sub-case of the more general case we examine here. Some specific case studies for which $a \gg b^2$ will be considered when we go through the process of actually *computing* LTI controllers that achieve close-to-optimal performance in a later section.

Rise Time Bound

For the plant of Eqn. 5.1.1

$$P(s) = \frac{a}{s(s - b)}$$

with $a > 0$, $b \in \mathbf{R}$, we are interested in deriving a lower bound on the 1% rise time of the step response T_r :

$$T_r = \min_{T \geq 0} \{T : y(T) = 0.99\}$$

where $y(t)$ is the step response of the plant $P(s)$ when the peak value of the control input $u(t)$ is bounded: $|u(t)| \leq 1$ for all $t \geq 0$. It is clear that the rise time T_r will be minimized by choosing the input $u(t)$ that maximizes $y(t)$ at each time t subject to the constraint $|u(t)| \leq 1$. First, assuming zero initial conditions $y(0) = \dot{y}(0) = 0$, note that $y(t)$ can be written as the convolution

$$y(t) = \int_0^t \frac{a}{b} (e^{b\tau} - 1) u(t - \tau) d\tau$$

whenever $b \neq 0$. Now,

$$|y(t)| \leq \int_0^t \left| \frac{a}{b} (e^{b\tau} - 1) u(t - \tau) \right| d\tau \leq \int_0^t \left| \frac{a}{b} (e^{b\tau} - 1) \right| d\tau = \int_0^t \frac{a}{b} (e^{b\tau} - 1) d\tau$$

where the equality follows from the fact that the impulse response

$$h(t) = \frac{a}{b} (e^{bt} - 1) \geq 0 \quad \forall t \geq 0$$

for any values of $a > 0$, $b \neq 0$. We conclude from the above inequalities that $y(t)$ is maximized for each t by picking $u(t) = 1$ for all $t \geq 0$. Hence, we can develop a lower bound on the 1% rise time T_r by picking $u(t) = 1$ for all $t \geq 0$. A similar (and simpler) proof holds in the case when $b = 0$, as well.

Now, when $u(t) = 1$ for all $t \geq 0$, $y(t)$ can be written explicitly as

$$y(t) = \frac{a}{b^2} e^{bt} - \frac{a}{b} t - \frac{a}{b^2}.$$

For an arbitrary $\epsilon > 0$, the equation we wish to solve to find a bound on the ϵ -rise time can be written as

$$e^{bt} - bt = 1 + \frac{b^2}{a} (1 - \epsilon). \quad (5.4.21)$$

While a simple closed form expression for the solution to Eqn. 5.4.21 is not obtainable, we can derive useful lower bounds on the value of t which solves Eqn. 5.4.21 by making use of the following inequalities, whose proofs are in the Appendix at the end of the chapter.

Proposition 5.4.19 *For any $x \geq 0$ and for any $n \in \mathbf{Z}^+$,*

$$1. \sum_{k=0}^{2n+2} \frac{(-x)^k}{k!} \geq e^{-x} \geq \sum_{k=0}^{2n+1} \frac{(-x)^k}{k!}.$$

$$2. e^x \geq \sum_{k=0}^n \frac{x^k}{k!}$$

We will find a bound on the rise time T_r by examining two separate cases: $b < 0$ and $b > 0$. When $b < 0$, by virtue of the first item of Prop. 5.4.19, the left hand side of Eqn. 5.4.21 satisfies

$$\begin{aligned} e^{bt} - bt &\leq 1 + bt + \frac{(bt)^2}{2} - bt \\ &= 1 + \frac{(bt)^2}{2}. \end{aligned}$$

from which we arrive at the lower bound

$$T_r \geq \sqrt{\frac{2(1 - \epsilon)}{a}}.$$

When $b > 0$, deriving a bound is slightly more complicated. First, note that Eqn. 5.4.21 can be equivalently written as

$$e^{bt} + 1 - bt = 2 + \frac{b^2}{a}(1 - \epsilon).$$

By the result of Prop. 5.4.19, the left hand side of the above equation can be upper bounded by $e^{bt} + e^{-bt}$. Hence, a lower bound for the rise time can be found by solving the equation

$$e^{2bt} - \left(2 + \frac{b^2}{a}(1 - \epsilon)\right) e^{bt} + 1 = 0$$

from which we can derive the explicit lower bound

$$T_r \geq \frac{1}{b} \ln \left(\frac{2 + \frac{b^2}{a}(1 - \epsilon) + \sqrt{\left(2 + \frac{b^2}{a}(1 - \epsilon)\right)^2 - 4}}{2} \right).$$

If we define γ in such a way that $b = \gamma\sqrt{a}$, then we can reparameterize the above bound in terms of γ and a such that $T_r \geq f(\gamma)/\sqrt{a}$ where

$$f(\gamma) = \frac{1}{\gamma} \ln \left(\frac{2 + \gamma^2(1 - \epsilon) + \sqrt{(2 + \gamma^2(1 - \epsilon))^2 - 4}}{2} \right).$$

Recall the implicit restriction that $a \geq b^2$. For $b > 0$, this constraint can be written in terms of the variable γ as $0 \leq \gamma \leq 1$. Numerical computation shows that, for $\epsilon = 0.01$, $f(\gamma)$ is decreasing for $\gamma \in [0, 1]$, so we conclude that the 1% rise time T_r satisfies the condition $T_r \geq f(1)/\sqrt{a}$, where

$$f(1) = \ln \left(\frac{3 - \epsilon + \sqrt{4(1 - \epsilon) + (1 - \epsilon)^2}}{2} \right)_{\epsilon=0.01} \approx 0.9579.$$

Finally, noting that the lower bound for $b > 0$ is smaller than the lower bound for $b < 0$, we conclude that the 1% rise time T_r satisfies the lower bound

$$T_r \geq \frac{0.95}{\sqrt{a}} \tag{5.4.22}$$

for all $b \in \mathbf{R}$ that satisfy $b^2 \leq a$.⁴

Upper bound on Settling Time Ratio

We are now prepared to find an upper bound on the ratio of the 1% settling time of the switching architecture T_s to the rise time bound T_r of Eqn. 5.4.22. If we, again,

⁴While we only formally proved this result for $b \neq 0$, simple calculations show that this bound holds for $b = 0$ as well.

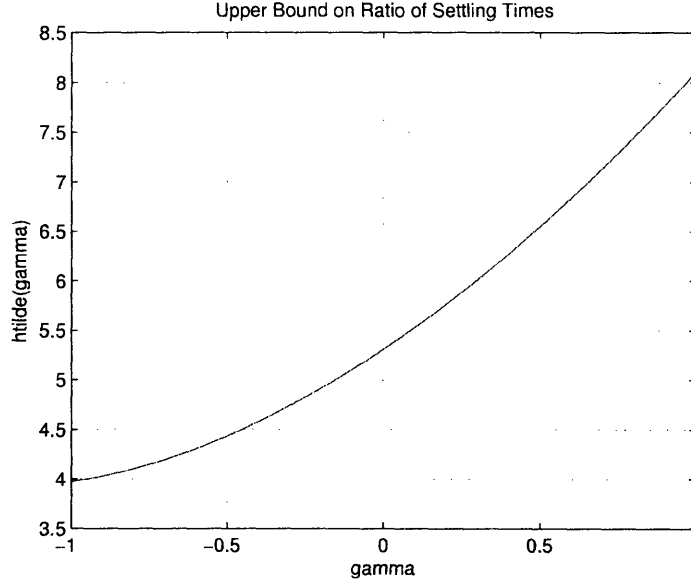


Figure 5.4.20: Plot of $\tilde{h}(\gamma)$ of Eqn. 5.4.24 for $\gamma \in [-1, 1]$.

let $b = \gamma\sqrt{a}$ where $\gamma \in [-1, 1]$, then the 1% settling time of the switching architecture T_s of Eqn. 5.2.12 can be reparameterized to be of the form $T_s = h(\gamma)/\sqrt{a}$ where $h(\gamma)$ is given by

$$h(\gamma) = \frac{\gamma + \sqrt{\gamma^2 + 4}}{2} \left(\ln \left(\frac{100}{\sqrt{2}} \right) + \sqrt{\frac{4 + \gamma^2}{4 - \gamma^2}} \operatorname{arccot} \left(\frac{2\gamma + \sqrt{\gamma^2 + 4}}{\sqrt{4 - \gamma^2}} \right) \right). \quad (5.4.23)$$

Using the above parameterization, we arrive at the following upper bound:

$$\frac{T_s}{T_r} \leq \frac{h(\gamma)}{0.95} \triangleq \tilde{h}(\gamma) \quad (5.4.24)$$

for all $a > 0$, $\gamma \in [-1, 1]$. A plot of $\tilde{h}(\gamma)$ is shown in Fig. 5.4.20. As the figure shows, $\tilde{h}(\gamma)$ increases with γ . Intuitively, this is sensible since larger γ corresponds to larger b , and the larger b , the “more unstable” the plant $P(s)$ of Eqn. 5.1.1. Also, since Fig. 5.4.20 shows that $\tilde{h}(\gamma) \leq 10$ for all $\gamma \in [-1, 1]$, we can conclude that the 1% settling time of the switching architecture is never more than a factor of 10 larger than the settling time that can be achieved via any control input that is bounded by 1, $|u(t)| \leq 1$ for all $t \geq 0$, for any value of $a > 0$ and any value of b with $b^2 \leq a$.

5.4.2 Time Optimal Control, Part II: Approximate Bound on Settling Time

While the previous section does provide us with a bound on the ratio of the settling times, as desired, the bound is somewhat conservative. A large part of this is due to the fact that the minimum achievable ϵ -rise time is, in general, a weak lower bound for the minimum achievable ϵ -settling time. In this section, we derive an *approximate* lower bound on the ϵ -settling time. While the bound we derive here is not exact, we will show that this new bound for the ϵ -settling time can be made arbitrarily close to the true ϵ -settling time for ϵ sufficiently small.

For a given plant $P(s)$ of Eqn. 5.1.1, the task of minimizing the ϵ -settling time of the step response $y(t)$ for some given $\epsilon \geq 0$ is the task of finding some control input $u(t)$ with $|u(t)| \leq 1$ so as to minimize the smallest time T_ϵ for which $|y(t) - 1| \leq \epsilon$ for all $t \geq T_\epsilon$. In general, this is a difficult problem to solve analytically for an arbitrary ϵ ; however, there is one exception for which an analytic solution can be obtained, namely the case when $\epsilon = 0$ exactly. We shall, therefore, compute the minimal settling time as a function of the plant parameters a and b when $\epsilon = 0$ and use this as an approximation to the true 1% settling time.

It is true, in theory, that the minimal 1% settling time could be markedly different from the settling time in the case when $\epsilon = 0$; however, one should naturally expect that when ϵ is small, the two values should be close. As we will show later, when ϵ is sufficiently small, the minimal ϵ -settling time of the step response over all control inputs that satisfy $|u(t)| \leq 1$ can be made arbitrarily close to the minimal settling time in the case that $\epsilon = 0$. Moreover, as we shall see when we examine a procedure for designing rational LTI controllers to minimize the settling time in the absence of overshoot, the 1% settling time that can be achieved through the design process is often remarkably close to the bound we derive here.

As a small technical note, in all the analysis that follows, all quantities are formally derived for the case $b \neq 0$, but results are stated for both $b \neq 0$ and $b = 0$. The proofs of statements for $b = 0$ are similar to those presented here (but often much simpler in terms of analysis and computation).

Approximate Bound: $\epsilon = 0$

If we again assume a state-space description of the plant $P(s)$ of the form

$$\begin{bmatrix} \dot{x}_1 \\ \dot{x}_2 \end{bmatrix} = \begin{bmatrix} 0 & \sqrt{a} \\ 0 & b \end{bmatrix} \begin{bmatrix} x_1 \\ x_2 \end{bmatrix} + \begin{bmatrix} 0 \\ \sqrt{a} \end{bmatrix} u \quad (5.4.25)$$

$$y = x_1 \quad (5.4.26)$$

then the problem of minimizing the settling time for $\epsilon = 0$ over all bounded control inputs $|u(t)| \leq 1$ for all $t \geq 0$ is one which fits the framework of the Pontryagin Maximum Principle [4], which is stated here for completeness:

Theorem 5.4.8 (Pontryagin Maximum Principle) *For the continuous-time dy-*

dynamic system,

$$\dot{x} = f(x(t), w(t)), \quad 0 \leq t \leq T, \quad x(0) : \text{given},$$

consider the problem of selecting $w(t)$ in an admissible control set W so as to minimize the cost functional

$$J(x(t), w(t)) = h(x(T)) + \int_0^T g(x(t), w(t)) dt$$

where g and h are continuously differentiable with respect to x and g is continuous with respect to w . Let $w^*(t)$ denote an optimal control trajectory and $x^*(t)$ denote the corresponding state trajectory, i.e.,

$$\dot{x}^*(t) = f(x^*(t), w^*(t)), \quad x^*(0) = x(0) : \text{given}.$$

Define the Hamiltonian function

$$H(x, w, p) = g(x, w) + p' f(x, w)$$

and let $p(t)$ denote the solution of the so-called adjoint equation

$$\dot{p}(t) = -\nabla_x H(x^*(t), w^*(t), p(t)),$$

with boundary condition

$$p(T) = \nabla h(x^*(T)).$$

Then, for all $t \in [0, T]$,

$$w^*(t) = \arg \min_{w \in W} H(x^*(t), w, p(t)).$$

Furthermore, there exists a constant C such that

$$H(x^*(t), w^*(t), p(t)) = C, \quad \forall t \in [0, T].$$

The condition $\epsilon = 0$ implies that $y(t) = 1$ and $\dot{y}(t) = 0$ for all $t \geq T$. One immediate condition that results from this is that, for the above state-space description, $x_1(T) = 1$, $x_2(T) = 0$. Moreover, since $\dot{y}(t) = x_2(t)$ is identically 0 for all $t \geq T$, it follows that $\dot{x}_2(t)$ is identically 0 for all $t \geq T$. But since

$$\dot{x}_2 = bx_2 + \sqrt{a}u,$$

it follows that $u(t) = 0$ for all $t \geq T$. Hence, any control input $u(t)$ which minimizes the settling time for $\epsilon = 0$ satisfies the constraints

$$\begin{aligned} |u(t)| &\leq 1 & 0 \leq t < T \\ u(t) &= 0 & t \geq T. \end{aligned}$$

In other words, the optimal choice of $u(t)$ is an input with finite horizon.

Now, to begin setting up the problem for the Pontryagin Maximum Principle, first note that the task of minimizing the settling time T can be expressed by choosing the integral cost $g(x, u) = 1$, i.e., we minimize the cost

$$\int_0^T 1 dt.$$

The problem can then be formulated as follows: we wish to find a control input $u : [0, T] \rightarrow [-1, 1]$ that minimizes the above integral cost subject to the initial and terminal constraints

$$x(0) = \begin{bmatrix} 0 \\ 0 \end{bmatrix} \quad x(T) = \begin{bmatrix} 1 \\ 0 \end{bmatrix}.$$

The Hamiltonian for this problem is given by

$$H(x, u, p) = 1 + \sqrt{a}p_1x_2 + p_2(bx_2 + \sqrt{a}u)$$

and the adjoint equation is

$$\begin{bmatrix} \dot{p}_1 \\ \dot{p}_2 \end{bmatrix} = \begin{bmatrix} 0 & 0 \\ \sqrt{a} & b \end{bmatrix} \begin{bmatrix} p_1 \\ p_2 \end{bmatrix}.$$

Note that because both the initial and terminal state are fixed, both the initial and final states of the adjoint equation are unrestricted [4]. For any arbitrary initial adjoint state $p(0) = [p_1(0) \ p_2(0)]'$, we find that $p_1(t) = 0$ for all time and $p_2(t)$ is given by

$$p_2(t) = \left(p_2(0) + \frac{\sqrt{a}p_1(0)}{b} \right) e^{bt} - \frac{\sqrt{a}p_1(0)}{b}.$$

Now, since the optimal control $u^*(t)$ must satisfy the constraint $u^*(t) = \arg \min_{|u| \leq 1} H(x, u, p)$ for all $t \in [0, T]$, we find that

$$u^*(t) = -\text{sgn}(p_2(t)).$$

For all values of $b \neq 0$, $\dot{p}_2(t) = (bp_2(0) + \sqrt{a}p_1(0))e^{bt}$ from which it is clear that $p_2(t)$ is either constant, monotonically increasing, or monotonically decreasing. Hence, $p_2(t)$ can change sign at most once. This leads to four possible candidates for the optimal control $u^*(t)$:

- $u_1^*(t) = 1$ for $0 \leq t < T$
- $u_2^*(t) = -1$ for $0 \leq t < T$
- $u_3^*(t) = \begin{cases} -1 & 0 \leq t \leq T_1 \\ 1 & T_1 < t < T \end{cases}$
- $u_4^*(t) = \begin{cases} 1 & 0 \leq t \leq T_1 \\ -1 & T_1 < t < T \end{cases}$

where T_1 is such that $0 < T_1 < T$. Simple calculations show that the first three options for $u^*(t)$ do not lead to solutions which satisfy both the initial and terminal conditions on the state; it is only $u_4^*(t)$ for which both constraints can be satisfied. With this parameterization, we now only need to solve for the parameters T_1 and T . If $b \neq 0$, then when $u(t) = u_4^*(t)$ above, we find via brute-force computation that, for $0 \leq t \leq T_1$,

$$\begin{aligned} x_1(t) &= \frac{a}{b^2} e^{bt} - \frac{a}{b} t - \frac{a}{b^2} \\ x_2(t) &= \frac{\sqrt{a}}{b} (e^{bt} - 1), \end{aligned}$$

while for $T_1 < t < T$,

$$x_1(t) = \frac{a}{b^2} (e^{bT_1} - 2) (e^{b(t-T_1)} - 1) + \frac{a}{b} (t - 2T_1) + \frac{a}{b^2} (e^{bT_1} - 1) \quad (5.4.27)$$

$$x_2(t) = \frac{\sqrt{a}}{b} (e^{bT_1} - 1) e^{b(t-T_1)} - \frac{\sqrt{a}}{b} (e^{b(t-T_1)} - 1). \quad (5.4.28)$$

From the terminal constraints $x_1(T) = 1$ and $x_2(T) = 0$, some algebraic manipulation yields an explicit expression for T in terms of the parameters a and b . If we let $\alpha = \exp(-b^2/2a)$, then we find that

$$T = \begin{cases} \frac{2}{\sqrt{A}} & b = 0 \\ \frac{2}{b} \ln \left(\frac{1+\sqrt{1-\alpha^2}}{\alpha} \right) & b > 0 \\ \frac{2}{b} \ln \left(\frac{1-\sqrt{1-\alpha^2}}{\alpha} \right) & b < 0 \end{cases}. \quad (5.4.29)$$

Moreover, the value of T_1 in the expression for $u_4^*(t)$ is related to T via the expression

$$T_1 = \begin{cases} -\frac{1}{b} \ln \left(\frac{1}{2} + \frac{1}{2} e^{-bT} \right) & b \neq 0 \\ \frac{T}{2} & b = 0 \end{cases}. \quad (5.4.30)$$

For $a = 1$, the time-optimal control $u^*(t)$ and the corresponding optimal output $y(t)$ are depicted in Fig. 5.4.21 for the values $b = -1, 0$, and 1 , respectively. For the cases when $b = -1$ and $b = 1$, the settling times are equal and given by $T \approx 2.1701$ (it can actually be shown that the expression for T given by Eqn. 5.4.29 is an even function of b , i.e., $T(b) = T(-b)$ for all $b \in \mathbf{R}$). Note, however, that the value of T_1 is quite different in each of these cases; when $b = -1$, $T_1 \approx 1.585$, whereas when $b = 1$, $T_1 \approx .585$.

When $b = 0$ (shown in the center of Fig. 5.4.21), we find that $T_1 = 1$ and $T_2 = 2$. Numerical examination indicates that, for a fixed value of a , the smallest value of the minimum settling time T over all $b \in \mathbf{R}$ occurs when $b = 0$, i.e., when the plant acts as a double integrator.

One feature which we would like to point out about the optimal outputs $y(t)$ in each of the above plots is that none of them exhibit any form of overshoot. Indeed, as we will now show, the optimal output $y(t)$ will never exhibit overshoot for any values

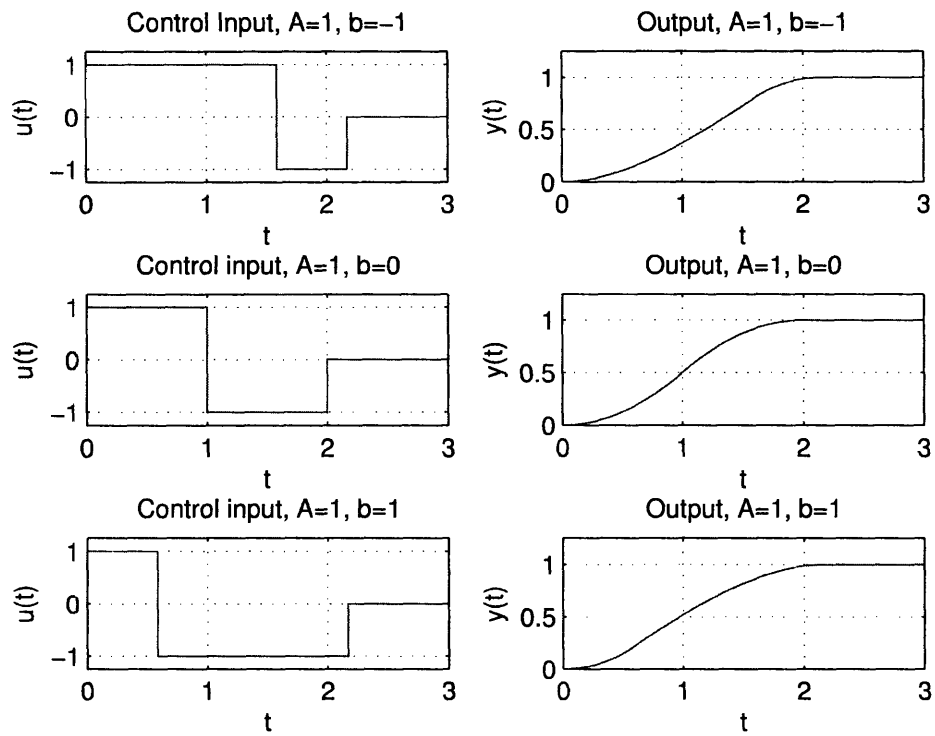


Figure 5.4.21: Time-optimal control $u^*(t)$ and corresponding optimal output $y(t)$ when $a = 1$ and for $b = -1, 0$ and 1 , respectively.

of $a > 0$ and $b \in \mathbf{R}$. Since $y(0) = 0$ and $y(T) = 1$, we simply need to show that $y(t)$ is monotonically nondecreasing in the range $0 \leq t \leq T$. Indeed, when $b \neq 0$,

$$\dot{y}(t) = \frac{a}{b} (e^{bt} - 1)$$

for $0 \leq t \leq T_1$, from which it immediately follows that $\dot{y}(t) \geq 0$ in this time range. For $T_1 \leq t \leq T$, we have that

$$\ddot{y}(t) = a (e^{bT_1} - 2) e^{b(t-T_1)} = -\frac{2ae^{bT}}{1 + e^{bT}} e^{b(t-T_1)} < 0.$$

Since $\dot{y}(T) = 0$, it then follows that $\dot{y}(t) > 0$ for $T_1 < t < T$. Hence, $y(t)$ is monotonically nondecreasing, and the optimal step response does not exhibit overshoot for any values of $a > 0$ and $b \neq 0$.

Continuity of ϵ -settling Time

We now seek to show that, for ϵ sufficiently small, the ϵ settling time of the step response for a plant $P(s)$ of the form Eqn. 5.1.1 can be made arbitrarily close to the settling time T of Eqn. 5.4.29 above. We will rely on the following fact whose proof can be found in the Appendix at the end of the chapter:

Proposition 5.4.20 *Consider a state trajectory $x(t) = [x_1(t) \ x_2(t)]'$ of the system with state space-description given by Eqn. 5.4.25 and Eqn. 5.4.26 with bounded input $|u(t)| \leq 1$ for all $t \geq 0$ and such that the following condition is satisfied: for some $0 \leq \epsilon \leq 1$, there exists $T \geq 0$ such that*

$$|x_1(t) - 1| \leq \epsilon \quad \forall t \geq T.$$

Then there exists a constant $M > 0$ such that for all $a > 0$, $b \in \mathbf{R}$ that satisfy $a > b^2$,

$$|x_2(t)| \leq M\sqrt{\epsilon} \quad \forall t \geq T.$$

In layman's terms, Prop. 5.4.20 states that any state trajectory that has corresponding output $y(t) = x_1(t)$ with ϵ -settling time T must satisfy the condition that the state $x(t)$ lies in a compact region for $t \geq T$. Moreover, as $\epsilon \rightarrow 0$, the compact region approaches the point $(1, 0)$ in the $x_1 - x_2$ plane.

Prop. 5.4.20 allows us to characterize bounds on the minimal ϵ -settling time of the step response subject to the control bound $|u(t)| \leq 1$ in the following way. For $\epsilon > 0$ fixed, consider the set X_0^ϵ given by

$$X_0^\epsilon = \{(x_1, x_2) : |x_1 - 1| \leq \epsilon, \ |x_2| \leq \sqrt{12e^2\epsilon}\}.$$

Now, for a given $x_0^\epsilon \in X_0^\epsilon$, consider the task of minimizing the cost functional

$$T(x_0^\epsilon) = \int_0^{T(x_0^\epsilon)} 1 dt$$

for the system with state-space description Eqn. 5.4.25 and Eqn. 5.4.26 subject to the constraints

$$\begin{aligned} |u(t)| &\leq 1 & 0 \leq t \leq T(x_0^\epsilon) \\ x(0) &= 0 \\ x(T(x_0^\epsilon)) &= x_0^\epsilon. \end{aligned}$$

Note that this is the exact problem that was formulated and solved using the Pontryagin Maximum Principle in the last section, with the exception that the terminal state is now allowed to be a point other than the point $(1, 0)$. Hence, all of the work that was used to derive the optimal solution for $\epsilon = 0$ applies to this problem, as well, and an optimal solution can be found by equating the expressions for $x_1(T)$ and $x_2(T)$ in Eqn. 5.4.27 and Eqn. 5.4.28 to the first and second components of x_0^ϵ , respectively.

Using the above characterization, we arrive at the following bounds on T_ϵ .

Proposition 5.4.21 *For every $\epsilon \geq 0$,*

$$\min_{x_0^\epsilon \in X_0^\epsilon} T(x_0^\epsilon) \leq T_\epsilon \leq T_0$$

where T_0 is the value of T_ϵ when $\epsilon = 0$.

Proof To establish the upper bound, consider the optimal trajectory $y(t)$ from the previous section which minimizes T_0 . It follows that the monotonicity of this $y(t)$ that there exists $T' \leq T$ for which $y(T') = 1 - \epsilon$ and for which $|y(t) - 1| \leq \epsilon$ for all $t \geq T'$. Since T_ϵ is the minimal value of T over all trajectories $y(t)$ which can be produced via a bounded control input $|u(t)| \leq 1$ that satisfy $|y(t) - 1| \leq \epsilon$ for all $t \geq T$, it follows that $T_\epsilon \leq T' \leq T_0$.

To establish the lower bound, note that because $x(T_\epsilon) \in X_0^\epsilon$, there exists $x_0^* \in X_0^\epsilon$ such that

$$T_\epsilon = T(x_0^*).$$

But, clearly

$$T(x_0^*) \geq \min_{x_0^\epsilon \in X_0^\epsilon} T(x_0^\epsilon).$$

□

We will show that T_ϵ is continuous at $\epsilon = 0$ in the following manner. Suppose we can show that, for every $\delta > 0$, there exists $\epsilon > 0$ such that $|T_0 - T(x_0^\epsilon)| < \delta$ for every

$x_0^\epsilon \in X_0^\epsilon$. Then by Prop. 5.4.21 we have that

$$\delta > \left| T_0 - \min_{x_0^\epsilon \in X_0^\epsilon} T(x_0^\epsilon) \right| \geq |T_0 - T_\epsilon|$$

from which we immediately conclude that T_ϵ is continuous at $\epsilon = 0$. If we note, now, that $T_0 = T(\tilde{x}_0)$ where $\tilde{x}_0 = \begin{bmatrix} 1 & 0 \end{bmatrix}'$, then the statement that $|T_0 - T(x_0^\epsilon)| < \delta$ for all $x_0^\epsilon \in X_0^\epsilon$ is equivalent to requiring that

$$|T(\tilde{x}_0) - T(x_0^\epsilon)| < \delta \quad \forall x_0^\epsilon \in X_0^\epsilon.$$

Hence, if we can prove that the map $T(x_0)$ is continuous at the point \tilde{x}_0 , then we will have effectively shown that T_ϵ is continuous at $\epsilon = 0$. In order to prove continuity of the map $T(x_0)$, we will rely on the following theorem [54, 55].

Theorem 5.4.9 (Inverse Function Theorem) *Consider a differentiable function $F : \mathbf{R}^n \rightarrow \mathbf{R}^n$ which can be written as $F = \begin{bmatrix} f_1(x) & f_2(x) & \dots & f_n(x) \end{bmatrix}$ where $f_i(x) : \mathbf{R}^n \rightarrow \mathbf{R}$ are differentiable for $1 \leq i \leq n$. Define the matrix $\partial F / \partial x$ as*

$$\frac{\partial F}{\partial x} = \begin{bmatrix} \frac{\partial f_1}{\partial x_1} & \frac{\partial f_1}{\partial x_2} & \dots & \frac{\partial f_1}{\partial x_n} \\ \frac{\partial f_2}{\partial x_1} & & & \vdots \\ \vdots & & & \vdots \\ \frac{\partial f_n}{\partial x_1} & \dots & \dots & \frac{\partial f_n}{\partial x_n} \end{bmatrix}$$

and consider the linear map $F'(p) : \mathbf{R}^n \rightarrow \mathbf{R}^n$ given by

$$F'(p) = \left. \frac{\partial F}{\partial x} \right|_{x=p}$$

where p is a point in \mathbf{R}^n . Then if $F'(p)$ is one-to-one, there exists an open set U containing p such that F restricted to U is a diffeomorphism⁵ of U onto an open set V .

Consider the map $F : \mathbf{R}^2 \rightarrow \mathbf{R}^2$ given by

$$F(T_1, T) = \begin{bmatrix} \frac{a}{b^2} (e^{bT_1} - 2) (e^{b(T-T_1)} - 1) + \frac{a}{b} (T - 2T_1) + \frac{a}{b^2} (e^{bT_1} - 1) \\ \frac{\sqrt{a}}{b} (e^{bT_1} - 1) e^{b(T-T_1)} - \frac{\sqrt{a}}{b} (e^{b(T-T_1)} - 1) \end{bmatrix}.$$

F is clearly differentiable with respect to both T_1 and T , and we recognize that $T(x_0^\epsilon)$ is given by the value of T for which

$$F(T_1, T) = x_0^\epsilon.$$

⁵Recall that F is a diffeomorphism which maps an open set U to an open set V if it has a differentiable inverse $F^{-1} : V \rightarrow U$.

Moreover, we have that

$$F(T_1^0, T_0) = \tilde{x}_0$$

where

$$T_1^0 = -\frac{1}{b} \ln\left(\frac{1}{2} + \frac{1}{2}e^{-bT_0}\right).$$

We would like to show that F has a continuous inverse in a sufficiently small neighborhood about the point (T_1^0, T_0) . If this is the case, then we have as an immediate consequence that $T(x_0)$ is continuous in a sufficiently small neighborhood of \tilde{x}_0 . To prove that this fact is indeed true, we consider the matrix $F'(T_1, T)$ given by

$$F'(T_1, T) = \begin{bmatrix} \frac{2a}{b} (e^{b(T-T_1)} - 1) & \frac{a}{b} (e^{bT} - 2e^{b(T-T_1)} + 1) \\ 2\sqrt{a}e^{b(T-T_1)} & \sqrt{a}(e^{bT} - 2e^{b(T-T_1)}) \end{bmatrix}.$$

A simple calculation shows that

$$\det(F'(T_1, T)) = -\frac{2a\sqrt{a}}{b}e^{bT} (e^{-bT_1} - 1).$$

From the above, we conclude that $F'(T_1, T)$ is a one-to-one mapping whenever $T_1 \neq 0$. Examination of the expression for T_1^0 shows that $T_1^0 \neq 0$, and we hence find that F is a diffeomorphism on an open set U containing the point (T_1^0, T_0) that maps to an open set V . Note that for ϵ sufficiently small, the set X_0^ϵ can be made to lie entirely inside V . Hence, we find that the map $T(x_0^\epsilon)$ is locally continuous for sufficiently small ϵ and conclude that T_ϵ is continuous at $\epsilon = 0$.

Approximate Bound on Ratio of Settling Times

We now return the main objective for this section: developing a bound on the ratio of the 1% settling time of the switching architecture T_s to the minimal 1% settling time that can be achieved via an arbitrary bounded input $|u(t)| \leq 1$ for all $t \geq 0$, i.e., computing a bound on

$$\frac{T_s}{T_\epsilon}.$$

Noting that $T_0 > 0$ for all a, b that satisfy $a > b^2$, we have via the continuity result of the previous section that, for ϵ sufficiently small

$$\frac{T_s}{T_\epsilon} \approx \frac{T_s}{T_0}.$$

Hence, to compute an approximate bound on the 1% settling times, we can compute the ratio of T_s/T_0 . Note that we have no guaranteed bound on the quality of this approximation; the continuity of T_ϵ tells us that, for ϵ sufficiently small, the difference $T_s/T_\epsilon - T_s/T_0$ will be small, but for a *given* value of $\epsilon > 0$, the difference may theoretically be quite large. Nevertheless, as we will see in the next section, the approximate bound T_s/T_0 is often quite accurate.

To develop an expression for the approximate bound, recall that T_s can be parameterized as $h(\gamma)/\sqrt{a}$ where $h(\gamma)$ is given as in Eqn. 5.4.23 where $\gamma = b/\sqrt{a}$. Examining the settling time for the set of a and b such that $a \geq b^2$ is equivalent to computing $h(\gamma)$ for $\gamma \in [-1, 1]$. We similarly can reparameterize T_0 of Eqn. 5.4.29 to be of the form $T_0 = f(\gamma)/\sqrt{a}$ where

$$f(\gamma) = \left| \frac{2}{\gamma} \ln \left(\frac{1 + \sqrt{1 - \exp(-\gamma^2)}}{\exp(-\gamma^2/2)} \right) \right|.$$

Therefore, we have for $\gamma \in [-1, 1]$:

$$\frac{T_s}{T_0} = \frac{h(\gamma)}{f(\gamma)}. \quad (5.4.31)$$

A plot of Eqn. 5.4.31 is shown in Fig. 5.4.22. Comparing this plot to the plot for the weak bound developed in the previous section shown in Fig. 5.4.20, the approximate bound predicts roughly a factor of two improvement in the ratio of the 1% settling time of the switching architecture vs. the achievable 1% settling time of arbitrary bounded control with $|u(t)| \leq 1$. For instance, whereas the weak bound predicts a factor of 8 difference for the case when $\gamma = 1$, the approximate bound predicts roughly a factor of 3.5 when $\gamma = 1$, down from roughly one order of magnitude difference to roughly half an order of magnitude. While, again, it must be advised that the approximate bound may actually differ from the true ratio quite significantly, we will see in the next section that the bound shown in Fig. 5.4.22 is often very close to the true ratio.

5.4.3 Designing LTI Controllers with Minimum Settling Time

We now turn to the problem of *designing* LTI controllers which minimize the 1% settling time of the step response for a given plant $P(s)$ of the form Eqn. 5.1.1. Formally, the problem we wish to investigate is this: for a given plant $P(s)$, we wish to design an LTI controller $K(s)$ connected in the servo configuration of Fig. 5.4.23 such that when the input $r(t)$ is a unit step and the plant and controller are both initially at rest, the following constraints are satisfied:

1. The closed-loop transfer function $S(s)$ from $r(t)$ to $y(t)$ is stable.
2. The control signal $u(t)$ is bounded: $|u(t)| \leq 1$ for all $t \geq 0$.
3. The 1% settling time is made as small as possible, i.e. the value of T for which $|y(t) - 1| \leq 0.01$ for all $t \geq T$ is minimized.
4. The percentage overshoot is less than 1%, i.e. $y(t) \leq 1.01$ for all $t \geq 0$.

For a given value of T , note that items 2 – 4 are linear constraints on the step response of the control input $u(t)$ and plant output $y(t)$. As we will see now, the

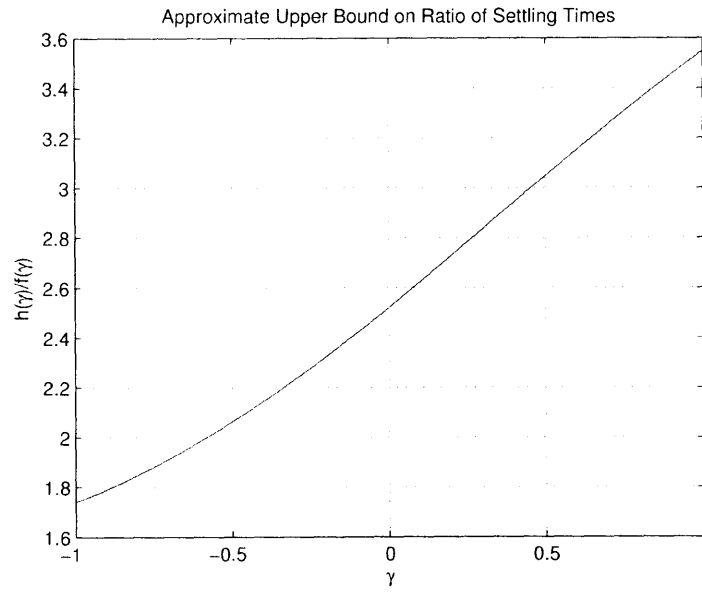


Figure 5.4.22: Plot of $h(\gamma)/f(\gamma)$ for $\gamma \in [-1, 1]$.

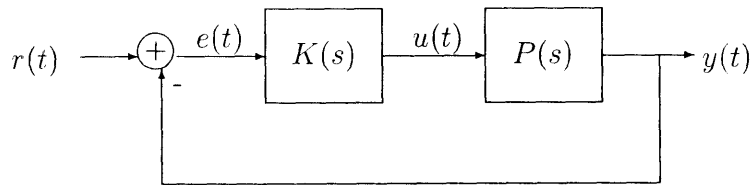


Figure 5.4.23: Servo configuration

problem we are attempting to solve here can be represented as an infinite dimensional linear programming problem which, upon appropriate discretization, yields an algorithm which can be implemented in MATLAB for finding $K(s)$ which satisfies all of the above constraints. All of the techniques we discuss here are presented in more detail in [5].

Characterization of Stabilizing Controllers

First, recall the *Q-parameterization Theorem* [52, 67] which, informally stated, says that the set of achievable stable, rational closed-loop transfer matrices $S(s)$ for a given plant $P(s)$ under LTI feedback $K(s)$ is an affine transformation of the set of stable, proper transfer matrices. That is, any stable closed-loop transfer matrix $S(s)$ for a given plant $P(s)$ can be represented as

$$S(s) = S_0(s) + S_1(s)Q(s)S_2(s)$$

for some stable, proper $Q(s)$, where $S_0(s)$, $S_1(s)$, and $S_2(s)$ are fixed, stable transfer matrices that depend on the plant $P(s)$. From the above we see that we can well-approximate any closed-loop transfer function $S(s)$ by well-approximating the set of stable transfer matrices. In other words, if we can find some basis $\{Q_i(s)\}_{i=1}^{\infty}$ for the set of stable transfer matrices, then any stable closed-loop transfer function $S(s)$ can be represented as

$$S(s) = S_0(s) + \sum_{i=0}^{\infty} a_i S_1(s)Q_i(s)S_2(s),$$

with $a_i \in \mathbf{C}$.

One common basis choice known as the *Ritz Basis* is given by

$$Q_i(s) = \left(\frac{c}{s+c} \right)^i \quad (5.4.32)$$

for any $c \in \mathbf{R}$, $c \neq 0$. We will use this basis in performing the numerical computations to be described.

While the above does characterize the set of stable-closed loop transfer matrices, for the case of the servo configuration of Fig. 5.4.23, an equivalent method of characterizing the set of closed-loop transfer functions (which is sometimes simpler to deal with when implementing numerical algorithms) is based on the classical *interpolation conditions* which state the following: for the feedback interconnection of Fig. 5.4.23, consider the closed-loop transfer function $S(s)$ given by

$$S(s) = \frac{P(s)K(s)}{1 + P(s)K(s)}$$

where $K(s)$ is a proper stabilizing controller and $P(s)$ has relative degree r . If we denote by p_1, p_2, \dots, p_n and z_1, z_2, \dots, z_m the unstable poles and zeros of the plant $P(s)$, respectively (i.e., those poles and zeros which lie in the closed right half-plane).

then the following conditions must be satisfied:

1. $S(s)$ is stable.
2. $S(p_1) = S(p_2) = \dots = S(p_n) = 1$.
3. $S(z_1) = S(z_2) = \dots = S(z_m) = 0$.
4. The relative degree of $S(s)$ is at least r .

Hence, for a given plant $P(s)$, we may characterize any stable closed-loop transfer function $S(s)$ via

$$S(s) = \sum_{i=r}^{\infty} a_i Q_i(s)$$

subject to the constraints

$$\begin{aligned} \sum_{i=r}^{\infty} a_i Q_i(p_j) &= 1, & 1 \leq j \leq n \\ \sum_{i=r}^{\infty} a_i Q_i(z_k) &= 0, & 1 \leq k \leq m \end{aligned}$$

For a given basis, note that the interpolation conditions impose a linear constraint on the coefficients a_i . Expressing the Q-parameterization through these interpolation conditions is often-times simpler computationally since it does not require one to explicitly find transfer function $S_0(s)$, $S_1(s)$ and $S_2(s)$.

Formulation of Linear Programming Problem

We utilize the results of the previous section in the following way. For some integer $N > 0$ that is potentially large, we consider the set of closed-loop transfer functions $S(s)$ from $r(t)$ to $y(t)$ in Fig. 5.4.23 of the form

$$S(s) = \sum_{i=2}^N a_i Q_i(s)$$

where $Q_i(s)$ is the i -th Ritz basis function of Eqn. 5.4.32, and where the a_i are coefficients to be determined. For the plant $P(s)$ given by

$$P(s) = \frac{a}{s(s-b)},$$

we have the interpolation condition

$$\sum_{i=2}^N a_i Q_i(0) = \sum_{i=2}^N a_i = 1.$$

When $b > 0$, we have the additional interpolation condition

$$\sum_{i=2}^N a_i Q_i(b) = \sum_{i=2}^N a_i \left(\frac{c}{c+b} \right)^i = 1.$$

To represent the conditions imposed on the step response $y(t)$ and the control signal $u(t)$. Let $s_i(t)$ represent the step response of $Q_i(s)$ and $u_i(t)$ represent the step response of $Q_i(s)/P(s)$. Then the overall step response $s(t)$ and control output $u(t)$ can be expressed as

$$\begin{aligned} s(t) &= \sum_{i=2}^N a_i s_i(t) \\ u(t) &= \sum_{i=2}^N a_i u_i(t). \end{aligned}$$

For a given settling time T , we can represent the control bound, and the 1% settling time and overshoot constraints as

$$\begin{aligned} \left| \sum_{i=2}^N a_i u_i(t) \right| &\leq 1 \quad \forall t \geq 0 \\ \left| 1 - \sum_{i=2}^N a_i s_i(t) \right| &\leq 0.01 \quad \forall t \geq T \\ \sum_{i=2}^N a_i s_i(t) &\leq 1.01 \quad \forall t \geq 0. \end{aligned}$$

Since all of the above constraints are linear constraints on the coefficients a_i , and, hence, is an infinite dimensional linear program. By finely gridding the time-axis, one may approximate this by a finite dimensional linear program which can be solved via existing software packages such as MATLAB's `sedumi` package. If the problem is feasible, the coefficients a_i determine for us a closed-loop transfer function whose output step response $y(t)$ and control step response $u(t)$ satisfies the desired conditions for some settling time T . A stabilizing controller $K(s)$ may then be obtained via the nonlinear transformation

$$K(s) = \frac{S(s)}{P(s)(1 - S(s))}.$$

Algorithm for Finding the Minimal 1% Settling Time T

Note in the above linear programming formulation, the 1% settling time T is not subject to optimization but must be supplied to the linear program. In addition to supplying T , we must also supply the parameter c for the Ritz basis functions of Eqn. 5.4.32, along with the parameter N to determine the number of basis elements we use in constructing $S(s)$.

The essence of the algorithm we use to estimate the minimal settling time is a bisection algorithm: we find bounds T_{upper} and T_{lower} on the settling time T , and consider the settling time $T' = 0.5(T_{\text{upper}} + T_{\text{lower}})$. If the linear program using the value T' is feasible, then we set $T_{\text{upper}} = T'$. If the program is infeasible, we would like to set $T_{\text{lower}} = T'$; however, we recognize that infeasibility of the program could be due to a poor choice of either c or N .

We modify the basic bisection algorithm by adding a “fine-tuning” phase at the beginning: we first set T to be some large value for which the program is feasible for some choice of c and N . Keeping T fixed, we then adjust the value of c to try to minimize the value of N for which the program remains feasible. Our aim here is to find a “good” value of c which will yield controller orders as low as possible.

Once we have found a good value of c , we proceed with a bisection algorithm as follows: whenever the program is feasible, we assign $T_{\text{upper}} = T'$ as before. When the program is infeasible, however, we increase the value of N and try again. We continue to increase the value of N until either the program is feasible or N has reached some large, pre-specified value N_0 . If the program is still not feasible with $N = N_0$, we assign $T_{\text{lower}} = T'$ and continue.

Results

We present the results of using the above algorithm for five different plants in Table 5.1. The table shows 4 quantities for each plant: the approximate settling time derived in the last section, the minimum 1% settling time that was achieved using the linear programming formulation, the smallest order of a controller that could be found that achieves the minimal settling time, and the 1% settling time of the switching architecture we derived at the beginning of the chapter (for reference). Note that the minimum 1% settling times are not too far from the analytical bound we derived earlier; the largest deviation of the five plants is about 7.5%. Hence, the approximate bound on the ratio of the settling times that we derived earlier is off by less than 10%.

After the 1% settling time was determined for each plant, the minimal controller order was determined by reducing the value of N until the program became infeasible. The controller order for the smallest value of N which did not make the program become infeasible is what is listed in the table. Extrapolating from the examples shown here, we see that the order of the controller needed to achieve the minimal 1% settling time using this method is, generally, quite high. Using standard model reduction techniques on the controller can provide some reduction in the order of the optimal controller. For instance, using Hankel model order reduction techniques, one can reduce the optimal controller for the double integrator down from a seventeenth order controller to a twelfth order controller. The control step response $u(t)$ and the output step response $y(t)$ is shown for the seventeenth order controller in Fig. 5.4.24 and for the twelfth order controller in Fig. 5.4.25. Similar reductions were seen performing Hankel model order reduction on the optimal controllers of the other plants.

A natural question to ask at this point is the following: how does the controller

$P(s)$	Analytical Approximation T_0	Measured 1% Settling Time	Controller Order	Switching Architecture 1% Settling Time T_s
$\frac{1}{s^2}$	2	1.85	17	5.08
$\frac{100}{s(s+1)}$	0.2002	0.185	17	.4849
$\frac{1}{s(s+1)}$	2.1701	2.04	15	3.7772
$\frac{100}{s(s-1)}$	0.2002	0.193	22	.5253
$\frac{1}{s(s-1)}$	2.1701	2.08	38	7.7013

Table 5.1: Summary of results for 5 different plants $P(s)$. The analytical approximation T_0 refers to the approximation for the 1% settling time given by Eqn. 5.4.29.

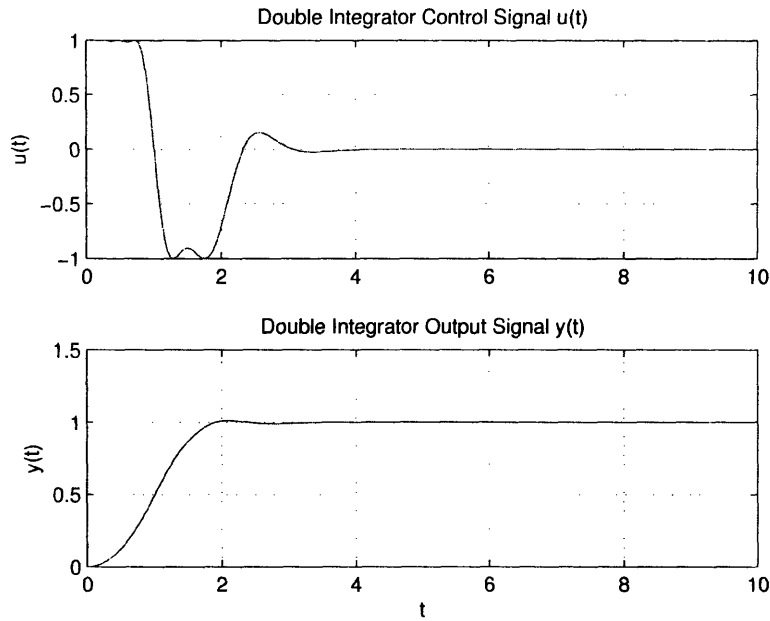


Figure 5.4.24: Control signal $u(t)$ and step response $y(t)$ which yield minimal 1% settling time (1.85 seconds) for the double integrator $P(s) = 1/s^2$ using a 17th order controller.

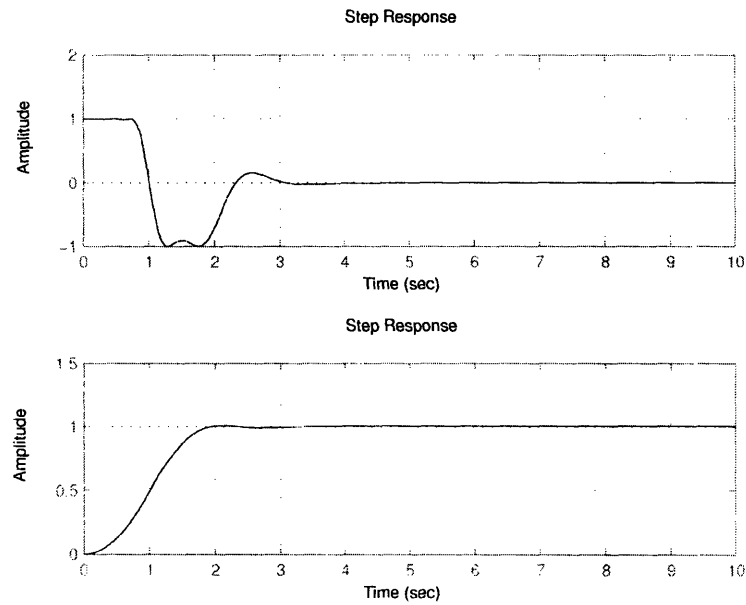


Figure 5.4.25: Control signal $u(t)$ and step response $y(t)$ which yield minimal 1% settling time (1.85 seconds) for the double integrator $P(s) = 1/s^2$ using a reduced order controller (12th order).

order change with the settling time? Can we increase the settling time and dramatically decrease the order of the optimal controller? The answer to this question is, in general, no. By increasing the settling time, it is possible to decrease the order of the required controller, but the order of the resulting controller is still generally fairly high using the method shown here. For instance, in the case of the double integrator, by increasing the 1% settling time to 2.53 seconds, we were able to design a 10th order controller (which could be reduced to a 9th order controller via Hankel model reduction), but an attempt to increase the settling time beyond that point did not reduce the order of the optimal controller at all.

While the method we used to construct controllers in this section is indicative that high order LTI control is necessary to achieve close-to-optimal performance, we *cannot* strictly conclude this on the basis of the analysis performed here. Indeed, the Q-parameterization method we used here typically does require a fairly large number of terms (large N) in order for the linear inequality constraints to be feasible. If one considers the problem of searching for an LTI controller of *minimal order* that achieves similar settling time and overshoot profiles to the ones we have shown here, the task is much more daunting since, to the knowledge of the author, there is no simple way of attempting to solve this problem, short of gridding the space of n -dimensional stabilizing controllers for a fixed value of n , starting with $n = 2$ and increasing n until a controller that satisfies the desired constraints is found. While this gridding process is not too difficult for low dimensions (as we demonstrated in this chapter), in general, an n -th dimensional controller requires $2n + 1$ free parameters, and assuming roughly uniform grids for each parameter, the number of grid points then grows exponentially with exponent $2n + 1$. Hence, attempting to solve the problem this way may easily become computationally intractable for even relatively small values of n .

5.5 Summary

In this chapter, we investigated the use of the switching architecture we have been studying to design a controller for a particular class of LTI plants for a step response application. The material that was presented can be broken down into three parts:

Synthesis of Switching Controllers We first showed how to use the tools that we had developed in the previous chapters to design switching controllers for the class of plants of interest to us in this chapter. We arrived at designs for a first order LTI observer and a static switching law (that depends upon the observer output) that allowed us to characterize the 1% settling time of the step response exactly and to show that the switching controller led to step responses with no overshoot.

Comparison to first Order LTI Control We investigated the performance of a particular LTI control architecture, namely a first order controller connected in a servo configuration about the plant. After formulating a formal comparison, we computed the achievable pairs of percentage overshoot and 1% settling time for the set of linear controllers that satisfied the mathematical constraints

we imposed and showed that the switching architecture outperforms the LTI controller in terms of both settling time and overshoot.

Comparison to Higher Order LTI Control We derived a fundamental limit on the minimum 1% settling time that can be achieved via an arbitrary bounded control input (as well as an approximate bound that is generally quite accurate) to show that, for a certain class of plants, the ratio of the settling time that can be achieved using the switching architecture to the settling time that can be achieved using an arbitrary bounded control input is, itself, bounded. Specifically, we showed that the 1% settling time of the switching architecture can never be more than a factor of 8 larger than the 1% settling time achievable via arbitrary bounded control. We then investigated a method of designing finite order LTI controllers which achieve close-to-optimal performance and saw, through the context of several examples, that the resulting controller order is generally quite large.

While it may be masked behind many of the mathematical details presented in this chapter, our main goal has to been to show that the switching architecture that we have been studying has the potential for application in the engineering world. While we have not addressed any of the real-world implementation issues that are inherent in turning any systems-level design into a physical realization, we have attempted to show that, at a systems level, we can design controllers with this particular switching architecture in a relatively simple manner. Moreover, this simple switching architecture can outperform linear controllers with dynamics of equal order. While it cannot outperform LTI controllers in general, the marginal improvement we can get comes at the high cost of potentially having to implement high order dynamical controllers. The studies shown here provide just a small glimpse into the power of switching, but we hope that this glimpse has been a powerful one.

5.6 Proof of Technical Statements

Proof of Prop. 5.3.15

If γ is an upper bound for the L_2 gain from $\begin{bmatrix} w(t) & w'(t) \end{bmatrix}$ to $y(t) = \Delta(w(t), w'(t))$, then

$$\inf_{T>0} \int_0^T (\gamma^2(\|w(t)\|^2 + \|w'(t)\|^2) - \|y(t)\|^2) dt > -\infty.$$

Now, if $|w(t)| = |w'(t)|$ for all $t > 0$, the above constraint can be re-written as

$$\inf_{T>0} \int_0^T (2\gamma^2\|w(t)\|^2 - \|y(t)\|^2) dt > -\infty.$$

Since the above constraint holds for *all* $w(t)$ that are square integrable over finite intervals, it follows that $\gamma' = \sqrt{2}\gamma$ is an upper bound for the L_2 gain from $w(t)$ to $y(t)$ subject to the constraint that $|w(t)| = |w'(t)|$ for all t .

Proof of Prop. 5.3.16

Using the notation $z = \Delta_1(w)$ and $y = \Delta_2(z)$, then by assumption

$$\begin{aligned} \inf_{T>0} \int_0^T (\gamma_1^2 \|w(t)\|^2 - \|z(t)\|^2) dt &> -\infty \\ \inf_{T>0} \int_0^T (\gamma_2^2 \|z(t)\|^2 - \|y(t)\|^2) dt &> -\infty \end{aligned}$$

Multiplying the top inequality by γ_2^2 and adding it to the second inequality yields

$$\inf_{T>0} \int_0^T (\gamma_1^2 \gamma_2^2 \|w(t)\|^2 - \|y(t)\|^2) dt > -\infty.$$

Since the above inequality holds for an arbitrary input $w(t)$, we conclude that $\gamma_1 \gamma_2$ is an upper bound on the L_2 gain of the composition.

Proof of Prop. 5.3.17

To prove item 1, we will prove the following equivalent fact: that the peak control value occurs at time 0, i.e. $|u(t)| < k$ for all $t > 0$ (note the strict inequality). To begin, note again that the transfer function from $r(t)$ to $u(t)$ in Fig. 5.3.8 is given by

$$H_{ru}(s) = \frac{ks^2(s+c)}{s^3 + ds^2 + ks + kc}.$$

In order for the above transfer function to represent an asymptotically stable system, we can deduce from the Routh criterion that $c > 0$, $d > 0$, $k > 0$ and that $d > c$. The above transfer function has a state-space description of the following form:

$$\begin{aligned} \dot{x}_1 &= x_2 \\ \dot{x}_2 &= k(r - x_1 + (c - d)x_3) \\ \dot{x}_3 &= r - x_1 - dx_3 \\ u &= k(r - x_1 + (c - d)x_3). \end{aligned}$$

When $r(t)$ is a constant, i.e. $r(t) = r$, if we make the change of variables

$$\begin{aligned} z_1 &= r - x_1 + (c - d)x_3 \\ z_2 &= x_2 \\ z_3 &= x_3. \end{aligned}$$

then the closed loop dynamics are characterized by the dynamics of the following autonomous system

$$\begin{aligned}\dot{z}_1 &= (c - d)z_1 - z_2 - c(c - d)z_3 \\ \dot{z}_2 &= kz_2 \\ \dot{z}_3 &= z_1 - az_3 \\ u &= kz_1.\end{aligned}$$

Note that the zero-state unit step response, which corresponds to the initial condition $x_1(0) = x_2(0) = x_3(0) = 0$, has a corresponding initial condition in terms of the z variables that is given by $z_1(0) = 1$, $z_2(0) = z_3(0) = 0$.

We will use the above state-space description in z coordinates to construct an argument $|u(t)| < k$ for all $t > 0$. Assume that the constraint does *not* hold, i.e., that there exists some time $t_0 > 0$ for which $u(t_0) = k$ or $u(t_0) = -k$. Suppose for the moment that $z_2(t_0) = z_3(t_0) = 0$. Then the state of the system $z = [z_1 \ z_2 \ z_3]'$ would satisfy the relationship $z(t_0) = \pm z(0)$. Moreover, the time-invariance of this system would imply that $z(mt_0) = \pm z(0) \neq 0$ for all $m \in \mathbf{Z}^+$ which would contradict the assumed asymptotic stability of the original system.

As it turns out, if $u(t_0) = \pm k$, then the remaining states $z_2(t_0)$ and $z_3(t_0)$ both *must* be 0, as we now show. Consider the quadratic Lyapunov function

$$V(z) = z_1^2 + \frac{1}{k}z_2^2 + c(d - c)z_3^2$$

which, along the system trajectories, satisfies

$$\dot{V}(x) = 2(c - d)(z_1 - cz_3)^2 \leq 0$$

for all $z \in \mathbf{R}^3$. Note that $V(z)$ satisfies the property that

$$V(z_1, z_2, z_3) > V(z_1, 0, 0) \quad \forall (z_2, z_3) \in \mathbf{R}^2 \setminus \{0\}.$$

Now, suppose that $u(t_0) = k$ or, correspondingly, that $z_1(t_0) = 1$, and that either or both of $z_2(t_0)$ and $z_3(t_0)$ are nonzero. Then we have that

$$V(1, z_2(t_0), z_3(t_0)) > V(1, 0, 0)$$

which contradicts the fact that $V(z)$ is nonincreasing along the system trajectories. By noting that $V(z) = V(-z)$, a similar proof holds to show that if $u(t_0) = -k$ then a similar contradiction holds. Hence, it follows that if $u(t_0) = \pm k$, then $z_2(t_0) = z_3(t_0) = 0$, and we conclude that $u(t_0)$ cannot equal either k or $-k$ for any $t_0 > 0$. By the continuity of the state trajectories, we further conclude that $|u(t)| < k$ for all $t > 0$ and that the peak control value (which occurs at time 0) is equal to k .

To prove the second item, let $H_1(s) = P(s)/(1 + P(s)K(s))$, and define $G_1(s) = H_1(\sqrt{k}s)$. It is clear that $\|G_1(s)\|_\infty = \|H_1(s)\|_\infty$. Note that $G_1(s)$ can be written in

the form

$$G_1(s) = \frac{s + \frac{d}{\sqrt{k}}}{s^3 + \frac{d}{\sqrt{k}}s^2 + s + \frac{c}{\sqrt{k}}} = \frac{P(s)}{1 + P(s)\tilde{K}(s)}$$

from which the norm bound constraint in item 2 immediately follows. Note also that $\tilde{K}(s)$ is a special form of Eqn. 5.3.14 with $k = 1$, so, by the result of item 1, the peak control value is equal to 1. Hence, $\tilde{K}(s)$ satisfies both constraints that we are imposing on the closed-loop system of Fig. 5.3.8.

Now, if we define the transfer functions

$$H_2(s) = \frac{P(s)K(s)}{1 + P(s)K(s)}, \quad G_2(s) = \frac{P(s)\tilde{K}(s)}{1 + P(s)\tilde{K}(s)}$$

which represent the closed-loop transfer functions from $r(t)$ to $y(t)$ in Fig. 5.3.8 for the controllers $K(s)$ and $\tilde{K}(s)$, respectively, then a simple calculation shows that $G_2(s) = H_2(\sqrt{k}s)$. Let $s(t)$ be the unit step response of the system with transfer function $H(s)$ and $\tilde{s}(t)$ be the unit step response of the system with transfer function $G(s)$, i.e.,

$$\begin{aligned} s(t) &= \int_0^t h_2(\tau) d\tau \\ \tilde{s}(t) &= \int_0^t g_2(\tau) d\tau \end{aligned}$$

where $h_2(t)$ and $g_2(t)$ are the impulse responses corresponding to the transfer functions $H_2(s)$ and $G_2(s)$, respectively. Because the impulse responses satisfy the relation

$$g_2(t) = \frac{1}{\sqrt{k}} h_2\left(\frac{t}{\sqrt{k}}\right),$$

we have

$$\tilde{s}(t) = \int_0^t g_2(\tau) d\tau = \int_0^t \frac{1}{\sqrt{k}} h_2\left(\frac{\tau}{\sqrt{k}}\right) d\tau = \int_0^{\frac{t}{\sqrt{k}}} h_2(\sigma) d\sigma = s\left(\frac{t}{\sqrt{k}}\right).$$

The above relationship makes clear that if the step response $s(t)$ has percentage overshoot M and 1% settling time T , then the step response $\tilde{s}(t)$ also has percentage overshoot M and has 1% settling time $T\sqrt{k}$.

Proof of Prop. 5.4.19

We will prove the statement via induction, starting with item 1. For the case $n = 0$, this implies verifying that

$$1 - x + \frac{x^2}{2} \geq e^{-x} \geq 1 - x$$

for any $x \geq 0$. We start with the inequality $\exp(-x) \leq 1$ for all $x \geq 0$. Integrating both sides of the above inequality yields the following:

$$\begin{aligned}\int_0^x e^{-y} dy &\leq \int_0^x dy \\ 1 - e^{-x} &\leq x \\ 1 - x &\leq e^{-x}\end{aligned}$$

which yields the desired lower bound. Integrating again yields

$$\begin{aligned}\int_0^x (1 - y) dy &\leq \int_0^x e^{-y} dy \\ x - \frac{x^2}{2} &\leq 1 - e^{-x} \\ e^{-x} &\leq 1 - x + \frac{x^2}{2}\end{aligned}$$

To prove the statement for arbitrary $n \in \mathbf{Z}^+$, assume that the bounds hold for a particular value of n . We wish to prove that bounds hold for $n + 1$, as well, i.e.,

$$\sum_{k=0}^{2(n+1)+2} \frac{(-x)^k}{k!} \geq e^{-x} \geq \sum_{k=0}^{2(n+1)+1} \frac{(-x)^k}{k!}.$$

Starting with the upper bound:

$$\begin{aligned}e^{-x} &\leq \sum_{k=0}^{2n+2} \frac{(-x)^k}{k!} \\ \int_0^x e^{-y} dy &\leq \sum_{k=0}^{2n+2} \int_0^x \frac{(-y)^k}{k!} dy \\ 1 - e^{-x} &\leq - \sum_{k=0}^{2n+2} \frac{(-x)^{k+1}}{(k+1)!} \\ \sum_{k=-1}^{2n+2} \frac{(-x)^{k+1}}{(k+1)!} &\leq e^{-x}\end{aligned}$$

Making the change of variable $m = k + 1$ yields

$$\sum_{m=0}^{2(n+1)+1} \frac{(-x)^m}{m!} \leq e^{-x}$$

which establishes the lower bound. Integrating this lower bound:

$$\begin{aligned} \sum_{m=0}^{2(n+1)+1} \int_0^x \frac{(-y)^m}{m!} dy &\leq \int_0^x e^{-y} dy \\ - \sum_{m=0}^{2(n+1)+1} \frac{(-x)^{m+1}}{(m+1)!} &\leq 1 - e^{-x} \\ e^{-x} &\leq \sum_{m=-1}^{2(n+1)+1} \frac{(-x)^{m+1}}{(m+1)!} \end{aligned}$$

Making the change of variable $p = m + 1$ yields

$$e^{-x} \leq \sum_{p=0}^{2(n+1)+2} \frac{(-x)^p}{p!}.$$

To prove the second item, note that the case $n = 0$ is true since it implies that

$$e^x \geq 1$$

for all $x \geq 0$. Now, assuming that the inequality holds for some arbitrary value of n ,

$$\begin{aligned} e^x &\geq \sum_{k=0}^n \frac{x^k}{k!} \\ \int_0^x e^y dy &\geq \sum_{k=0}^n \int_0^x \frac{y^k}{k!} dy \\ e^x - 1 &\geq \sum_{k=0}^n \frac{x^{k+1}}{(k+1)!} \\ e^x &\geq \sum_{k=-1}^n \frac{x^{k+1}}{(k+1)!}. \end{aligned}$$

Making the change of variable $m = k + 1$ yields

$$e^x \geq \sum_{m=0}^{n+1} \frac{x^m}{m!}.$$

Proof of Prop. 5.4.20

To begin, first note that it is sufficient to establish that given property holds for $t = T$, i.e., that $|x_2(T)| \leq M\sqrt{\epsilon}$. To see this, consider an arbitrary time $T' > T$ for which we desire to show the property

$$|x_1(t) - 1| \leq \epsilon \quad \forall t \geq T \implies |x_2(T')| \leq M\sqrt{\epsilon}.$$

A sufficient condition for the above implication to be true is that

$$|x_1(t) - 1| \leq \epsilon \quad \forall t \geq T' \implies |x_2(T')| \leq M\sqrt{\epsilon}.$$

Due to the time-invariance of $P(s)$, by making the change of variable $t' = t - (T' - T)$, the above reduces to

$$|x_1(t') - 1| \leq \epsilon \quad \forall t' \geq T \implies |x_2(T)| \leq M\sqrt{\epsilon}.$$

Moreover, note that without loss of generality, we may take $T = 0$.

Now, if $|x_1(t) - 1| \leq \epsilon$ for all $t \geq 0$, we have

$$\begin{aligned} |x_1(t) - x_1(0)| &= |x_1(t) - 1 - (x_1(0) - 1)| \\ &\leq |x_1(t) - 1| + |x_1(0) - 1| \\ &\leq 2\epsilon \end{aligned}$$

for all $t \geq 0$. Note that $x_1(t)$ can be written explicitly as

$$x_1(t) = x_1(0) + \frac{\sqrt{a}}{b} (e^{bt} - 1) x_2(0) + \frac{a}{b} \int_0^t (e^{b\tau} - 1) u(t - \tau) d\tau.$$

Now,

$$\begin{aligned} |x_1(t) - x_1(0)| &\geq \frac{\sqrt{a}}{b} (e^{bt} - 1) |x_2(0)| - \left| \frac{a}{b} \int_0^t (e^{b\tau} - 1) u(t - \tau) d\tau \right| \\ &\geq \frac{\sqrt{a}}{b} (e^{bt} - 1) |x_2(0)| - \frac{a}{b} \int_0^t (e^{b\tau} - 1) d\tau \\ &= \frac{\sqrt{a}}{b} (e^{bt} - 1) |x_2(0)| - \frac{a}{b} t + \frac{a}{b^2} (e^{bt} - 1) \end{aligned}$$

where we use the fact that

$$\frac{1}{b} (e^{bt} - 1) \geq 0 \quad \forall t \geq 0$$

for any $b \neq 0$.⁶ In order for the constraint $|x_1(t) - x_1(0)| \leq 2\epsilon$ to be satisfied for all $t \geq 0$, we must have that

$$\frac{\sqrt{a}}{b} (e^{bt} - 1) |x_2(0)| - \frac{a}{b} t + \frac{a}{b^2} (e^{bt} - 1) < 2\epsilon$$

for all $t \geq 0$. A simple calculation shows that if $|x_2(0)| \geq \sqrt{a}/b$, then the left hand side of the above expression is always increasing and, hence, the above condition cannot be satisfied for all $t \geq 0$. When $|x_2(0)| < \sqrt{a}/b$, we can compute the maximum value of the left hand side over all $t \geq 0$, and we find that the above condition is satisfied

⁶We only prove the statement for the case $b \neq 0$ here; the proof for $b = 0$ is similar and is left to the reader.

for all $t \geq 0$ if and only if

$$-\frac{b}{\sqrt{a}}|x_2(0)| - \ln \left(1 - \frac{b}{\sqrt{a}}|x_2(0)| \right) < 2\epsilon \frac{b^2}{a}. \quad (5.6.33)$$

When $b > 0$, the left hand side of the above expression is of the form $-x - \ln(1 - x)$ with $x > 0$. From item 1 of Prop. 5.4.19 for $n = 1$, we have by taking logarithms:

$$\begin{aligned} -x - \ln(1 - x) &\geq \ln \left(1 - x + \frac{x^2}{2} - \frac{x^3}{6} \right) - \ln(1 - x) \\ &\geq \ln \left(1 - x + \frac{x^2}{6} - \frac{x^3}{6} \right) - \ln(1 - x) \\ &= \ln \left((1 - x) \left(1 + \frac{x^2}{6} \right) \right) - \ln(1 - x) \\ &= \ln \left(1 + \frac{x^2}{6} \right). \end{aligned}$$

Similarly, when $b < 0$, the left hand side of Eqn. 5.6.33 is of the form $x - \ln(1 + x)$, $x > 0$, and we have from item 2 of Prop. 5.4.19:

$$\begin{aligned} x + \ln(1 + x) &\geq \ln \left(1 + x + \frac{x^2}{2} + \frac{x^3}{6} \right) - \ln(1 + x) \\ &\geq \ln \left(1 + x + \frac{x^2}{6} + \frac{x^3}{6} \right) - \ln(1 + x) \\ &= \ln \left(1 + \frac{x^2}{6} \right). \end{aligned}$$

We hence conclude that the following condition must be satisfied:

$$\ln \left(1 + \frac{b^2}{a}|x_2(0)|^2 \right) < 2\epsilon \frac{b^2}{a}$$

which can be rewritten as

$$|x_2(0)| < \frac{\sqrt{6a}}{b} \sqrt{\exp \left(2\epsilon \frac{b^2}{a} \right) - 1}. \quad (5.6.34)$$

Recall the Mean Value Theorem [30] which states that a function $f(x)$ which is continuous on an interval $[c, d]$ and differentiable on (c, d) satisfies the condition

$$f(d) = f'(m)(d - c) + f(c)$$

for some $m \in (c, d)$. Applying this theorem to the function $f(x) = e^x - 1$, we have that

$$e^x - 1 = xe^m$$

for some $m \in (0, x)$, which, in turn, implies that

$$e^x - 1 \leq xe^x.$$

We hence conclude from Eqn. 5.6.34 that

$$|x_2(0)| \leq \sqrt{12 \exp\left(2\epsilon \frac{b^2}{a}\right) \epsilon} \leq \sqrt{12e^{2\epsilon}\epsilon} \leq \sqrt{12e^2\epsilon}$$

where, in the above, we have used the fact that $b^2 < a$ and $\epsilon \leq 1$.

Chapter 6

Moving Beyond the Phase Plane: Higher Order Design Example

While all of the techniques we have developed to this point have focused on second order LTI plants, the L_2 gain techniques we developed in Chapter 4 actually allow us to extend our design capabilities to a larger class of systems—including higher order LTI, nonlinear, and time-varying systems—which are well-approximated by a second order LTI model in an L_2 gain sense. By making use of the so-called *Small Gain Theorem*, in many instances, we can actually reduce the design of a controller for a more complicated system model to that of designing a second order LTI model. More importantly, even though our design will be based upon a simpler model, we will be able to provide a performance bound for the *original* plant (or, as in the case we examine here, a performance bound for an entire *class* of plants).

In this chapter, we will consider an example in which we design a switching controller using the techniques we have developed to stabilize a class of fourth order LTI plants which, in an L_2 gain sense, are close to a double integrator. We will provide a method of designing controllers for the fourth order plant based upon a second order approximation and will provide a bound on the L_2 gain from the input of the plant to the output of the plant for all plants within the class we consider. For reference, we will compare this bound to the “nominal” bound we computed for the double integrator in the previous chapter. Finally, we will compute the step responses for various plants within the class to show numerically that, as the fourth order plant model approaches a double integrator in an L_2 gain sense, the corresponding step response of the fourth order plant well-approximates the step response of a double integrator.

6.1 Preliminaries: Small Gain Theorem

The main result from robust control theory which will allow us to extend our design results beyond plants which are second order LTI systems is embedded in a form of the *Small Gain Theorem* given below (adapted from [52]):

Theorem 6.1.10 (Small Gain Theorem) *Consider systems S and Δ as shown in*

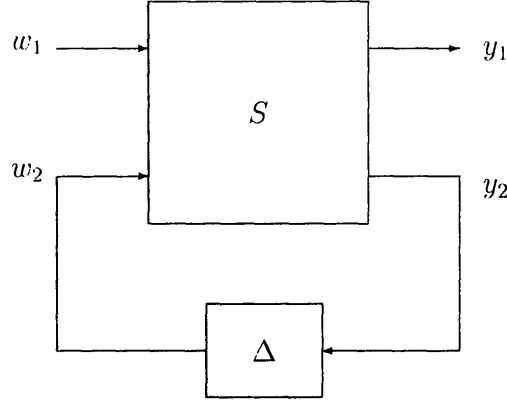


Figure 6.1.1: Block diagram description of systems S and Δ for Small Gain Theorem.

Fig. 6.1.1. If system S has L_2 gain less than or equal to γ_S and system Δ has L_2 gain less or equal to γ_Δ , then if $\gamma_S\gamma_\Delta \leq 1$, the feedback interconnection of Fig. 6.1.1 has L_2 gain from w_1 to y_1 less than or equal to γ_S .

Proof By assumption,

$$\inf_{T>0} \int_0^T (\gamma_S^2(\|w_1\|^2 + \|w_2\|^2) - (\|y_1\|^2 + \|y_2\|^2)) dt > -\infty$$

$$\inf_{T>0} \int_0^T (\gamma_\Delta^2\|y_2\|^2 - \|w_2\|^2) dt > -\infty.$$

Multiplying the bottom relationship by γ_S^2 and adding it to the first yields

$$\inf_{T>0} \int_0^T (\gamma_S^2\|w_1\|^2 - \|y_1\|^2 - (1 - \gamma_S^2\gamma_\Delta^2)\|y_2\|^2) dt > -\infty.$$

If $\gamma_S\gamma_\Delta \leq 1$, then we conclude

$$\inf_{T>0} \int_0^T (\gamma_S^2\|w_1\|^2 - \|y_1\|^2) dt > -\infty.$$

□

We will use the above version of the Small Gain Theorem in the following way: for a given plant P (which may be higher than second order, nonlinear, or time-varying), we derive a second order LTI approximation $\hat{P}(s)$ which we incorporate into the system model S of Fig. 6.1.1 and we represent the “unwanted” dynamics of P in the block depicted Δ in Fig. 6.1.1. If the L_2 gain of Δ is sufficiently small, we can conclude that if we design a stabilizing controller for the second order LTI approximation (which yields an L_2 gain stable system S), then the controller actually stabilizes the original plant P . Moreover, the L_2 gain from the external input w_1

to the output y_1 is upper bounded by the *open-loop* joint L_2 gain from (w_1, w_2) to (y_1, y_2) .

For the reader who is unfamiliar with the standard results of robust control, the utility of the above-described process may not be immediately apparent (for an introduction to robust control theory, see [67]). In this chapter, we present a specific design example to illustrate the above procedure in a concrete manner. The design example considers a class of fourth order LTI systems which can be well-approximated by a double integrator and is described in the next section.

6.2 Design Example: Robust Design for a Class of Fourth Order LTI Systems

In this chapter, we consider a set of LTI plants parameterized by a single real number $\tau > 0$:

$$P_\tau(s) = \frac{1}{\tau^2 s^4 + 2\tau s^3 + (1 - \tau^2)s^2 - 2\tau s}.$$

Since the above transfer function has a single pole at $s = 0$, by factoring the denominator and applying the Routh criterion to the resulting third order polynomial, one can easily see that the above transfer function is exponentially unstable for any value of $\tau \neq 0$. Note, however, that when $\tau = 0$, $P_0(s)$ is a pure double integrator (and is marginally stable). Our goal in this chapter is to design a *single* stabilizing switching controller for the plant $P_\tau(s)$ for a range of $\tau > 0$. We will accomplish this by first approximating $P_\tau(s)$ by a double integrator and using the switching controller for the double integrator we designed in the last chapter. While this may initially seem a bit alarming since we are approximating an exponentially unstable system by a marginally unstable one, by appropriate use of the Small Gain Theorem, we will be able to accomplish the following three goals:

1. We will determine an explicit range of values of $\tau \in [0, \tau_0]$ for which stabilizability of the double integrator guarantees stabilizability of $P_\tau(s)$ for all $\tau \in [0, \tau_0]$.
2. Continuing in the vein of the comparison to first order LTI control we made in the last chapter, we will be able to compute an upper bound on the L_2 gain from a disturbance to the input of the plant $w(t)$ to the output $y(t)$ of the plant $P_\tau(s)$ that holds for *all* values of $\tau \in [0, \tau_0]$.
3. We will show via numerical simulation that the step response of $P_\tau(s)$ under our switching control algorithm well-approximates the step response of the true double integrator for small values of τ .

6.2.1 Range of τ and L_2 Gain Bound

The design setup we consider is depicted in Fig. 6.2.2. Here, $r(t)$ represents a command input which, in the sequel, will be a step input. For this section, however, we will assume $r(t)$ is identically 0. The input $w(t)$ is a disturbance input. The observer

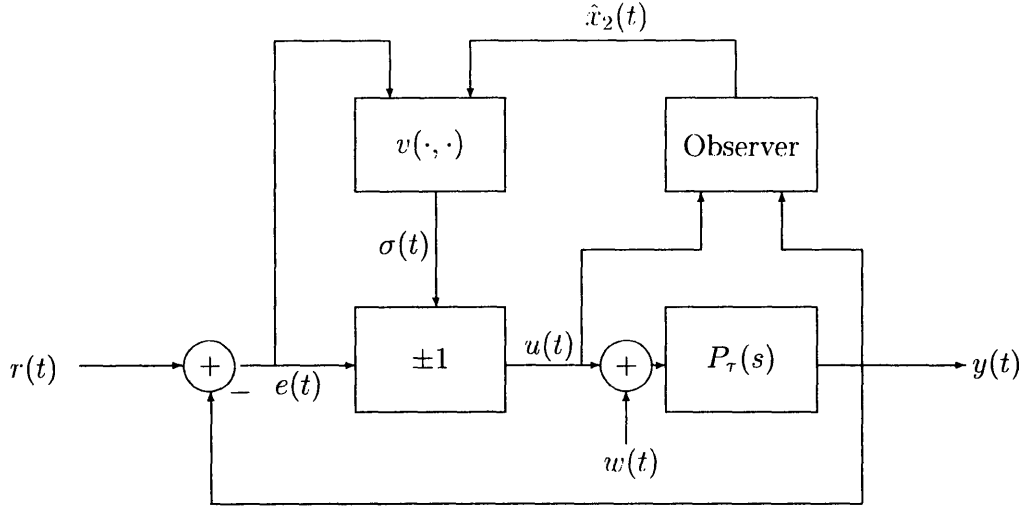


Figure 6.2.2: Design setup for fourth order plant $P_\tau(s)$.

and supervisor are still a first order LTI estimator and a memoryless switching law, respectively. Our objective in this section is to use the Small Gain Theorem to find a number $\tau_0 > 0$ such that a switching controller that stabilizes a double integrator also stabilizes $P_\tau(s)$ for all $\tau \in [0, \tau_0]$. Moreover, we also wish to determine an upper bound on the L_2 gain from $w(t)$ to $y(t)$ that is valid for all $P_\tau(s)$ with $\tau \in [0, \tau_0]$.

We begin first by noting that $P_\tau(s)$ has the block diagram realization of Fig. 6.2.3. Note that for $\tau > 0$, the dynamics of the first block are stable. Moreover, when τ is very small, the two additional poles introduced by the $1/(\tau s + 1)$ terms become very large and, intuitively, one would expect that their effect on the overall system dynamics should become negligible. We prove this statement rigorously using the Small Gain Theorem in the following way: we first rewrite the block diagram of Fig. 6.2.3 so that it appears as in Fig. 6.2.4 where $\Delta(s)$ is given by

$$\Delta(s) = \frac{1}{s+1} \left(\frac{1}{(\tau s + 1)^2} - 1 \right) \quad (6.2.1)$$

If we now label the input and output of Δ as $y_2(t)$ and $w_2(t)$, respectively, and remove the $\Delta(s)$ block from Fig. 6.2.4, we arrive at the system of Fig. 6.2.5. According to the Small Gain Theorem if the product of the L_2 gain of Δ and the L_2 gain of this two-input two-output system is less than or equal to 1, then the closed-loop L_2 gain from $w(t)$ to $y(t)$ with Δ in place (i.e., as in Fig. 6.2.4) will be less than the open loop *joint* L_2 gain from the composite input $\begin{bmatrix} w(t) & w_2(t) \end{bmatrix}'$ to the composite output $\begin{bmatrix} y(t) & y_2(t) \end{bmatrix}'$. Again, denoting this joint L_2 gain as γ_S , explicit computation of γ_S will lead us to two conclusions:

1. If $\|\Delta(s)\|_\infty \leq 1/\gamma_S$, L_2 gain stability will be preserved. Moreover, the condition $\|\Delta\|_\infty \leq 1/\gamma_S$ will directly lead to calculation of an explicit value of τ_0 such

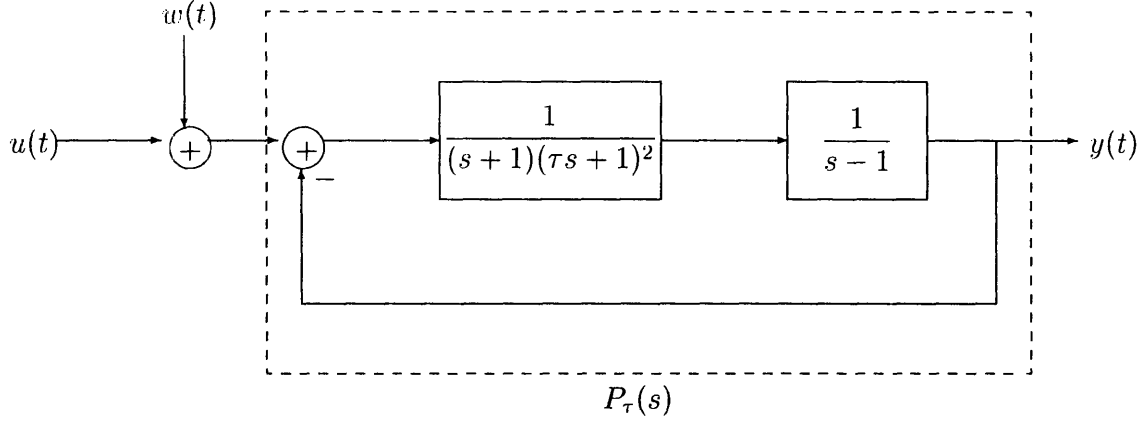


Figure 6.2.3: Block diagram realization of $P_\tau(s)$.

that $P_\tau(s)$ will be stabilized for any $\tau \in [0, \tau_0]$.

2. The L_2 gain from $w(t)$ to $y(t)$ with $\Delta(s)$ in place will be less than or equal to γ_S for all $\tau \in [0, \tau_0]$.

Now, because we have already designed a stabilizing switching controller for the double integrator, we will omit those details here; the switching law and observer are exactly as they are given in Section 5.2.2. In order to compute an upper bound on the joint L_2 gain of the system in Fig. 6.2.5, it is again necessary to introduce a “slack” variable that we denote $q(t)$ (equivalent to the slack variable $v(t)$ in the last chapter, but we use a different variable name so as not to confuse the slack variable with the memoryless switching law). This slack variable enters the system dynamics the same way that it entered the system dynamics in the last chapter (as an input to the second argument of the switching law $v(\cdot, \cdot)$, and is depicted as such in Fig. 6.2.6 where $\hat{z}(t)$ is the second input to the switching law $v(\cdot, \cdot)$.

Now, if we let $w_1(t) = [w(t) \ q(t)]'$ and $y_1(t) = y(t)$, then an upper bound on the joint L_2 gain from $[w_1(t) \ w_2(t)]'$ to $[y_1(t) \ y_2(t)]'$ can be obtained with a minor modification to the procedure that was outlined in Chapter 4. Notice that because u is either y or $-y$ at any given time t , the output y_2 is a *nonlinear* function of the plant state x . Specifically, in the specific coordinate system that we chose to perform the L_2 gain calculation of Section 5.3.1, at any time t , $y_2(t)$ is equal to either $w(t)$ or $w(t) - 2x_1(t)$. While it does not immediately follow from the results of chapter 4 (which proved finite L_2 gain boundedness for outputs which were *linear* functions of the state and exogenous inputs), we will show now that we can compute an upper bound on the L_2 gain with a small adjustment. For notational simplicity (the general case follows in exactly the same way), consider the task of computing the L_2 gain from $w(t)$ to $y_2(t)$ which involves the task of finding a storage function $V(x)$ and a value of γ such that

$$\gamma^2 \|w(t)\|^2 - \|y_2(t)\|^2 - \frac{d}{dt} V(x(t)) > 0$$

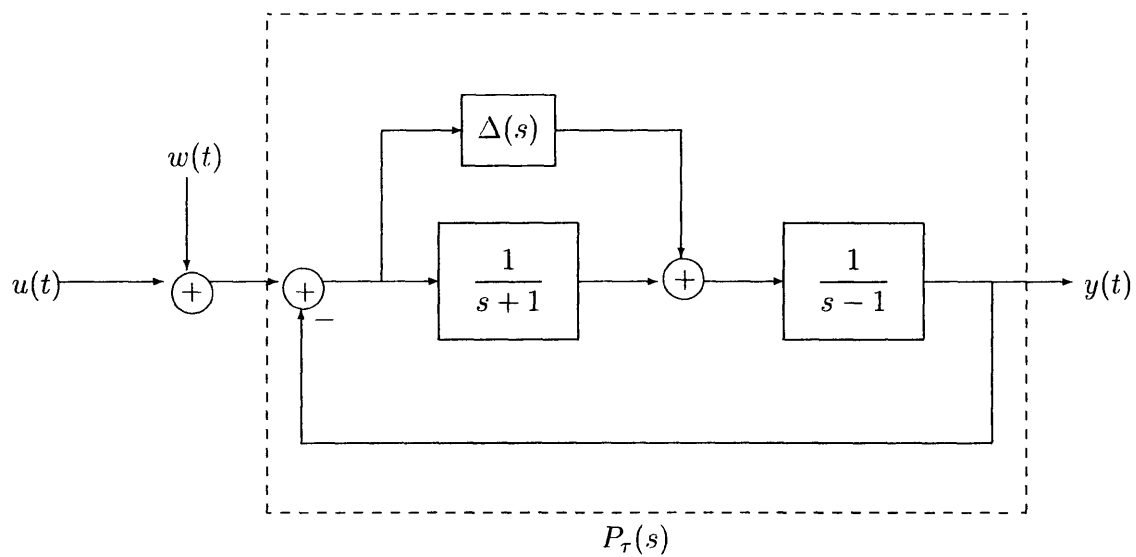


Figure 6.2.4: Block diagram realization of $P_\tau(s)$ with $\Delta(s)$ given as in Eqn. 6.2.1.

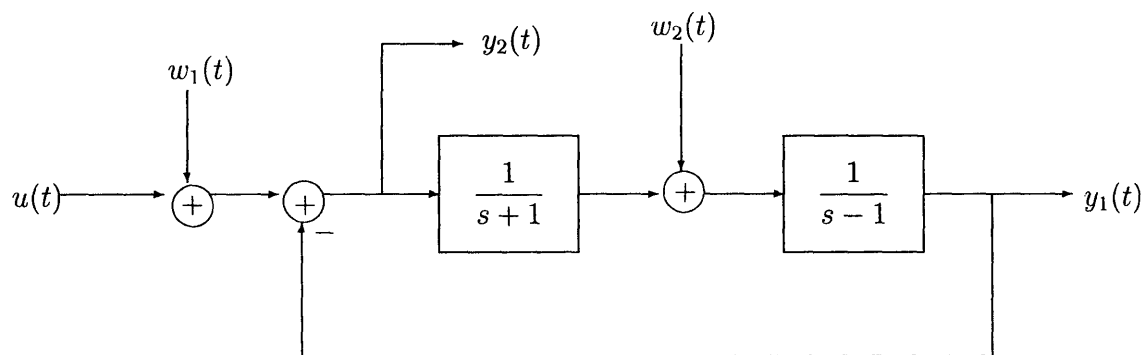


Figure 6.2.5: Block diagram of system to which we apply the Small Gain Theorem.

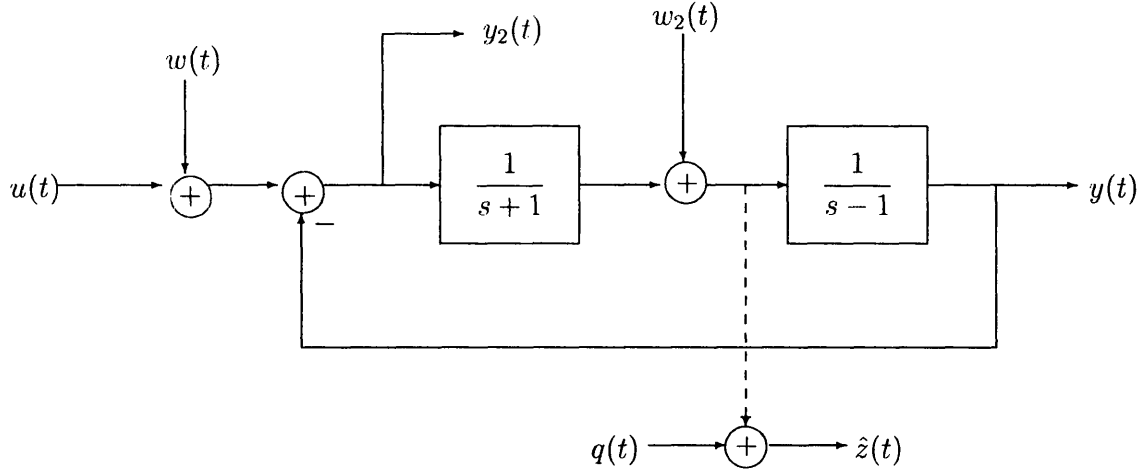


Figure 6.2.6: Block diagram of system for joint L_2 gain calculation.

along system trajectories. It follows that γ is an upper bound for the L_2 gain if there exists a storage function $V(x)$ such that

$$\gamma^2 \|w(t)\|^2 - \max\{\|w(t)\|^2, \|w(t) - 2x_1(t)\|^2\} - \frac{d}{dt}V(x(t)) > 0$$

along system trajectories for all t . The above can equivalently be written as the pairwise conditions

$$\begin{aligned} \gamma^2 \|w(t)\|^2 - \|w(t)\|^2 - \frac{d}{dt}V(x(t)) &> 0 \\ \gamma^2 \|w(t)\|^2 - \|w(t) - 2x_1(t)\|^2 - \frac{d}{dt}V(x(t)) &> 0 \end{aligned}$$

and a corresponding semidefinite program can be set up to find an upper bound on γ .

Performing the above procedure for the system of Fig. 6.2.6 yields a joint L_2 gain bound of 21.16. Numerical computation shows that $\|\Delta(s)\|_\infty \leq 1/21.16$ for $0 \leq \tau \leq 0.024 \triangleq \tau_0$. Hence, we conclude that $P_\tau(s)$ is stabilizable via the switching algorithm of Section 5.2.2 for all values of $\tau \in [0, 0.024]$. Moreover, accounting for the $\sqrt{2}$ factor that is introduced from the slack variable $q(t)$, we find that the joint L_2 gain from $w(t)$ to $y(t)$ is less than or equal to 29.92 for *all* values of $\tau \in [0, 0.024]$. Note in Chapter 5 that we computed an upper bound on the L_2 gain from $w(t)$ to $y(t)$ for the double integrator of 8.38. Hence, extension from a *single* plant to an entire *family* of plants only increases the upper bound by less than a factor of 4.

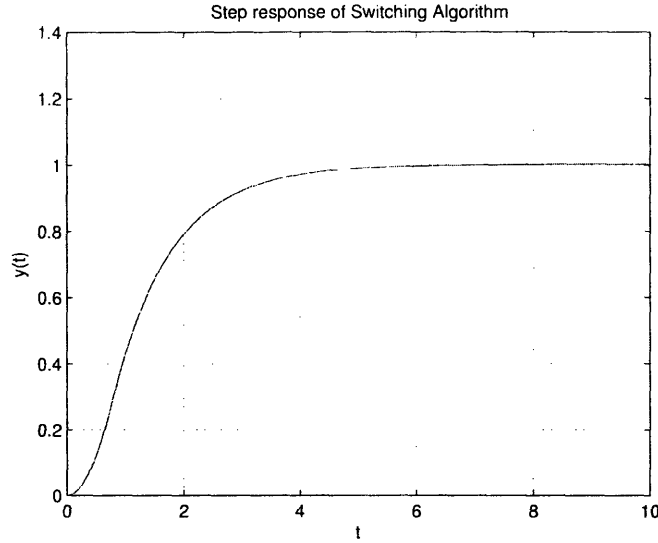


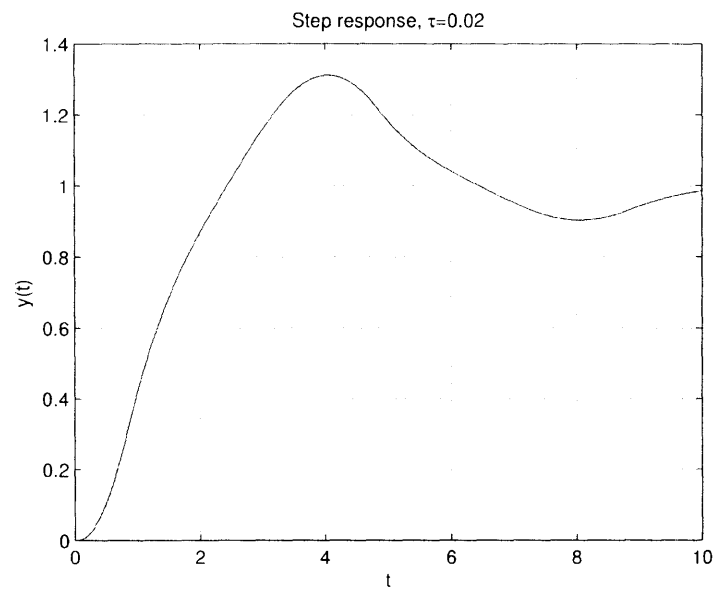
Figure 6.2.7: Step response of double integrator.

6.2.2 Step Response Performance

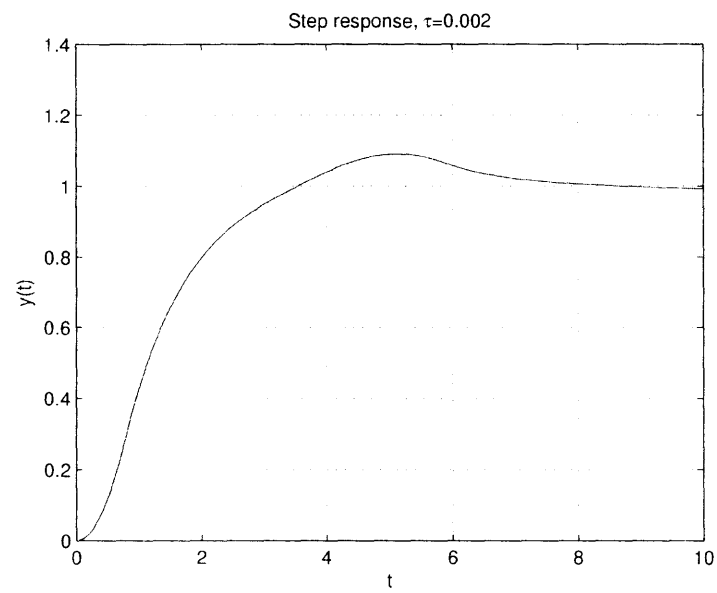
Now that we have computed a range of τ for which stability is guaranteed, we can investigate the behavior of the step response for various values of τ in this range. We naturally expect that as τ approaches 0, the step response of the fourth order system should begin to more closely resemble the step response of the double integrator which is repeated in Fig. 6.2.7 for reference. The step responses for four different values of τ are shown in Fig. 6.2.2 (for $\tau = 0.02$ and 0.002) and 6.2.2 (for $\tau = 0.0002$ and 0.00002). For values of τ that lie close to τ_0 , we see that the discrepancy between the step response of the double integrator and the fourth order system is quite large; however, examination of successive plots as we decrease τ indicates that as τ becomes small, the step response of the controlled fourth order system appears to approach the step response of the double integrator. To formally prove the statement that the step response of the fourth order system approaches the step response of the double integrator in some metric requires the notion of *incremental L_2 gain stability* [53] which has yet to be investigated for this particular class of switching systems and is beyond the scope of this document. We offer these pictures more as a “sanity check” of sorts to verify that the switching controller yields closed-loop behavior that agrees with natural intuition.

6.3 Summary

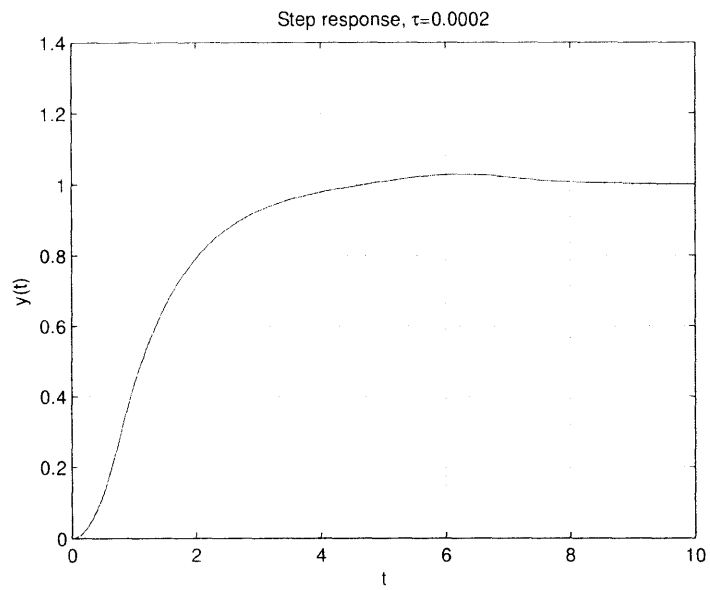
While we illustrated Small Gain techniques in this section through an LTI example, it should be reiterated that the plant we wish to stabilize need *not* be LTI for these techniques to be fruitful. Small gain techniques can also be applied to nonlinear and time-varying systems and, hence, our design techniques can be extended outside



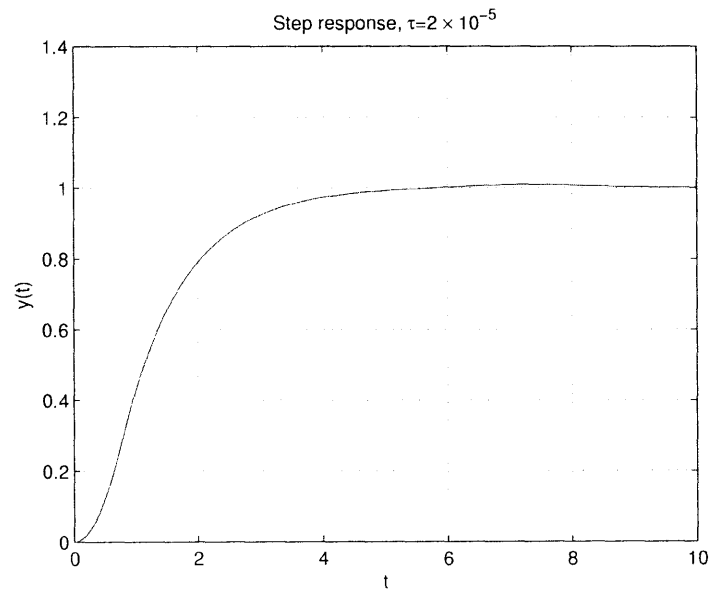
(a) Step response, $\tau = 0.02$.



(b) Step response, $\tau = 0.002$



(c) Step response, $\tau = 0.0002$.



(d) Step response, $\tau = 0.00002$

the realm of LTI systems--provided that the plant model can be represented as a “small” perturbation of a second order LTI model of relative degree two. It is also important to point out that the manner in which the dynamics of the Δ block of Fig. 6.2.4 enter the system do not need to take the additive form shown here; other standard methods of representing uncertainty include multiplicative and feedback perturbations (see [46]), and both of these forms of perturbations can be handled by the techniques outlined in this section, as well.

Chapter 7

Conclusion and Future Work

We begin with a passage:

To read a poem (so the King of Hearts told the White Rabbit), “Begin at the beginning and go on till you come to the end: then stop.” Books, like poems, are sequentially ordered structures, and thus inevitably have a beginning and an end; this is the final paragraph of this book. But the theory of systems and signals, as we have seen, is not simply a cascaded arrangement of topics. There are multiple loops and branches, many parallel and crossing paths. Most ideas are linked directly and indirectly to many others. There is no simple step-by-step route by which this multidimensional web can be systematically explored and comprehended. There is really no beginning, and no end. We cannot expect to appreciate one topic fully until we have considered others. And so we must continually circle back to examine earlier concepts from a new vantage point.

—from William McConway Siebert, Epilogue to *Circuits, Signals and Systems*, 1986.

The work that we have performed here is by no means an end. Nor, as Siebert points out, is it actually a beginning, either. Many of the concepts that we investigated in this document are direct applications of already existing methods and techniques; it is the *way* in which we apply these techniques that we feel is a new contribution, as is often the case with many new contributions in engineering and, in particular, in both the theoretical and applied areas related to signals and systems research.

We have developed tools for synthesizing output feedback controllers using a simple switching architecture for a class of LTI plants and have demonstrated that this architecture can be used to better performance when compared to more traditional control architectures. This provides not only a set of tools for a specific class of problems, but, more importantly, it provides both insight into the power of switching and hope that a more general framework for the synthesis of switching controllers may someday exist. The natural question is now: where do we go from here? Because of the nature of the “multidimensional web” we have entered into, clear paths are

not immediate conclusions. Indeed, the paths leading up to this work have been far greater than what we show here, as it is so often the case that we must discover the paths to failure before we discover a path to success. Nevertheless, we attempt now to provide some insight into potentially fruitful continuations of the research we have developed here, starting with some of the more “obvious” extensions and continuing to somewhat broader research levels.

Second Order Systems of Relative Degree One

While the work here is tailored toward systems of relative degree two, systems of relative degree one have very similar results to the ones shown here. The majority of the parallel work in designing control laws that optimize the rate of convergence and have finite L_2 gain has been mostly completed but is omitted due to time constraints. One interesting fact to note about the case of relative degree one systems from a technical perspective is that, while the optimal algorithm for maximizing the rate of convergence is still a bang-bang algorithm, the eigenmodes are real for *both* the maximum and minimum control gain. Hence, the optimal algorithm in this case does *not* require the use of complex eigenvalues to rotate onto the stable manifold; rotation is induced by switching between two systems with real eigenmodes in a stable way. This statement, of course, only holds true for systems of relative degree one that satisfy the necessary and sufficient conditions developed in Chapter 1.

Choice of Controller Boundaries and Observer Design

Many of the tools we developed in this document provide a *class* of structures from which to choose to achieve stability. For instance, in designing our memoryless switching law, we have the freedom to choose one of the boundaries (the “ q ” parameter) anywhere in a cone whose boundaries are the stable and unstable eigenvectors. Similarly, we determined a class of observers which can be used to construct estimators whose outputs converge asymptotically to the true state. In this work, we picked particular instances in each of these regimes and were able to construct switching architectures which had clear performance benefits over particular LTI structures. The natural question then arises as to whether we could have achieved even better performance by picking a *different* memoryless switching law and observer. While the specific choice of either of these components does not make a difference when considering just asymptotic stability, the specific choice *does* make a difference when computing L_2 gain. Also, when the initial condition of the observer does not match the initial condition of the plant, the specific choice of observer determines the asymptotic rate at which the observer output will converge to the true state. It is clear, then, that investigation of how these specific choices affect performance (which may or may not be embedded in corresponding optimization problems) is important for figuring out how to best design switching systems of the type shown here.

Robustness-related Issues

We briefly discussed a robustness related issue in Chapter 4 (namely robustness with respect to time delays), but this issue deserves more attention. Robustness with respect to errors in the switching boundaries, the observer gains, and the plant itself are all very important issues that should be investigated in-depth in order to assess the sensitivity of the control laws developed here. Fortunately, the main obstacle in performing robustness analysis has been resolved in the work here; since we have computational tools for computing upper bounds on L_2 gains, any case studies for specific forms of uncertainty are applications of the L_2 gain tools we have developed here.

Some preliminary work on a specific case study (again, the double integrator) indicates that the sensitivity of the control laws studied here is not necessarily very high, though we make no attempt to formally quantify that statement here. Of particular interest to note is that, unlike many sliding mode controllers (which, in essence, drive the state onto a stable manifold like we do here, with the major difference that the driving element is a relay), the case study that we have examined is remarkably *insensitive* to the phenomenon of chatter. In fact, a brief experiment indicates that, even in the presence of time delays, if one “over-designs” the switching boundary to account for the potential of time delay and error in the controller parameters, we can design a controller that stabilizes the double integrator with no overshoot, no “visible” chatter, and with settling time very close to the settling time we derived here for the nominal case. If these observations hold in some generality, then this could even provide motivation for using the control structures shown here (or similar variants) for problems which use more “standard” forms of sliding mode control (i.e., with relays).

Applications to Operational Amplifier Design

As mentioned in the introduction, one of the reasons for looking at this particular switching architecture was motivated via problems in operational amplifier design. In designing operational amplifiers, it is typical to add some sort of *compensation network* to reduce oscillations in the closed-loop step response when the op amp is configured in some sort of feedback configuration (which is how an op amp is almost *always* configured for any practical purpose) [15, 22, 59]. In designing compensators, the feedback mechanisms that can be implemented must be stable and are practically constrained to be either first or zeroth order structures. In fact, the first comparison we made in Chapter 5 with first order LTI control models a typical op amp compensation problem as the model of $1/s^2$ is not too distant from a “true” op amp model (one of the transfer functions we investigated, namely $P(s) = 100/s/(s + 1)$ is actually fairly accurate). The implementation of switching between gains of plus and minus one involves implementing a set of switches to essentially invert the open loop gain of the op amp and is, hence, easily implementable. The one major question is then whether the supervisor we use can be implemented easily, the memoryless switching law in particular. Because the switching law we implement is the product

of two linear combinations of the state, we can implement an equivalent control law by computing the signs of each of these linear combinations. For instance, if we desire to check whether

$$x_1(x_1 + x_2)$$

is positive or negative, it is equivalent to compute whether

$$\text{sgn}(x_1)\text{sgn}(x_1 + x_2)$$

is positive or negative, where $\text{sgn}(\cdot)$ is the standard signum function. Because the $\text{sgn}(\cdot)$ function can be computed using a circuit element known as a *comparator*, we have hope that the control laws given here can be implemented rather simply and, hence, may be an option for replacing some of the current techniques of operational amplifier compensation. This hope is further supported by the fact that there has been a recent trend toward the design of hybrid analog/digital circuit structures [61].

Lowpass Filter Design

It is natural to expect that the switching controller of Chapter 5 that is designed to track a step input may also well-track sinusoidal inputs of sufficiently low frequencies. Preliminary simulation for the double integrator indicates that this is, indeed, the case. Moreover, the settling time and overshoot profiles are quite similar to what we observe for a step input when the input frequencies are not too high. When the input frequencies increase beyond a certain point, however, the amplitude of the output decreases with a “roll-off” very akin to a 40dB per decade decrease in amplitude per unit frequency that is observed in LTI filters of relative degree two. This raises the question as to whether the structures we have investigated here may be suitable for lowpass filter design with the possible advantage of having better transient characteristics than LTI lowpass filters with equivalent bandwidth/roll-off characteristics.

Higher Order Systems

The one million dollar question is whether the techniques developed here can be extended to *arbitrary* higher dimensional systems. We have made headway into extending beyond the class of second order LTI systems via the Small Gain Techniques discussed in Chapter 6, but these techniques are not general because they require the plant model being considered to be relatively close to a second order LTI model. For instance, the plant $1/s^3$ does *not* have a good second order LTI approximant in an L_2 gain sense and, thus, the techniques of Chapter 6 cannot be applied.

Currently, we do have some preliminary results on stabilizability in higher dimensions. For instance, a *sufficient* condition for stabilizability by a controller much like the one in Chapter two can be derived to show that if the root locus satisfies the conditions that

- There exists one value of gain for which *only one* eigenvalue lies in the closed right half-plane, and

- There exists another value of gain for which a pair of *dominant* complex eigenvalues,

then a control law which switches between one gain on a stable manifold and another gain everywhere else can be used to achieve asymptotic stability. For instance, a triple integrator $P(s) = 1/s^3$ can be stabilized in this way by switching between gains of $+1$ and -1 in an appropriate manner. The design of control laws of the form listed in Chapter 3 and beyond, however, has yet to be investigated, and the issue of assessing finite L_2 gain has yet to be investigated either. Because the phase portraits of third order systems can be visualized, it seems like investigating the third order case is the best place to start if one wants to move to general higher dimensional problems. In performing this extension, however, it is important to keep one's mind open to the possibility of new, more appropriate feedback structures and a large degree of experimentation may be required to find a switching architecture with performance benefits that are similar to the ones we saw here (e.g., by considering switching between low order dynamical controllers rather than static controllers, by increasing the number of controllers among which switching takes place, etc.). On the whole, this extension is still very much an open problem, and the set of directions we may take in the multidimensional web we have entered are many.

Bibliography

- [1] Malcolm Adams and Victor Guillemin. *Measure Theory and Probability*. Birkhäuser, 1996.
- [2] Dirk Aeyels and Jacques L. Willems. Output feedback: Periodic and memoryless as an alternative for time-invariant and dynamic. pages 2218–2219, Tucson, AZ, December 1992. Proceedings of 31st Conference on Decision and Control.
- [3] Z. Artstein. Example of stabilization with hybrid feedback in *hybrid systems iii*. volume 1066, pages 173–185. Lecture Notes in Computer Science, 1996.
- [4] Dimitri P. Bertsekas. *Dynamic Programming and Optimal Control*. Athena Scientific, second edition, 2000.
- [5] Stephen P. Boyd and Craig H. Barratt. *Linear Controller Design: Limits of Performance*. Prentice Hall, 1991.
- [6] M. S. Branicky. *Studies in Hybrid Systems: Modeling, Analysis, and Control*. Ph.d. thesis, MIT, June 1995.
- [7] M. S. Branicky. Multiple lyapunov functions and other tools for switched and hybrid systems. *IEEE Transactions on Automatic Control*, 43(4):475–482, April 1998.
- [8] D. Chatterjee and D. Liberzon. Stability analysis of deterministic and stochastic switched systems via a comparison principle and multiple lyapunov functions. *SIAM Journal on Control and Optimization*, 45(1):174–206, 2006.
- [9] H. Dym and H. P. McKean. *Fourier Series and Integrals*. Academic Press, 1972.
- [10] Johan Eker and Jörgen Malmberg. Design and implementation of a hybrid control strategy. *IEEE Control Systems Magazine*, 19(4):12–21, August 1999.
- [11] Irmgardd Flüge-Lotz. *Discontinuous and Optimal Control*. McGraw Hill Series in Applied Mathematics, 1968.
- [12] J. M. Gonçalves. Quadratic surface lyapunov functions for global stability analysis of saturation systems. pages 4183–4188. Proceedings of the 2001 American Control Conference, 2001.

- [13] J. M. Gonçalves. Global stability analysis of on/off systems. pages 1382–1387. Proceedings of the 39th Conference on Decision and Control, December 2000.
- [14] Jorge Gonçalves. *Constructive Global Analysis of Hybrid Systems*. Ph.d. thesis, MIT, September 2000.
- [15] Paul R. Gray and Robert G. Meyer. *Analysis and Design of Analog Integrated Circuits*. John Wiley & Sons, Inc., third edition, 1993.
- [16] John P. Greschak and George C. Verghese. Periodically varying compensation of time-invariant systems. *Systems and Control Letters*, 2(2):88–93, August 1982.
- [17] J. Hespanha. Uniform stability of switched linear systems: Extensions of lasalle’s invariance principle. *IEEE Transactions on Automatic Control*, 49(4):470–482, April 2004.
- [18] J. Hespanha and A. S. Morse. Switching between stabilizing controllers. *Automatica*, 38(11):1905–1917, November 2002.
- [19] J. P. Hespanha. *Logic Based Switching Algorithms in Control*. Ph.d. dissertation, Yale University, 1998.
- [20] J. P. Hespanha. Root-mean-square gains of switched linear systems. *IEEE Transactions on Automatic Control*, 48(11):2040–2045, 2003.
- [21] Mikael Johansson and Anders Rantzer. Computation of piecewise quadratic lyapunov functions for hybrid systems. *IEEE Transactions on Automatic Control*, 43(4):555–559, April 1998.
- [22] David A. Johns and Ken Martin. *Analog Integrated Circuit Design*. John Wiley & Sons, Inc., 1997.
- [23] Pierre T. Kabamba. Control of linear systems using generalized sampled-data hold functions. *IEEE Transactions on Automatic Control*, AC-32(9):772–783, September 1987.
- [24] T. Kaczorek. Pole placement for linear discrete-time systems via periodic output feedbacks. *Systems and Control Letters*, 6:267–269, October 1985.
- [25] Hassan K. Khalil. *Nonlinear Systems*. Prentice-Hall, Inc., second edition, 1996.
- [26] D. Liberzon. Stabilizing a linear system with finite-state hybrid output feedback. Proceedings of the 7th IEEE Mediterranean Conference on Control and Automation, 1999.
- [27] D. Liberzon and A. S. Morse. Basic problems in stability and design of switched systems. *IEEE Control Systems Magazine*, 19(5):59–70, October 1999.
- [28] Daniel Liberzon. *Switching in Systems and Control*. Birkhäuser, 2003.

- [29] M. Margaliot and D. Liberzon. Lie algebraic stability conditions for nonlinear switched systems and differential inclusions. *Systems and Control Letters*, 55(1):8–16, January 2006.
- [30] Arthur P. Mattuck. *Introduction to Analysis*. Prentice Hall, 1999.
- [31] B. Hu, G. Zhai and A. N. Michel. Hybrid output feedback stabilization of two-dimensional linear control systems. pages 2184–2188, Chicago, Illinois, June 2000. Proceedings of the 2000 American Control Conference.
- [32] E. Litsyn, Y. V. Nepomnyashchikh and A. Posonov. Stabilization of linear differential systems via hybrid feedback controls. *SIAM Journal of Control Optimization*, 38(5):1468–1480, 2000.
- [33] G. Zhai, B. Hu, K. Yasuda and A. N. Michel. Disturbance attenuation properties of time-controlled switched systems. *Journal of the Franklin Institute*, 358(7):765–779, 2001.
- [34] Guisheng Zhai, Hai Lin and Youngbok Kim. L2 gain analysis for switched systems with continuous-time and discrete-time subsystems. pages 658–663. SICE 2004 Annual Conference, August 2004.
- [35] J. M. Gonçalves, A. Megretski, and M. A. Dahleh. Global stability of relay feedback systems. *IEEE Transactions on Automatic Control*, 46(4):550–562, April 2001.
- [36] J. M. Gonçalves, A. Megretski, and M. A. Dahleh. Global analysis of piecewise linear systems using impact maps and surface lyapunov functions. *IEEE Transactions on Automatic Control*, 48(12):2089–2106, December 2003.
- [37] J. P. Hespanha, D. Liberzon and A. S. Morse. Logic-based switching of a nonholonomic system with parametric modelling uncertainty. *Systems and Control Letters*, 38(3):167–177, November 1999.
- [38] J. P. Hespanha, D. Liberzon, and A. S. Morse. Overcoming the limitations of adaptive control by means of logic-based switching. *Systems and Control Letters*, pages 49–65, 2003.
- [39] J. P. Hespanha, D. Liberzon and A. S. Morse. Hysteresis-based switching algorithms for supervisory control of uncertain systems. *Automatica*, pages 269–275, 2004.
- [40] K. R. Santarelli, A. Megretski and M. A. Dahleh. Stabilizability of two-dimensional linear systems via switched output feedback. *Systems and Control Letters* [submitted, May 2006].
- [41] K. R. Santarelli, A. Megretski, and M. A. Dahleh. New results on the stabilizability of two-dimensional linear systems via switched output feedback. pages 3778–3783, Portland, OR, June 2005. Proceedings of the 2005 American Control Conference.

- [42] K. R. Santarelli, M. A. Dahleh and A. Megretski. Optimal controller synthesis for second order lti plants with switched output feedback. San Diego, CA, December 2006. Proceedings of the 45th Conference on Decision and Control.
- [43] K. R. Santarelli, M. A. Dahleh and A. Megretski. Optimal controller synthesis of second order linear systems of relative degree two with switched output feedback. Technical report, MIT, March 2006.
- [44] L. A. Gould, W. R. Markey, J. K. Roberge, and D. L. Trumper. *Control Systems Theory*. Lecture notes for MIT Course 6.302 *Feedback Systems*, 1997.
- [45] L. Vu, D. Chatterjee and D. Liberzon. Input-to-state stability of switched systems and switching adaptive control. To appear in *Automatica*, available at http://decision.csl.uiuc.edu/~liberzon/research/iss_auto.pdf.
- [46] Mohammed Dahleh, Munther A. Dahleh, and George C. Verghese. *Lectures on Dynamic Systems and Control*. Lecture notes for MIT Course 6.241 *Dynamic Systems and Control*, 1999.
- [47] Pramod P. Khargonekar, Kameshwar Poola and Allen Tannenbaum. Robust control of linear time-invariant plants using periodic compensation. *IEEE Transactions on Automatic Control*, AC-30(11):88–93, November 1985.
- [48] Stephen Boyd, Laurent El Ghaoui, Eric Feron, and Venkataramanan Balakrishnan. *Linear Matrix Inequalities in System and Control Theory*. SIAM Studies in Applied Mathematics, 1994.
- [49] Vadim Utkin, Jürgen Guldner, and Jingxin Shi. *Sliding Mode Control in Electromechanical Systems*. Taylor & Francis, 1999.
- [50] Vishwesh Kulkarni, Myungsoo Jun and João Hespanha. Piecewise quadratic lyapunov functions for time-delay hybrid systems. pages 3885–3889. Proceedings of the 2004 American Control Conference, June 2004.
- [51] A. Megretski. Course 6.243 lecture notes. 2003.
- [52] Alexandre Megretski. *6.245 Lecture Notes*. Lecture notes for MIT Course 6.245 *Multivariable Control Systems*, 2002.
- [53] Alexandre Megretski. *6.242 Lecture Notes*. Lecture notes for MIT Course 6.242 *Model Reduction*, 2004.
- [54] Barrett O’Neill. *Semi-Riemannian Geometry With Applications to Relativity*. Academic Press, 1983.
- [55] Barrett O’Neill. *Elementary Differential Geometry*. Academic Press, 1997.
- [56] Alan V. Oppenheim and Alan S. Willsky with Hamid S. Nawab. *Signals and Systems*. Prentice Hall Signal Processing Series. 1997.

- [57] N.B.O.L. Pettit. *Analysis of Piecewise Linear Systems*. John Wiley and Sons, 1995.
- [58] A. Rantzer and A. Megretski. *A Tutorial on Integral Quadratic Constraints. Part I: IQC Models and Their Feasibility*. Personal correspondence, 2002.
- [59] James K. Roberge. *Operational Amplifiers: Theory and Practice*. John Wiley & Sons, Inc., 1975.
- [60] Walter Rudin. *Principles of Mathematical Analysis*. McGraw-Hill, 1976.
- [61] Rahul Sarpeshkar. Analog vs. digital: Extrapolating from electronics to neurobiology. *Neural Computation*, 10:1601–1638, 1998.
- [62] Stephen D. Senturia and Bruce D. Wedlock. *Electronic Circuits and Applications*. John Wiley & Sons, 1975.
- [63] William McC. Siebert. *Circuits, Signals, and Systems*. The MIT Press, 1986.
- [64] Karl. J. Åström and Tore Hägglund. *PID Controllers: Theory, Design, and Tuning*. Instrument Society of America, second edition, 1995.
- [65] Ya. Z. Tsypkin. *Relay Control Systems*. Cambridge University Press, 1984.
- [66] Stephen A. Ward and Robert H. Halstead Jr. *Computation Structures*. The MIT Press, 1990.
- [67] Kemin Zhou with John C. Doyle. *Essentials of Robust Control*. Prentice Hall, 1998.
- [68] X. Xu and P. J. Antsaklis. Stabilization of second-order lti switched systems, *ISIS Technical Report isis-99-001*,. Technical report, Dept. of Elec. Enging., University of Notre Dame, January, 1999.
- [69] X. Xu and P. J. Antsaklis. Design of stabilizing control laws for second-order switched systems. volume C, pages 181–186, Beijing, P. R. China, July 1999. Proceedings of the 14th IFAC World Congress.
- [70] J. L. Yanesi and A. G. Aghdam. High-performance simultaneous stabilizing periodic feedback control with a constrained structure. pages 839–844, Minncapolis, MN, June 2006. Proceedings of 2006 American Control Conference.
- [71] Jun Zhao and David J. Hill. On stability and l2 gain for switched systems. pages 3279–3284, Seville, Spain, December 2005. Proceedings of the 44th Conference on Decision and Control.